TECHNICAL REPORT STANDARD TITLE PAGE

1. Report No.	2. Government Accession No.	3. Recipient's Catalog No.
FHWA/TX-78/01+23-3F		

4. Title and Subtitle	5. Report Date
TEMPERATURE INDUCED STRESSES IN HIGHWAY BRIDGES BY FINITE ELEMENT ANALYSIS AND FIELD TESTS	July 1978
	6. Performing Organization Code
7. Author(s)	8. Performing Organization Report No.
Atalay Yargicoglu and C. Philip Johnson	Research Report 23-3F
9. Performing Organization Name and Address	10. Work Unit No.
Center for Highway Research The University of Texas at Austin Austin, Texas 78712	11. Contract or Grant No. Research Study 3-5-74-23
	13. Type of Report and Period Covered
12. Sponsoring Agency Name and Address	Final
Texas State Department of Highways and Public Transportation; Transportation Planning Division P. O. Box 5051 Austin, Texas 78763	14. Sponsoring Agency Code

15. Supplementary Notes

Study conducted in cooperation with the U. S. Department of Transportation, Federal Highway Administration. Research Study Title: "Temperature Induced Stresses in Highway Bridges by Finite Element Analysis and Field Tests"

16. Abstract

This research focused on the application of finite element computer programs to the transient heat conduction and static stress analysis of bridge-type structures. The temperature distribution is assumed to be constant along the centerline of the bridge but can vary arbitrarily over its cross section.

A computer program, TSAP, was developed for the prediction of the transient temperature distribution due to either daily variations of the environment such as solar radiation, ambient air temperature, and wind speed, or measured surface temperatures. This program, which also included thermal stress analysis based on elastic beam theory, was used extensively in this work to establish quantitatively typical magnitudes of temperature induced stresses for selected bridge types located in the state of Texas. Specific attention was given to the extreme summer and winter climatic conditions representative of the city of Austin, Texas.

A static analysis program, SHELL8, which utilizes two-dimensional finite elements in a three-dimensional global assemblage with six degrees of freedom at each node point, was also developed to determine the thermally induced stresses and bridge movements. A concrete slab bridge was analyzed using this program to investigate skew and transverse behavior. Also, correlations between the field measured slope changes on two prestressed concrete bridges, and results that were obtained using the finite element programs, have been included.

17. Key Words	18. Distribution Statement
bridges, temperature, stresses, finite element, analysis, field tests, computer	No restrictions. This document is available to the public through the National Technical Information Service, Springfield, Virginia 22161.

19. Security Classif. (of this report)	20. Security Classif. (of this page)	21. No. of Pages	22. Price
Unclassified	Unclassified	196	

Form DOT F 1700.7 (8-69)

TEMPERATURE INDUCED STRESSES IN HIGHWAY BRIDGES BY FINITE ELEMENT ANALYSIS AND FIELD TESTS

by

Atalay Yargicoglu
C. Philip Johnson

Research Report Number 23-3F

Temperature Induced Stresses in Highway Bridges
by Finite Element Analysis and Field Tests

Research Project 3-5-74-23

conducted for

Texas
State Department of Highways and Public Transportation

in cooperation with the
U. S. Department of Transportation
Federal Highway Administration

by the

CENTER FOR HIGHWAY RESEARCH
THE UNIVERSITY OF TEXAS AT AUSTIN

July 1978

The contents of this report reflect the views of the authors, who are responsible for the facts and the accuracy of the data presented herein. The contents do not necessarily reflect the official views or policies of the Federal Highway Administration. This report does not constitute a standard, specification, or regulation.

There was no invention or discovery conceived or first actually reduced to practice in the course of or under this contract, including any art, method, process, machine, manufacture, design or composition of matter, or any new and useful improvement thereof, or any variety of plant which is or may be patentable under the patent laws of the United States of America or any foreign country.

PREFACE

This is the third report resulting from the research project "Temperature Induced Stresses in Highway Bridges by Finite Element Analysis and Field Tests." The first two reports (Refs 39 and 43) are a result of Ph.D. dissertations written by Drs. Thaksin Thepchatri and Kenneth M. Will at The University of Texas at Austin. Their contributions which are especially noteworthy were made during the first two years of the project. This report summarizes their work as well as the research performed during the third year of the project. Program documentations, listings and example problems are also contained in this final report.

Several individuals have made contributions in this research. Special thanks are given to Professor Hudson Matlock for his contribution in supervising the field tests. The interest shown by John Panak and his inputs during the course of this work are appreciated. In addition, thanks are given to Mr. Hector Reyes, Mr. Dewaine Bogard, and Mr. Mike Hoblet for their assistance in the field tests and to Kay Lee for typing the draft and final copy of this report. The help given by the staff of the Center for Highway Research in producing this report is also appreciated.

Atalay Yargicoglu

C. Philip Johnson

ABSTRACT

This research focused on the application of finite element computer programs to the transient heat conduction and static stress analysis of bridge-type structures. The temperature distribution is assumed to be constant along the center-line of the bridge but can vary arbitrarily over its cross section.

A computer program, TSAP, was developed for the prediction of the transient temperature distribution due to either daily variations of the environment such as solar radiation, ambient air temperature, and wind speed, or measured surface temperatures. This program, which also included thermal stress analysis based on elastic beam theory, was used extensively in this work to establish quantitatively typical magnitudes of temperature induced stresses for selected bridge types located in the state of Texas. Specific attention was given to the extreme summer and winter climatic conditions representative of the city of Austin, Texas.

A static analysis program, SHELL8, which utilizes two-dimensional finite elements in a three-dimensional global assemblage with six degrees of freedom at each node point, was also developed to determine the thermally induced stresses and bridge movements. A concrete slab bridge was analyzed using this program to investigate skew and transverse behavior. Also, correlations between the field measured slope changes on two prestressed concrete bridges, and results that were obtained using the finite element programs, have been included.

SUMMARY

Finite element procedures for the prediction of temperature induced stresses in highway bridges caused by daily environmental changes have been developed. This research indicates that the amplitude and form of the temperature distribution are mainly functions of the daily solar radiation, ambient air temperature and wind speed. The shape and depth of the bridge cross-section and its material thermal properties such as absorptivity, emissivity, and conductivity, are also factors. For example, due to the low thermal conductivity of concrete, the nonlinearity of the temperature distribution in deep concrete bridges was found to be considerably greater than that occurring in composite steel bridges. In addition to stresses caused by the nonlinear form of the temperature gradient, temperature induced stresses also arise from statical indeterminancy of the bridge. Analytical procedures which can account for both effects were developed and implemented into two computer programs.

The first program, TSAP, which is able to predict both the temperature distribution and the temperature induced stresses, was extensively used to establish typical magnitudes of temperature induced stresses for three types of highway bridges located in the state of Texas. The environmental data required in the analysis were obtained from daily weather reports. The most extreme environmental conditions were found to occur on a clear night followed by a clear day with a large range of air temperature. Specific attention was given to the extreme summer and winter climatic conditions representative of the city of Austin, Texas.

In general, it was found that thermal deflections are small. Thermal stresses, however, appear to be significant. For the weather conditions considered, temperature induced tensile stresses in a prestressed concrete slab bridge and a precast prestressed I-beam were found to be in the order of 60-65 to 80-90 percent respectively of the cracking stress of concrete suggested by the AASHTO specifications. Compressive stresses as high as 45 percent of the allowable compressive strength were predicted in a prismatic slab having a depth of 17 inches. For a composite steel-concrete bridge, on

the other hand, temperature induced stresses were approximately 10 percent of the design dead and live load stresses.

The other program, SHELL8, is a finite element static analysis program. This program, which employs two-dimensional finite elements in a three-dimensional global assemblage, may be used to predict temperature induced stresses and movements for complex bridge-type structures. Thermal forces are calculated from a quartic distribution of temperature through the thickness and a linear distribution over the mid-surface of each element. Hence the nonlinearity of the temperature distribution found in concrete structures is accurately considered in the analysis.

During this research, field measurements were performed on two bridges: an entrance ramp in Pasadena, Texas, which was skewed and post-tensioned with three continuous spans and a two-span pedestrian overpass in Austin, Texas, with pretensioned beams made continuous for live loads. A portable temperature probe was developed to measure surface temperatures at various locations on the bridges. A mechanical inclinometer was available for determining slope changes induced by temperature changes. Correlations of measured slope changes with results obtained using the finite element procedures were made for each test. Measured surface temperatures were used to predict the internal temperature distribution which is required in the static analysis. These correlations clearly demonstrate the capability and the accuracy of the subject finite element procedures in predicting temperature induced stresses and movements under field conditions.

IMPLEMENTATION STATEMENT

As a result of this research two computer programs, TSAP and SHELL8, have been developed to predict temperature induced stresses in highway bridges due to daily changes of temperature. The CDC 6600 computer at The University of Texas at Austin was used during the course of this investigation. The final versions of programs TSAP and SHELL8 have also been adapted to the IBM computer facilities of the Texas State Department of Highways and Public Transportation for ongoing use. In regard to implementation, this report contains:

(a) the documentation of programs TSAP and SHELL8 (Chapter 4);

(b) an example problem for input and output for program TSAP (Appendix 1);

(c) an example problem for input and output for program SHELL8 (Appendix 2);

(d) a listing of the IBM version of program TSAP (Appendix 3); and

(e) a listing of the IBM version of program SHELL8 (Appendix 4).

This information is presented for the purpose of enhancing inhouse use by the engineers of the State Department of Highways and Public Transportation for direct determination of temperature induced stresses in highway bridges of future interest.

Although the time required in preparing data and executing these programs is significant, they may be used effectively to determine the effects of skew, transverse behavior, and the stiffness contributions of the parapets and sidewalks, if any. There are other immediate applications of the heat conduction and/or thermal stress analysis programs. They can be readily applied to reinforced concrete pavement to evaluate the effects of temperature. Another area of interest is that of polymer-impregnated concrete in which the surface is dried for several hours at 200-300^{o} F before the bridge deck is impregnated. This drying process could be investigated with the subject procedures, and could help locate potential problems even though the conductivity and tangent stiffness of concrete changes considerably at elevated temperatures.

The method used in program TSAP is based on a two-dimensional model for predicting the temperature distribution and one-dimensional beam theory for the stress analysis; the program is relatively easy to use. Environmental data are available through regular Weather Bureau Reports while material thermal properties may be obtained from one of the handbooks on concrete engineering. By using the program TSAP, typical magnitudes of temperature induced stresses were analytically established for three types of highway bridges subjected to daily climatic changes found in Texas. Specific attention was given to the extreme climatic conditions of the city of Austin, Texas. Thermal stresses obtained from ordinary beam theory were magnified by less than 15 percent at only a very limited number of locations on the bridge due to skew and transfer behavior according to the results obtained for a three-span slab bridge.

Field tests were performed on two prestressed concrete bridges using the portable temperature probe developed for measuring the surface temperatures and the mechanical inclinometer for measuring slope changes. Correlations with field results demonstrated that relatively simple instrumentation with a few selected measurements may be used in the study of the diurnal heating of bridges under field conditions when coupled with the subject finite element procedures. The thermally induced stresses predicted in the analysis for both bridges tested are well within design limits. However, it should be emphasized that these stresses are only for the days of the tests which are not believed to be the most severe days for thermal effects. The low magnitude of the stresses in the entrance ramp is also due to the overdesign of the structure since the stiffness of the sidewalks and parapets was neglected in the design process.

TABLE OF CONTENTS

CHAPTER 1. INTRODUCTION

Nature of the Problem

The purpose of this report is to summarize the results of the research project "Temperature Induced Stresses in Highway Bridges by Finite Element Analysis and Field Tests," which was conducted during the period of September 30, 1973, to August 30, 1976, under the sponsorship of the Texas Highway Department and the Federal Highway Administration. This project was motivated by the need for a general analysis procedure which could establish quantitatively typical magnitues of temperature induced stresses and movements caused by daily variations in temperature for complex bridge structures.

Stresses and movements caused by daily and seasonal fluctuations of temperature in bridges have been studied by several researchers during the past decade as summarized in Ref 35. Current technology is being applied at an accelerating rate towards the development and utilization of predictive models in an effort to assess the role of temperature in highway bridges (24, 34).

The results of studies which have been made to date indicate that temperature induced stresses may be of sufficient magnitude when coupled with their cyclic nature to damage or hasten deterioration of bridge decks. For example, compressive stresses in a prismatic thick slab section in the range of 40 percent of the allowable compressive strength have been cited (34). Tensile stresses of approximately 600 psi have been predicted in this research (39) for a composite prestressed section. This stress is caused by daily changes in temperature which are representative of Austin, Texas. Temperature stresses may be more severe for other locations and other bridge types. In addition, these stresses may be amplified by skew as well as other three-dimensional effects.

It is recognized that the daily variation of temperature is a significant source of thermal strains and stresses. These induced strains and stresses may be attributed to two types of behavior: (1) the nonlinear form of the temperature gradient over the depth of the section which within itself is a source of thermal stress, and (2) the form of statical indeterminancy of the

structure. The temperature stresses in a single span structure are due solely to the nonlinear temperature while two- and three-span structures share this same stress plus flexural stresses due to the restraint of the interior support in preventing upward movement which would take place since the upper portion of the section heats more rapidly. The amplitude and form of the temperature gradient are principally a function of the intensity of the solar radiation and ambient air temperature combined with the shape and depth of the cross section and its material properties.

A general method of analysis is required to determine the transient temperature distributions and temperature induced movements and stresses for bridge-type structures. The finite element method, the subject of texts by Desai and Abel (17) and Zienkiewicz (47), is such a general method. Fortunately, highly developed finite element analysis programs were available at the onset of this work. Thus only minimal modifications and extensions were necessary to address problems of current interest.

Review of Objective and Scope of the Study

The objective of this study was to demonstrate quantitatively typical magnitudes of temperature induced stresses and movements under field conditions for selected highway bridges in the state of Texas. The study was separated into four phases to accomplish the objective:

(1) development of a computational procedure to solve for the temperature distribution and temperature induced movements and stresses of bridges,

(2) field measurements of bridge temperatures and temperature induced movements,

(3) correlation of measured bridge movements with computer results, and

(4) providing the State Department of Highways and Public Transportation with information regarding the magnitude of temperature induced stresses and internal temperature distributions for various bridge types at three different locations in the state of Texas.

Two finite element programs, TSAP and SHELL8, were developed for the purpose of predicting temperature distributions and temperature induced stresses of bridges in order to accomplish the first phase of this study. The method of analysis is discussed in detail in the next section.

Selected field measurements were performed on two bridges. The first bridge tested was the same one tested by Matlock and co-workers as discussed in Ref 30. The second bridge tested was a two-span continuous for live load pedestrian overpass. Both tests were performed during daylight hours. Summaries of the field measurements and computer results are presented in Chapter 3. More detailed information regarding these field tests is presented in Refs 39 and 43. It should be emphasized that it was not within the intended scope of this study to take extensive field measurements to accomplish the second phase of this study. Rather, selected measurements of temperatures and bridge movements were taken to validate the computational procedure.

Based on the favorable comparisons between the predicted and the measured results, the proposed approach thus offers an excellent opportunity to determine bridge types and environmental conditions for which temperature effects may be severe. This study was limited to three typical types of highway bridges subjected to climatic changes found in the state of Texas. These bridges as shown in Fig 1 are:

(1) a post-tensioned concrete slab bridge,
(2) a composite precast pretensioned bridge, and
(3) a composite steel bridge.

Analyses of several environmental conditions representative of summer and winter conditions were carried out for three locations: Austin, El Paso, and Brownsville. Past records of the solar radiation levels and the daily air temperature distributions during the years 1967-1971 were obtained from either the U.S. Weather Bureau or local newspapers for these locations. Temperature effects in both statically determinate and indeterminate bridges were studied, including skew and transverse behavior.

It should be noted that this study concerns primarily the stresses induced by a temperature differential over the depth of highway bridges. Combined effects of dead and live load plus impact are therefore ignored.

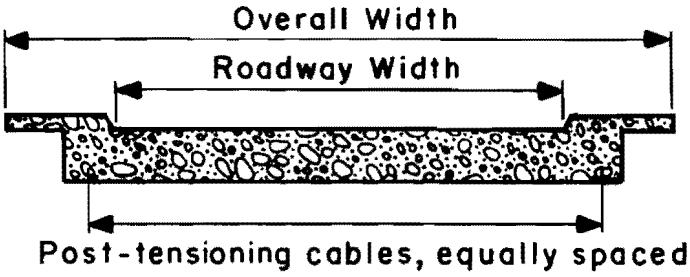

(a) Post-tensioned concrete slab bridge

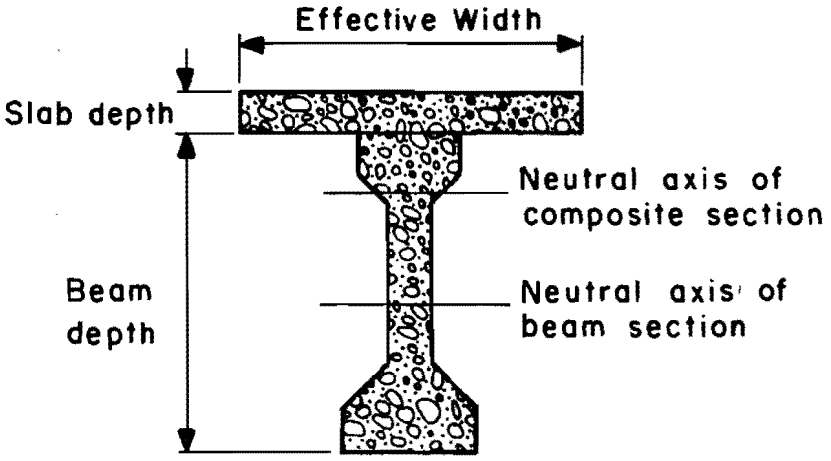

(b) Composite precast pre-tensioned bridge

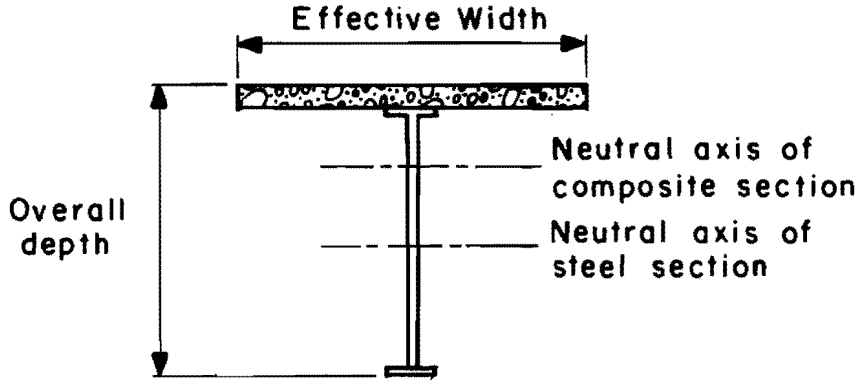

(c) Composite steel bridge

Fig 1. Cross-section of highway bridges.

Analysis Procedures

Classical solutions are available for thermal stresses and transient temperature distributions in plates, cylinders, and beams. Solutions for these cases may be found in Refs 8, 9, and 40. Unfortunately, these classical solutions are restricted to a limited boundary and geometrical configurations. For bridge-type structures, a more general method of analysis is required to determine the transient temperature distributions and temperature induced movements and stresses.

In the analysis of bridge temperature distribution, the flow of heat will be negligible in the longitudinal direction of the bridge. The heat will flow primarily over the bridge cross section since the top and bottom surfaces are the main locations of heat input due to solar radiation and/or convection.

The shape of the bridge cross section will influence the temperature distribution. The temperature distribution over the sections of Fig 1b and 1c will be two-dimensional since the temperature in the girders will be a result of the heat propagating from the top surface and that of the ambient air temperature exposed to the exterior surfaces of the girders. Studies that have been made in this research show that the temperature is nonlinear both vertically and horizontally, thus requiring the use of two-dimensional heat flow theory.

The temperature distribution over the bridge cross section at a given time can be calculated by solving the heat-conduction equation. To solve this equation, however, it is necessary that the temperature on the boundary and the initial condition be specified at the starting time. At this time, it is assumed that the bridge temperature is uniform and equal to the surrounding air temperature.

The two heat codes which were used in this work follow from Emerson (20). and Wilson (46). The first is a one-dimensional model based on finite differences. Temperature predicted by this model has been shown to compare favorably with experimental results. The second is a two-dimensional model using finite elements. Both procedures have been extended to account for outgoing radiation, thus enabling the determination of temperature through a full 24-hour period or over a period of several days. Temperature distribution may be obtained from inputs consisting of either solar radiation and ambient air temperature or measured surface temperatures.

Two computer programs are presented in this report for determining temperature induced stresses. The first program (TSAP) includes the heat flow and the thermal stress analysis in a complete system. In this program, the two-dimensional heat code is used in combination with the one-dimensional stress model. Its advantages lie in the relative economy of data preparation and computation time. Its use is limited to straight bridges with orthogonal supports. The second program (SHELL8) is more general and has been shown to be effective for a detailed stress analysis for complex bridge structures (25). In this program, the bridge is idealized as an assemblage of one- and two-dimensional finite elements. Each element may have a quartic distribution of temperature over its thickness. In this way, nonlinear temperature gradients may be systematically and accurately accounted for; however, the required inputs are quite extensive.

The stress model used in TSAP is the simplest one. The one-dimensional beam theory is employed in conjunction with the principle of superposition. All materials are assumed to behave elastically. Structural stiffness is computed based on the uncracked section. In brief, the temperature induced stresses are computed as follows. The bridge is considered to be completely restrained against any movement, thus creating a set of built-in stresses. This condition also induces a set of end forces which are applied back at the ends since the bridge is free from external end forces. This causes another set of stresses which vary linearly over the depth. The final stresses are then obtained by superimposing the above two sets of stresses.

The subject procedures, which have yielded satisfactory correlation with field measurements, provide a mechanism for investigating a wide range of conditions in an effort to isolate types and locations of structures that are most severely affected by daily variations of temperature. The documentation of the computer programs is presented in Chapter 4.

CHAPTER 2. THERMAL EFFECTS IN HIGHWAY BRIDGES

Bridge Type and Location

In this work, three bridge types as shown in Fig 1 were considered: (1) a post-tensioned concrete slab bridge, (2) a composite precast pretensioned bridge, and (3) a composite steel bridge. Special attention was given to the extreme summer and winter conditions found in the city of Austin, Texas (39). In the final phase of this research, a limited number of investigations were carried out for two other cities in Texas (El Paso and Brownsville) so as to provide information regarding the magnitude of temperature induced stresses and internal temperature distributions for other locations in the state of Texas.

Types of Temperature Induced Stresses

Temperature behavior in highway bridges is caused by both short-term (daily) and long-term (seasonal) environmental changes. Seasonal environmental fluctuations from winter to summer, or vice versa, will cause large overall expansion and contraction. If the bridge is free to expand longitudinally, the seasonal change will not lead to temperature induced stresses. However, daily changes of the environment result in a temperature gradient over the bridge cross section that causes temperature induced stresses. The magnitude of these stresses depends on the nonlinear form of the temperature gradient and the flexural indeterminacy of the bridge. Past research in this area indicates that the most significant environmental variables which influence the temperature distribution are solar radiation, ambient air temperature and wind speed. These are discussed in the following sections.

Environmental Variables

Solar radiation, also known as insolation (incoming solar radiation), is the principal cause of temperature changes over the depth of highway bridges. Solar radiation is maximum on a clear day. The sun's rays which are absorbed directly by the top surface cause the top surface to be heated more rapidly than the interior region, thus resulting in nonlinear temperature gradient

over the bridge cross section. The amount of solar radiation actually received by the surface depends on its orientation with respect to the sun's rays. The intensity is maximum if the surface is perpendicular to the rays and is zero if the rays become parallel to the surface. The variation of daily solar radiation intensity on a horizontal surface is approximately sinusoidal. It is found, however, that the maximum surface temperature generally takes place around 2 p.m. This lag of surface temperature is attributed to the influence of the daily air temperature variation which normally reaches its maximum value around 4 p.m.

Field measurements on solar radiation intensity also indicate that the amount of radiation received each day varies with the time of year and the latitude. Local conditions, such as atmospheric contamination, humidity, and elevation above sea level, affect the total solar energy received by a surface. Values of the total insolation in a day are available through the U.S. Weather Bureau Reports. The average of the maximum insolation values as recorded during the years 1967-1971 are given in Table 1 for the city of Austin, Texas. From Table 1, it can be seen that in December, the radiation is the minimum due to the reduced angle of incidence of the sun's rays, their longer path through the atmosphere, and the shorter period of sunlight.

Air temperature varies enormously with locations on earth and with the seasons of the year. The manner in which daily air temperature varies with time must be known in order to accurately predict temperature effects in a bridge. The maximum and the minimum value of air temperatures in a day are regularly recorded at almost all weather stations in the nation. The hourly temperature distribution, however, can only be obtained from local weather reports.

On clear days with little change in atmospheric conditions, the air temperature generally follows two cycles. The normal minimum temperature is reached at or shortly before sunrise, followed by a steady increase in temperature due to the sun's heating effect. This increase continues until the peak temperature is reached during the afternoon, usually around 4 to 5 p.m. Then the temperature decreases until the minimum reading is reached again the next morning. This cyclic form of temperature variation can be changed by the presence of clouds, rain, snow, etc. Clouds, for example, form a blanket so that much of the sun's radiation fails to reach the earth; this results in lowering air temperature during the day. At night, back radiation from the clouds causes a slight increase in air temperature.

TABLE 1. AVERAGE MAXIMUM TOTAL INSOLATION IN A DAY ON THE HORIZONTAL SURFACE (1967-1971) AND LENGTH OF DAYTIME (AUSTIN, TEXAS)

Month	Insolation (btu/ft^2)	Time(CST)		Length of Daytime(hr.)
		Sunrise(A.M.)	Sunset(P.M.)	
JAN	1500	7:30	6:00	10.5
FEB	1960	7:15	6:15	11.0
MAR	2289	6:30	6:30	12.0
APR	2460	6:00	7:00	13.0
MAY	2610	5:30	7:00	13.5
JUN	2631	5:30	7:30	14.0
JUL	2550	5:30	7:30	14.0
AUG	2380	6:00	7:00	13.0
SEP	2289	6:30	6:30	12.0
OCT	1925	6:30	6:00	11.5
NOV	1570	7:00	5:30	10.5
DEC	1329	7:30	5:30	10.0

It is worth noting that the times of high and low ambient air temperature do not coincide with the times of maximum and minimum solar radiation intensity. This is true for both the daily and the yearly conditions. The month of August is generally considered the hottest month of the year, January the coldest; yet the greatest intensity of radiation occurs in June and the lowest in December. On a daily basis, the maximum air temperature normally occurs at 4 p.m., yet the maximum solar radiation intensity occurs at noon. Table 2 summarizes temperature data as recorded in Austin, Texas, with normal and extreme air temperatures tabulated for each month of the year.

Studies done in this research have shown that during a period of clear days and nights, variations of bridge temperature distribution over the concrete cross section are small at about two hours after sunrise. At this time, it is possible to assume a thermal equilibrium state in which the bridge temperature is the same as that of the surrounding air temperature. In this study, it was also found that the range of air temperature from a minimum value to a maximum value during a given day affects the bridge temperature distribution. A large range of air temperature will cause a large temperature differential over the bridge depth which in turn causes high temperature induced stresses. It is of interest to note that the range of air temperature is higher in winter than in summer. In January, the range is 45^{o} F, while 34^{o} F is found in August.

Wind is known to cause an exchange of heat between surfaces of the bridge and the environment. The speed of the wind has an effect in increasing and lowering surface temperatures. From this research study, it was found that maximum temperature gradients over the bridge depth are reached on a still day. On a sunny afternoon, wind decreases temperatures on the top surface and increases temperatures at the bottom. This effect, of course, results in lowering the temperature gradient during the day. At night, maximum reversed temperature gradients are also decreased by the presence of the wind.

Wind speed is recorded by all weather stations. Table 2 gives the average wind speed for each month of the year as recorded in Austin, Texas.

Heat Flow Conditions

The prediction of time varying bridge temperature distributions involves the solution of the heat flow equations governing the flow of heat at the bridge boundaries and within the bridge. In general, heat is transferred

TABLE 2. NORMALS, MEANS AND EXTREMES (REF 39)
LATITUDE 30° 18'N, LONGITUDE 97° 42'N
ELEVATION (GROUND) 597 FEET

Austin, Texas

Month	Temperature							Wind			
	Normal			Extremes				Mean Hourly Speed	Fastest Mile		
	Daily Max.	Daily Min.	Monthly (Av.)	Record Highest	Year	Record Lowest	Year		Speed	Direction	Year
JAN	60.3	40.5	50.4	86	1963	12	1963	9.9	47	N	1962
FEB	64.0	43.5	53.8	87	1962	22	1967	10.2	57	N	1947
MAR	70.6	48.7	59.7	96	1967	23	1962	10.9	44	W	1957
APR	78.0	57.3	67.7	98	1963	39	1962	10.9	44	NE	1957
MAY	85.2	64.9	75.1	99	1967	52	1968	10.2	47	NE	1946
JUN	92.0	71.7	81.9	100	1967	55	1964	9.6	49	SE	1956
JUL	95.1	73.9	84.5	103	1964	64	1968	8.7	43	S	1953
AUG	95.6	73.7	84.7	105	1962	61	1967	8.3	47	N	1959
SEP	89.7	68.5	79.1	102	1963	47	1967	8.0	45	NE	1961
OCT	81.9	59.5	70.7	95	1963	39	1966	8.1	47	NW	1967
NOV	69.6	47.9	58.8	89	1963	31	1966	9.1	48	NW	1951
DEC	62.8	42.6	52.7	84	1966	21	1966	9.2	49	NW	1956

between the bridge boundaries and the environment by radiation and convection. Heat, on the other hand, is transferred within the bridge boundaries by conduction.

Radiation is the primary mode of heat transfer which results in warming and cooling bridge surfaces. The top surface gains heat by absorbing solar radiation during the day and loses heat by emitting out-going radiation at night. The amount of heat exchange between the environment and the bridge boundaries depends on the absorptivity and emissivity of the surface, the surface temperature, the surrounding air temperature, and the presence of clouds. Values of absorptivity of a plain concrete surface depends on its surface color. In general, its values lie between 0.5 and 0.8. Concrete with asphaltic surface has higher absorptivity and published values are between 0.85 and 0.98. The emissivity, on the other hand, is independent of the surface color. Its value lies between 0.85 and 0.95. For steel, the absorptivity varies from 0.65 to 0.80, and the emissivity is between 0.85 and 0.95.

The two types of heat exchange by convection between bridge boundaries and the environment are termed free and forced convection. In the absence of the wind, heat is transferred from the heated surface by air motion caused by density differences within the air. This process is known as free convection. It is known that heat loss by forced convection is greater than by free or natural convection. Heat loss by convection from a dry surface is given as

$$Q_c = h_c (T_s - T_a)$$

where

Q_c = heat loss by convection, $btu/ft^2/hr$,

T_s = surface temperature, ^oF ,

T_a = air temperature, ^oF ,

h_c = convection film coefficient,

= $0.665 + 0.133u$, $btu/ft^2/hr/^oF$, and

u = wind speed, mph .

The effect of the wind on the loss of heat by convection is recognized in the film coefficient, h_c .

Heat is transferred within the bridge boundaries by conduction. The thermal conductivity, k , is a specific characteristic of the material. It indicates the capacity of a material for transferring heat. It has been shown that its magnitude increases as the density of the material increases. Normally, the average thermal conductivity of concrete and steel are 0.81 and 26.6 btu/hr/ft/^{o}F respectively. Whether the material is wet or dry affects the thermal conductivity. It has been shown that wet concrete has higher thermal conductivity than dry concrete.

Sensitivity Analysis of the Bridge Thermal Behavior

The significant factors that affect the bridge thermal behaviors are daily total insolation intensity, surface absorptivity, thermal conductivity, specific heat, unit weight, bridge geometry, the range of daily air temperature, and initial conditions.

Before the bridge temperature distributions can be predicted the initial condition must be specified. This condition includes the reference time and the initial temperature distribution. A study of a typical daily solar radiation and air temperature variation indicates that the temperature in a bridge will be relatively uniform early in the morning. At about two hours after sunrise, it is possible to assume a thermal equilibrium state in which the bridge temperature is the same as that of the surrounding air temperature. In this research, it has been found that different starting conditions, at about this time, do not have significant effects on the temperature induced stresses.

In order to study the significance of the other variables, temperature distributions and stresses were calculated using the data given in Table 3 for a concrete slab bridge having three equal spans. The predicted results are also listed in Table 3. By keeping the rest of the variables at their average values, one variable at a time was increased by 10 percent. A summary of comparisons is given in Table 4. It can be seen that the most significant factor with respect to the material thermal properties is the absorptivity of the surface to the solar radiation. Also of importance is the coefficient of thermal expansion and contraction, since the thermal induced stresses vary linearly with this variable. However, an

TABLE 3. SELECTED AVERAGE VALUES FOR THE SENSITIVITY ANALYSIS (AUGUST)

Average total insolation intensity	2380	btu/ft^2
Air temperature distribution	Fig 12a	
Wind speed	10	mph
Absorptivity of surface to solar radiation	0.5	
Emissivity	0.9	
Thermal conductivity	0.81	btu/ft/hr/°F
Specific heat	0.23	btu/lb/°F
Unit weight	150	lb/ft^3
Depth	17	inches
Modulus of elasticity of concrete	4.25×10^6	lb/in^2
Coefficient of thermal expansion	6.0×10^{-6}	in/in/°F

PREDICTIVE RESULTS (3-equal-span-bridge)

Maximum top surface temperature	120	°F
Maximum temperature gradient	30	°F
Maximum reverse temperature gradient	7	°F
Maximum tensile stress (bottom half)	239	psi
Maximum tensile stress (top)	318	psi
Maximum compressive stress (top)	818	psi
Maximum vertical deflection (downward)	0.125	inch
Maximum mean bridge temperature range	35	°F

TABLE 4. THE EFFECTS OF A 10% INCREASE IN ONE-VARIABLE AT A TIME ON TEMPERATURES AND STRESSES IN A THREE EQUAL SPAN CONCRETE SLAB BRIDGE (AUGUST)

	Temp. (top)	Temp. gradient	Tensile stress	Comp. stress	Reverse gradient	Tensile stress(top)	Vertical deflection	Mean bridge temp.
Average	0%	0%	0%	0%	0%	0%	0%	0%
Insolation	2.5	10	9.2	8.1	0	1.6	9.6	2.9
Absorptivity	2.5	10	9.2	8.1	0	1.6	9.6	2.9
Conductivity	-0.8	-3.3	-0.8	-3.3	0	-2.5	-0.8	0
Specific heat	-0.8	-3.3	-2.9	-0.1	0	-2.5	-2.4	-2.9
Density	-0.8	-3.3	-2.9	-0.1	0	-2.5	-2.4	-2.9
Wind speed	-0.8	-3.3	-2.1	-1.5	0	0	-2.4	0
Thickness	0	0	-0.8	3.3	0	-0.3	-11.2	-5.7
Range of air temperature	1.7	0	2.1	3.1	14.3	4.7	0.8	2.9
Insolation (Eq 3.1)	3.3	13.3	9.2	11.4	0	0.3	10.4	-0.3

increase in the thermal conductivity, specific heat and density reduces the temperature gradient and thus decreases the induced stresses.

With respect to the environmental variables, an increase in the solar radiation intensity and the daily air temperature range amplifies the predicted temperature gradient and the temperature induced stresses. An increase in the wind speed, on the other hand, decreases the computed results. Consequently, the extreme climatic condition is believed to take place on a still day with a maximum value of the solar radiation and a maximum range of daily ambient air temperature.

Extreme Summer and Winter Conditions

Although the maximum air temperature is found in August, a maximum solar radiation intensity is recorded in June. Therefore, in order to study the bridge thermal behaviors associated with summer daytime conditions, daily climatic changes in June, July, and August need to be investigated.

In this research, it has been found that the daily environmental variations in August are the extreme summer conditions for the city of Austin (Ref 39). The environmental data for these conditions are given in Fig 2 and Table 3.

In order to establish extreme environmental conditions for the rest of the state, the days having either a maximum solar radiation intensity or a maximum range of daily air temperature have been selected from the Weather Bureau Reports for the cities of El Paso, Midland, Fort Worth, San Antonio, and Brownsville. The maximum insolation values and ranges of daily air temperatures as recorded during the years 1961-1971 are given in Table 5 for these locations. For each selected day, the resulting environmental data have been input to the program TSAP so as to predict the thermal stresses in a typical slab bridge. The extreme climatic condition is then defined herein as the one which produces the maximum tensile stress in concrete.

The extreme summer conditions found in the cities of Midland, Fort Worth, and San Antonio produced thermal stress distributions approximately similar to those obtained from the conditions of the city of Austin. Therefore, the summer conditions given for Austin are applicable to these cities. On the other hand, the extreme summer conditions for both El Paso and Brownsville have been found to take place in the month of June and to produce different stress distributions. The recommended extreme summer conditions for these

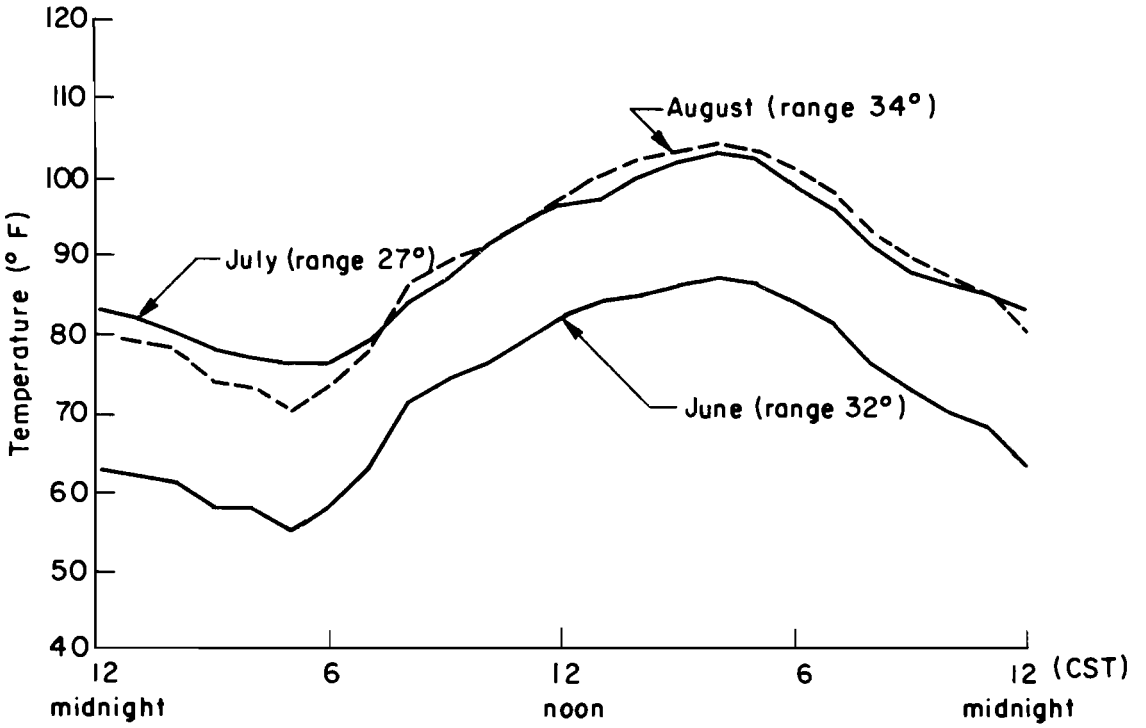

a) Summer

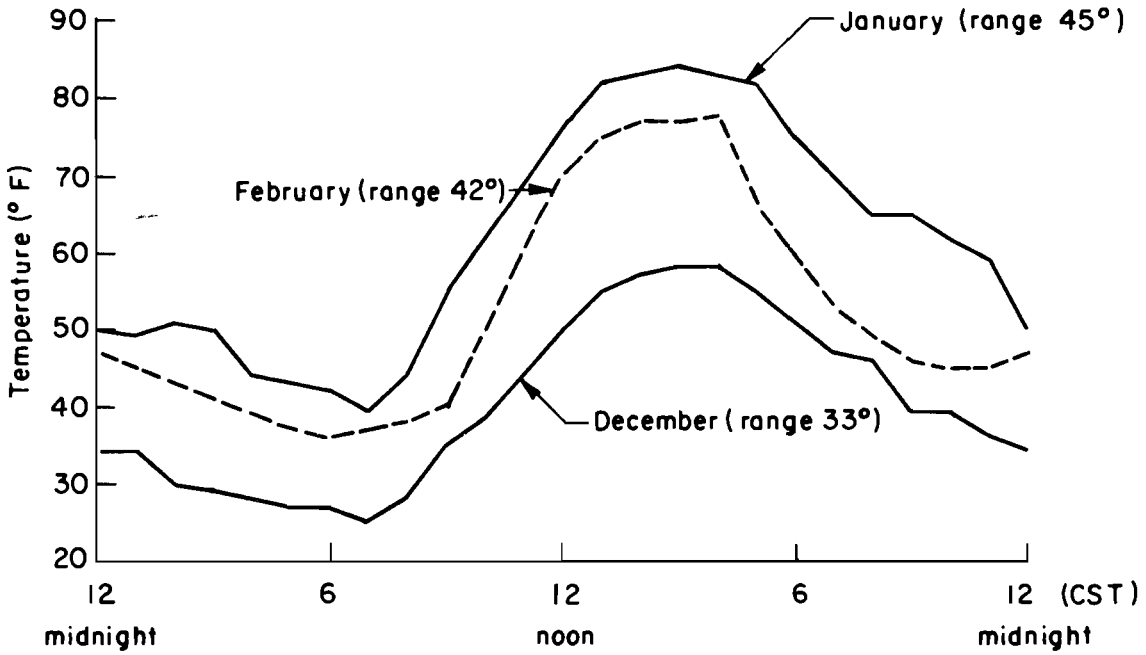

b) Winter

Fig 2. Hourly distributions of air temperature (Austin, Texas).

TABLE 5. CLIMATIC CONDITIONS IN THE STATE OF TEXAS AS RECORDED DURING THE YEARS 1961-1971 (SUMMER CONDITIONS)

City	Month	Maximum Daily Insolation, btu/ft^2	Maximum Range of Air Temperature, ^oF	Average Wind Speed, mph
Brownsville	June	3025	24	13
	July	2800	24	10.2
	August	2707	27	9
El Paso	June	3077	30	9.2
	July	2980	32	9.0
	August	2770	33	8.5
Fort Worth	June	2900	29	10.6
	July	2880	29	10
	August	2766	30	9.8
Midland	June	2870	30	10.0
	July	2860	32	9.8
	August	2680	35	9.0
San Antonio	June	2750	30	12
	July	2710	29	11.4
	August	2490	30	10.4

DAILY VARIATION OF AIR TEMPERATURE

	Time	06 a.m.	07	08	09	10	11	12 noon	13 p.m.	14	15	16	17	18
Brownsville (June)	^oF	76	79	83	89	90	91	92	92	92	92	91	90	88
El Paso (June)	^oF	55	63	70	77	85	89	90	92	94	95	93	92	91

cities are shown in Table 5. In the light of these investigations, El Paso has the most severe summer conditions in the state of Texas. Brownsville, on the other hand, is less severe because of the mild ocean climate.

In contrast to the summer conditions, large reverse temperature gradients occur during a still winter night with a maximum amount of outgoing radiation and a large range of air temperature. In view of these factors, the daily atmospheric variations in December, January, and February were investigated to study the extreme winter conditions. It was found that the daily environmental variations in January are the extreme winter conditions in the city of Austin (39). The extreme winter conditions found in the city of Austin are also recommended for the other locations in the state of Texas, because of the similar ranges of air temperatures and wind speeds recorded at the other cities.

As can be seen in the following sections, the extreme winter conditions gave the most severe thermal stresses only for slab bridge types. In composite bridges, on the other hand, winter conditions produced relatively small temperature effects compared to summer conditions.

Thermal Effect in Slab Bridges

Temperature induced stresses for a single span statically determinate bridge and statically indeterminate structures with two and three spans are shown in Fig 3. The stresses were computed at the section of symmetry of the bridge and the summer conditions of Austin were used. A maximum difference of 35° F is found between the top and the bottom temperature at 2:00 p.m. At this time, the top surface is approximately 20° F warmer than the air temperature. Figure 3(a) depicts the thermal stress distributions in a concrete slab bridge with a thickness of 17 inches. For the one-span case, compressive stresses predominate at the top as well as at the bottom surface with a maximum value of 460 psi at 1:00 p.m. A maximum tensile stress of approximately 180 psi, however, is predicted at the neutral surface of the section at 2:00 p.m. For the two- and three-span case, all sections below the neutral axis are subjected to tension with a maximum value of 330 psi located near the bottom surface at 4:00 p.m. At the top surface, on the other hand, a maximum compressive stress of 1000 psi was observed at 2:00 p.m. The length effect of the center span in the three-span case was also studied.

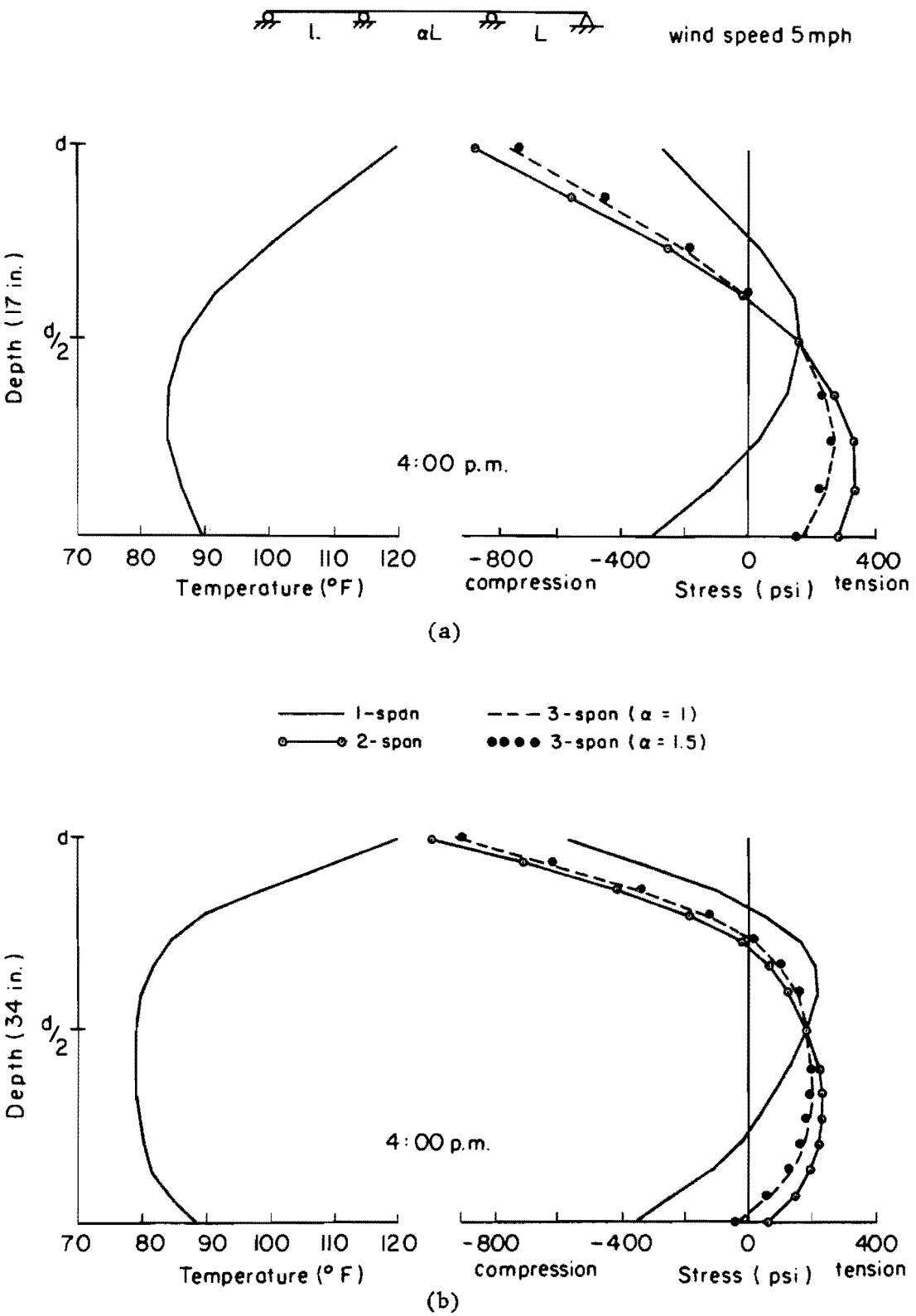

Fig 3. Temperature induced stresses for a one-, two-, and three-span bridge (August, Austin).

It is evident from Fig 3(a), however, that this parameter has an insignificant contribution on the state of stress. It is also of interest to note that all stress distributions coincide at mid-depth, i.e., the neutral surface of the section. This is due to the fact that the interior supports prevent only vertical movement of the bridge, thus affecting only the bending stress component.

Temperature and temperature induced stress distributions in a 34-inch concrete slab at 4:00 p.m. are shown in Fig 3(b). Although a lower magnitude of tensile stress is computed below the neutral axis, i.e., 230 psi, a higher compressive stress is predicted at the top surface with the maximum value of 1100 psi at 2:00 p.m.

Figure 4(a) depicts the temperature and thermal stress distributions in a 17-inch concrete slab due to the extreme summer conditions found in El Paso. A maximum tensile stress of approximately 410 psi is predicted near the bottom surface at 3:00 p.m. for the two-span case. At the top surface a maximum compressive stress of 1100 psi was found at 2:00 p.m. These stresses have larger magnitudes than those predicted for Austin. Figure 4(b) depicts the predicted thermal effects for the same slab bridge due to the summer conditions of Brownsville.

Figure 5, on the other hand, depicts the maximum reverse gradients and the associated stresses computed under winter conditions (39). Temperature and stress distributions over the depth of 17 inches are shown in Fig 5(a). A maximum tensile stress of 180 psi is found at the bottom surface in the one-span structure. At the top surface, however, the two-span case yields higher tensile stress with a maximum value of 400 psi. Similar forms of stress distribution are found in a deeper section, Fig 5(b). Higher tensile stresses, nevertheless, are predicted at the exterior surfaces, i.e., 490 and 250 psi at the top and bottom surfaces, respectively.

The above study (39) indicated that the temperature induced stresses in any statically indeterminate bridge will be bounded by the stresses computed from a one- and two-span case. An approximate analysis is given in Ref 39 in order to determine temperature effect in non-prismatic concrete slab bridges.

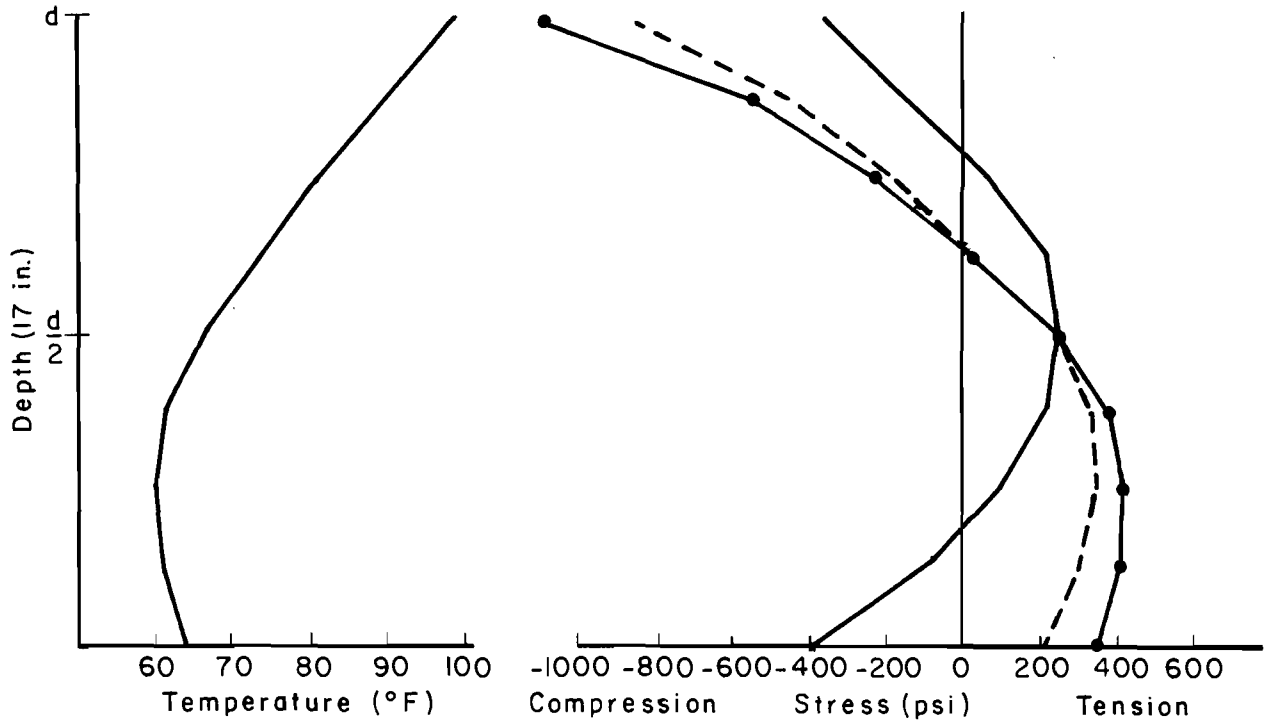

(a) El Paso - June

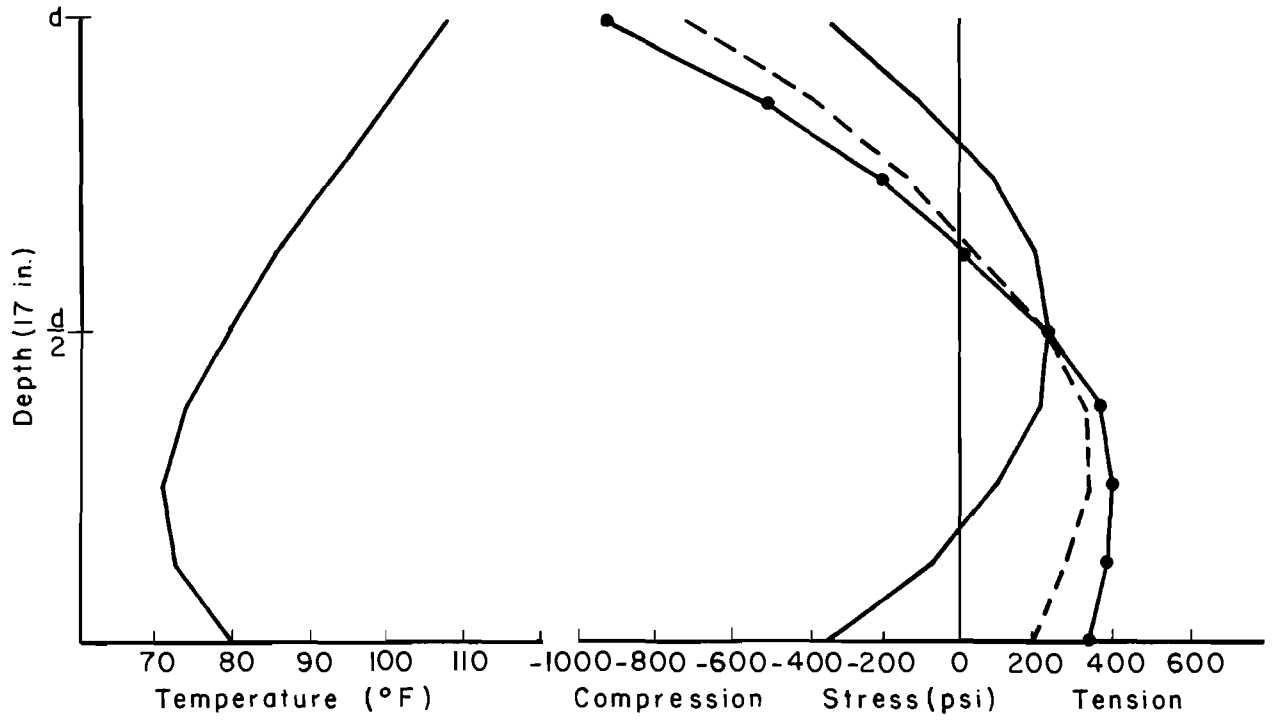

(b) Brownsville - June

1-span 2-span 3-span

Fig 4. Temperature induced stresses for a one-, two-, and three-span slab bridge with thickness of 17 in.

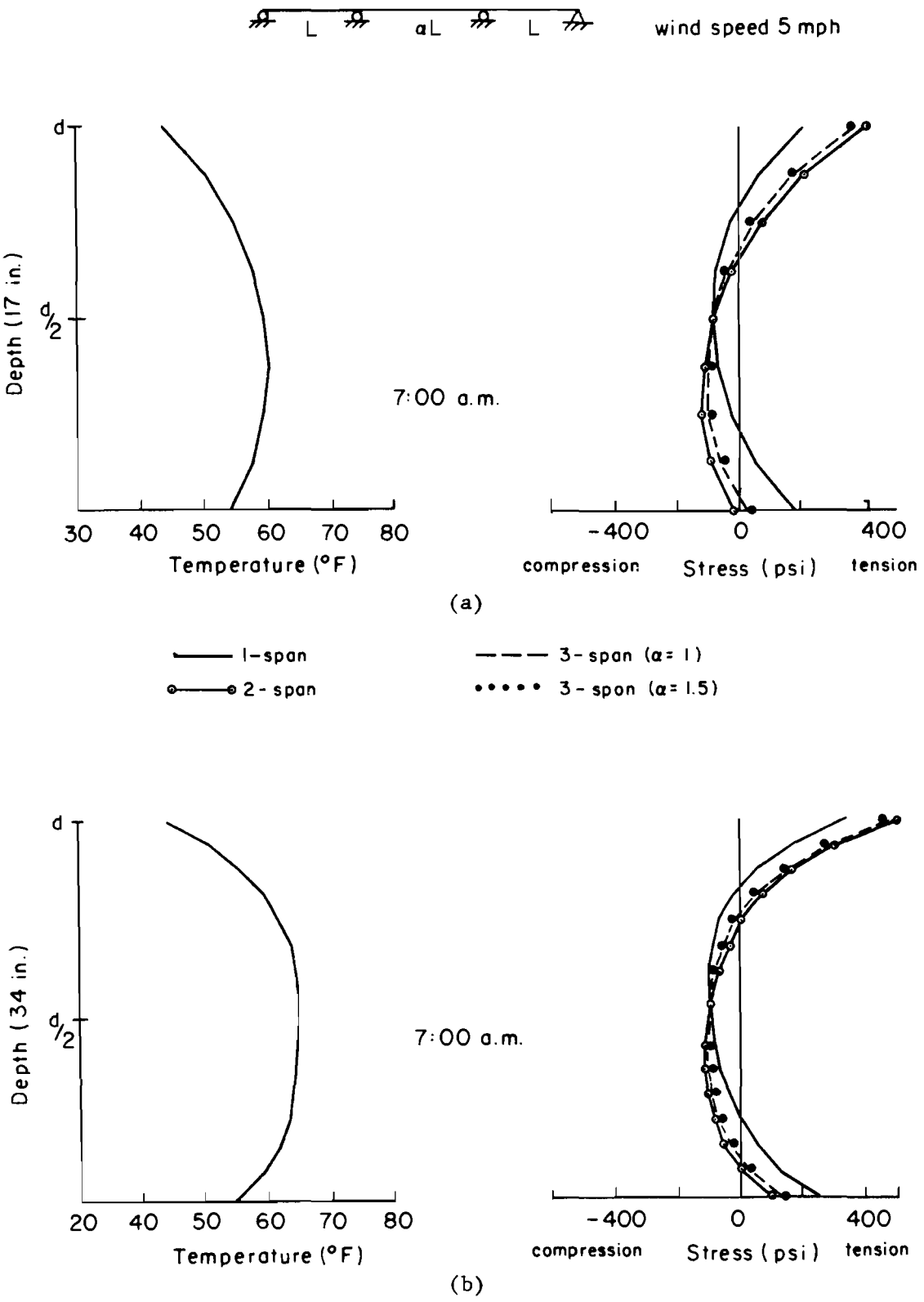

Fig 5. Temperature induced stresses for a one-, two-, and three-span bridge (January, Austin).

Thermal Effects in Composite Precast Pretensioned Bridges

A typical interior girder, Texas standard type-B, of a composite precast pretensioned bridge is shown in Fig 6. The bridge is made continuous for live load by placing reinforcing steel in the slab over the piers. The beam spacing is 8 ft center to center with a cast-in-place concrete slab 6.5 in. thick. The finite element mesh used by the TSAP program of Ref 39 had a total number of 90 elements with 117 nodal points. Triangular as well as rectangular elements are used to represent the true I-shape of the beam cross section. The concrete thermal properties which were used are given in Table 3. The compressive strength of the concrete slab and beam are 3000 and 6000 psi respectively.

Temperature distribution resulting from the TSAP program due to the summer conditions of Austin is depicted in Fig 7(a). Only a portion of the slab is included in Fig 7(a) because the temperature was found to be uniform over the rest of the slab. The top surface temperature at this time is about 20° F warmer than the surrounding air temperature. The temperature at the bottom surface of the slab is found to be warmer than the surface temperature along the side of the beam. This is as expected since additional heat energy is gained by conduction at the bottom slab surface while along the side of the beam heat exchange is taking place only by convection and radiation. At the center of the cross section, the temperature distribution over the depth shows changes in curvature; see Fig 8(a). This is due to the varying thickness of the precast beam. A thinner section will, of course, have higher temperature than a thicker section, thus explaining the increase of temperature at the middle portion of the beam. A temperature difference as high as 9° F occurs between the exterior and the interior face at the bottom portion of the beam. Figure 7(a) also shows that although temperature distribution in the slab varies constantly in the transverse direction, temperature distribution in the beam, on the other hand, varies nonlinearly in both the vertical and transverse directions. The predicted maximum temperature gradient is 27° F and takes place at 2:00 p.m.

At 3:00 p.m., the longitudinal thermal induced stresses calculated at the center of the middle span of the three-span bridge are shown in Fig 7(b). The stress distribution varies considerably over the cross section. High tensile stresses are found near the bottom portion of the beam with a maximum value of 465 psi at six inches above the bottom surface of the beam. At the

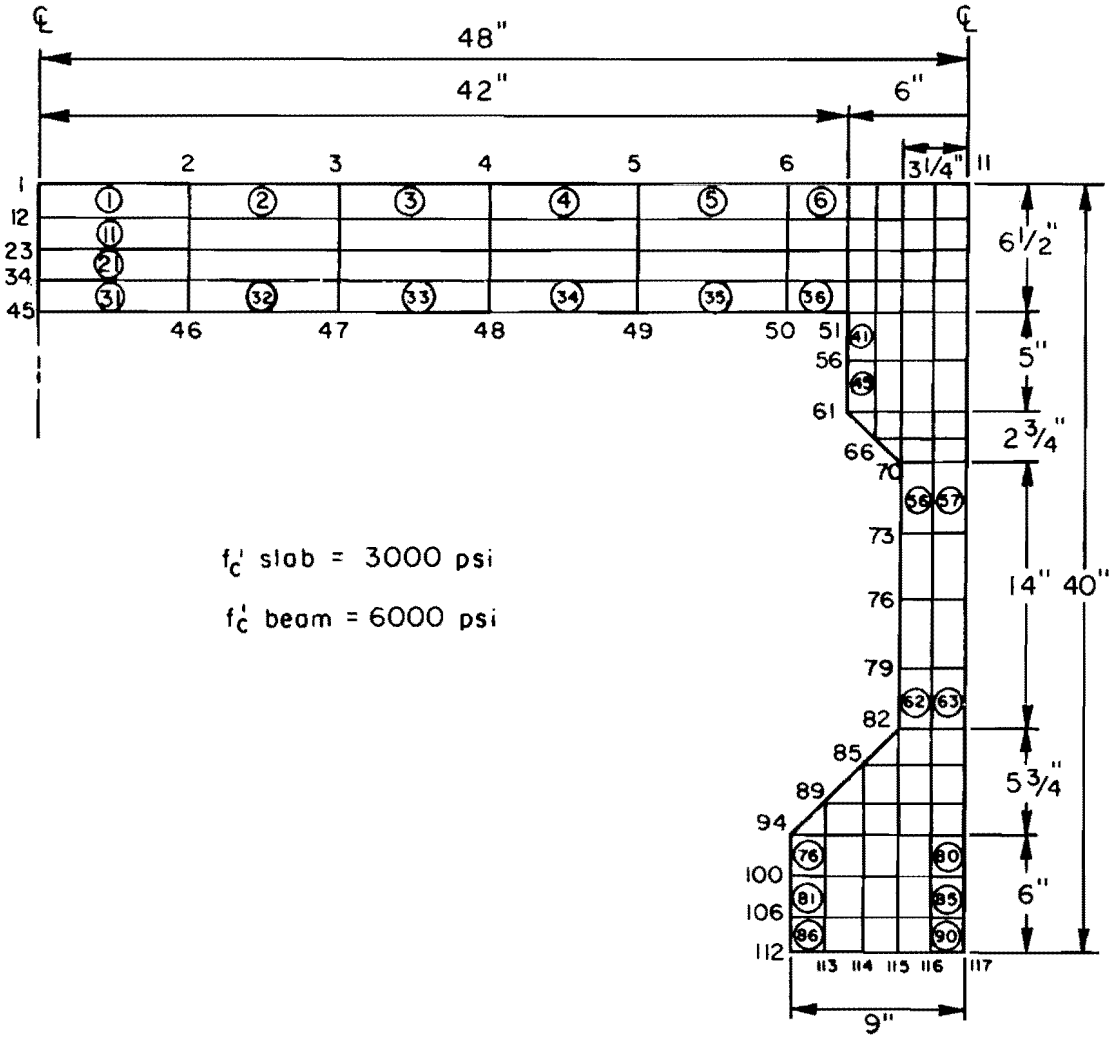

Fig 6. Typical interior girder idealization of a composite precast pretensioned bridge (Texas standard type B-beam).

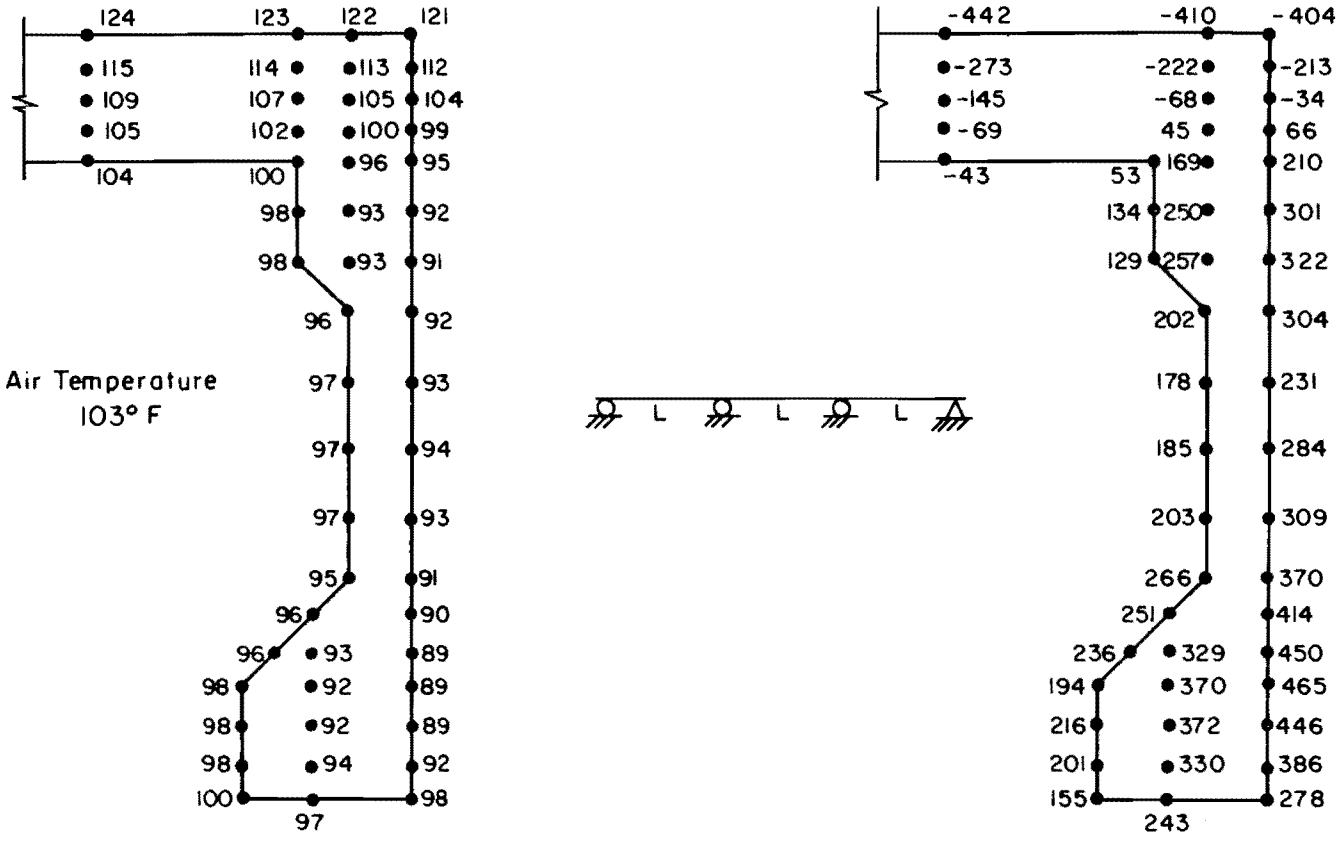

(a) Temperature distribution (°F)

(b) Stress distribution (psi)

Fig 7. Temperature and stress distributions (August, Austin).

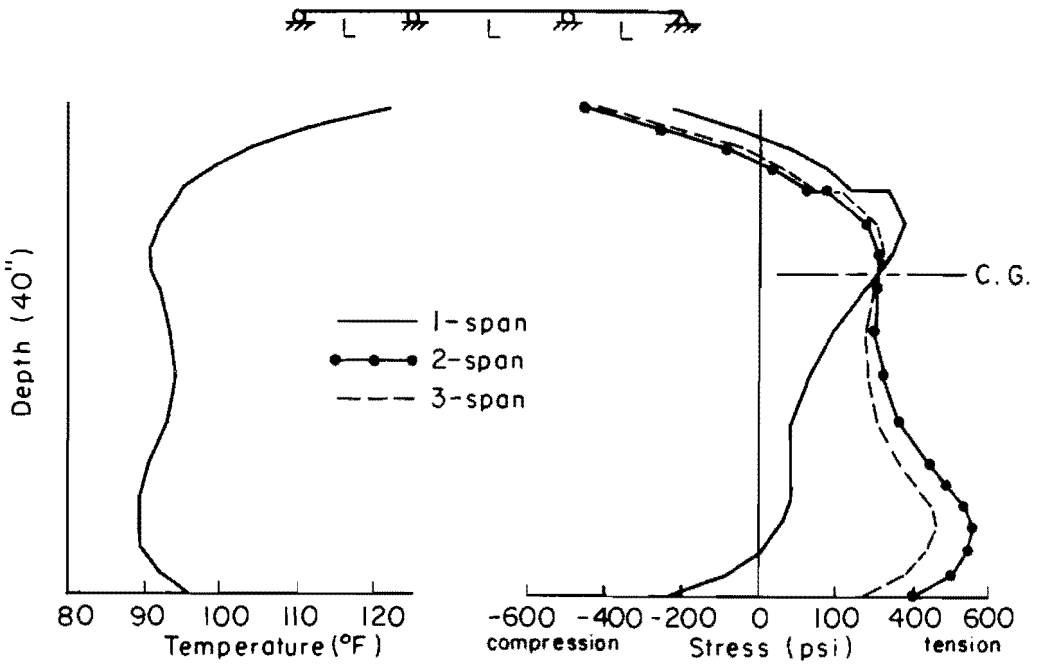

(a) August

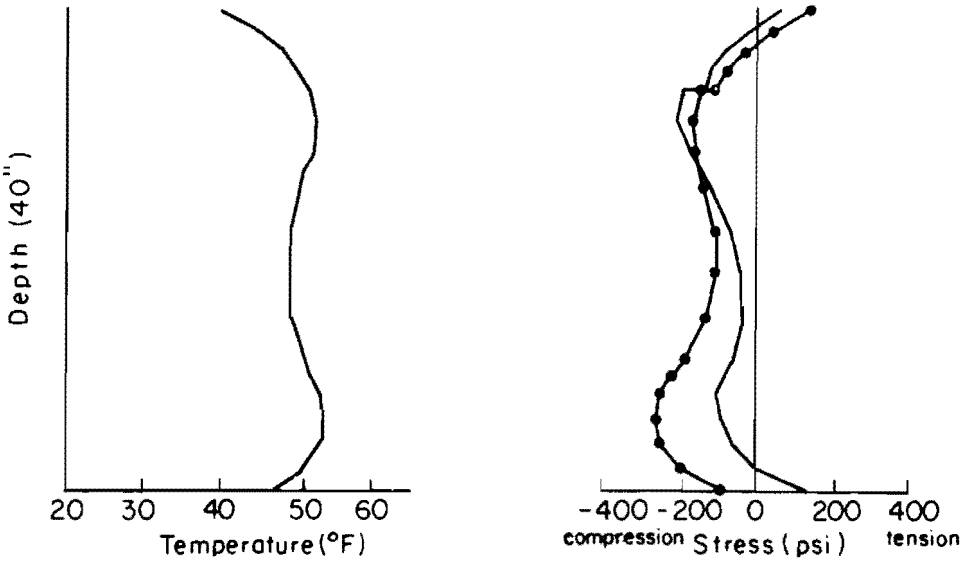

(b) January

Fig 8. Temperature and stress distributions at the section of symmetry (Austin).

same level on the exterior face, a tensile stress of only 194 psi is given. Maximum compressive stress of 477 psi, however, takes place at 2:00 p.m. and is found at the top surface of the slab. Figure 8(a) depicts temperature stresses induced in a one-, two-, and three-span bridge. In each case the individual spans have the same length. The difference in stress distribution, caused by the indeterminacy of the bridge, is noteworthy. For the one-span case, a maximum tensile stress of 380 psi is calculated at a location close to the neutral surface of the section. Compressive stresses predominate at the top as well as at the bottom surface. Larger tensile stresses, on the other hand, are found near the bottom portion of the beam in the two- and three-span cases. These high stresses were anticipated since the neutral surface of the composite section is located high in the upper portion of the beam causing thermal bending stresses to be large in the bottom region.

The temperature distribution and temperature induced stresses resulting from the summer conditions of the city of El Paso are shown in Fig 9(a). The predicted maximum temperature gradient is 31° F and takes place at 2:00 p.m. A maximum tensile stress of 810 psi is found near the bottom of the beam at this moment. This is also the maximum value of temperature induced tensile stresses found in this composite bridge type in the state of Texas. A maximum compressive stress of 620 psi takes place at 1:00 p.m. and is found at the top of the slab. Temperature effects resulting from the summer conditions of Brownsville are depicted in Fig 9(b). In this study it was found that the days having relatively larger values of daily solar insolation give the most critical temperature induced stress distributions in composite bridges.

Temperature distribution at 7:00 a.m. on a cold sunny day, in the month of January, is shown in Fig 10(a). Again, a temperature difference as high as 9° F is observed between the exterior and the interior face at the bottom portion of the beam. The maximum temperature gradient is found to be 7° F. The temperature induced stresses in a simply supported bridge is shown in Fig 10(b). Tensile stress of 239 psi is found at the bottom surface of the beam on the exterior face. Figure 8(b) depicts temperature and stress distributions over the depth of the composite section. Tensile stress of 148 psi is found at the top surface at section over interior support in the two-span case.

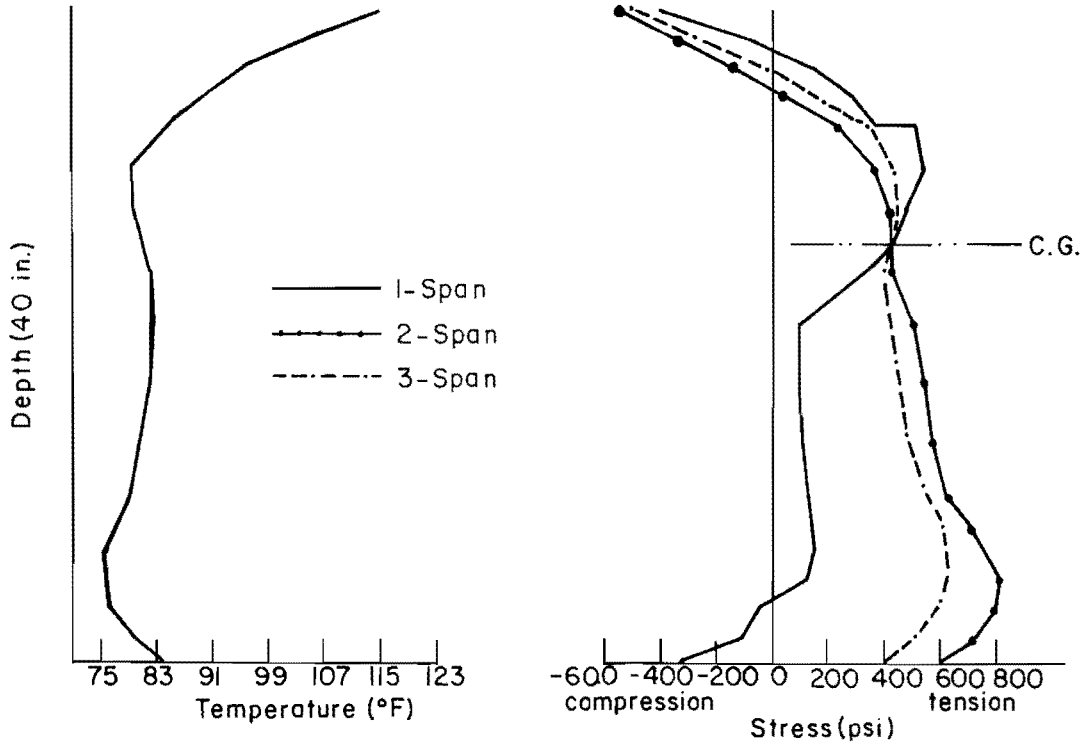

(a) El Paso

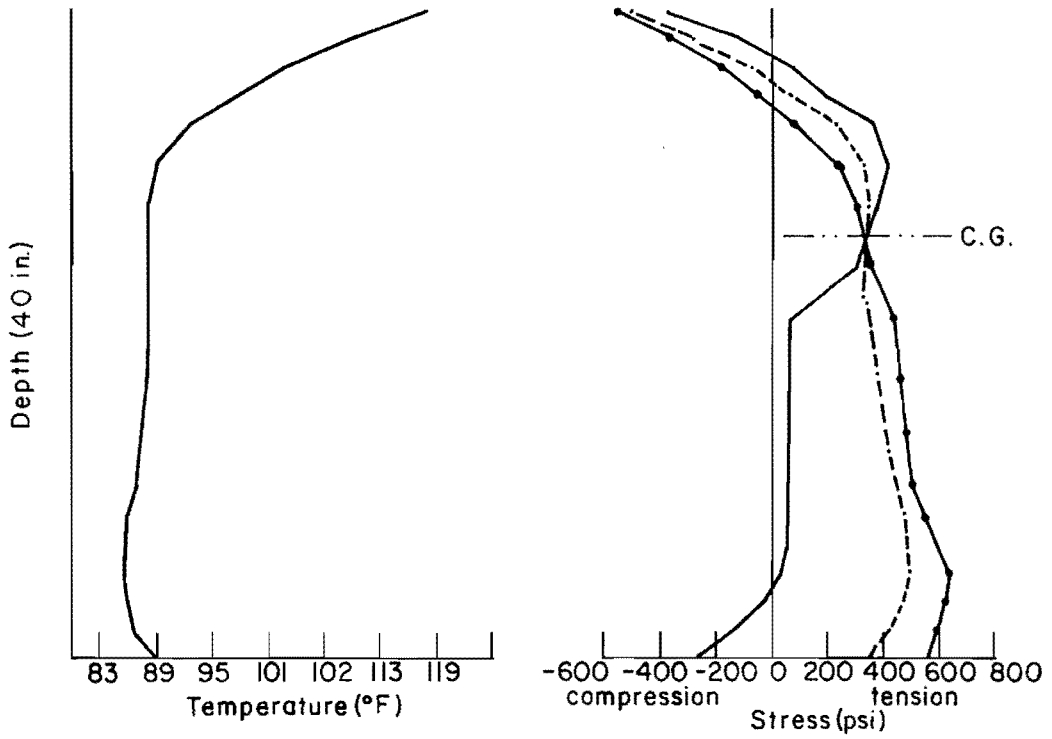

(b) Brownsville

Fig 9. Temperature and stress distributions at the section of symmetry.

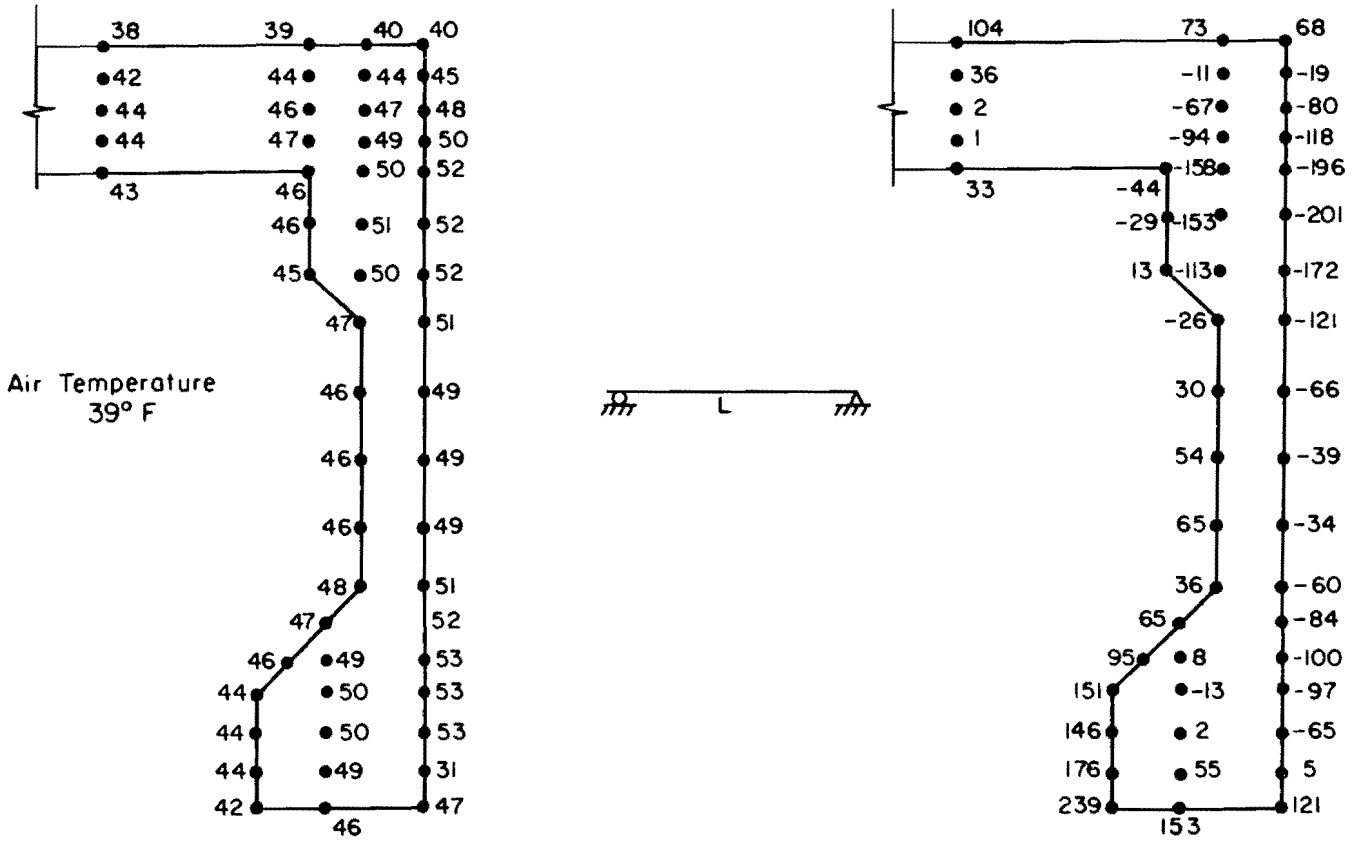

(a) Temperature distribution (°F)

(b) Stress distribution (psi)

Fig 10. Temperature and stress distributions (January, Austin).

Thermal Effects in Composite Steel Bridges

Figure 11 depicts the idealization of a typical interior composite steel beam. A total number of 46 rectangular elements with 71 nodal points were used. The compressive strength of the concrete slab was assumed to be 3000 psi. Its average thermal properties are listed in Table 3. The modulus of elasticity of the steel girder was taken to be 29×10^6 psi with a density of 490 lb/ft^3. The average thermal properties of structural steel are

coefficient of thermal expansion	6.5×10^{-6}	$in/in/^oF$
thermal conductivity	26.6	$btu/ft/hr/^oF$
specific heat	0.11	$btu/lb/^oF$

Figure 12(a) shows predicted surface temperature distributions on a warm sunny day in August (Austin). It is found that the maximum temperature differential through the depth of the bridge occurs at 2:00 p.m. and is 22^o F. In addition, the top surface temperature is about 21^o F warmer than the surrounding air temperature. Reference 48 reported this value to be 20^o F to 30^o F depending on the color of the concrete surface. The bottom flange temperature is very close to the air temperature. This is due to the steel's high conductivity. It is observed that in the late afternoon and during the night, the bottom flange temperature is warmer than the air temperature.

Although a maximum temperature gradient occurs at 2:00 p.m., the maximum tensile stress in the steel beam is found to take place a few hours later. Consequently, it is the shape of the temperature distribution over the cross section and not necessarily the highest thermal differential between the top and bottom surface that induces the highest internal thermal stress. Temperature distribution at 6:00 p.m. is shown in Fig 12(b). As is anticipated, bottom slab temperature affects the temperature at the top of the steel beam. Temperature distribution in the concrete slab is nonlinear, while a uniform gradient is found over a large portion of the steel beam. Stress distributions at the section of symmetry in a one-, two-, and three-span bridge are also presented in Fig 12(b). For the three-span case, maximum induced tensile stress in the beam is about 1000 psi. Maximum compressive stress, however, is 330 psi at the top of the concrete slab and occurs at 2:00 p.m.

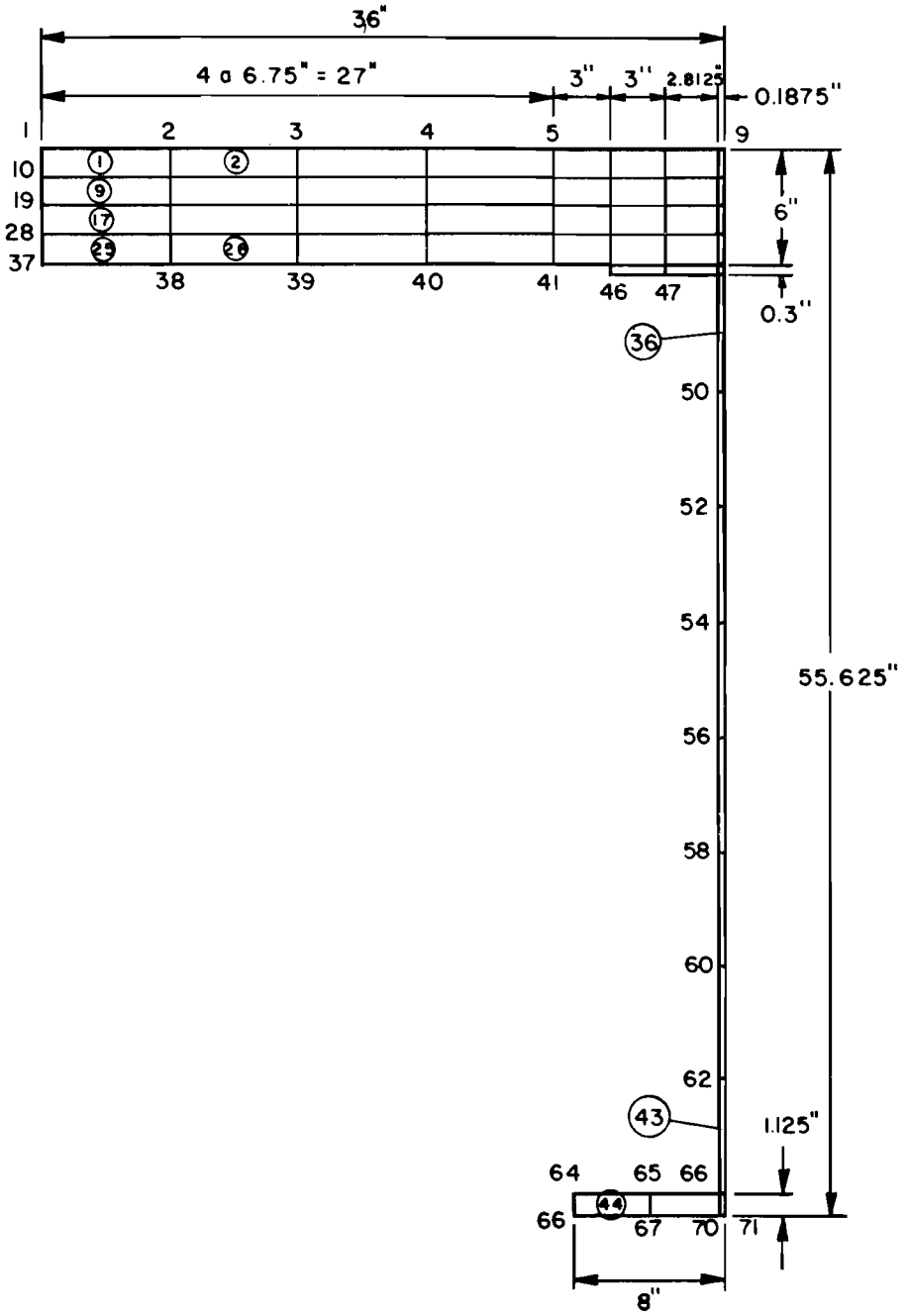

Fig 11. Typical interior girder idealization of a composite steel bridge.

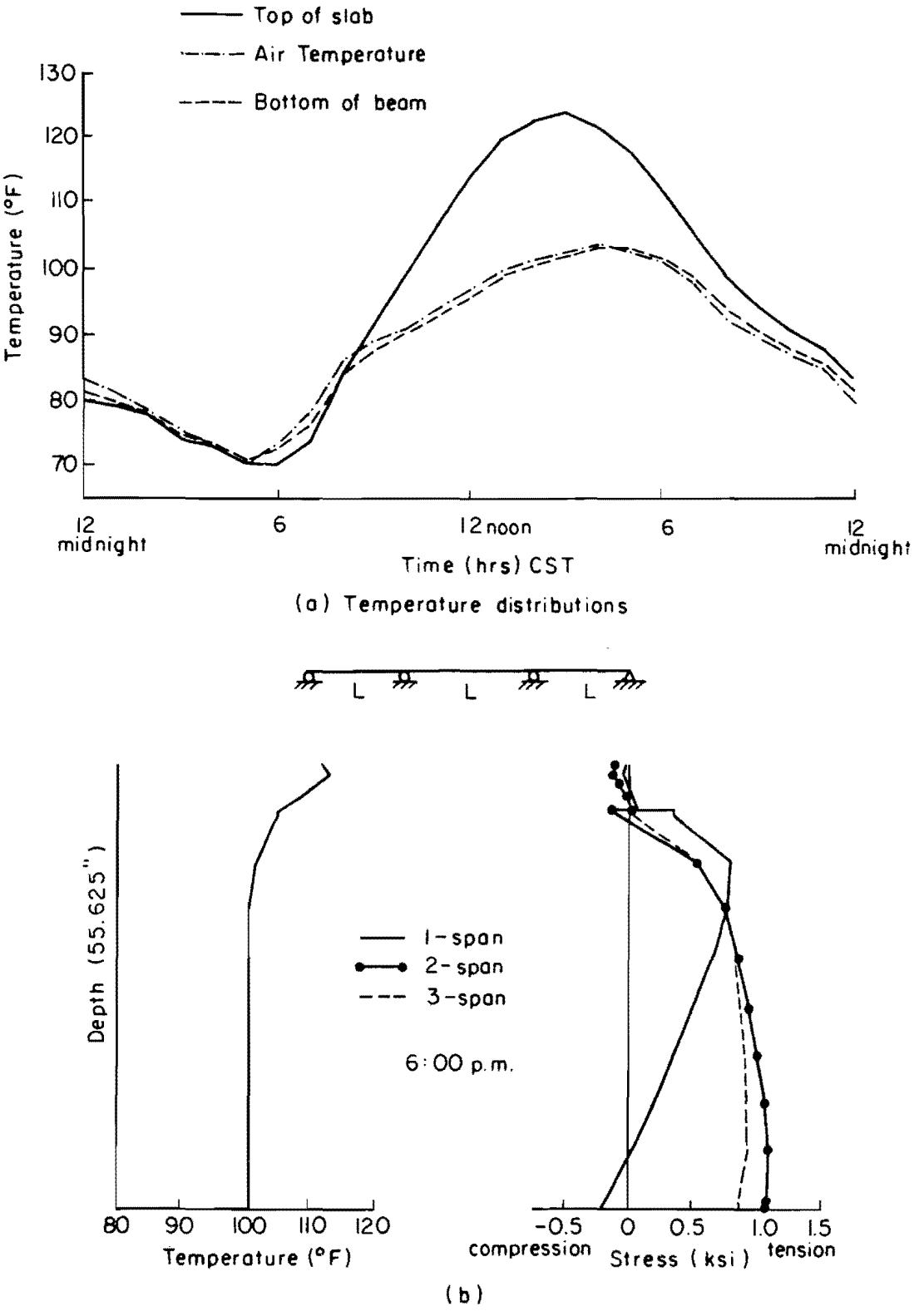

Fig 12. Temperature and stress distributions at the section of symmetry (August, Austin).

Because of the steel's high conductivity which is approximately 30 times that of concrete, the steel beam will have rapid responses to air temperature. The critical environmental conditions would, therefore, take place during a hot sunny afternoon followed by a quick drop of air temperature. Figure 13(a) depicts two kinds of daily air temperature distribution. Curve A represents a normal increase and decrease of air temperature. Curve B represents a normal increase up to the maximum value and a sudden decrease of air temperature of 10° F during the next hour. Temperature and stress distributions throughout the depth are shown in Fig 13(b). It can be seen that thermal induced stresses in case B are about twice as much as stresses induced in case A. Maximum tensile stress of 1910 psi is found at the bottom portion of the steel beam. For an A36 steel beam, stress induced by temperature will be about 10 percent of the allowable stress. This temperature stress is, however, less than the AASHO allowable 25 percent overstress for group loadings, Section 1.2.22.

Surface temperature distributions of a typical interior beam during a cold sunny day in January (Austin) are shown in Fig 14(a). In contrast to the hot sunny afternoon, the top slab temperature is only 10° F warmer than the air temperature. This is due to the lower value of solar radiation intensity in winter than in summer. Temperature variation at the bottom flange of the beam again follows the same trend as that of air temperature. The maximum reverse temperature gradient is found to be 5° F and takes place at 9:00 a.m.

Temperature and stress distribution at 11:00 a.m. are shown in Fig This is the time at which the maximum compressive stress is induced in the beam. For a two-span bridge, a compressive stress of 1750 psi is found at the bottom portion of the steel beam at the section over the interior support.

With regard to longitudinal movements, it is found that the range of the rise and fall of the bridge temperature from an assumed temperature, 60° F, at the time of erection is 45° F. This is the same range of mean bridge temperature found in the prestressed composite bridge discussed earlier.

Interface Forces

In composite bridges, the ends of the beam are subjected to special shear forces due to temperature difference between the slab and the beam. Interface shear forces are computed by integrating temperature stresses over the slab

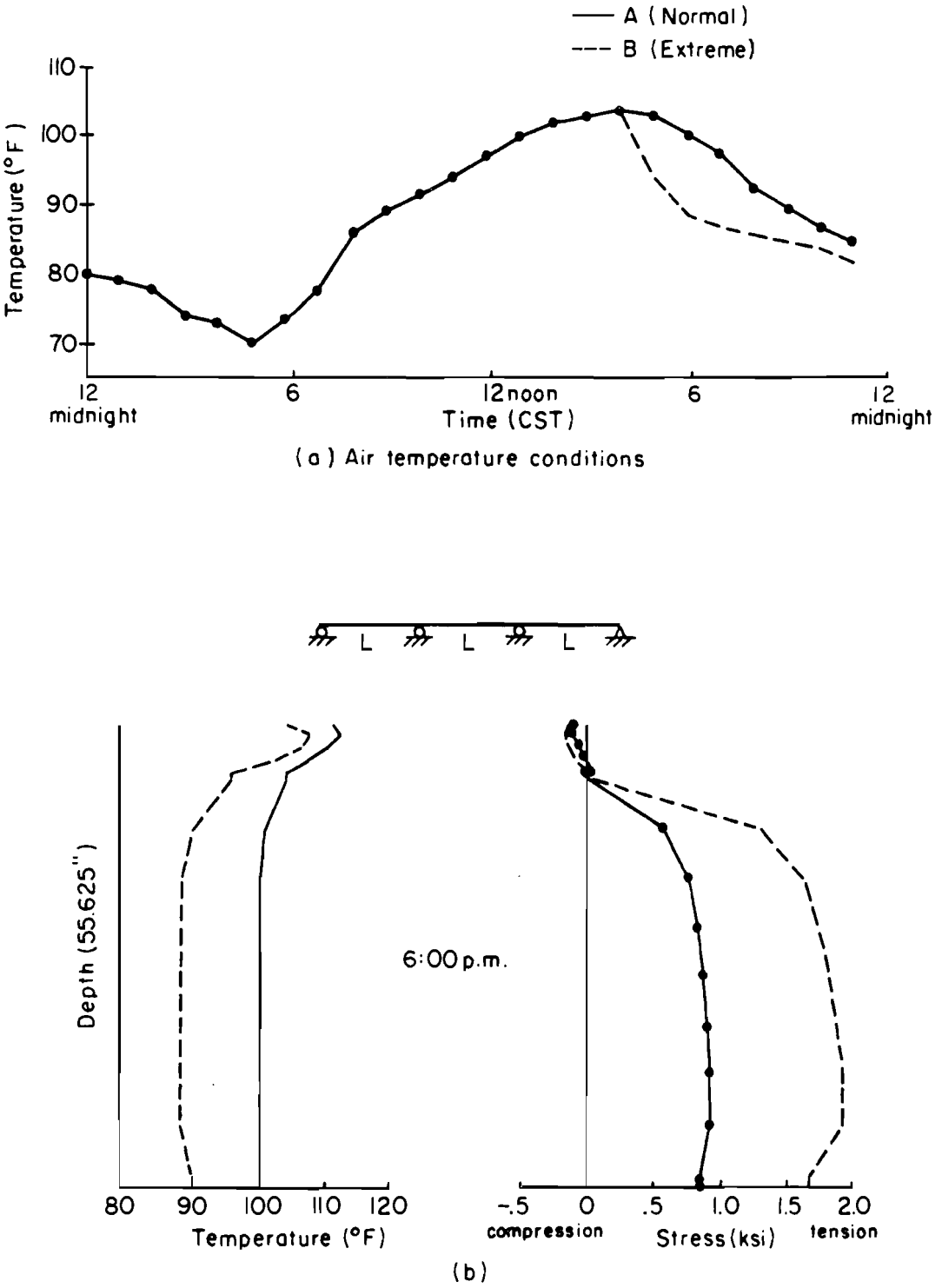

Fig 13. Temperature and stress distributions at the section of symmetry (August, Austin).

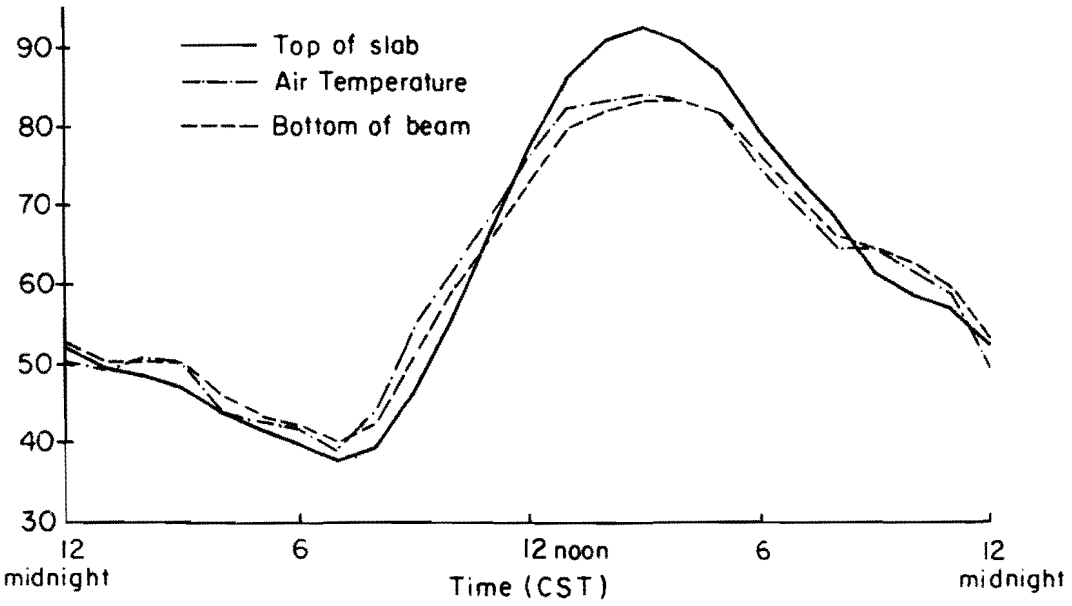

(a) Temperature distributions

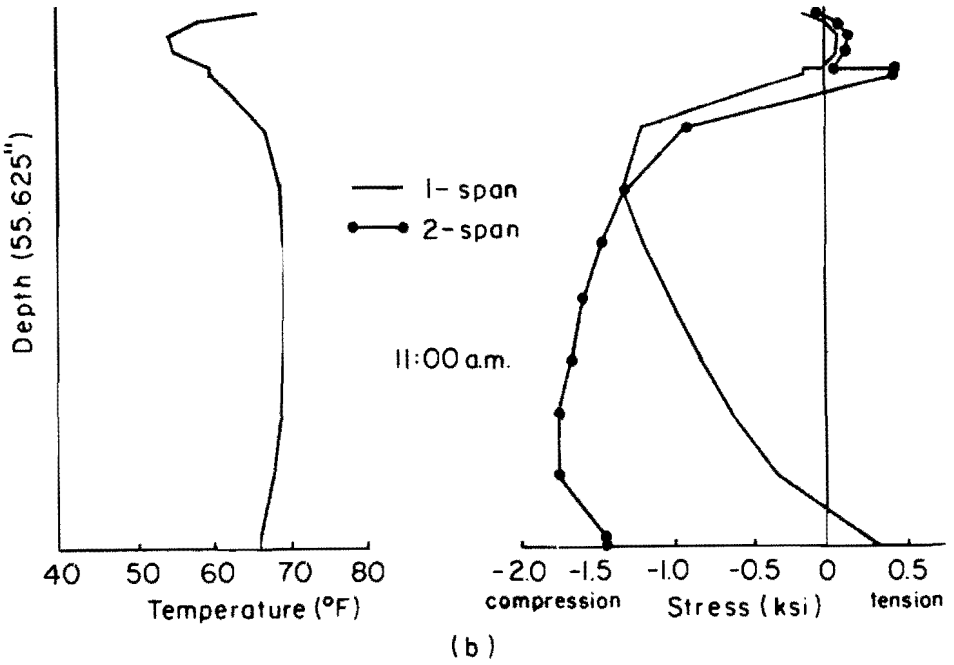

(b)

Fig 14. Temperature and stress distributions at the section of symmetry (January, Austin).

cross section in the single span case. Since these shear forces result from the strain compatibility requirements, their magnitudes are, therefore, independent of the presence of interior supports.

According to the analyses given in Ref 39, temperature induced interface shear force will require additional shear connectors of approximately 50 percent of that required by the design load over the length of the effective width of the slab for both composite bridge types discussed previously.

Effects of Longitudinal Restraining Forces on Temperature Induced Stresses

In the preceding studies, the stresses were calculated based on the assumption that the bridge was unrestrained longitudinally. In general, as a thermal movement occurs, restraining forces are developed at the supports, thus yielding another set of stresses. For a friction bearing, the translational force will be transmitted directly to the support until the magnitude of thermal force equals μR, where μ is the coefficient of friction which normally depends on the type of the bearing, corrosion of the bearing, etc. The reaction R must also include the additional reaction change caused by a temperature differential in the bridge. According to the analyses given in Ref 39, the stresses caused by restraining forces have been found to be insignificant.

Effects of Skew and Transverse Behavior

The thermal stresses in bridges presented in the previous discussions were computed by using the program TSAP. As mentioned previously in this program, the thermal stress analysis is based on the one-dimensional beam theory and is therefore limited to straight bridges with orthogonal supports. In order to investigate the effect of skew and transverse behavior on thermal stresses, a three-span bridge, shown in Fig 15(a), was analyzed by using the three-dimensional program SHELL8. The computed thermal stresses for the skewed case (with a skew angle of 30 degrees) and the non-skewed case were then compared to those obtained from the stress analysis of TSAP.

The results of this investigation are summarized in Figs 15 and 16. In this study, only the stresses acting in the longitudinal direction of the bridge are considered since these stresses have the same direction with those caused by design loads. The thermal stresses acting in the transverse direction of the bridge were either equal or smaller in magnitude than the ones acting in the longitudinal direction.

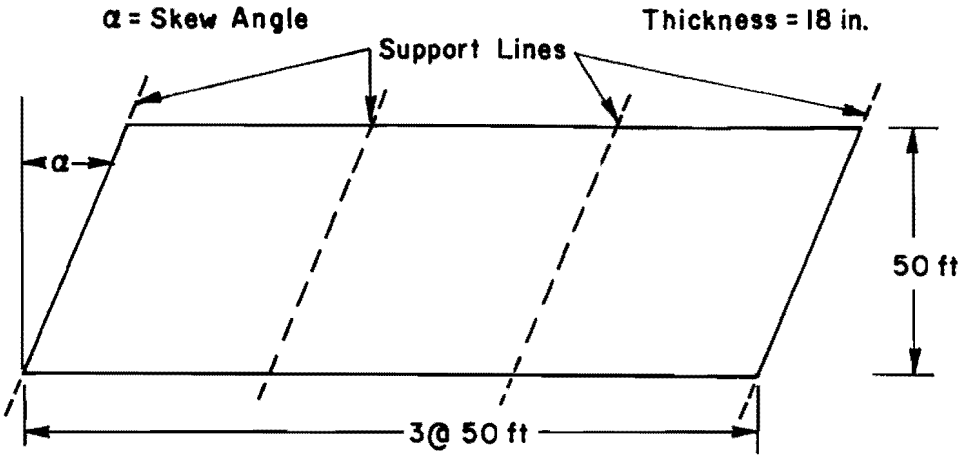

(a) Plan view of the bridge

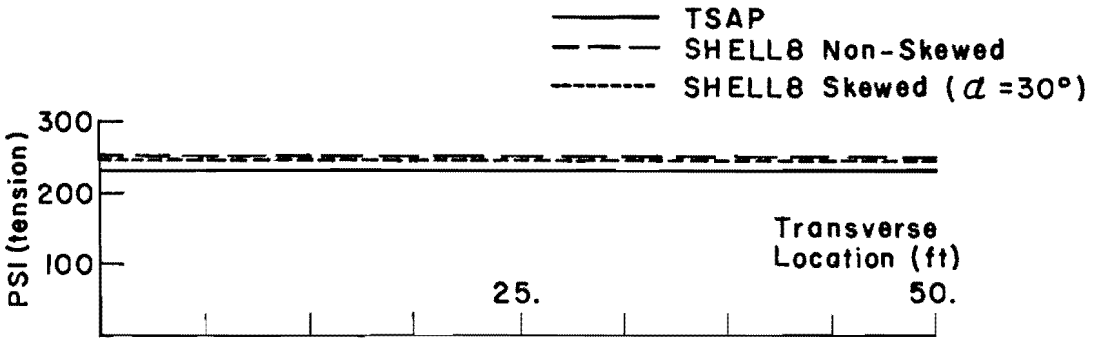

(b) Tensile stresses along the neutral surface

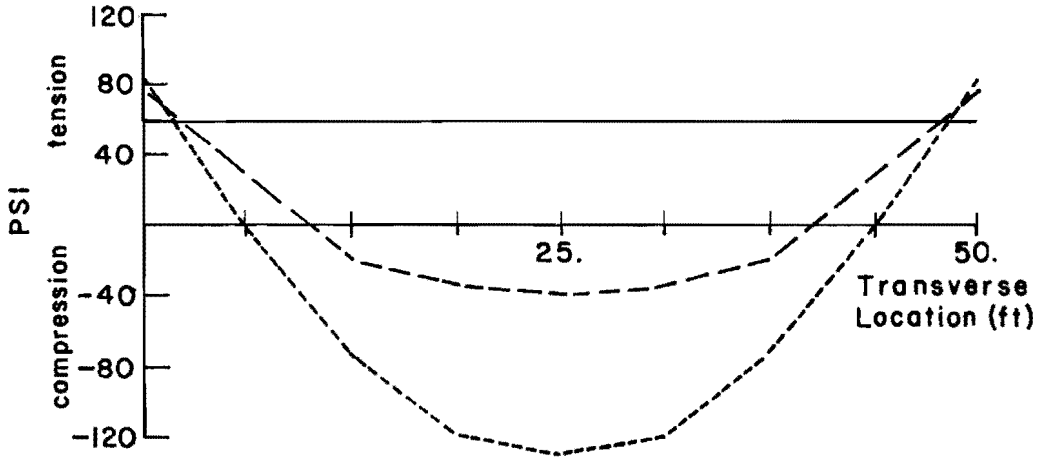

(c) Bottom fiber stress distribution along the center of the interior span

Fig 15. Effect of skew and transverse behavior.

(All stresses are acting in the direction parallel to the longitudinal direction of the bridge).

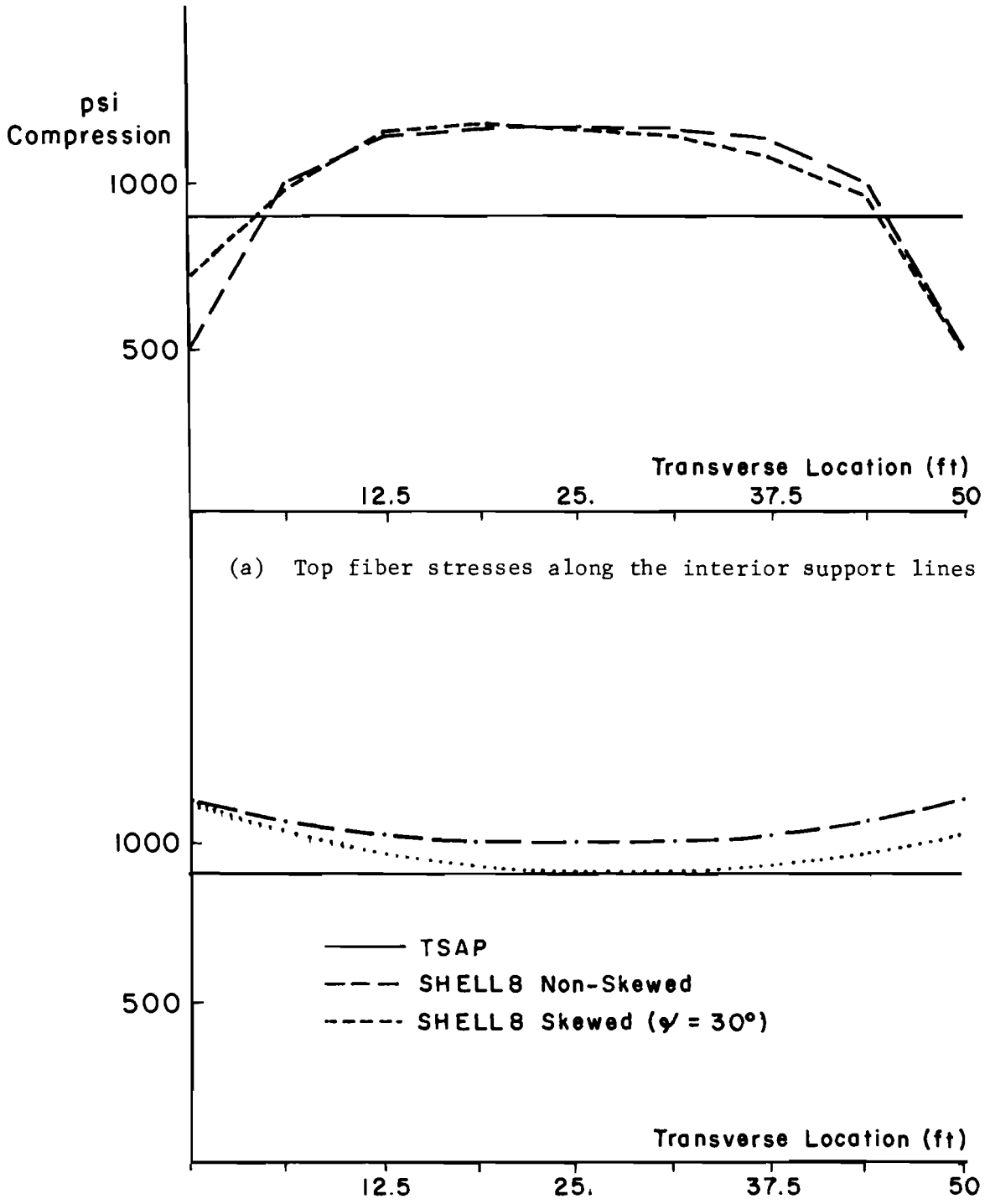

(a) Top fiber stresses along the interior support lines

(b) Top fiber stresses along the center of the interior span

Fig 16. Effect of skew and transverse behavior.

(All stresses are acting in the direction parallel to the longitudinal direction of the bridge.)

The tensile stress on the neutral surface of the bridge (Fig 15(b)) was 236 psi from the one-dimensional analysis and 250 psi from the three-dimensional analyses for both skewed and non-skewed cases. Tensile stress was not magnified at any location by skew and transverse behavior except there was a 15 percent increase near the sides of the bridge at the center of the interior span as shown in Fig 15(c). Also, as seen in Fig 15(c), along the interior part of this section, bottom fiber longitudinal stresses were compressive instead of being tensile as predicted by the one-dimensional analysis. Since the design stresses are generally tensile in this case along the bottom of this section, this reversal in the sign of stress should not have any practical implications.

The longitudinal stress distribution along the top fibers of the interior support lines is shown in Fig 16(a). As seen from this figure, there is a 28 percent magnification in the compressive stress at the middle of this section. This magnification of stress may partially result from the displacement constraints imposed on the bridge by the interior support lines. Without these constraints, the bridge under thermal effects would have double curvature and the interior support lines would lift up vertically. Due to transverse curvature of the bridge surface, the center of the support line would lift up more than its sides. When the support constraints are applied to the bridge, the interior support lines are pulled down to have no vertical displacement. Since the middle is pulled down more than the sides, the resulting compressive stresses are maximum at the middle and minimum at the sides of the support lines as in Fig 16(a). Figure 16(b) depicts the distribution of longitudinal stresses along the top fibers at the center of the interior span. There is a 22 percent magnification in compressive stress at the side of the bridge at this location for both skewed and non-skewed cases.

The results of this investigation indicate that thermal tensile stresses were magnified by less than 15 percent by skew and transverse behavior at only a very limited number of locations on the bridge. The thermal compressive stresses, however, were magnified by 28 and 22 percent at the middle of the interior support lines and at the side of the bridge at the center of the interior span, respectively. The thermal compressive stresses were magnified by less than 22 percent elsewhere on the bridge. Although these results were limited to a three-span slab bridge, the investigator believes that a slab bridge which would have the maximum ratio of the transverse bending rigidity to the longitudinal one, compared to the other bridge types, should demonstrate the effect of skew and transverse behavior effectively.

CHAPTER 3. CORRELATION OF FIELD MEASUREMENTS AND COMPUTER ANALYSES

Field measurements were performed on two bridges. The first bridge tested was the same one tested by Matlock and co-workers (30) for the live load effect. The second bridge tested was a two-span continuous for live load pedestrian overpass. As previously stated, it was not within the intended scope of this study to perform extensive field tests nor to use elaborate instrumentation. Only selected measurements were taken to validate the computational procedure. These measurements were divided into two categories: the first containing those measurements necessary to determine the surface temperature distribution (top and bottom of section), and the second containing those measurements necessary to determine the thermally induced movement of the structure at various locations. The first category, field measurements and surface temperatures, was required to predict the temperature distribution over the depth of the bridge section for computer simulation by TSAP and SHELL8. The second category was merely used for correlation with results from the computer simulation.

Instrumentation to Determine Bridge Temperature Distribution

Six mechanical surface thermometers manufactured by Pacific Transducer Corporation were acquired for evaluation purposes. The accuracy of the thermometers was found to be insufficient for this study. In addition, the thermometers were not practical for measuring the surface temperatures under the bridges.

A portable temperature probe was developed utilizing a temperature sensor gage. This gage is commercially available and is configured like a strain gage. The strain gage indicator was connected to the contact head containing the temperature sensor gage by wires running along the length of the pole. By adjusting the length of the pole, a practical method of determining the temperature on the bottom surfaces was achieved. Plan and elevation views of the probe are shown in Fig 17.

Two different pyranometers were used to measure the solar radiation. Both the Eppley pyranometer and the Casella pyranometer measured the global

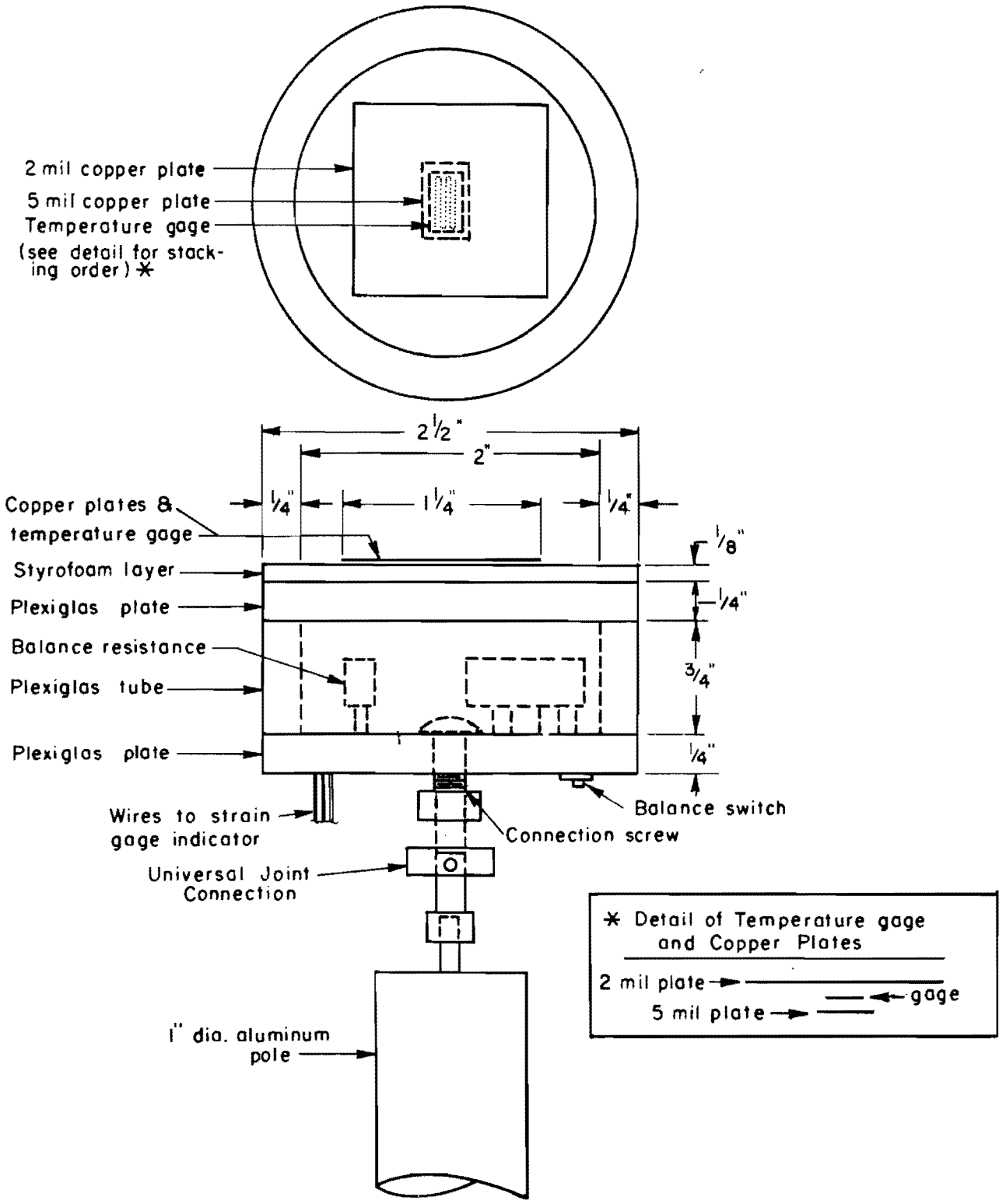

Fig 17. Temperature probe used to measure surface temperature.

radiation on a horizontal plane, i.e. the total of the direct, diffuse, and reflected radiation. Solar radiation measurements observed during one of the field tests were used by Thepchatri (39) to predict the surface temperatures and to compare them with measured quantities. This prediction of the surface temperatures also required the air temperature and wind speed measurements during the first test.

Instrumentation to Measure Bridge Movement

A mechanical inclinometer had been developed by Matlock and co-workers (30) to measure slope changes on a bridge tested for live load effects in Pasadena, Texas. Basically, the inclinometer measures the change in elevation between pairs of ball bearing test points that are cemented to the bridge deck at 24-inch spacings. The slope between the two points is then computed by dividing the difference in elevation between the two points by the length of the inclinometer, 24 inches. Slope changes are computed by subtracting a reference slope from any other reading.

The inclinometer which was used and a typical ball point are shown in Fig 18. The inclinometer has two steel feet in line with the level bubble, one with a V-grooved foot and the other the flat end of a micrometer screw. The lateral support six inches to the side of the longitudinal axis has a circular hole in the bottom of the foot to seat on auxiliary points. This provides for precise repositioning of the inclinometer during later readings. The ball points are cemented to the bridge deck using a quick setting epoxy cement. An aluminum template is used to accurately position the four ball points required at each station while they are being cemented.

Each slope reading was taken using two observations of the micrometer with the inclinometer reversed end-for-end between the two readings. This provides a self-checking system for the readings and also cancels instrument errors. Using this system only instrument errors that occurred between the two readings would not be canceled.

Summary of Field Measurements on Pasadena Bridge

The Right Entrance Ramp Structure at Richey and Margrave Streets on State Highway 225 in Pasadena, Texas, was selected for the first field test. The bridge was a skewed, post-tensioned three-span continuous slab structure. A previous test for live load effects on this structure had found that thermal response was of the same order of magnitude as the live load response. A

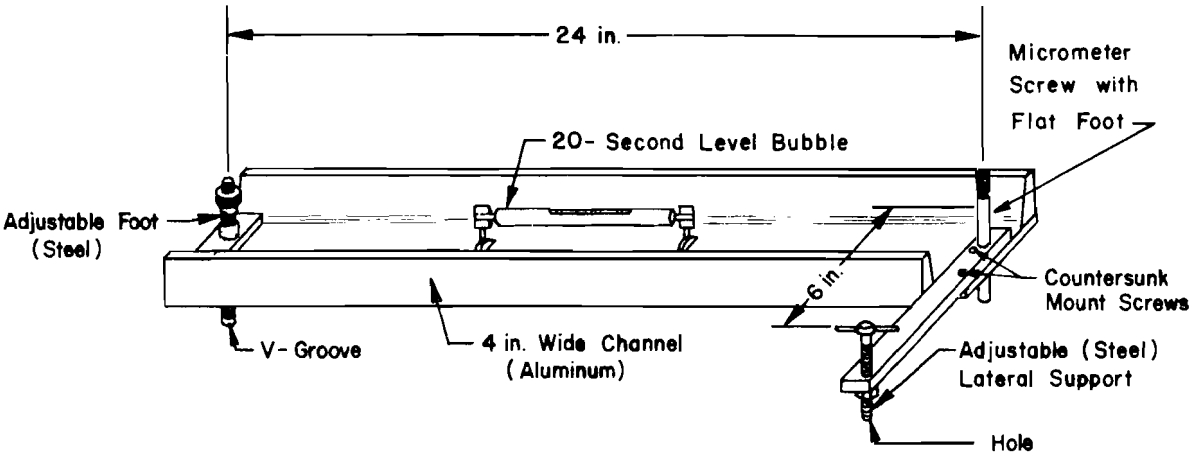

(a) Inclinometer.

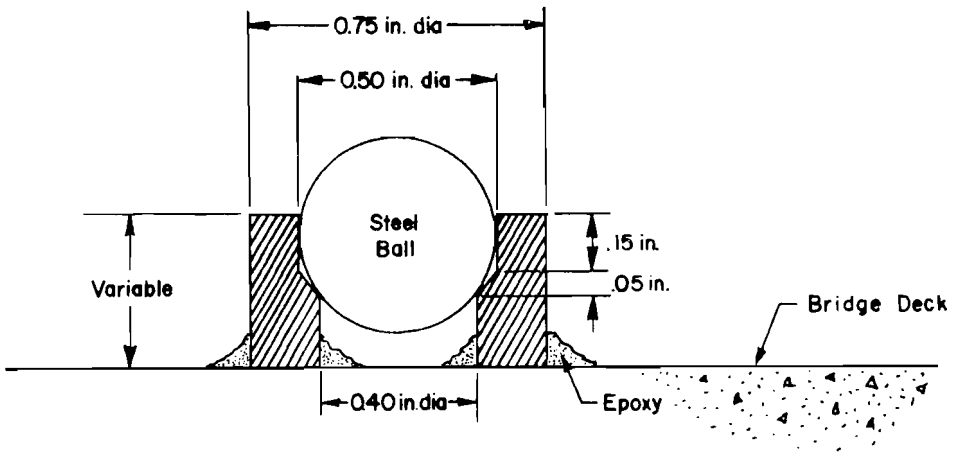

(b) Ball point.

Fig 18. Slope measuring instrument and test point (Ref 30).

partial plan view and cross section of the bridge are shown in Fig 19(a) and (b).

The bridge was tested on 24 August 1974 between 0615 and 1800 hours (CDT). Instrument locations and measurement stations were established the previous night. Inclinometer measurements were taken at nine locations on the slab: three locations at the northern abutment, three over the northernmost interior supports, and three locations in the center of the structure. All inclinometer stations were located so as to measure the change in slope along the longitudinal axis. Surface temperatures were measured at 40 stations: 12 stations on the top of the slab, 12 on the bottom of the slab, and 16 stations on the parapet and sidewalk. Solar radiation readings were observed using both the Casella and Eppley pyranometers located on the top surface of the bridge. Wind speed and air temperature readings were also observed. Positions of all the inclinometer and surface temperature measurement stations are described in Appendix A of Ref 42.

Weather conditions for the day of test were generally poor for purposes of the test. Considerable cloudiness was present almost the entire day and a heavy rain fell between 1615 and 1745 hours (CDT). Only a few spot inclinometer and surface temperature measurements were taken after the rain stopped. After these measurements the test was terminated. The cloudiness is illustrated by the rapid changes in the Eppley solar radiation measurements shown in Fig 20. Shown in Fig 21 are the average top and bottom slab temperatures and the air temperature measured during the test. The maximum slab temperature observed was 107.1° F. Normally for that time of the year and clear weather, one would expect slab temperatures as high as $120\text{-}130^{\circ}$ F (39).

The maximum slope changes recorded were from inclinometer stations located at the northern abutment. Despite the undesirable testing conditions, a maximum slope change of 5.73×10^{-4} was measured. This compares with a maximum slope change of 5.63×10^{-4} measured in a previous field test (30) due to a live load. Plots of all inclinometer and temperature measurements are also presented in Appendix A of Ref 42.

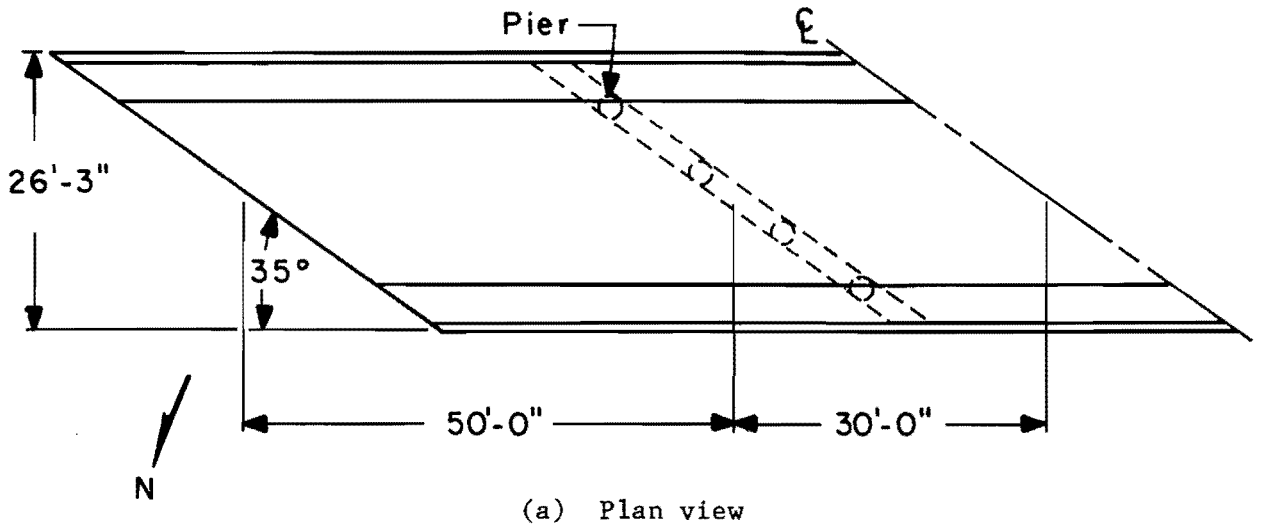

(a) Plan view

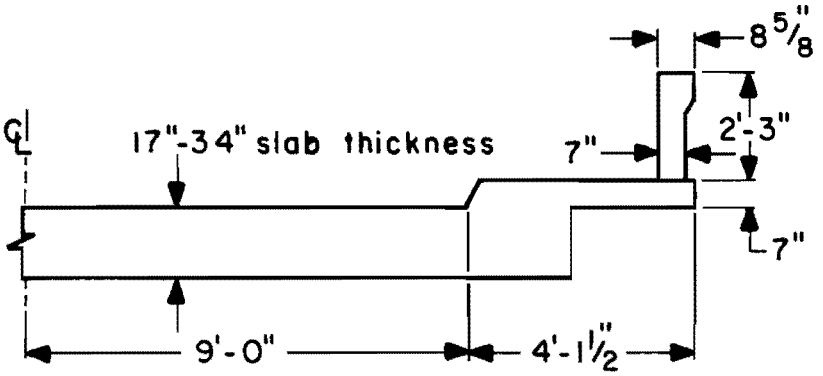

(b) Cross section

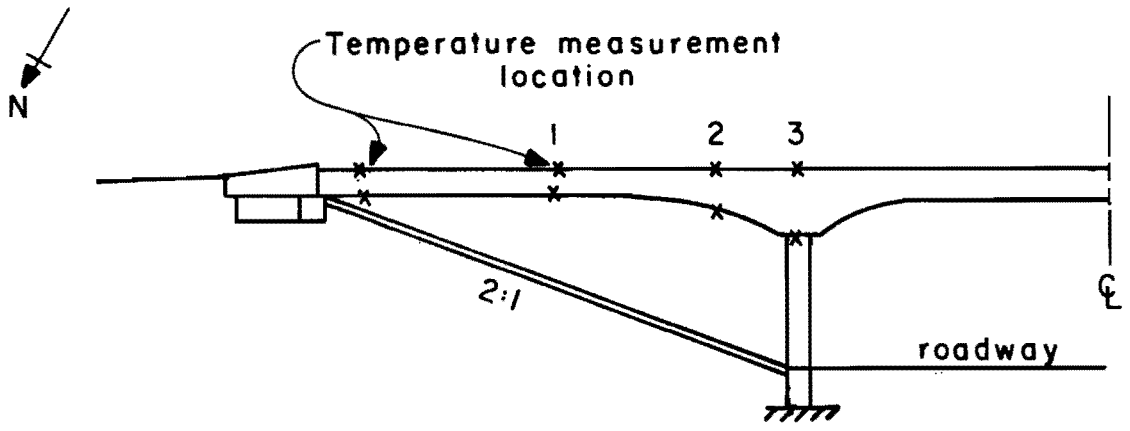

(c) Elevation view

Fig 19. Pasadena bridge.

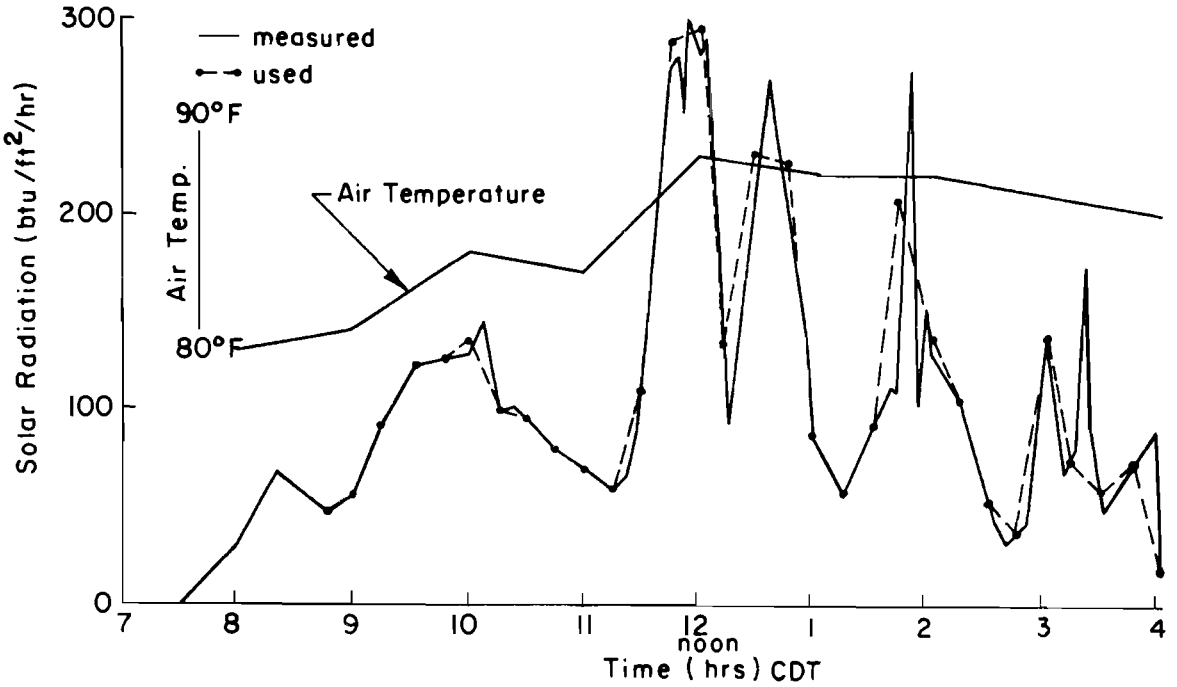

Fig 20. Measured air temperature and solar radiation intensity.

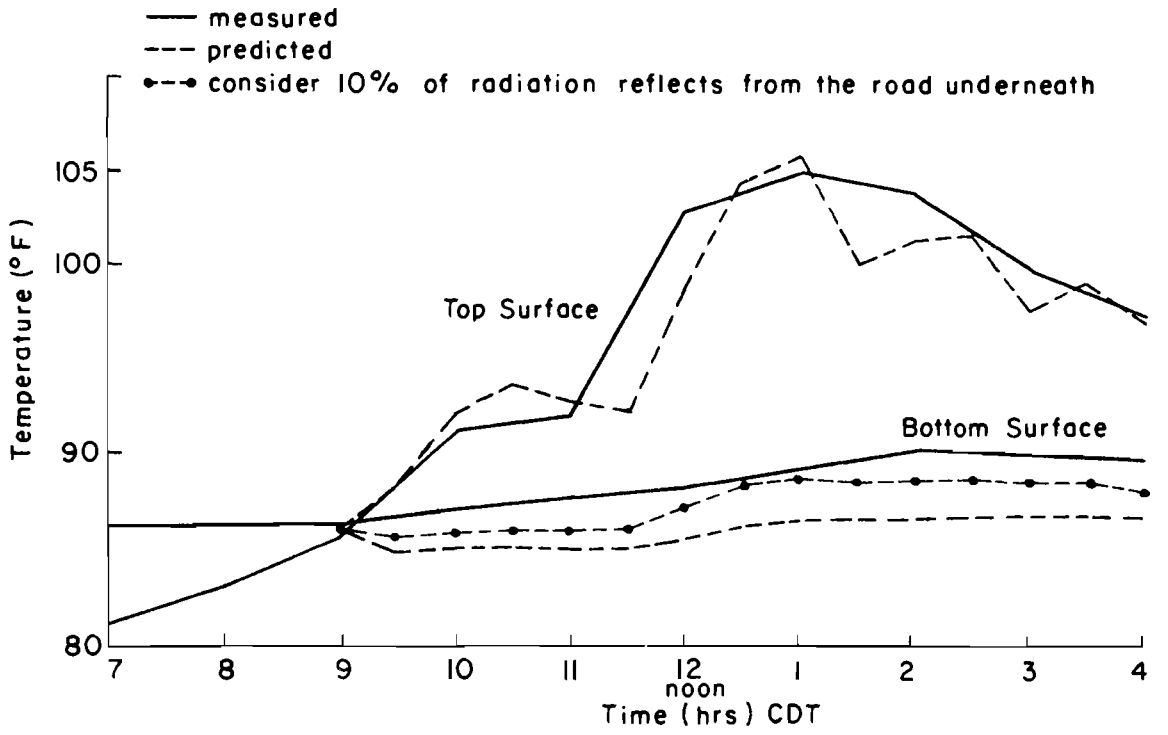

Fig 21. Measured and predicted surface temperatures.

Heat Flow Analyses for the Pasadena Bridge

The first step in the analysis of the Pasadena bridge was to determine the transient internal temperature distribution using the measured surface temperatures. One-dimensional heat flow was used since the heat flow in the longitudinal and transverse directions of the bridge had been found to be negligible. Heat flow in the longitudinal direction was confirmed to be negligible by a later analysis of the haunch region of the slab using the two-dimensional heat flow program (TSAP).

To predict mathematically the temperature distributions throughout the bridge deck, the starting condition, i.e., the reference time and the initial temperature distribution, must be known. As there was no experimental information concerning the temperature variation inside the slab, the reference time was assumed to take place at the time when the top and the bottom surface temperatures reached the same value. Thus, from Fig 21, the starting time at 9:00 a.m. was used with the initial uniform temperature distribution 86^{o} F.

Variations of the measured surface temperatures are depicted in Fig 21. The average top surface temperature at any particular time was used since the maximum temperature difference measured was approximately 2^{o} F. This was also true at the bottom surface of the bridge.

In the analysis, a time increment of 15 minutes was selected. Solar radiation intensities at the 15-minute intervals were extracted from the measured values as shown in Fig 20 in such a way that the area under extracted and measured curves were approximately the same. Since no information was available on the thermal properties of the concrete for the test bridge, the material properties were assumed to be at their typical values. Table 6 gives the average values of concrete thermal properties and pertinent data used in the analysis.

Three different slab thicknesses, i.e., 17 inches, 25.5 inches, and 34 inches at sections 1, 2, and 3, respectively, Fig 19(c), were considered in the analysis. In each case, however, the temperatures computed at the surfaces were identical. The predicted top and bottom surface temperatures are shown in Fig 21. The comparison between measured and predicted top surface temperatures was found to be satisfactory. However, there was a greater discrepancy at the bottom surface of the bridge which has been attributed to the fact that the sun's rays reflected from the roadway underneath were neglected in the analysis. Since the orientation of the bridge

TABLE 6. AVERAGE VALUES OF CONCRETE THERMAL PROPERTIES AND PERTINENT DATA

Solar radiation intensity	Fig 20
Air temperature	Fig 20
Wind speed	10 mph
Initial uniform temperature	86^{o} F
Absorptivity of surface to solar radiation	0.5
Emissivity	0.9
Density	150 lb/ft^3
Thermal conductivity	0.81 $btu/ft/hr/^{o}F$
Specific heat	0.23 $btu/lb/^{o}F$

is not in the east-west direction, the bottom surface receives a portion of the solar radiation intensity, thus influencing its temperature. Subsequently an additional analysis was made by assuming that the bottom surface absorbed 10 percent of the measured solar radiation intensity. The results of this analysis are also shown in Fig 21. It should be noted that the above. assumption, which is felt to be reasonable, results in a better agreement with the measured temperatures.

The above comparison of measured and predicted temperature variations, although limited to the surfaces of the bridge, provide positive evidence that actual bridge temperature distributions over the depth under daily environmental changes can be predicted in a satisfactory way.

Thermal Stress Analyses for the Pasadena Bridge

Once the transient temperature distributions had been predicted for all the sections, static analyses were performed using the predicted temperature changes from the 0900 initial temperatures at one-hour intervals from 0900 to 1600. An example of the temperature distributions predicted by the temperature analysis for the 17-inch slab section is shown in Fig 22. As can be seen from this figure, heat entering the top and bottom of the slab required considerable time to penetrate to the interior of the slab. A plan view and cross section of the finite element mesh (for the program SHELL8) used for these analyses are shown in Fig 23.

Boundary conditions used in the static analyses are as follows:

(1) vertical movement restrained at all pier supports and nodal points along both end abutments, and

(2) rotation about the surface coordinate ξ_2 shown in Fig 23(a) restrained at all nodal points along both abutments.

The surface coordinate system was used only at the abutments in order to provide rotational restraint about ξ_2 since the bottom surface of the slab rested on the abutments continuously along the skew. The expansion joints shown in Fig 23 were only in the parapets and sidewalks at the indicated locations. These joints were idealized in the finite element representation by providing nodal points on both sides of the expansion joints. These nodal points were not connected to each other. Therefore, movement of a nodal point on one side of the expansion joint did not directly induce movement in the

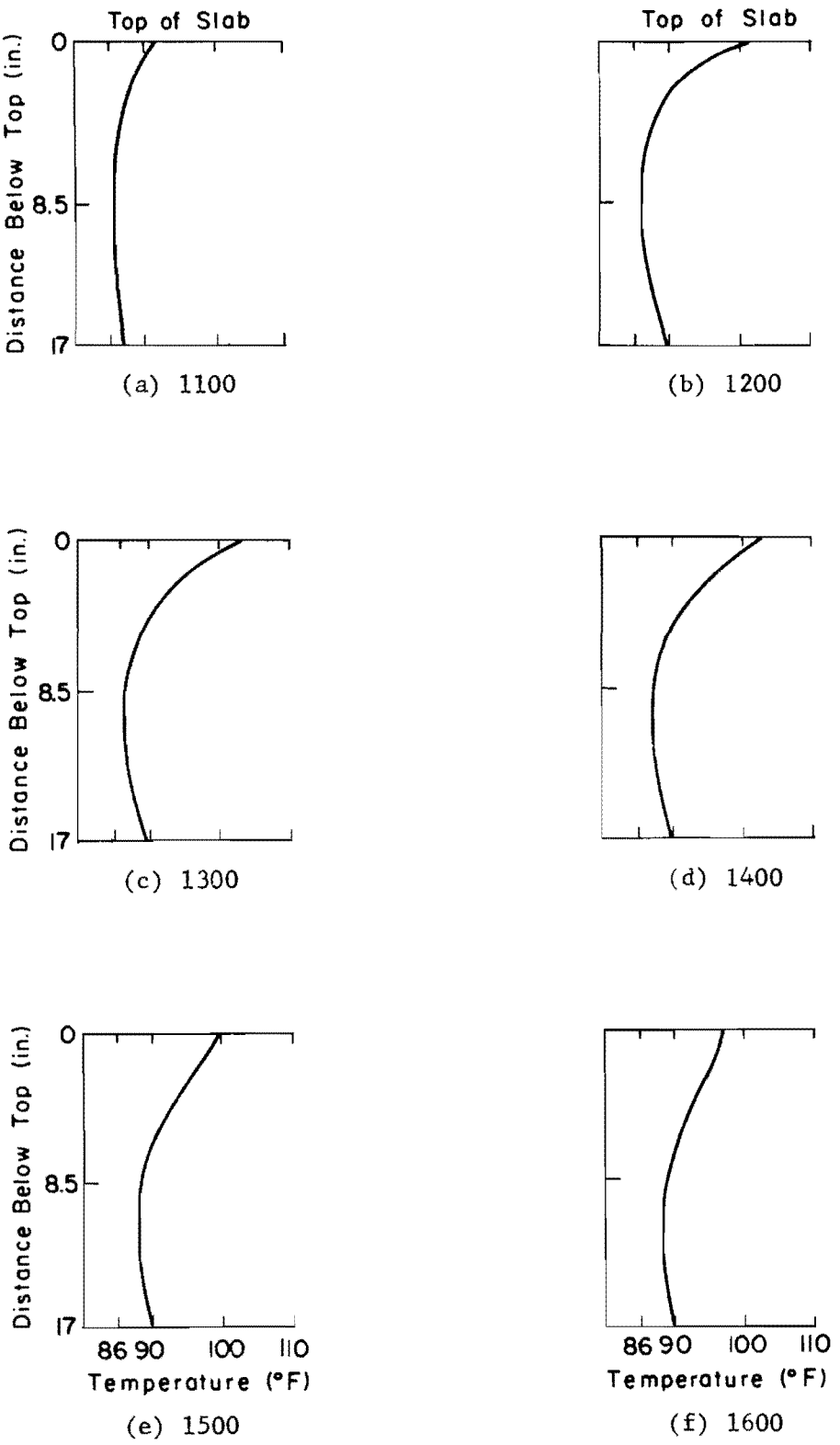

Fig 22. Predicted temperature distributions at several times for 17-inch-thick section on Pasadena bridge.

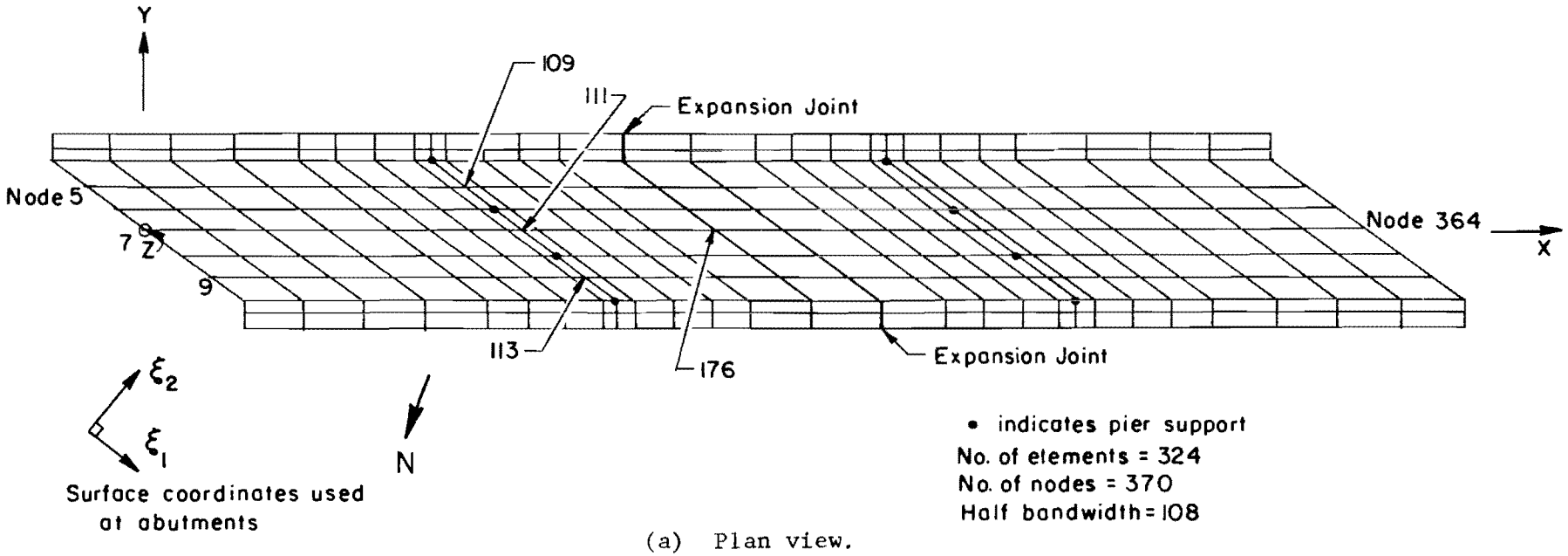

(a) Plan view.

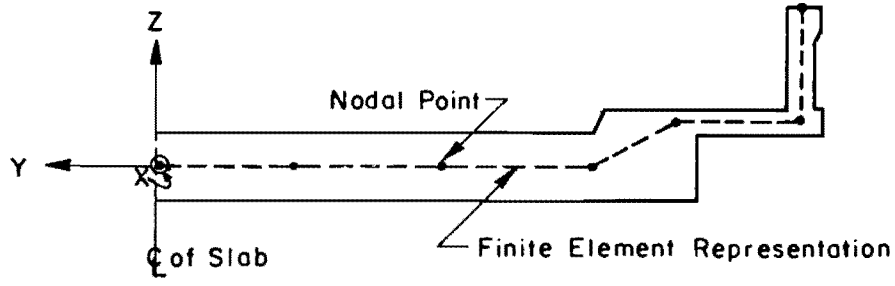

(b) Cross section.

Fig 23. Static analysis finite element mesh for Pasadena bridge.

nodal point on the other side. The following material properties were used for the static analyses:

(1) a modulus of elasticity for 4,690,000 psi for the slab based on a compressive strength of 6000 psi,
(2) a modulus of elasticity of 3,320,000 psi for the sidewalk and parapets based on a compressive strength of 3000 psi,
(3) Poisson's ratio of 0.15, and
(4) a coefficient of thermal expansion of .000006 in/in/^{o}F .

Correlations of the measured and computer predicted slope changes for locations along the northeast abutment are presented in Fig 24. As shown in Appendix A of Ref 42, three inclinometer points, numbers 1, 2, and 3, were measured along this abutment. These locations corresponded to nodal points 5, 7, and 9 respectively in the finite element mesh. Since measured slope changes were about the Y-axis in Fig 23 and the computer results were about ξ_1 , the computer results were transformed so that they too were about the Y-axis. The inclinometer measurements shown in Fig 24 were obtained by subtracting the 0900 slope changes interpolated from the measurements presented in Appendix A of Ref 2. This was necessary since the static analyses slope changes were from the 0900 starting time. The following observations may be made from Fig 24:

(1) the computer results follow the same trend as the field measurements with the exception of the computer results at 1100 hours,
(2) the computer results are generally less than the field measurements, and
(3) the difference between the maximum slope change measured at inclinometer point and the corresponding computer result at nodal point 9 is approximately 15 percent.

The comparison in (3) above was selected since nodal point 9 exhibited the maximum slope change in the field measurements.

Correlations of the measured and computer predicted slope changes for locations along the line of the northeast pier supports are presented in Fig 25. Three inclinometer locations, points 4, 5, and 6, were measured along this line of pier supports. These locations corresponded to nodal points 109, 111, and 113 respectively of the finite element mesh. The slope

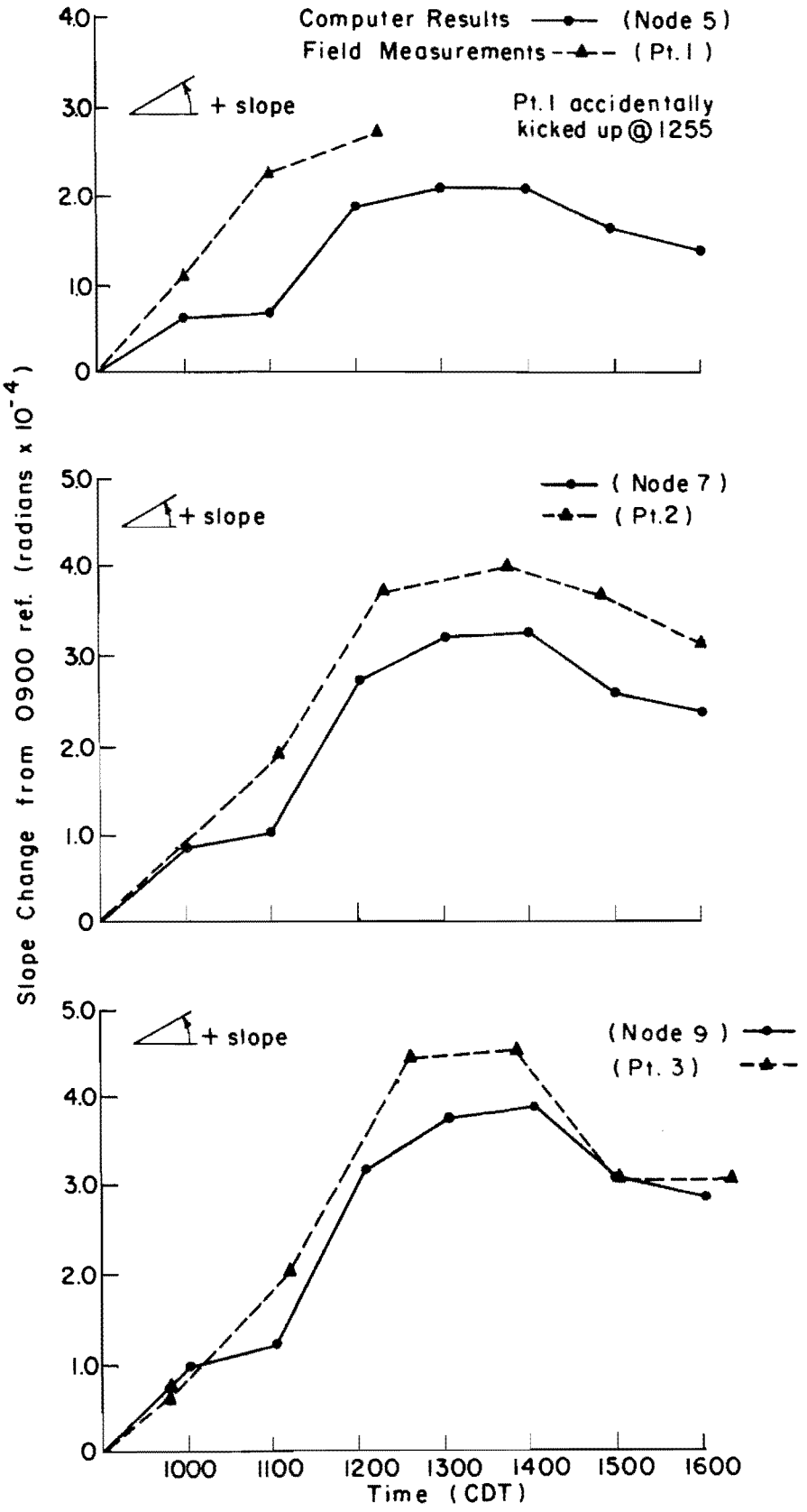

Fig 24. Correlation of measured and computer slope changes for locations along abutment.

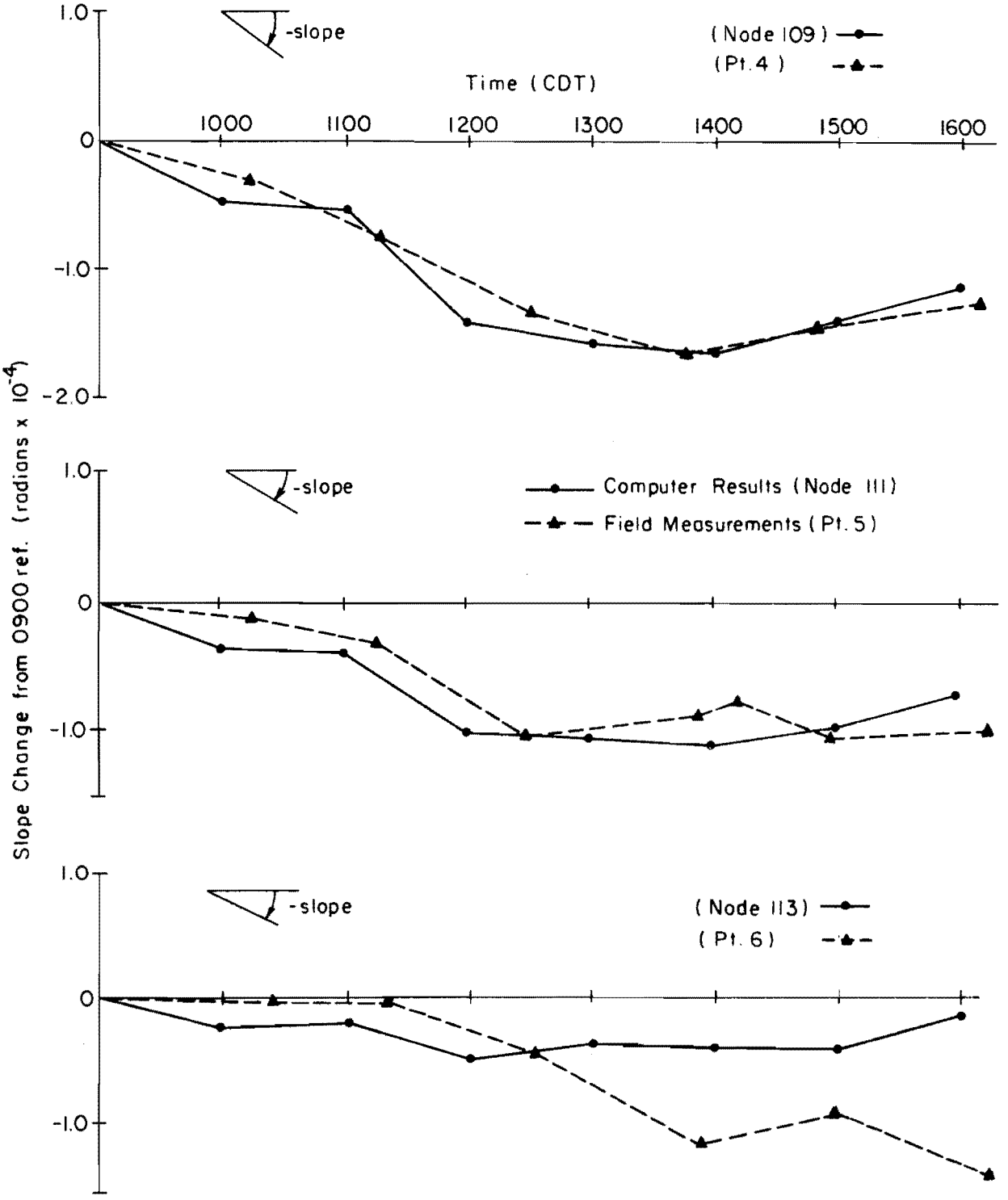

Fig 25. Correlation of measured and computer slope changes for locations along line of pier supports.

changes obtained from the inclinometer measurements and the computer results were about the Y-axis in Fig 23. The following observations may be made from Fig 25:

(1) the computer results generally follow the same trend as the field measurements with the exception of the results at node 113 and inclinometer point 6,
(2) the computer results are of the same order of magnitude as the field measurements, and
(3) the slope changes measured and computed along the line of the pier supports are approximately one-third or less of the slope changes measured or computed at the abutment.

No explanation is available for the discrepancies between the measured results obtained at inclinometer point 6 and the computer results obtained at node 113. A parameter study to explore possible sources of discrepancies in the computational procedure will be presented in a later section. However, the correlations as presented both along the abutment and the line of pier supports are considered favorable.

The temperature induced stresses obtained from the static analyses showed that the top of the slab was in compression at all nodal points and at all times that the stresses were evaluated. Stresses predicted at mid-depth of the slab were tensile while stresses predicted for the bottom of the slab varied from small magnitudes of tension to small magnitudes of compression. An example of the temperature induced stresses for node 176 of the finite element mesh is illustrated in Fig 26. This figure shows the variation in the longitudinal stress with time for the top, bottom, and middle surfaces of the slab. The maximum tensile stress predicted at this node was 147 psi while the maximum compressive stress predicted was 545 psi. Both of these stresses occurred at 1300 hours. The rapid increase in the stresses shown in Fig 26. between 1100 and 1200 is attributed to the rapid increase in the surface temperatures due to the cloud cover clearing between these hours.

The temperature induced stresses shown in Fig 26 are the changes in stress from the assumed 0900 reference time. The low magnitudes of these stresses are due to the poor testing conditions for temperature effects on the day of the test. Based on studies performed by Thepchatri (39), one would expect the maximum temperature induced stresses to be approximately twice

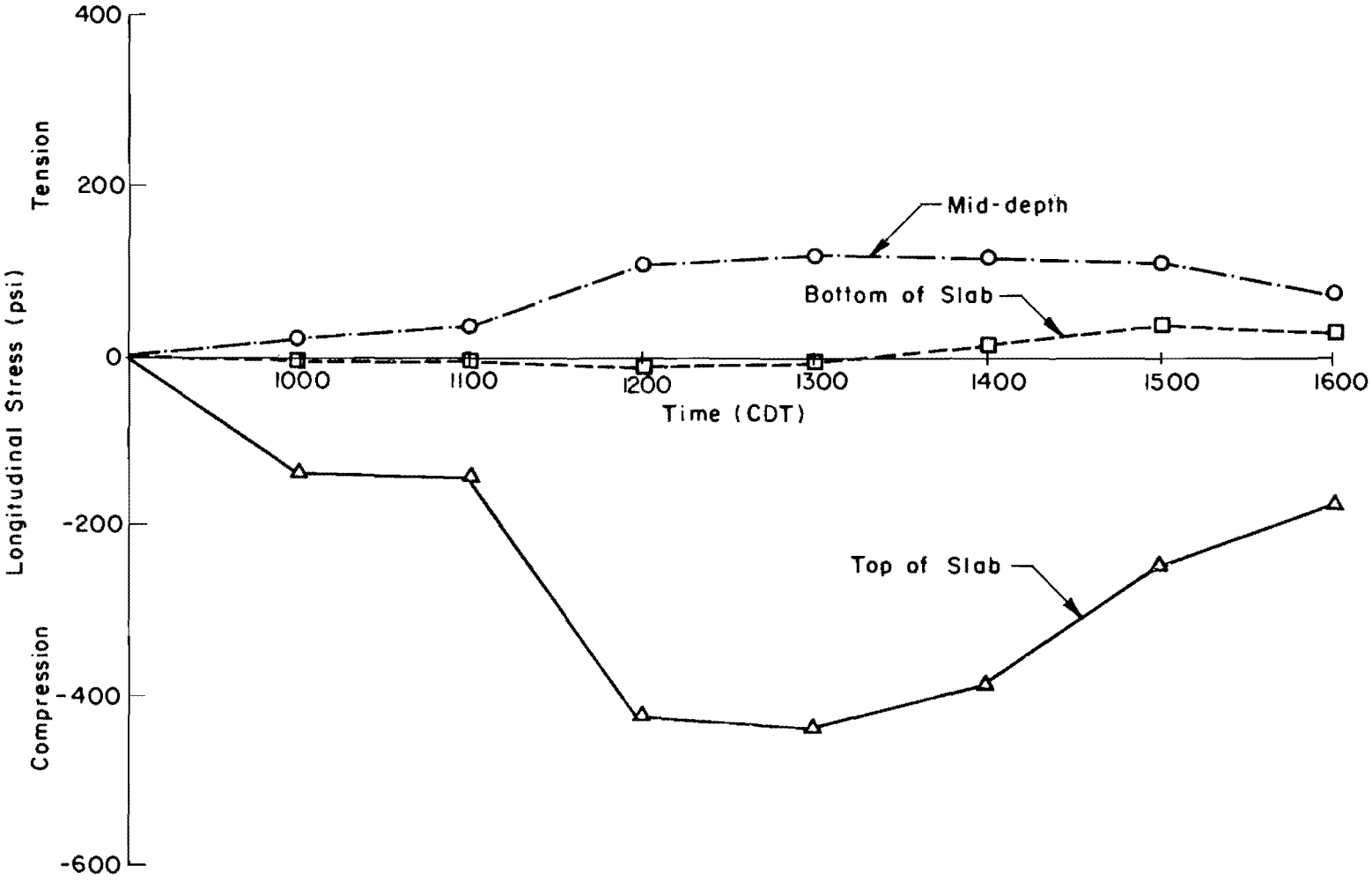

Fig 26. Variation of the longitudinal temperature stresses at node 176 with time.

those shown in Fig 26 under environmental conditions such as clear skies and little wind.

Temperature, Dead Load, and Prestress Stresses on Pasadena Bridge

The final study performed on the Pasadena bridge was the superposition of the temperature effects with those of the dead load and prestress. The temperatures used were those from the day of the field test at 1300 hours. The time, 1300, was selected since the temperature induced stresses had been found to be a maximum then. The equivalent loading method suggested by Lin (29) and Khachaturian (27) was used to determine the prestress effects on the structure. The dead load effects were determined by simply specifying the unit weight of the concrete in the static analysis program.

The equivalent prestress loading for a unit width of the structure was computed using the prestress conduit layout and the geometric shape of a longitudinal section of the slab. The longitudinal section and conduit layout are shown in Fig 27. The equivalent loading that was computed is depicted in Fig 28. This loading is for a unit width of the slab and a unit force of one kip of prestress force. The final loading was computed by multiplying the unit loading from Fig 28 by the total prestressing force after losses and then distributing the load over the width of the slab. Eleven prestressing tendons were distributed over the width of the slab with a final prestressing force of 368 kips in each tendon at release. These forces were reduced to account for losses due to friction, shrinkage, elastic shortening, creep, etc. An average force was computed and assumed to be constant over the length of the bridge to simplify the calculations. A loss of 33000 psi in each tendon was used to account for losses other than friction. This figure was obtained from the 1975 AASHTO Interim Specifications for Bridges (3). The loss of 33000 psi is recommended for conrete with a compressive strength of 5000 psi while the slab strength was 6000 psi. Friction losses were calculated at each point of angle change in the conduit using the formula suggested in the 1973 AASHO Bridge Specifications (1). The friction losses were calculated assuming the tendons were jacked at both ends of the bridge. These friction losses were then averaged and assumed to be constant over the length of the bridge. The average friction loss computed was 22500 psi. The total loss in prestress reduced the force in each tendon to 262 kips, or 29 percent total losses.

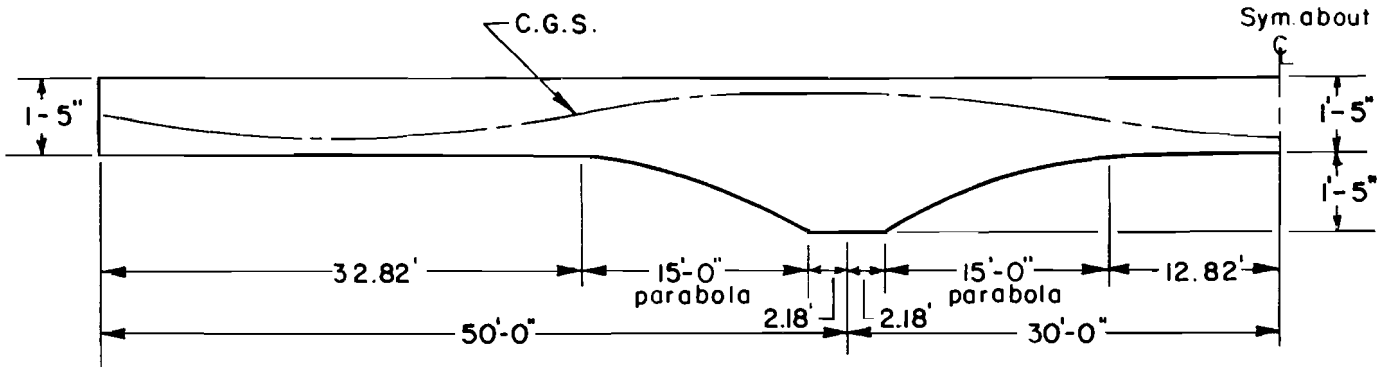

(a) Typical longitudinal section of slab.

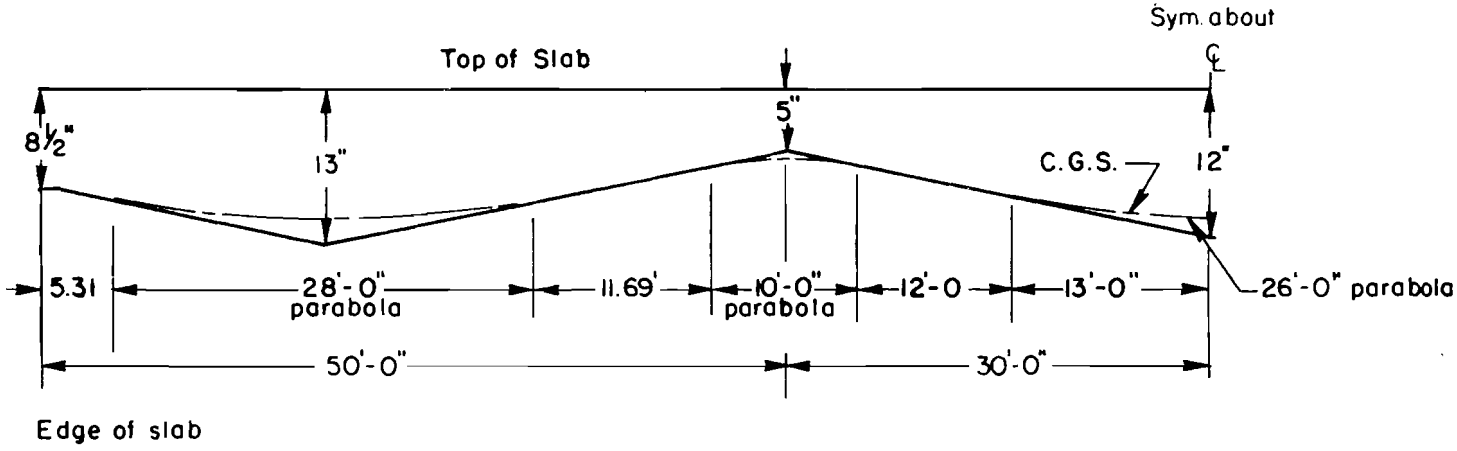

(b) Prestressing conduit layout using the top of the slab as a level datum.

Fig 27. Typical longitudinal section and prestressing conduit layout for Pasadena bridge.

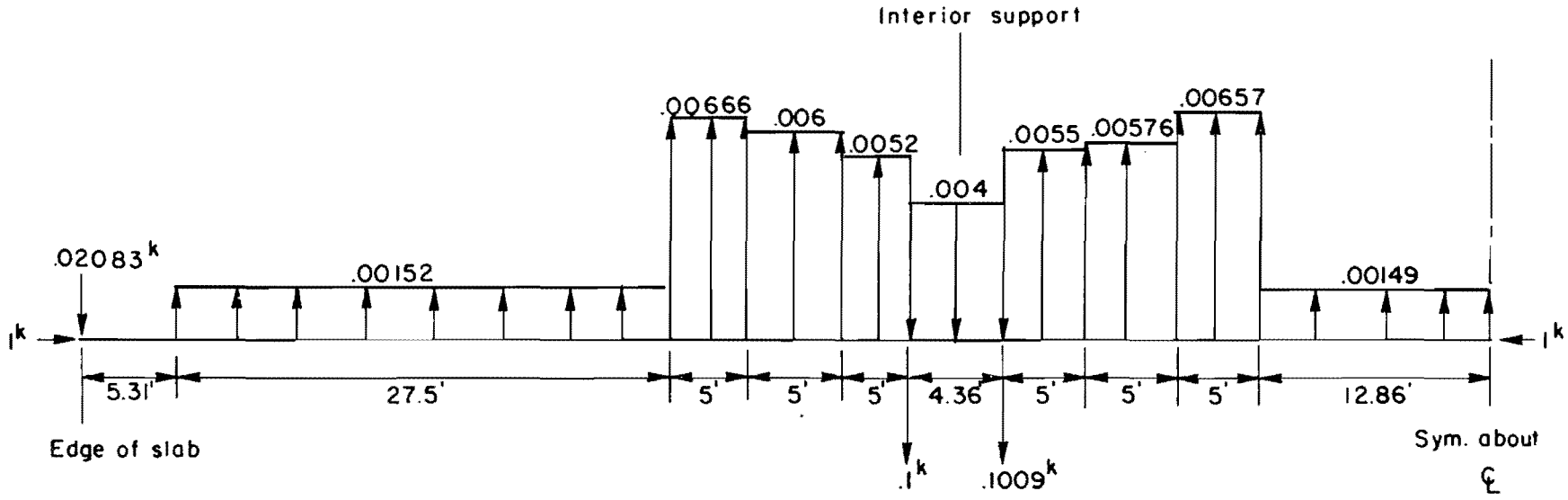

Note: All uniform loads in units of kips/ft of length
Equivalent loads shown are for 1 k of prestress force

Fig 28. Equivalent prestress loading for unit width of Pasadena bridge.

Stresses due to the dead loading and prestressing forces were computed first and then the stresses due to the temperature changes were included. The results obtained from the analyses are illustrated in Fig 29 for a longitudinal section of the slab at the center of the roadway. Stresses are presented in Fig 29 for the top, middle, and bottom surfaces of the slab. In general, the temperature induced stresses would not be symmetrical due to the different distributions in the parapets and sidewalks on opposite sides of the bridge. However, at the time used in the analysis, 1300 hours, the difference in temperatures of the parapets and sidewalks on opposite sides was small; thus, the difference in stresses on each side of the axis of symmetry were negligible. The following observations can be made from Fig 29:

(1) the temperature stresses increase the top surface compressive stresses due to the dead loading and prestressing by at least 400 psi at all locations along the length of the section;
(2) the temperature stresses had little or no effect on the stresses at the bottom and middle surfaces of the slab;
(3) the superposition of the dead loading, prestressing, and temperature did not produce tensile stresses at any location; and
(4) all stresses were within allowable design limits (compressive allowable = $0.4\ f'_c$ (1)).

The low magnitudes of the stresses are attributed to the over-design of the bridge since the inertia and area of the parapets and sidewalks are neglected in the design process. Even though the parapet and sidewalks are lower strength concrete and are assumed to have a lower modulus of elasticity, they contribute considerably to the stiffness of the structure. Also, the temperatures measured on the day of the field test were less than would normally be encountered on a clear day.

Summary of the Investigations for Pedestrian Overpass (14 March 1975)

The second field test was performed on a two-span pedestrian overpass in Austin, Texas, with pretensioned beams made continuous for live load (Fig 30). The large variation in the measured temperatures about the cross section of this bridge required a two-dimensional heat conduction analysis to determine the transient internal temperature distribution. The finite element mesh used for the heat conduction analysis is depicted in Fig 30(a). The temperature distribution was assumed to be constant along the longitudinal

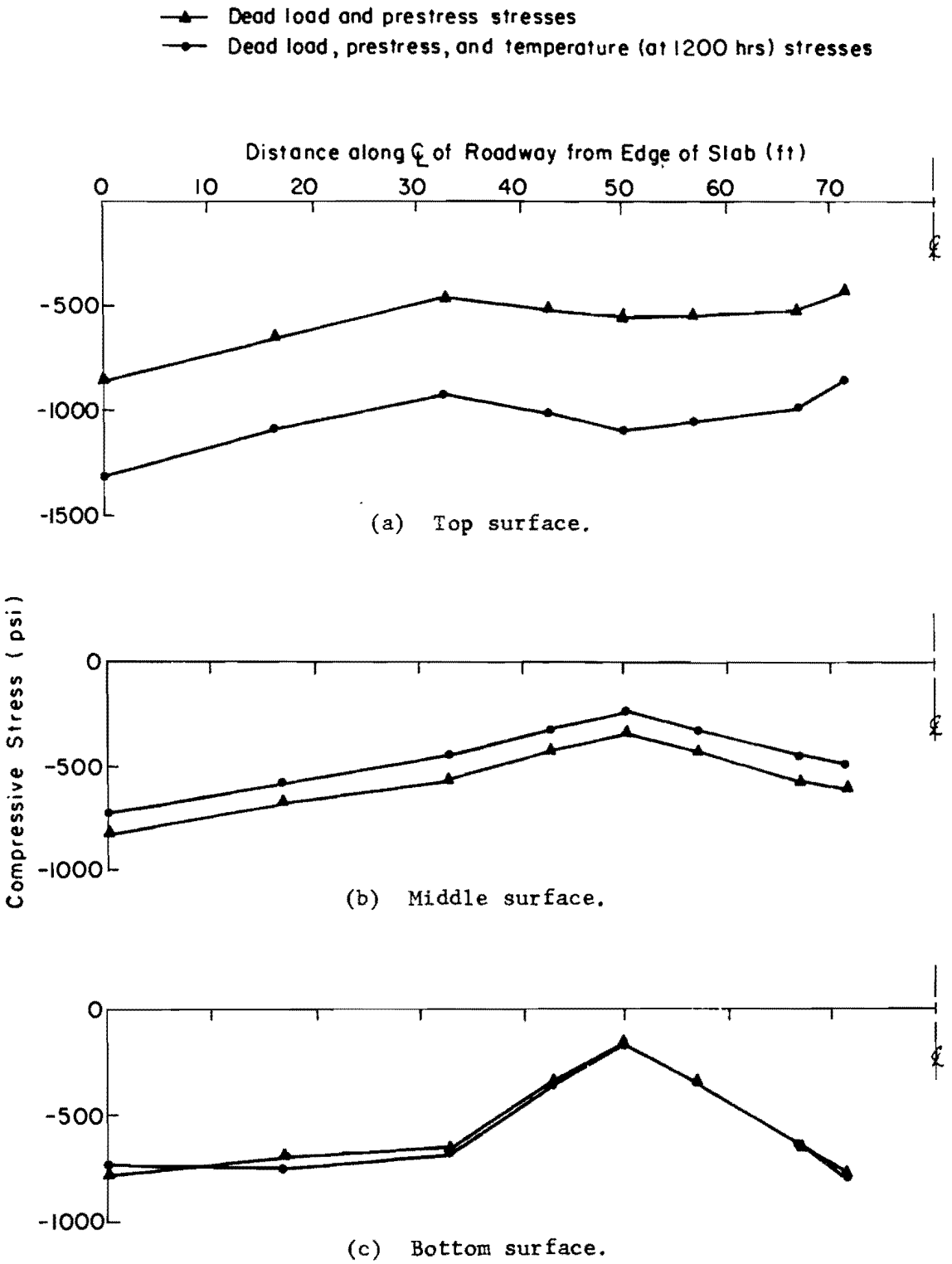

Fig 29. Dead load, prestress, and temperature (1300 hours) stresses along length of slab.

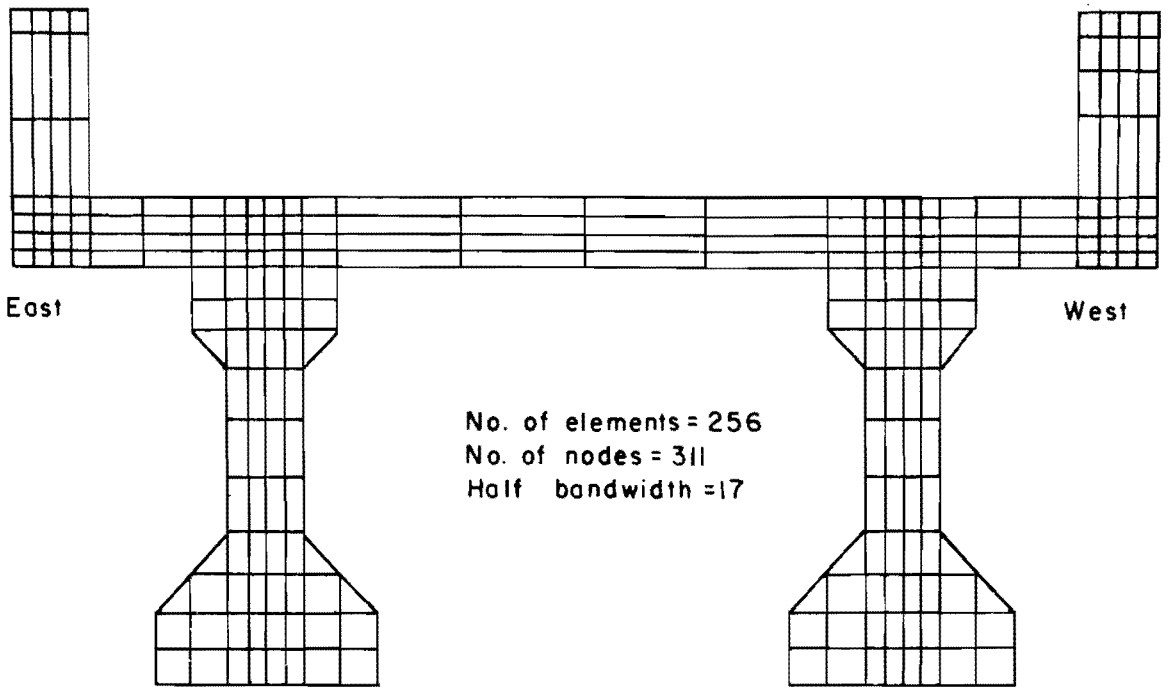

(a) Heat conduction mesh.

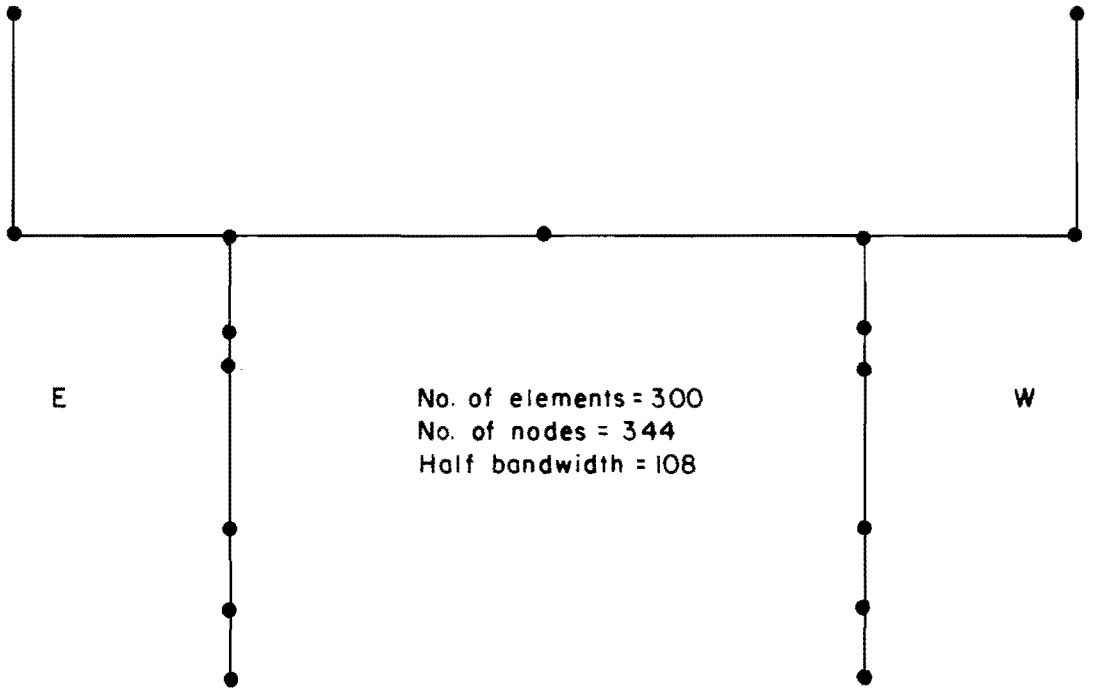

(b) Cross section of static analysis mesh.

Fig 30. Finite element meshes used for pedestrian overpass analysis.

axis of the bridge. Average concrete thermal properties as used for the analysis of the Pasadena bridge were used for the analysis of the pedestrian overpass also. Surface temperatures obtained from measurements at 56 locations about the cross section were specified as boundary conditions. The locations and the measured temperature variation with time are presented in Appendix B of Ref 43. Linear interpolation between measurement locations was used to approximate the surface temperatures at nodal points in the finite element mesh where measurements were not taken. The most difficult problem faced in the analysis, other than the large amount of input data required, was the determination of the initial uniform temperature distribution and starting time approximations. This was due to the side heating of the east side of the bridge in the early morning while the rest of the bridge remained relatively cool. An analysis of the measured surface temperatures revealed that a 41° F initial uniform temperature distribution at 0830 (CDT) would provide the smallest variation in temperature around the cross section.

The heat conduction analysis was performed every hour between 0830 and 1830 hours (CDT). Temperatures were also calculated at 1000 hours since a static analysis had to be performed at this time to obtain a reference slope for comparison with the inclinometer slope changes. An example of the internal temperature approximations and the specified surface temperatures at 1530 is shown in Fig 31 for both girders. The time, 1530, was selected for comparison since the maximum measured slope change occurred at that time. The temperature distributions along the centerline of the girders were nonliner as can be observed in Fig 31. The nonlinearity occurred primarily in the flanges of both girders and in the slab. Temperatures in the east girder were slightly higher at this time as a result of side heating in the morning. The temperatures in the top of the slab were slightly higher over the west girder due to the shading of the east side of the slab by the parapet in the morning.

Temperature changes from the 41° F initial temperature distribution were then used for the static analyses. A cross section of the mesh used for the static analyses is shown in Fig 30(b). Longitudinal divisions were specified every five feet in this mesh. The bridge response was assumed to be symmetric about the interior support; therefore, only the north span of the bridge was idealized for the static analyses. Expansion joints in the parapets were

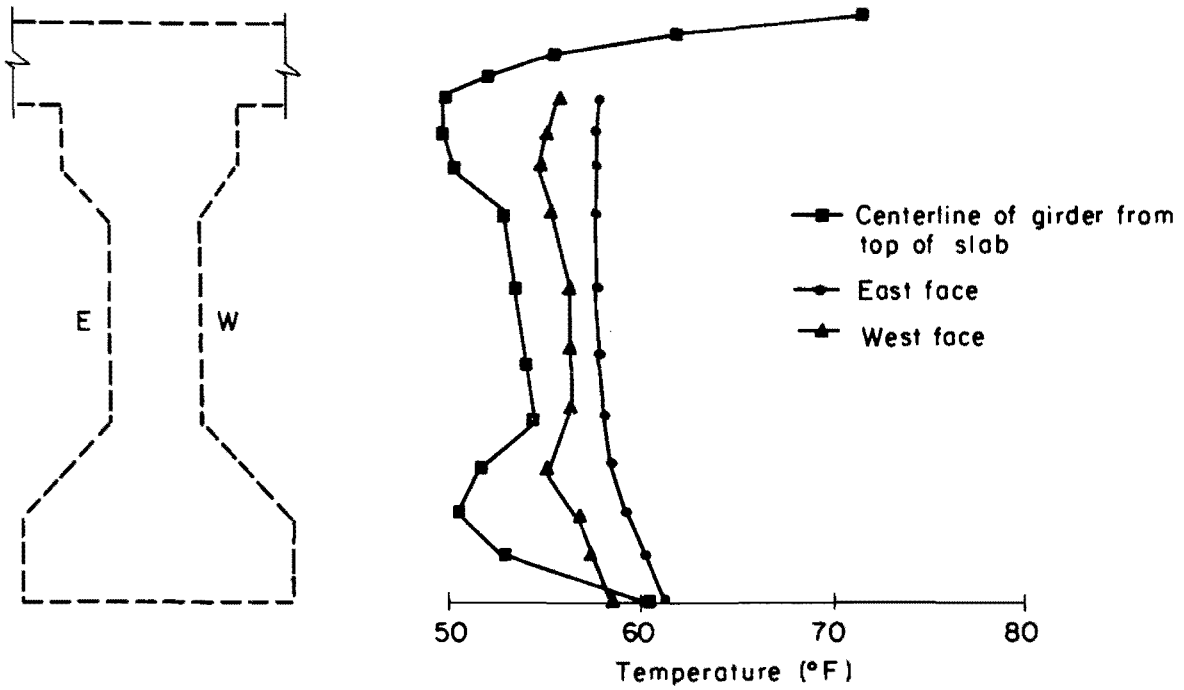

(a) Temperature distribution in East girder at 1530 hours.

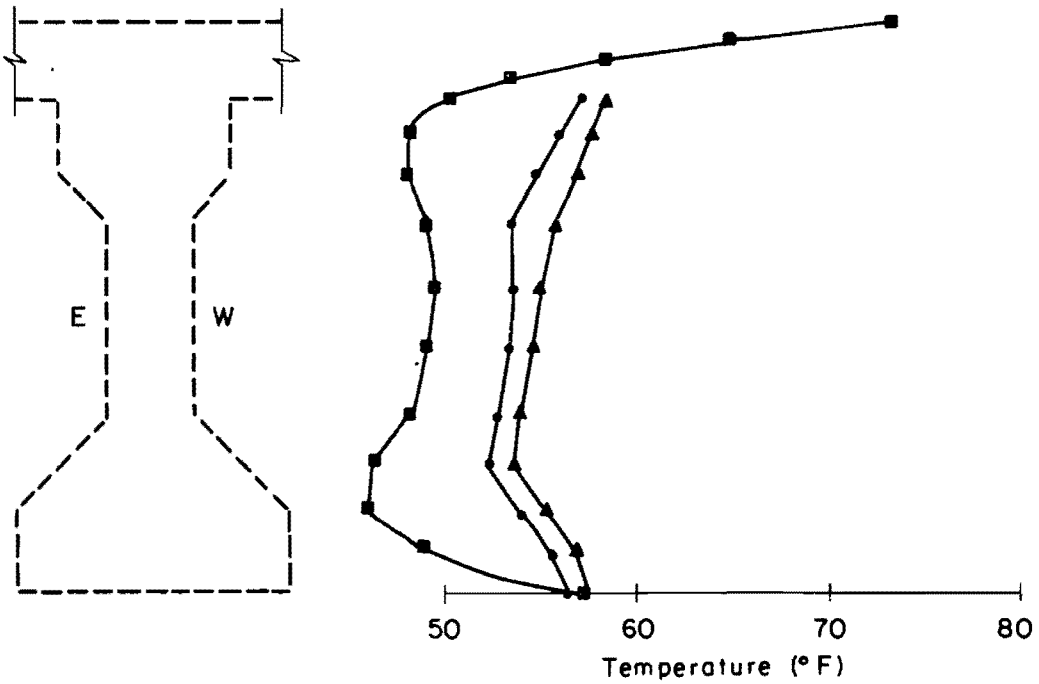

(b) Temperature distribution in West girder at 1530 hours.

Fig 31. Girder temperature distributions at 1530 hours.

neglected in the finite element idealization. The following material properties were used in the analyses:

(1) a modulus of elasticity of 4,690,000 psi for the girders based on a compressive strength of 6000 psi,
(2) a modulus of elasticity of 3,320,000 psi for the slab and parapets based on a compressive strength of 3000 psi,
(3) Poisson's ratio of 0.15, and
(4) a coefficient of thermal expansion of .000006 in/in/^{o}F .

The concrete was assumed to be uncracked for the analyses.

Analyses were performed at 1000 and then from 1030 until 1830 in one-hour time intervals. The 1000 analysis was performed to provide a reference slope for comparison with the inclinometer results. The slope obtained at this time was subtracted from slopes at other times at the nodal point corresponding to the inclinometer location. This was necessary to obtain the slope change from 1000 since inclinometer measurements were not observed until 1010 on the day of the test. The ten-minute difference in reference times was assumed to be negligible. Correlation of the measured slope changes and static analyses results is shown in Fig 32. The correlation was excellent as can be observed from Fig 32. The finite element analysis was able to accurately track the slope change as it increased and decreased. Slope changes were obtained at only one location during the field test due to a malfunction of a new inclinometer. The slope change about the transverse axis of the bridge was found to be a maximum at the location of the inclinometer from the finite element analyses.

An example of the longitudinal stress distributions at 1530 in the girders at the exterior support is presented in Fig 33. The time and location were selected for illustration since the maximum tensile stress obtained in the analyses, 415 psi, was predicted at 7 inches from the bottom of the west girder at the interior support. Stresses in the slab were compressive at all locations and times analyzed. The stresses at the middle of the slab width at the interior support at 1530 were as follows: top of the slab, 384 psi compression; mid-depth of the slab, 90 psi compression; and bottom of the slab, 47 psi compression. Vertical movements predicted by the analyses were small with a maximum movement of 0.05 inches predicted at 1530 hours.

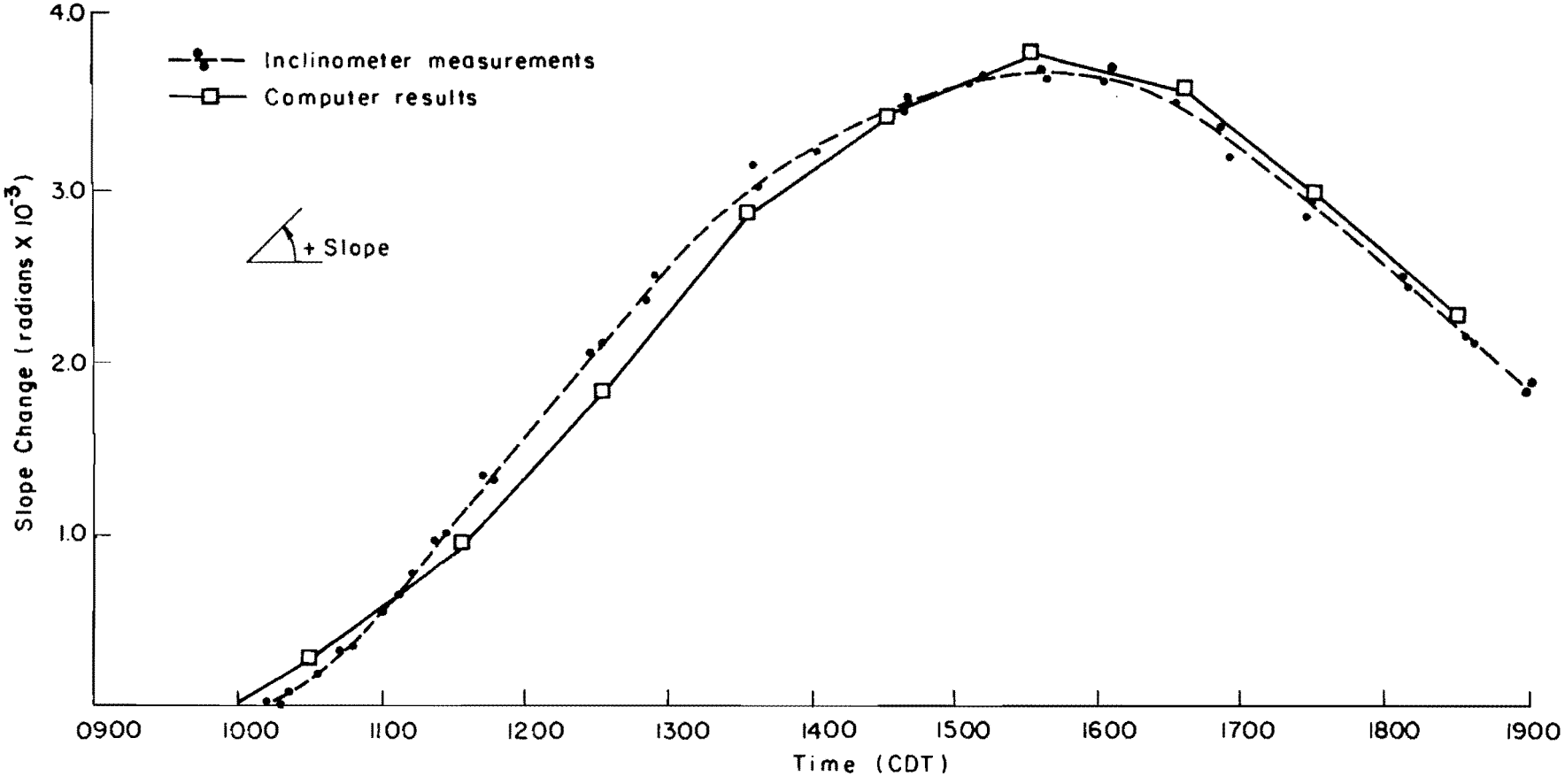

Fig 32. Correlation of measured slope changes and computer results for pedestrian overpass (14 March 1975).

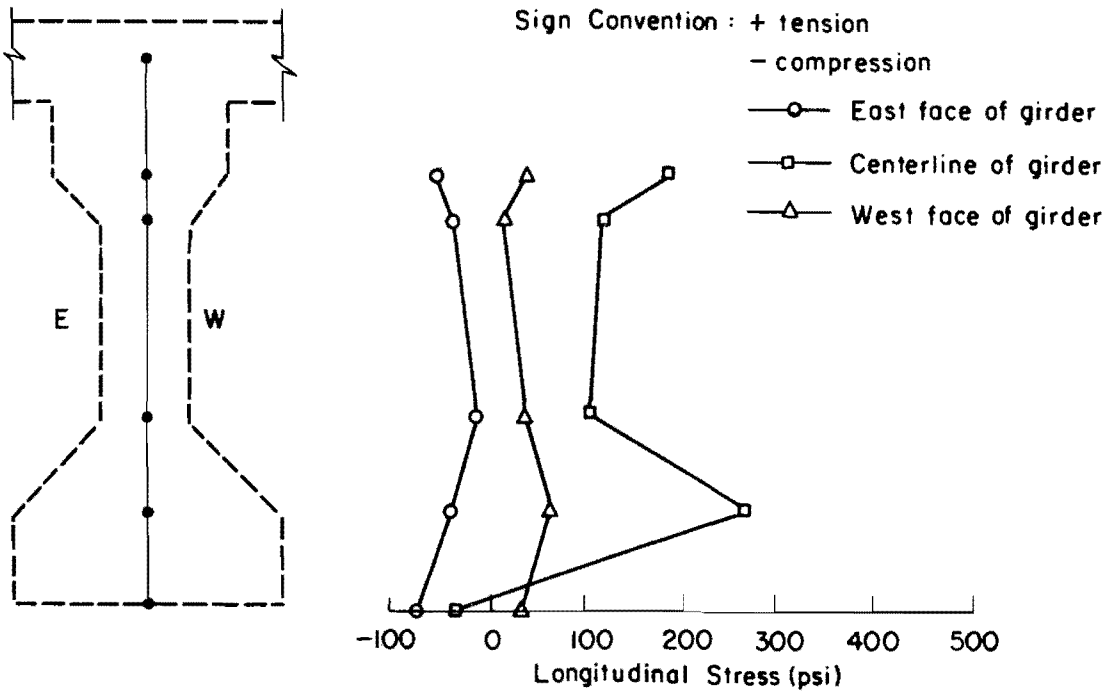

(a) Stress variation thru depth of East girder @ 1530.

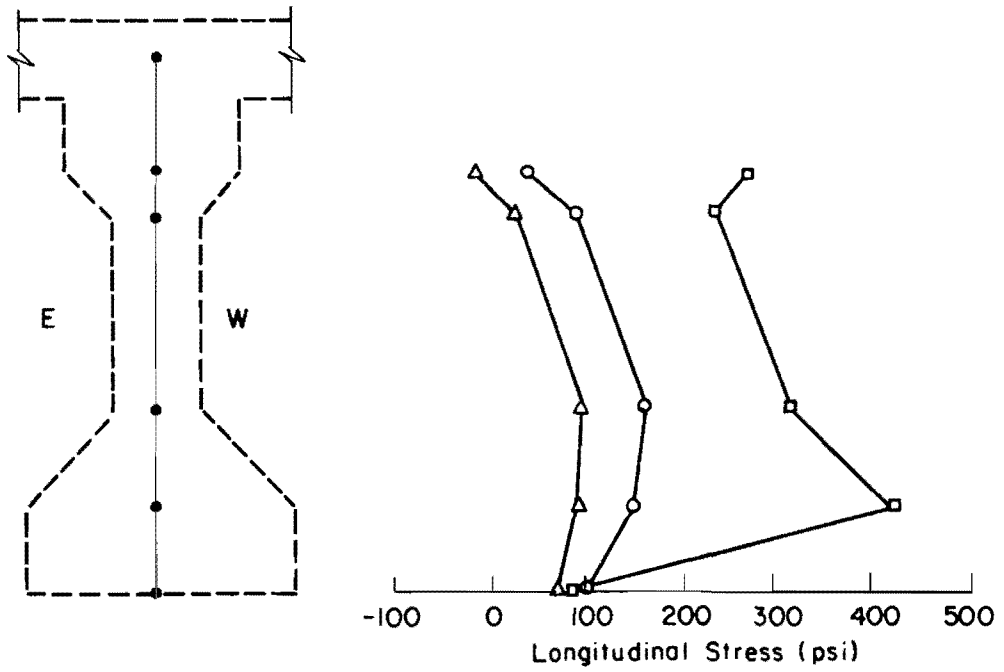

(b) Stress variation thru depth of West girder @ 1530.

Fig 33. Girder temperature stresses over interior support at 1530 hours.

CHAPTER 4. DOCUMENTATION OF COMPUTER PROGRAMS

Introduction

The programs, TSAP and SHELL8, were used extensively in this research. They provide a general capability for predicting bridge temperature distributions and the corresponding temperature induced stresses caused by daily environmental changes.

The program TSAP includes the heat flow and the thermal stress analysis in a complete system. In this program, the cross-section of the structure is idealized as an assemblage of two-dimensional finite elements to predict the temperature distribution due to either specified environmental conditions or measured surface temperatures. Temperature induced stresses and deformations are calculated based on one-dimensional beam theory. Hence, the method is limited to straight bridges with supports perpendicular to the longitudinal direction of the bridge. The program is applicable to both simple span and continuous span bridges.

The program SHELL8 utilizes one and two-dimensional finite elements in a three-dimensional global assemblage with six degrees-of-freedom at each nodal point. This program provides a general capability for the analysis of complex bridge structures having arbitrary geometry and support conditions, as well as variable thickness over the individual elements and orthotropic material properties. The temperature distributions that are obtained from the heat conduction analysis are used as input data to predict the thermally induced movements and stresses. The thermal stress analysis is based on a quartic representation of the temperature distribution through the thickness of each element and a linear representation of the temperature distribution over the surface of the element.

Both programs, which are written in FORTRAN IV, have automatic mesh generation options in order to reduce and simplify the task of preparing input data. The program TSAP is divided into a main program and three subroutines. Overlay features are utilized to save storage in SHELL8. In this program, there are four overlays and 52 subroutines which are called sequentially by

the resident (MAIN) program. Six FORTRAN logical units are used for intermediate storage during the execution of this program. DOUBLE PRECISION is used for all real variables in the IBM versions of these programs presented in this report.

Use of the Program TSAP

1.1 Coordinate System and Mesh Construction. A global coordinate system x, y , for example, as shown in Fig 6, must be chosen for the cross-section of the bridge which is to be analyzed. Input nodal coordinates could be simplified by the proper orientation for this coordinate system.

As shown in Fig 6, a finite element mesh is obtained by subdividing the cross-section of the bridge into quadrilateral and triangular elements. The mesh may require refinement, i.e. reduction in element size, in regions having steep heat flow gradients. In this idealization, 400 nodes, 300 elements, and 5 different material types are possible.

The nodal point numbering should run in the direction with the smallest number of elements in order to minimize the nodal point half band width (maximum element nodal difference plus one) of the assemblage and consequently the computational efforts during the solution process.

1.2 Finite Element Types. Two types of finite elements are available in the program, as shown in Figs 34 and 35. The triangular element employs a linear temperature distribution over the element. The quadrilateral element is formed from four triangular elements. The interior node is then eliminated by employing the method of static condensation.

1.3 Heat Flow Conditions. Heat is transferred between the bridge boundaries and the environment by radiation and convection. It is also transferred with the bridge boundaries by conduction.

Heat flow by radiation primarily depends on the daily variation of solar radiation intensity and on the absorptivity and emissivity of the concrete surface. In the program, an empirical equation is used to define the daily variation of solar radiation when the total radiation and the times of sunrise and sunset are input (see Sec. 2.6).

Heat flow by convection depends on the wind speed and on the temperature difference between air and bridge surface. Ambient air temperature needs to be input for each time step (see Sec. 2.8.1). The effect of the wind on

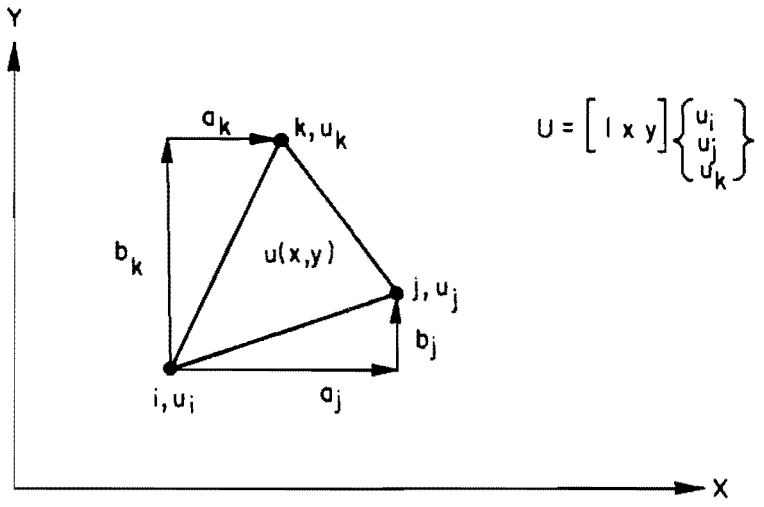

Fig 34. A typical triangular element.

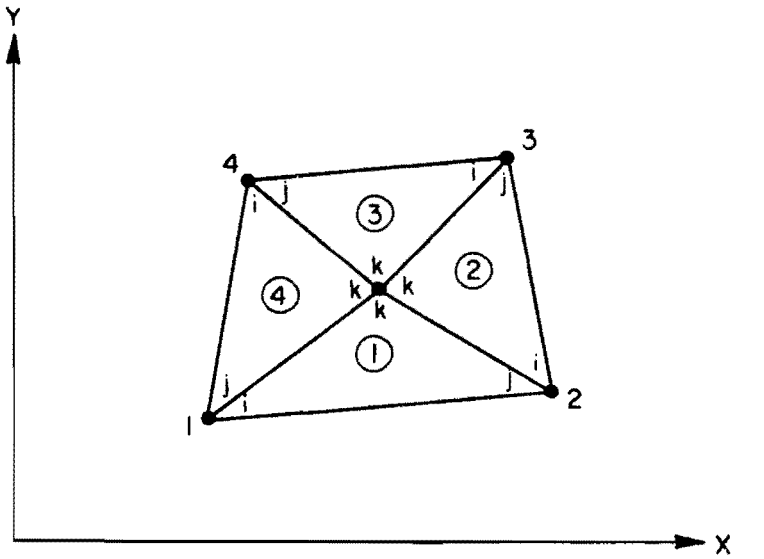

Fig 35. A typical quadrilateral element.

convection is recognized in the film coefficient h_c. Wind speed is assumed to have a constant average value with respect to time.

For a known time-dependent boundary temperature distribution, the interior temperature distribution is governed by the well-known transient heat-conduction equation. Hence, in this case, measured surface temperatures are sufficient in order to predict the interior temperature distribution. Surface temperatures need to be input for each time step (see Sec. 2.8.2).

Preparation of Input Data

Abbreviations: A = alphanumeric field
I = integer value (must be packed to the right of the field)
F = floating point number (must be punched with a decimal)

2.1 Title Card

Cols. 1-70 (A) Problem identification

2.2 Control Cards (Two cards)

Card 1

Cols. 1- 5 (I) Number of nodal points (400 max)
6-10 (I) Number of elements (300 max)
11-15 (I) Number of different material types (5 max)
16-20 (I) Number of convective boundary conditions (sidewise, 200 max)
25 (I) = 0 if external heat flow is specified
= 1 if nodal temperatures are specified
26-30 (I) Number of nodal points with specified external heat flow or nodal temperature (200 max)
31-35 (I) Number of time increments (no limit)
40 (I) = 0 for no stress computation
= 1 for stress computation
45 (I) = 0 if only moment about X-axis is considered
= 1 if both M_x and M_y are considered
46-50 (I) Time interval for print of output

Card 2

Cols.	1-10	(F)	Time increment (fraction of hour, assumed constant in the problem)
	11-20	(F)	Uniform initial temperature for all nodal points
	21-30	(F)	Absorptivity of the top surface
	31-40	(F)	Emissivity of the material
	41-50	(F)	Span ratio (= -1 for 1 span; = 0 for 2 spans; and 1 for 3 equal spans)

2.3 Element Material Cards. Two cards per element type must be input. Material properties are assumed constant over each individual element.

Card 1

Cols.	5	(I)	Element material type

Card 2

Cols.	1-10	(F)	Conductivity in the X-direction (btu/ft/hr/^{o}F)
	11-20	(F)	Conductivity in the Y-direction
	21-30	(F)	Conductivity in the XY-direction (for isotropic material, X = Y and XY = 0)
	31-40	(F)	Specific heat of material (btu/lb/^{o}F)
	41-50	(F)	Density of material (lb/ft^{3})
	51-60	(F)	Rate of heat generated per unit volume (internal heat generation)
	61-70	(F)	Modulus of elasticity (either psi or psf; same unit for stress output)
	71-80	(F)	Thermal coefficient of expansion

2.4 Nodal Coordinate Cards. Two cards per nodal point except when mesh generation option is used. These cards need not be input in numerical sequence; however, the node having the largest number must be input last. The increment between nodal points and coordinates along the line must be constant.

Card 1

Cols.	1- 5	(I)	Nodal point I of straight line
	6-10	(I)	Nodal point J of straight line (J = I if no generation in J-direction)

Cols.	11-15	(I)	Nodal point K of straight line (K = I if no generation in K-direction)
	16-20	(I)	Increment between successive nodes in the J-direction
	21-25	(I)	Increment between successive nodes in the K-direction

Card 2

Cols.	1-10	(F)	X-coordinate of nodal point I
	11-20	(F)	Y-coordinate of nodal point I
	Omit the following items if only one node is input:		
	21-30	(F)	X-coordinate of nodal point J
	31-40	(F)	Y-coordinate of nodal point J
	41-50	(F)	X-coordinate of nodal point K
	51-60	(F)	Y-coordinate of nodal point K

2.5 Element Nodal Point Number and Material Type Cards. One card per element, except when mesh generation option is used. This card need not be input in numerical sequence; however, the element having the largest number must be input last.

Cols.	1- 5	(I)	Element number II
	6-10	(I)	Last element number to be generated in JJ-direction (JJ = II if no generation)
	11-15	(I)	Last element number to be generated in KK-direction (KK = II if no generation)
	16-20	(I)	Element material type
	21-25	(I)	Element nodal point I of element number II
	26-30	(I)	Element nodal point J of element number II
	31-35	(I)	Element nodal point K of element number II
	36-40	(I)	Element nodal point L of element number II (for a triangle, L = I)
	41-45	(I)	Element number increment in JJ-direction (= 0 if JJ = II)
	46-50	(I)	Element number increment in KK-direction (= 0 if KK = II)

Cols. 51-55 (I) Element nodal point increment in JJ-direction (= 0 if JJ = II)

56-60 (I) Element nodal point increment in KK-direction (= 0 if KK = II)

2.6 External Heat Flow or Nodal Temperature Cards (At Time Zero). This set of data is omitted if item 6 in Sec. 2.2 is zero. Otherwise, the number of nodal points in item 6 in Sec. 2.2 must be input. One card per nodal point, except when mesh generation option is used. These cards need not be input in numerical sequence.

Cols. 1- 5 (I) Nodal point I

6-10 (I) Nodal point J

11-15 (I) Increment between successive nodes

21-30 (F) Nodal temperature or external heat flow intensity or total solar radiation intensity in a day

If item 4 is the total solar radiation intensity in a day, then input the following:

31-40 (F) Time at sunrise (if 6:30 a.m., input 6.5)

41-50 (F) Time at sunset (if 6:30 p.m., input 18.5)

51-60 (F) Time at this moment

2.7 Convective Boundary Condition Cards. This set of data is omitted if item 4 in Sec. 2.2 is zero. Otherwise, the number of nodal points in item 4 (Sec. 2.2) must be input. One card per nodal point, except when mesh generation option is used. These cards need not be input in numerical sequence.

Cols. 1- 5 (I) Nodal point I

6-10 (I) Nodal point J

11-15 (I) Increment between successive nodes

21-30 (F) Film coefficient ($h_c = 0.663 + 0.133u$ where u = wind speed, mph)

2.8 Transient Information

2.8.1 Environmental Temperature Card. This data card is omitted if item 4 in Sec. 2.2 is zero.

Cols. 1-10 (F) Air temperature (^{o}F)

2.8.2 External Heat Flow or Nodal Temperature Cards. This set of data is omitted if item 4 in Sec. 2.6 is the total solar radiation intensity in a day. If item 4 in Sec. 2.6 is the external heat flow intensity, then input

Cols. 1-10 (F) Heat flow intensity (btu/ft^2/hr).

However, if item 4 in Sec. 2.6 is the specified nodal temperature, then input

Cols.	1- 5	(I) Nodal point I
	6-10	(I) Nodal point J
	11-15	(I) Increment between successive nodes
	21-30	(F) Nodal temperature.

Use of the Program SHELL8

3.1 Mesh Construction. A finite element mesh is obtained by subdividing the structure into quadrilateral or triangular elements. An example of a finite element mesh for a typical segment used in segmental bridge construction is shown in Fig 36. Element nodes lie in the mid-surface of the individual plates comprising the segment. Although the exact proportions of the individual elements are arbitrary, care should be taken to insure that the element proportions do not become overly exaggerated.

In this program, the frontal method is employed during the solution process (Ref 22). In this procedure, the element numbering, rather than nodal numbering, should run in the direction with the smallest number of elements, as shown in Fig 36. In this way, the maximum front width of the entire assemblage is minimized in order to reduce storage and computational efforts. The program is dimensioned for a maximum front width of 150 degrees-of-freedom (or 25 node points).

When the entire mesh or a portion of it has the same number of subdivisions in two directions throughout as shown in Fig 37, a reduction of the required input is possible. The assumed nodal and element numbering for a mesh of this type, which is referred to herein as a regular mesh, is illustrated in Fig 37. Element nodal point numbers for a regular mesh may be generated with a single input data card as described in Sec. 4.5. Element nodal points I, J, K, and L are numbered counterclockwise with node I having the smallest number as illustrated for element I in Fig 37 for a regular mesh. Regular meshes should be used when possible. This simplifies the required input, thereby reducing possibilities of error in preparing the input data.

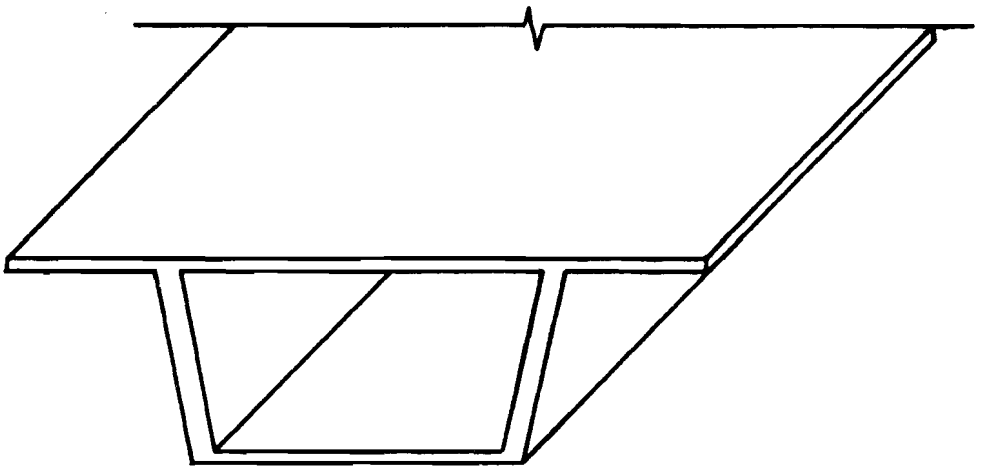

a. Partial three-dimensional view.

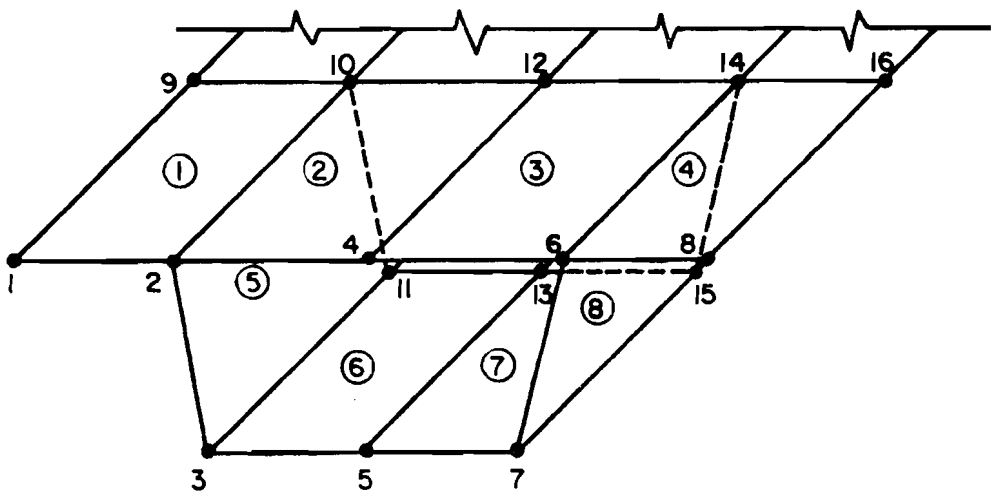

b. Partial finite element idealization.

Fig 36. Box girder bridge.

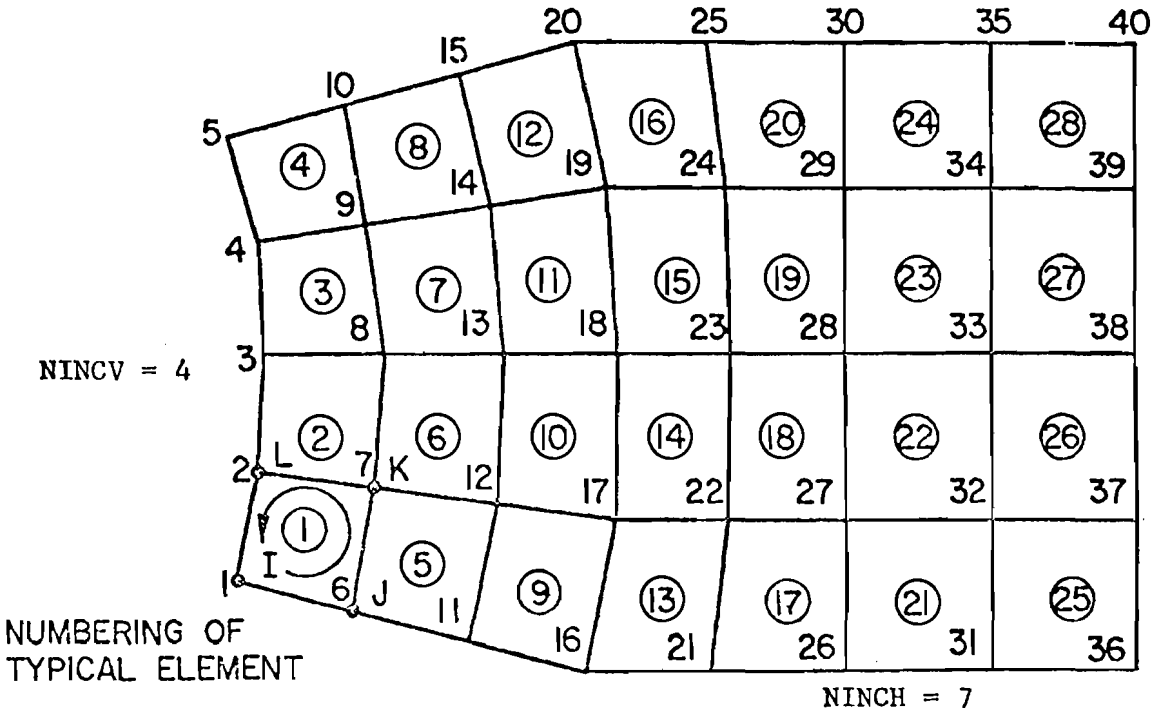

Fig 37. Regular mesh with nodal and element numbering.

Moreover, regular meshes usually result in minimum front width, hence reducing storage and the computation time for a given problem.

The mesh may require refinement, i.e., reduction in element size, in regions having steep stress and moment gradients. A regular mesh is graded by a gradual decrease in element sizes. In addition, a mesh may be graded by the use of triangular elements.

3.2 Coordinate Systems. A global coordinate system x, y, z , for example, as shown in Fig 38, must be chosen for the structure which is to be analyzed. This choice is arbitrary; however, simplification of input nodal coordinates usually dictates the proper orientation for this coordinate system.

Another set of coordinates ξ_1, ξ_2, and ξ_3 (Fig 38), called surface coordinates, must be selected. If IFLAG = 0 in Sec. 4.2, i.e. all translations and rotations are specified to be in global coordinates as is the usual case, then no input data is required. These coordinates are internally generated by the program to be in the global directions at all node points. However, if the structure is skewed, for example, then support boundary constraints should have directions other than those defined by the global coordinates. In this case, surface coordinates should be specified so that either ξ_1 or ξ_2 is normal to the skewed support in order to ensure zero rotation normal to that support (see also Appendix 2). In such problems, IFLAG = 1 in Sec. 4.2, and surface coordinates must be either generated (see Secs. 5.1 through 5.4) or input at each node point.

Local coordinates ($\bar{x}$, $\bar{y}$, and $\bar{z}$) for each triangle are constructed automatically by the program as shown in Fig 39. This coordinate system is referred to as element coordinates and is defined as follows: The axis $\bar{x}$ is directed along side I-J while the axis $\bar{y}$ is perpendicular to $\bar{x}$ and lies in the plane of the element and is directed toward node K. The axis $\bar{z}$ is constructed normal to the plane of the element to complete a right-handed system for the coordinates $\bar{x}$, $\bar{y}$, and $\bar{z}$.

Another local coordinate system (η_1 , η_2 , and η_3) for each quadrilateral is constructed automatically as shown in Fig 40. This coordinate system is referred to as η-coordinates and is constructed as follows. The coordinate η_1 bisects sides I-L and J-K, while η_2 bisects sides I-J and K-L. Positive directions for η_1 and η_2 are shown in Fig 40. Subsequently, η_3 is

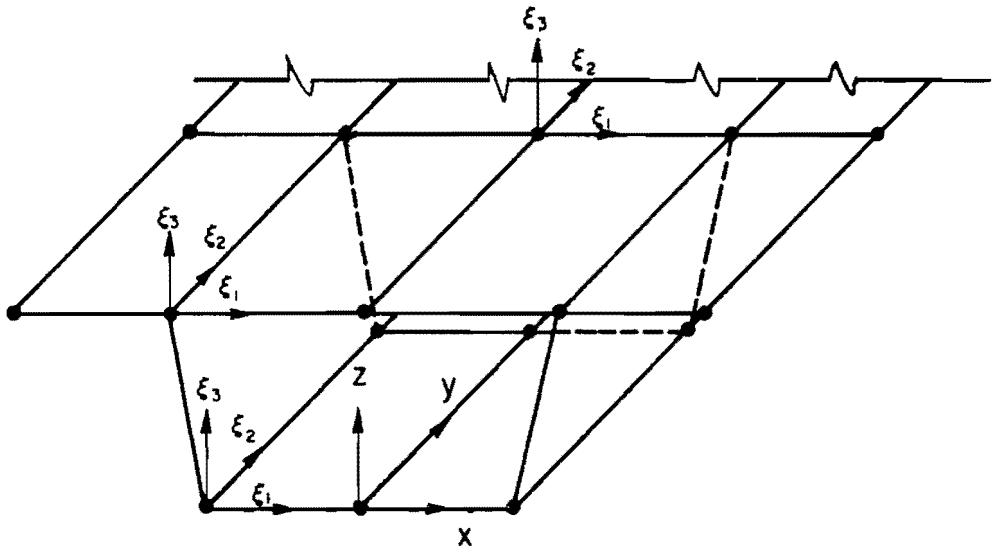

Fig 38. Surface coordinate systems for box girder bridge.

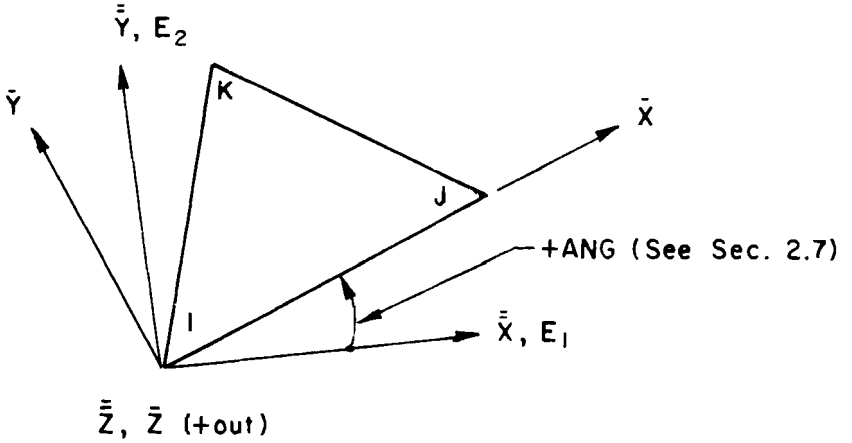

Fig 39. Definition of $\bar{x}$ - $\bar{y}$ coordinates for triangle and orientation of orthotropic moduli, E_1 and E_2 .

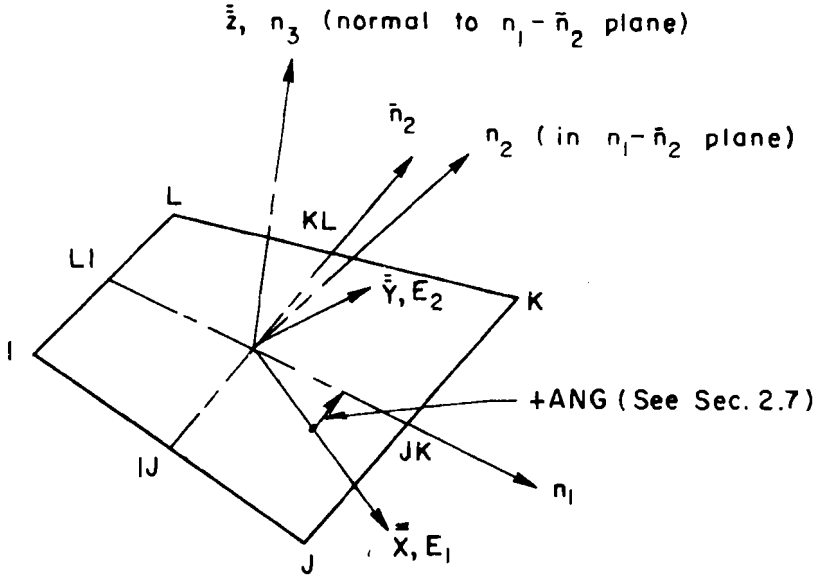

Fig 40. Definition of $\bar{r}$-coordinates for quadrilateral and orientation of orthotropic moduli, E_1 and E_2 .

constructed normal to the $\eta_1 - \eta_2$ plane and then η_2 is taken normal to the $\eta_1 - \eta_3$ plane to complete the right-handed system (η_1, η_2, η_3).

These two local systems, i.e., element and η-coordinates, must be considered in specifying orthotropic material orientations ($\bar{x}$ and $\bar{y}$) and element distributed loadings, and also in determining the orientations of stress and moment resultants which are output by the program.

3.3 Finite Element Types. In addition to a truss element, three types of finite elements are available in the program, all of which include membrane and bending stiffnesses.

a. Triangular Element
   Membrane stiffness . . . Constant strain triangle (CST)
   Bending stiffness . . . Fully compatible plate bending element after Hsieh, Clough and Tocher (HCT)

b. Nonplanar Quadrilateral Element
   Membrane stiffness . . . An assemblage of four linear strain triangles with linear displacements along exterior sides (CLST)
   Bending stiffness . . . An assemblage of four bending elements as per a

c. Planar Quadrilateral Element
   Membrane stiffness . . . A refined membrane element (QM5)
   Bending stiffness . . . Same as for nonplanar quadrilateral

d. One-Dimensional Element . . . Axial stiffness only

The superior stiffness properties of the quadrilateral versus the triangle motivate the general use of the quadrilateral.

3.4 Nodal Point Degrees of Freedom and Base Coordinates. A six-degree-of-freedom nodal point displacement system for the assemblage is utilized. These six degrees of freedom consist of three linear translations and three rotations, and are defined as follows:

D1 ≡ Translation in either global x-dir. or surface ξ_1-dir.,
D2 ≡ Translation in either global y-dir. or surface ξ_2-dir.,
D3 ≡ Translation in either global z-dir. or surface ξ_3-dir.,

D4 ≡ Rotation about either global x-dir. or surface ξ_1-dir.,
D5 ≡ Rotation about either global y-dir. or surface ξ_2-dir.,
D6 ≡ Rotation about either global z-dir. or surface ξ_3-dir.

It should be noted that all translations and rotations are either in global coordinates or in surface coordinates.

3.5 Element Distributed Loads. Equivalent nodal forces are automatically generated for element unit weight and pressure load for each element of the assemblage. Only translational nodal force components are considered to result from element weight and pressure load. The element nodal forces are computed by assuming linear variations of in-plane and out-of-plane displacements over each triangle and each subelement of the quadrilateral. The nodal forces resulting from both shell weight and pressure will be superimposed onto input nodal forces.

Element unit weight is considered uniform over each triangle and each quadrilateral in the idealization, but may have a different value for each element. Element weight per surface area is computed by multiplying the element unit weight by the element thickness at each corner of the triangular element and each subelement of the quadrilateral. Therefore, a linear variation in element weight is accounted for in the program. Positive element weight is assumed to act in the positive global z-direction.

The pressure load is assumed to act normal to each triangular element. For the quadrilateral, the pressure load is assumed to act normal to each of the four subelements. Input positive pressure is assumed to act in the z-direction for the triangle while input positive pressure for the quadrilateral is assumed to produce loads in each subelement which act in the positive η_3 direction for a planar quadrilateral. For a nonplanar quadrilateral, positive pressure on each subelement produces loads which have positive components in the direction of η_3 ; however, in this case, components will result in the $\eta_1 - \eta_2$ plane, since the normal component for each subelement is not exactly parallel to η_3 . The pressure load may vary linearly over each triangular element and linearly over each subelement of the quadrilateral since the pressure at the central interior node is taken as the average of the pressure at the four exterior nodes. See Figs 39 and 40 for triangular and quadrilateral coordinate definition.

Temperature effects are accounted for by computing "equivalent" element nodal point forces from the specified temperature distribution. Shapes of temperature distribution over the bridge depth depend mainly on its conduction property. A steel beam, for example, because of its high thermal conductivity, will quickly reach the temperature of the surrounding air. However, this is not true for a concrete beam. Nonlinear temperature distribution is usually found in the concrete structures as a result of its low thermal conductivity. In this program, expressions for the "equivalent" forces are based on the quartic approximation of the temperature distribution through the thickness of each element and a linear approximation to the temperature distribution over the surface of each element. These approximations give a more accurate representation of the nonlinear temperature distribution in concrete structures than the approximation based on a linear temperature distribution over the depth of each element.

In order to define a quartic temperature distribution, five different temperatures over the thickness of the element need to be input at each node point. Input nodal temperatures may be specified by either node points or elements (see Sec. 4.9). When nodal temperatures are input by node points, the corners of elements sharing a common node have the same temperature. The corners of elements sharing a common node could have different temperatures by specifying nodal temperatures by elements.

3.6 Orthotropic Material Properties. The principal elastic axes for the orthotropic properties are $\bar{x}$, $\bar{y}$, and $\bar{z}$, as shown in Figs 39 and 40. The principal elastic axes may have arbitrary orientation with respect to the quadrilateral and triangular coordinates as shown in Figs 39 and 40. The angle, ANG , between the principal elastic axes and element coordinates is measured from the principal elastic axis, $\bar{x}$ to η_1 and $\bar{x}$ for the quadrilateral and triangle, respectively. Positive angles are indicated in Figs 39 and 40.

The stress-strain relation referred to the principal elastic axes is

$$\begin{Bmatrix} \sigma_{\bar{\bar{x}}} \\ \sigma_{\bar{\bar{y}}} \\ \tau_{\bar{\bar{x}}\bar{\bar{y}}} \end{Bmatrix} \quad \begin{bmatrix} E_1/X & E_2\nu_{12}/X & \cdot \\ E_1\nu_{21}/X & E_2/X & \cdot \\ \cdot & \cdot & G_{12} \end{bmatrix} \quad \begin{Bmatrix} \epsilon_{\bar{\bar{x}}} \\ \epsilon_{\bar{\bar{y}}} \\ \gamma_{\bar{\bar{x}}\bar{\bar{y}}} \end{Bmatrix}$$

where

E_1 , E_2 are principal elastic moduli in the $\bar{\bar{x}}$ and $\bar{\bar{y}}$ directions, respectively;

ν_{12} , ν_{21} = Poisson's ratios ($E_2\nu_{12} = E_1\nu_{21}$);

$X = (1 - \nu_{12}\nu_{21})$; and

G_{12} is the shear modulus.

To simplify the input, the following material constants will be defined:

$E = \sqrt{E_1E_2}$ mean modulus;

$\rho = E_1/E_2$ modulus ratio;

$\nu = \sqrt{\nu_{12}\nu_{21}}$ mean Poisson's ratio;

$\nu_{G12} = \left[E/(2G_{12})\right] - 1$ fictitious Poisson's ratio associated with G_{12} .

The in-plane stress-strain relation in the principal elastic axes becomes

$$\begin{Bmatrix} \sigma_{\bar{\bar{x}}} \\ \sigma_{\bar{\bar{y}}} \\ \tau_{\bar{\bar{x}}\bar{\bar{y}}} \end{Bmatrix} = \frac{E}{1-\nu^2} \begin{bmatrix} \sqrt{\rho} & \nu & \cdot \\ \nu & 1/\sqrt{\rho} & \cdot \\ \cdot & \cdot & \frac{1-\nu^2}{2(1+\nu_{G12})} \end{bmatrix} \begin{Bmatrix} \epsilon_{\bar{\bar{x}}} \\ \epsilon_{\bar{\bar{y}}} \\ \gamma_{\bar{\bar{x}}\bar{\bar{y}}} \end{Bmatrix}$$

The moment curvature relation is obtained by multiplying this matrix by $t^3/12$, where t is the plate thickness, and by associating a factor of two with the twisting curvature.

If the material is isotropic, $E_1 = E_2 = E$, $\nu_{12} = \nu_{21} = \nu = \nu_{G12}$ and $\rho = 1.0$. For the isotropic case, ANG (Figs 39 and 40) is arbitrary and should be input as zero or simply left blank.

Preparation of Input Data

Abbreviations: A = alphanumeric field
I = integer value (must be packed to the right of the field)
F = floating point number (must be punched with a decimal)

4.1 Title Card (A) - Alphanumeric information for problem identification

4.2 Control Card

Cols.				
1- 5	(I)	NUMEL	=	Number of elements (2000 max)
6-10	(I)	NUPTS	=	Number of nodal points (400 max)
11-15	(I)	NUBPTS	=	Number of points with displacement boundary conditions (100 max)
16-20	(I)	IBANDP	=	This field must be left blank.
21-25	(I)	NDFRE	=	Nodal point degrees of freedom ≡ 6
26-30	(I)	IFLAG	=	Base coordinates for translations: If 0, translations and rotations are in global coordinates. If 1, translations and rotations are in surface coordinates.
31-35	(I)	NUMAT	=	Number of different material types (30 max)
36-40	(I)	ISHEAR	=	This field must be left blank.
41-45	(I)	NRED	=	This field must be left blank.

Cols.	46-50	(I)	IREACT	This field must be left blank.
	51-55	(I)	LPROB	Specifies if another problem is to follow: If 0, this is the last problem. If 1, another problem follows.
	56-60	(I)	IGEN	IGEN, which may have values of 0, 1, 2, 3, or 4, governs the level of output desired - for example, when IGEN = 0, maximum amount of output is obtained; when IGEN = 4, minimum amount of output is obtained.
	61-65	(I)	ISIG	Specifies whether element stress and moment resultants or element stresses and principal stresses are to be printed. Refer to Appendix 2 for definitions of the quantities. If 0, stress and moment resultants are printed. If 1, stresses and principal stresses are printed.
	66-70	(I)	IROT	Fictitious rotational stiffness: when IROT = 0 , fictitious rotational stiffness is considered; when IROT = 1 , it is not considered.
	71-75	(I)	ITEMP	Element or nodal point temperature desired to be input. If 0, nodal point temperatures are to be input.

			If 1, element temperatures are to be input.
76-80	(I)	NLVT	Must be 1.

4.3 Nodal Coordinate Cards. One card per nodal point, except when mesh generation options are used. These cards need not be input in numerical sequence; however, the node having the largest number must be input last.

Cols.	1- 5	(I)	Nodal point number
	21-30	(F)	Global x-coordinate
	31-40	(F)	Global y-coordinate
	41-50	(F)	Global z-coordinate

For generation options see Nodal Coordinate Generation (Secs. 5.1-5.6).

4.4 Surface Coordinate Direction Cosine Cards. The surface coordinate direction cosines as described in Sec. 3.2 are specified by this set of cards. From the input cosines described below, ξ_3 is automatically constructed by a cross-product of ξ_1 and $\overline{\xi}_2$, and ξ_2 is then determined by the cross-product of ξ_3 and ξ_1 to insure a right-handed orthogonal system.

If IFLAG in Sec. 4.2 is 0, then only the blank card is required to terminate this data set. Surface coordinates will be generated to be in the global directions at all node points.

If IFLAG in Sec. 4.2 is 1, then direction cosines must be specified for all node points. When the options of Secs. 5.1-5.6 are exercised, each point for which coordinates are generated will also be assigned direction cosines. If only some of the nodes are generated as per Secs. 5.1-5.6, the direction cosines must be input for all other nodes. These cards need not be input in numerical sequence. A blank card must be used to terminate this data set.

Cols.	1- 5	(I)	Nodal point number I
	6-10	(I)	LIM
	11-15	(I)	MOD
	21-30	(F)	Component in global x-dir. of unit vector ξ_1 *
	31-40	(F)	Component in global y-dir. of unit vector ξ_1
	41-50	(F)	Component in global z-dir. of unit vector ξ_1
	51-60	(F)	Component in global x-dir. of unit vector $\overline{\xi}_2$ **

Cols. 61-70 (F) Component in global y-dir. of unit vector $\bar{\xi}_2$

71-80 (F) Component in global z-dir. of unit vector $\bar{\xi}_2$

*If Cols. 21-50 are left blank, input cosines for ξ_1 are suppressed.

**If Cols. 51-80 are left blank, input cosines for $\bar{\xi}_2$ are suppressed.

The suppression option allows one to redefine one set of previously established cosines (either from input or generation options) without changing the other at a given point. Note that $\bar{\xi}_2$ is an approximate value to ξ_2.

If LIM > I and MOD > 0, then the direction cosines of points

I + MOD , I + 2*MOD , . . . , LIM

will be set equal to these specified for point I.

4.5 Element Nodal Point Number Cards. One card per element, except when mesh generation options are used. These cards need not be input in numerical sequence; however, the element having the largest number must be input last.

Cols. 1- 5 (I) Element Number N

6-10 (I) Element nodal point I

11-15 (I) Element nodal point J

**16-20 (I) Element nodal point K

*21-25 (I) Element nodal point L

26-30 (I) NINCV = number of elements in direction of nodal numbering; see Fig 37.

31-35 (I) NINCH = number of layers with similar element nodal numbering; see Fig 37.

*A triangular element is assumed if Cols. 21-25 are left blank.

**A truss element is assumed if Cols. 16-25 are left blank.

If NINCV > 0 and NINCH > 0, a regular mesh will be constructed for the quadrilateral elements N through N+NINCV*NINCH - 1, as shown in Fig 37. Care should be taken to order the node numbers I, J, K, and L for the N'th element as shown in Fig 37.

See Secs. 6.1-6.2 for additional generation options.

4.6 Element Material Table. One card per element type must be input. Material properties are assumed constant over each individual element. See Sec. 3.6 for definition of terms used below.

Cols. 1- 5 (I) Element material type

11-20 (F) Mean modulus = $\sqrt{E_1 E_2}$

Cols.	21-30	(F)	Modulus ratio = E_1/E_2
	31-40	(F)	Mean Poisson's ratio = $\sqrt{\nu_{12}\nu_{21}}$
	41-50	(F)	Fictitious Poisson's ratio = $\left[\sqrt{E_1E_2}/(2G_{12})\right] - 1$
	51-55	(F)	Field must be left blank
	56-60	(F)	Field must be left blank
	61-70	(F)	Thermal coefficient of expansion
	71-80	(F)	Initial temperature distribution - uniform temperature throughout the thickness and over the surface of the material (TINIT).

4.7 Element Property Cards. One card per element, except when mesh generation options are used. These cards need not be input in numerical sequence; however, the element having the largest number must be input last.

Cols.	1- 5	(I)	Element number N
	6-10	(I)	Element material type (see Sec. 4.6)
	11-15	(I)	LIM
	16-20	(I)	MOD
	21-25	(I)	Specifies type of membrane stiffness for the quadrilateral. If 0, four CLST's are used (see Sec. 3.3b). If 1, a QM5 is used (see Sec. 3.3c).
	31-40	(F)	Thickness at node I (or cross-sectional area for a truss member)
	41-50	(F)	Thickness at node J
	51-60	(F)	Thickness at node K
	61-70	(F)	Thickness at node L
	71-80	(F)	ANG = Angle in degrees between principal elastic axis and element coordinates; see Figs 39 and 40.

If LIM > N and MOD > 0 , then the element type, thicknesses, and ANG of elements

N + MOD , N + 2*MOD , . . . , LIM

will be set equal to those specified for element N .

4.8 Element Distributed Load Cards. One card per element, except when mesh generation options are used. Loads acting on all elements must be specified (elements with zero loads must be included). These cards need not be input in numerical sequence; however, the element having the largest number must be input last.

Cols.	1- 5	(I)	Element number N
	6-10	(I)	LIM
	11-15	(I)	MOD
	21-30	(F)	Element unit weight (positive in global z-direction)
	31-40	(F)	Pressure at node I
	41-50	(F)	Pressure at node J
	51-60	(F)	Pressure at node K
	61-70	(F)	Pressure at node L

Note: See Sec. 3.5 for sign conventions.

If LIM > N and MOD > 0 , then the element unit weight and pressures of elements

$$N + MOD \ , \ N + 2*MOD \ , \ . \ . \ . \ , \ LIM$$

will be set equal to those specified for element N .

4.9 Nodal Temperature Cards. If ITEMP = 0 as specified in Sec. 4.2, item 15, then temperatures must be input by nodal point numbers for all nodal points. If NLVT = 0 , then all nodal point temperatures must be input as zero.

Cols.	1- 5	(I)	Nodal point number I
	6-10	(I)	LIM
	11-15	(I)	MOD
	21-30	(F)	Temperature at top surface at node I (TT)
	31-40	(F)	Temperature at $t/4$ below top surface at node I (TT4)
	41-50	(F)	Temperature at $t/2$ below top surface at node I (TM)
	51-60	(F)	Temperature at $3t/4$ below top surface at node I (TB4)
	61-70	(F)	Temperature at bottom surface at node I (TB)

A blank card must follow this data set.

If ITEM = 1 , then temperatures are input by elements with four cards required for each generation.

Element Temperature Generation (4 cards):

Card 1	Cols.	1- 5	(I)	Element number
		6-10	(I)	LIM
		11-15	(I)	MOD
		21-30	(F)	TT at node I of element generated
		31-40	(F)	TT4 at node I of elements generated
		41-50	(F)	TM at node I of elements generated
		51-60	(F)	TB4 at node I of elements generated
		61-70	(F)	TB at node I of elements generated
Card 2	Cols.	21-30	(F)	TT at node J of elements generated
		31-40	(F)	TT4 at node J of elements generated
		41-50	(F)	TM at node J of elements generated
		51-60	(F)	TB4 at node J of elements generated
		61-70	(F)	TB at node J of elements generated
Card 3	Cols.	21-30	(F)	TT at node K of elements generated
		31-40	(F)	TT4 at node K of elements generated
		41-50	(F)	TM at node K of elements generated
		51-60	(F)	TB4 at node K of elements generated
		61-70	(F)	TB at node K of elements generated
Card 4	Cols.	21-30	(F)	TT at node L of elements generated
		31-40	(F)	TT4 at node L of elements generated
		41-50	(F)	TM at node L of elements generated
		51-60	(F)	TB4 at node L of elements generated
		61-70	(F)	TB at node L of elements generated

Temperatures must be generated for all elements. A blank card must follow this data set.

The temperature input in Sec. 4.9 will be reduced by subtracting TINIT in Sec. 4.6 to determine the temperature change from the original uniform temperature distribution for each material type.

If LIM > I and MOD > 0 , then the temperature at points

I + MOD , I + 2*MOD , . . . , LIM

will be set equal to those specified for Node I. Temperatures need not be input in numerical sequence but they must be specified for all nodes. A blank card must be used to terminate this data set.

4.10 Boundary Condition Cards. One card per nodal point having a specified displacement component (whether zero or nonzero), except when mesh generation options are used. Boundary condition cards need not be input in numerical sequence. The six degrees of freedom are ordered as follows:

Cols.	1- 5	(I)	Nodal point number I
	7	(I)	1 for specified value for D1; 0 otherwise
	8	(I)	1 for specified value for D2; 0 otherwise
	9	(I)	1 for specified value for D3; 0 otherwise
	10	(I)	1 for specified value for D4; 0 otherwise
	11	(I)	1 for specified value for D5; 0 otherwise
	12	(I)	1 for specified value for D6; 0 otherwise
	13-15	(I)	LIM
	16-18	(I)	MOD
	21-30	(F)	Specified value* for D1
	31-40	(F)	Specified value for D2
	41-50	(F)	Specified value for D3
	51-60	(F)	Specified value for D4
	61-70	(F)	Specified value for D5
	71-80	(F)	Specified value for D6

*Specified value may be nonzero.

If LIM > I and MOD > 0 , then values for points

I + MOD , I + 2*MOD , . . . , LIM

will be set equal to those specified for element I.

4.11 Control Card for Elastic Supports

Cols.	1- 5	(I)	Number of points with elastic supports (max 50)

4.12 Spring Constant Cards. If the number of points with elastic springs is specified as zero, no cards are required for this set. These cards need not be input in numerical sequence.

Cols.	1- 5	(I)	Nodal point number I
	6-10	(I)	LIM
	11-15	(I)	MOD
	21-30	(F)	Spring constant for D1 displacement
	31-40	(F)	Spring constant for D2 displacement
	41-50	(F)	Spring constant for D3 displacement
	51-60	(F)	Spring constant for D4 rotation
	61-70	(F)	Spring constant for D5 rotation
	71-80	(F)	Spring constant for D6 rotation

If LIM > 1 and MOD > 0 , then values for points

I + MOD , I + 2*MOD , . . . , LIM

will be set equal to those specified for node I. This set is terminated when the number of points specified in Sec. 4.11 has been input.

4.13 Control Card for Nodal Point Loads. Only one load case for a single problem is allowed. A blank card must follow this card.

Cols.	1- 5	(I)	Must be 1
	6-10	(I)	Number of loaded nodes

Joints with all six applied force components equal to zero need not be included as a loaded joint. Nodal forces are input as described below.

4.14 Nodal Point Load Cards. Input nodal forces correspond in an energy sense to the nodal point displacement components, i.e., $P_i D_i$, $i = 1, 6$. The number of input cards for the load case must equal the number specified in Sec 4.13 above, except when mesh generation options are used. The input format for the load case is as follows:

Cols.	1- 5	(I)	Nodal point number I
	6-10	(I)	LIM
	11-15	(I)	MOD
	21-30	(F)	Value of P1 which corresponds to D1
	31-40	(F)	Value of P2 which corresponds to D2
	41-50	(F)	Value of P3 which corresponds to D3

Cols.	51-60	(F)	Value of P4 which corresponds to D4
	61-70	(F)	Value of P5 which corresponds to D5
	71-80	(F)	Value of P6 which corresponds to D6

These cards need not be input in numerical sequence.

If LIM > I and MOD > 0 , then loads for points

$$I + MOD \ , \ I + 2*MOD \ , \ . \ . \ . \ , \ LIM$$

will be set equal to those specified for point I.

Nodal Coordinate Generation

The previous section provided a general input format by which all the information which is necessary to completely define a given problem is input via data cards. The generation options in Secs. 5.1-5.6 and Secs. 6.1-6.2 are intended to simplify and to reduce the amount of that required input.

Six types of automatic generation options are available. The first four types treat surface generations which occur frequently in structures; straight lines, circular arcs, parabolas and ellipses. Nodal numbering along each generator must be in increasing order and the difference between adjacent nodes must be constant over the entire generator. The fifth and sixth types of generation are useful when the coordinates of a set of points may, by constant increments (in nodal numbering and global coordinates), be defined from a previous set of points which have been input.

If any of these six types of generation are used, then two sets of direction cosines are generated. The procedure for the generation of these direction cosines is described below for each type of coordinate generation. In many cases, these generated direction cosines will correspond with the chosen surface coordinates ξ_1 and ξ_2 , thereby eliminating the need of inputting these direction cosines; in other cases, the generated direction cosines will have to be replaced by manually computed values.

5.1 Straight Line (Fig 41)

Cols.	1- 5	(I)	Node I of straight line
	6-10	(I)	Node J of straight line
	11-15	(I)	Increment between successive nodes ≡ K
	20	(I)	= 1
	21-30	(F)	Global x-coordinate of point I
	31-40	(F)	Global y-coordinate of point I

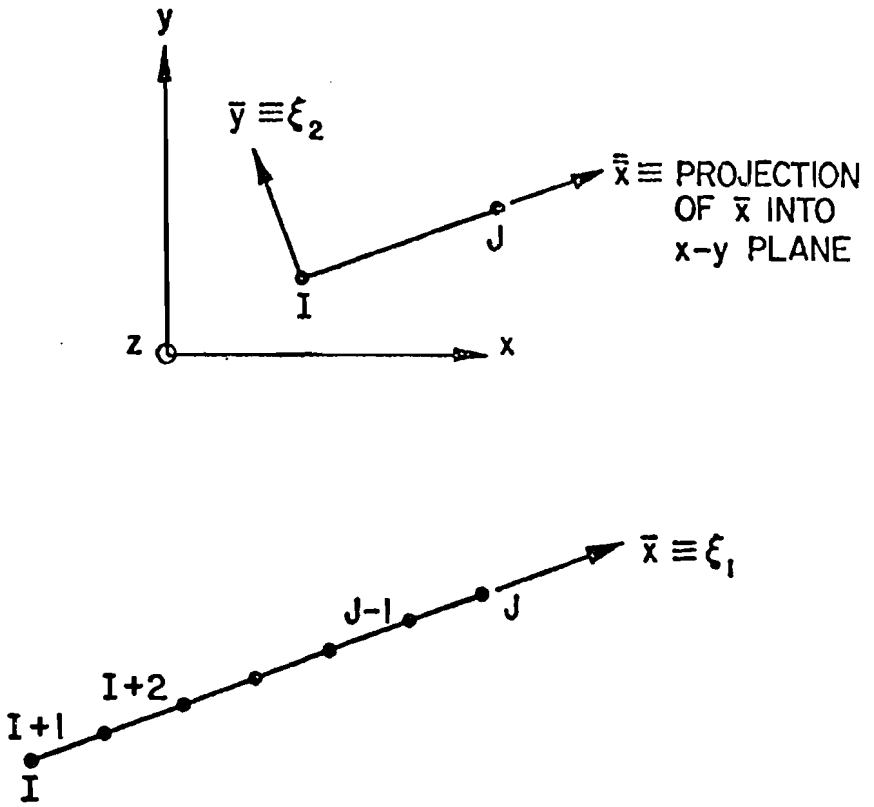

Fig 41. Straight line.

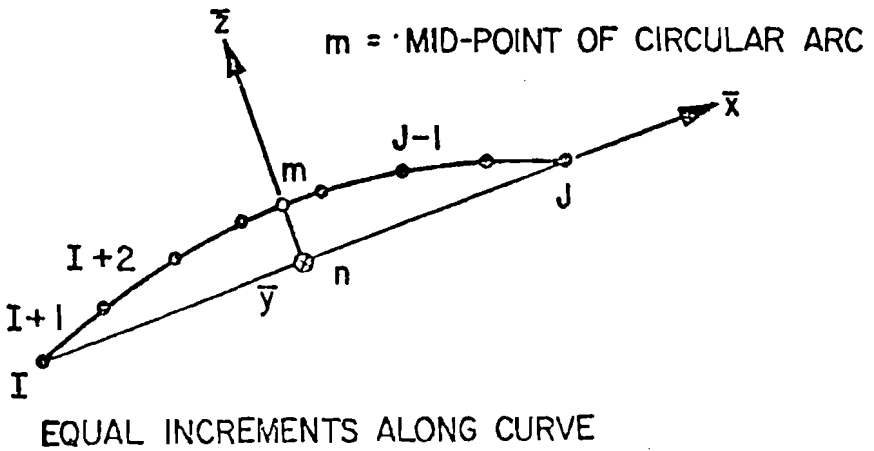

Fig 42. Circular arc.

Cols.	41-50	(F)	Global z-coordinate of point I
	51-60	(F)	Global x-coordinate of point J
	61-70	(F)	Global y-coordinate of point J
	71-80	(F)	Global z-coordinate of point J

The straight line is subdivided into (J-I)/K equal parts and the intermediate global nodal coordinates are computed.

The two sets of direction cosines are computed by

a. Assuming ξ_1 is in the direction from point I to point J.
b. Assuming ξ_2 lies in the x-y plane and is normal to the line obtained by projecting line I-J onto the x-y plane, i.e., $\xi_2 \equiv \bar{y}$ (Fig 41), and by ensuring a right handed system for $\bar{x}$, $\bar{y}$, $\bar{z}$.

For example, if the numbering had required a reversed direction for $\bar{x}$ and hence ξ_1, then $\bar{y}$ and ξ_2 would be reversed in order to maintain a right-handed system without changing the direction of ξ_3. In the case where ξ_1 is parallel to z (either direction), then ξ_2 is assumed to be in the same direction as the global y-coordinate.

5.2 Circular Arc (Fig 42) (Two cards)

Card 1

Cols.	1- 5	(I)	Node I of circular arc
	6-10	(I)	Node J of circular arc
	11-15	(I)	Increment between successive nodes ≡ K
	20	(I)	= 2
	21-30	(F)	Global x-coordinate of point I
	31-40	(F)	Global y-coordinate of point I
	41-50	(F)	Global z-coordinate of point I
	51-60	(F)	Global x-coordinate of point m
	61-70	(F)	Global y-coordinate of point m
	71-80	(F)	Global z-coordinate of point m

Card 2

Cols.	21-30	(F)	Global x-coordinate of point J
	31-40	(F)	Global y-coordinate of point J
	41-50	(F)	Global z-coordinate of point J

The circular arc is subdivided into (J-I)/K parts of equal arc length and the intermediate global nodal coordinates are computed. The local right-handed Cartesian coordinate system $\bar{x}$, $\bar{y}$, $\bar{z}$ is constructed as follows:

a. $\bar{x}$ is positive from I to J.

b. $\bar{z}$ is positive from n, a point equidistant from I and J, to point m, the midpoint of the circular arc.

c. $\bar{y}$ is established by a cross-product of $\bar{x}$ and $\bar{z}$ (+inward as shown in Fig 42).

Surface coordinate direction cosines are computed by assuming

d. ξ_1 lies in the plane $\bar{x}$-$\bar{z}$ and is tangent to the circular arc at each node. It is directed along the arc going from I to J.

e. ξ_2 is assumed to be in the positive direction of $\bar{y}$. Note that if the nodal point numbers had increased from right to left in Fig 42, $\bar{y}$, and hence ξ_2, would be positive outward.

The circular arc may have an arbitrary orientation with respect to the global coordinates.

5.3 Parabola (Fig 43) (Two cards)

Card 1

Cols.	1- 5	(I)	Node I of parabola
	6-10	(I)	Node J of parabola
	11-15	(I)	Increment between successive nodes = K
	20	(I)	= 3
	21-30	(F)	Global x-coordinate of origin point O
	31-40	(F)	Global y-coordinate of origin point O
	41-50	(F)	Global z-coordinate of origin point O
	51-60	(F)	Local $\bar{x}$-coordinate of point I
	61-70	(F)	Local $\bar{x}$-coordinate of point J
	71-80	(F)	Largest absolute value of $\bar{z}_i$ and $\bar{z}_j$

Card 2

Cols.	21-30	(F)	Counterclockwise angle ω (in degrees) from x to $\bar{x}$

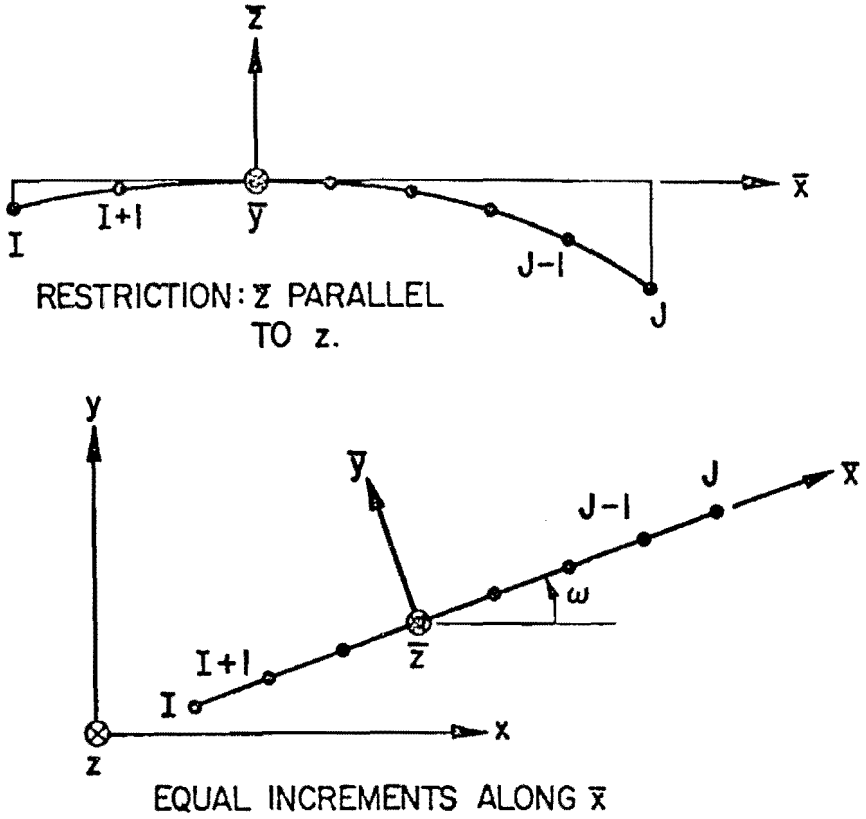

Fig 43. Parabola.

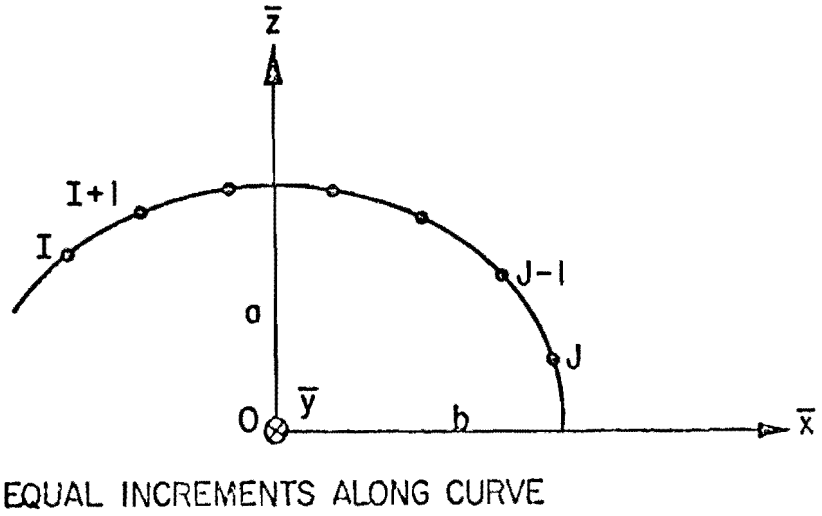

Fig 44. Ellipse.

The horizontal distance between I and J is subdivided into (J-I)/K equal intervals and the intermediate global nodal coordinates are computed.

The local coordinate system $\bar{x}$, $\bar{y}$, and $\bar{z}$ is constructed as follows:

a. $\bar{x}$ is positive in the direction from I to J.

b. $\bar{z}$ is parallel and in the same direction as z.

c. $\bar{y}$ forms a counterclockwise angle of $\omega + 90^{o}$ from the global x-axis.

Surface coordinate direction cosines are computed by assuming

d. ξ_1 lies in the plane $\bar{x}$-$\bar{z}$ and is tangent to the parabola at each node. It is directed along the parabola going from I to J.

e. ξ_2 is parallel to and in the same direction as $\bar{y}$.

5.4 Ellipse (Fig 44) (Two cards)

Card 1

Cols.	1- 5	(I)	Node I of ellipse
	6-10	(I)	Node J of ellipse
	11-15	(I)	Increment between successive nodes ≡ K
	20	(I)	= 4
	21-30	(F)	Global x-coordinate of origin point O
	31-40	(F)	Global y-coordinate of origin point O
	41-50	(F)	Global z-coordinate of origin point O
	51-60	(F)	Local $\bar{x}$-coordinate of point I
	61-70	(F)	Local $\bar{x}$-coordinate of point J
	71-80	(F)	Distance, a , from O to ellipse along $\bar{z}$

Card 2

Cols.	21-30	(F)	Distance, b , from O to ellipse along $\bar{x}$
	31-40	(F)	Counterclockwise angle from x to $\bar{x}$ in degrees

The ellipse arc length between nodes I and J is subdivided into (J-I)/K equal arc lengths and the intermediate global nodal coordinates are computed.

The local coordinate system $\bar{x}$, $\bar{y}$, and $\bar{z}$ is constructed as follows:

a. $\bar{x}$ is positive in the direction from I to J.

b. $\bar{z}$ is parallel and in the same direction as z.

c. $\bar{y}$ forms a counterclockwise angle of $\omega + 90^{o}$ from the global x-axis.

Surface coordinate direction cosines are computed by assuming

d. ξ_1 lies in the plane $\bar{x}$-$\bar{z}$ and is tangent to the ellipse at each node. It is directed along the parabola going from I to J.

e. ξ_2 is parallel to and in the same direction as $\bar{y}$.

Restriction: $\bar{z}$ must be parallel to the global z-axis and angle $IOJ < 180^{o}$.

5.5 Incremental Generation - Type 1

Cols.			
	1- 5	(I)	Node I of generator
	6-10	(I)	Node J of generator
	11-15	(I)	-MOD, where MOD = nodal difference of adjacent generators
	16-20	(I)	-LIM, where LIM = number of new lines to be generated
	21-30	(F)	XINC = Increment in x-dir. from old to new generator
	31-40	(F)	YINC = Increment in y-dir. from old to new generator
	41-50	(F)	ZINC = Increment in z-dir. from old to new generator

This card causes (J-I)*LIM points to be generated as follows:

$$X_K = X_{K-MOD}+XINC*L \qquad (\xi_1)_K = (\xi_1)_{K-MOD}$$

$$Y_K = Y_{K-MOD}+YINC*L \quad \text{and} \quad (\xi_2)_K = (\xi_2)_{K-MOD}$$

$$Z_K = Z_{K-MOD}+ZINC*L \qquad (\xi_3)_K = (\xi_3)_{K-MOD}$$

where L = 1 , 1 , LIM , and K = (I+MOD*(L-1)) , 1 , (J+MOD*(L-1)) .

This option assumes that XINC, YINC, and ZINC are constant for all generators considered. Also, nodal numbering as for a regular mesh is assumed as shown in Fig 45. Assuming that Line 1 (Fig 45) had been generated, then the following would generate the remaining Lines 2-6:

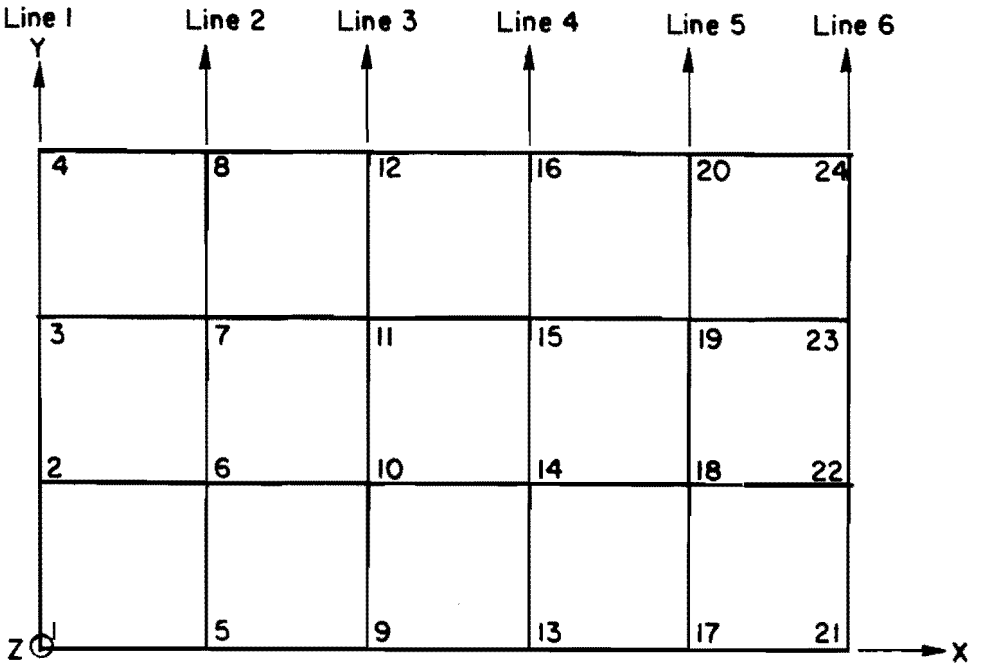

Fig 45. Sample for nodal point generation.

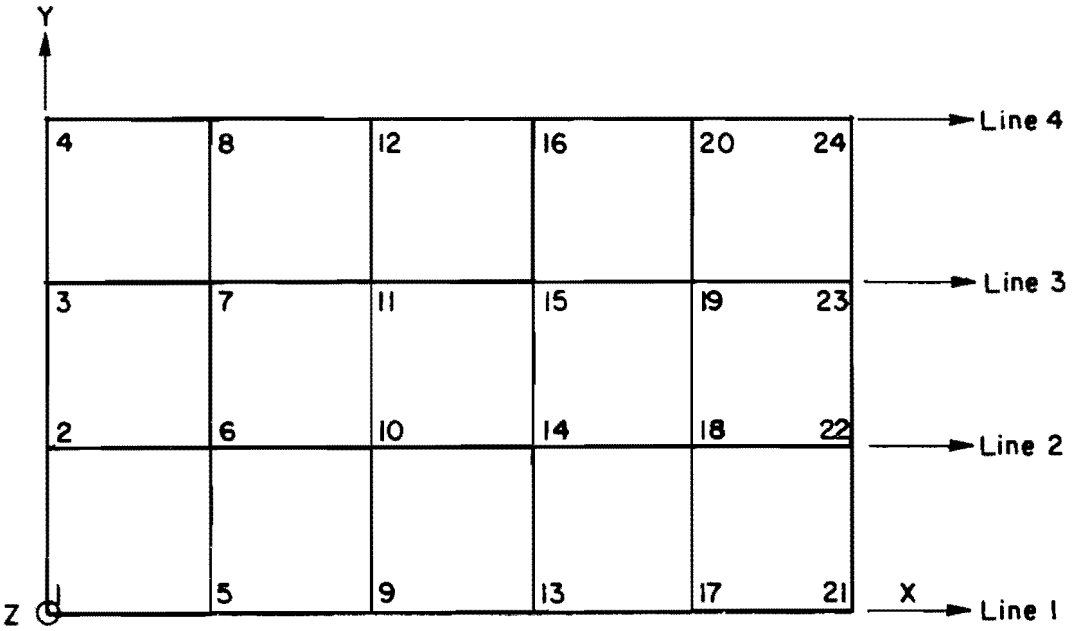

Fig 46. Sample for nodal point generation.

I = 5 , J = 8 , MOD = 4 , LIM = 5 and

XINC = X_5-X_1 , YINC = Y_5-Y_1 , ZINC = Z_5-Z_1 .

5.6 Incremental Generation - Type 2

Cols. 1- 5 (I) Node I of generator
6-10 (I) Node J of generator
11-15 (I) MOD (same as for Type 1)
16-20 (I) -LIM, where LIM = number of new lines to be generated
21-30 (F) XINC
31-40 (F) YINC } same as for Type 1
41-50 (F) ZINC

This card causes ((J-I)/MOD)*MOD*LIM points to be generated as follows:

$X_K = X_{K-1}+XINC*L$ $\qquad$ $(\xi_1)_K = (\xi_1)_{K-1}$

$Y_K = Y_{K-1}+YINC*L$ $\qquad$ and $\qquad$ $(\xi_2)_K = (\xi_2)_{K-1}$

$Z_K = Z_{K-1}+ZINC*L$ $\qquad$ $(\xi_3)_K = (\xi_3)_{K-1}$

where L = 1 , 1 , LIM and K = (I+L-1) , MOD , (J+L-1) .

As for Type 1, a regular mesh is assumed as shown in Fig 46; however, Type 2 generates lines opposite to the direction of nodal numbering. Assuming that Line 1 (Fig 46) had been generated, then the following would generate the remaining Lines 2-4:

I = 2 , J = 22 , MOD = 4 , LIM = 3 .

Element Nodal Point Number Generation

6.1 Type 1. If M element cards are omitted with NINCV = NINCH = 0 in Sec. 4.5 these missing elements will be generated by increasing the nodal numbers I, J, K, L of each of the preceding elements by 1.

6.2 Type 2. If on the card for element N (Sec. 4.5) we specify

Cols. 26-30 (I) -MOD
31-35 (I) NLAY
36-40 (I) LASTEL

then elements N + NLAY , N + 2N*LAY , . . . , LASTEL will be constructed by adding MOD to the nodal numbers of each preceding element. If LASTEL equals NUMEL , the input of the element nodal point numbers will be terminated.

CHAPTER 5. SUMMARY AND CONCLUSIONS

General

This research has focused on establishing typical magnitudes of temperature induced stresses and movements in highway bridges caused by daily variations of temperature representative of the state of Texas. Computer programs were developed for predicting temperature induced stresses and were correlated with experimental data from two field tests. Further, they were used to access the role of temperature in three typical highway bridge types: (1) post-tensioned concrete slab bridges; (2) composite precast pretensioned bridges; and (3) composite steel bridges. Environemntal data for six locations in the state of Texas (Austin, El Paso, Brownsville, Fort Worth, Midland, and San Antonio) were obtained to study the influence of bridge location on thermal stresses. Results for three of these locations (Austin, El Paso, and Brownsville) are presented in this report. In the various analyses structural response was assumed to be in the elastic range with the structural stiffness based on an uncracked section.

Environmental, Material and Geometric Variables

As a result of this research it may be concluded that the important environmental variables that affect bridge temperature are radiation, ambient air temperature and wind speed. Incoming solar radiation which increases the temperature on the top surface is the principal source of thermal stress during the day while outgoing radiation during the night decreases the temperature and leads to different forms of thermal stresses. Thermal behavior is amplified by increasing intensities of solar radiation and larger ranges of air temperature during a given day. Increasing wind speed serves to lower the temperature gradient and thus decrease the thermal stress. Thus extreme environmental conditions are considered to take place on a clear night followed by a clear still day with a large change in air temperature.

Important material thermal properties are stiffness, absorptivity, emissivity, and thermal conductivity.

Geometric variables which have an important effect on temperature induced stresses are depth and shape of the cross section and the flexural indeterminancy of the bridge. Thick sections with low thermal conductivity have a nonlinear distribution through their depth. The sun's rays heat the top surface more rapidly than the interior region causing the nonlinear temperature gradient and an upward curling of the bridge. The nonlinear temperature gradient thereby causes thermal stresses which are independent of the flexural indeterminancy of the bridge while additional flexural stresses take place in multispan bridges due to the restraint against upward curling offered by the interior supports. Composite steel bridges, on the other hand, behave differently when subjected to the same environmental conditions. This is due to the high conductivity of the steel causing it to respond quickly to air temperature and thereby decreasing the temperature differential over the depth.

Extreme Thermal Conditions

Based on this research, thermal effects appear to be more severe for bridges with low thermal conductivity having thick sections which are subjected to large intensities of solar radiation and large changes in air temperature over a given day. For weather conditions representative of Austin, Texas, predicted temperature induced tensile stresses in a prestressed concrete slab bridge and a composite precast pretensioned bridge were found (39) to be in the order of 60 to 80 percent respectively of the cracking stress of concrete suggested by the AASHTO Specifications. Compressive stresses as high as 40 percent of the allowable compressive strength were predicted in a prismatic thick slab having a depth of 17 inches. On the other hand, for a composite steel bridge temperature stresses were predicted to be approximately 10 percent of the design dead and live load stresses.

Thermal conditions are more severe for El Paso largely due to greater amounts of solar radiation. For example, for a uniform slab bridge with a depth of 17 inches, compressive stresses of 1000 psi and 1100 psi were predicted for Austin and El Paso, respectively, while corresponding tensile stresses were 330 psi and 410 psi. Tensile stresses in a precast pretensioned bridge were predicted to be 565 psi for Austin and 810 psi for El Paso. These thermal stresses are representative of an afternoon in the months of August in

Austin and June in El Paso. In general, it was found (39) that extreme summer conditions which result in compression at the top of the section with tension in the lower regions occur in June or August while extreme reverse conditions take place in January. Investigations carried out for a skewed three span slab bridge with a uniform thickness of 18 in. yielded a small increase in tensile stresses (about 15 percent) for the extreme summer conditions while compressive stresses were increased by about 28 percent.

Finite Element Procedures

As a result of this research two computer programs, TSAP and SHELL8, were developed and adapted to the IBM computer facilities of the Texas State Department of Highways and Public Transportation for ongoing use. In each case temperature distribution is predicted by using a two-dimensional finite element model. Required inputs consist of either surface temperatures or environmental data (i.e., solar radiation intensity, ambient air temperature and wind speed). In TSAP temperature induced stresses are computed from beam theory. On the other hand, SHELL8 utilizes two-dimensional finite elements in a three-dimensional global assemblage with six degrees of freedom at each nodal point. Thermal forces are calculated from a quartic distribution of temperature through the thickness of each element. TSAP provides a versatile and economical method for predicting thermal stress in regular sections with orthogonal supports. Although greater amounts of data and computer time are required, the use of program SHELL8 is required for more complex sections with skewed supports.

Field Tests and Correlation

Field tests were performed on two bridges located in the state of Texas to determine temperature induced slope changes and surface temperatures. A portable temperature probe was used to measure surface temperatures while a mechanical inclinometer was used to measure slope changes on the top surface of the two bridges. The first bridge tested was a skewed, post-tensioned, three-span continuous slab bridge located in Pasadena, Texas. The test was conducted on 24 August 1974, a day with considerable cloudiness and heavy rain between 1615 and 1745 hours (CDT). Despite these undesirable testing

conditions for thermal effects, the thermal slope changes were of the same magnitude as the live load response observed in a previous test (30).

The second field test was performed on 14 March 1975 on a two-span structure with precast pretensioned beams made continuous for live load. This two girder bridge is a pedestrian overpass and is located in Austin, Texas. Surface temperature was complex in this narrow bridge due to the side heating of the two girders and partial shading of the top of the slab by the parapet. Thus surface temperatures were measured at 53 stations while slope changes were measured at only one location since one of the inclinometers malfunctioned. Correlations of measured slope changes and results from computer simulation were made for each field test. Measured surface temperatures were used to predict the internal temperature distributions. Static analysis programs were then used to computer thermal movements and stresses. Correlations of the measured slope changes and finite element results were considered to be satisfactory for both structures.

REFERENCES

1. American Association of State Highway Officials, Standard Specifications for Highway Bridges, AASHO, Washington, D.C., 1973.

2. American Association of State Highway and Transportation Officials, Interim Specifications for Bridges 1974, AASHTO, Washington, D.C., 1974.

3. American Association of State Highway and Transportation Officials, Interim Specifications for Bridges 1975, AASHTO, Washington, D.C., 1975.

4. Barber, E. S., "Calculation of Maximum Pavement Temperatures from Weather Reports," Bulletin 168, Highway Research Board, 1957.

5. Becker, E. B., and C. H. Parr, "Application of the Finite Element Method to Heat Conduction in Solids," Technical Report 5-117, U.S. Army Missile Command, Redstone Arsenal, Alabama, November 1968.

6. Berwanger, C., "Thermal Stresses in Composite Bridges," Proceedings, ASCE Specialty Conference on Steel Structures, Engineering Extension Series, No. 15, University of Missouri - Columbia, Columbia, Missouri, June 1970.

7. Billington, N. S., Thermal Properties of Buildings, Cleaver-Hume Press Ltd, 1952.

8. Boley, B., and J. Weiner, Theory of Thermal Stress, John Wiley and Sons, Inc., 1960.

9. Brisbane, J., "Heat Conduction and Stress Analysis of Anisotropic Bodies," Vol. 1, Rohm and Haas Company, Redstone Research Laboratories, Huntsville, Alabama, October 1969.

10. Capps, M. W. R., "The Thermal Behavior of Beachley Viaduct/Wye Bridge," RRL Report No. 234, Road Research Laboratory, Ministry of Transport, London, 1968.

11. Carslaw, H. S., and J. C. Jaeger, Conduction of Heat in Solids, Oxford University Press, Second Edition, London, 1959.

12. Climates of the States, Volume II, Western Series, U.S. Department of Commerce, 1974.

13. Clough, R. W., and J. L. Tocher, "Finite Element Stiffness Matrices for the Analysis of Plate Bending," Proceedings, Conference on Matrix Methods in Structural Mechanics, Air Force Institute of Technology, Wright-Patterson Air Force Base, Ohio, 1965.

14. Colville, J., "A General Solution of the Von Karman Plate Equations by the Finite Element Method," Ph.D. Dissertation, The University of Texas at Austin, 1970.

15. Cruz, Carlos, "Elastic Properties of Concrete at High Temperature," Journal of the PCA Research and Development Laboratories, January 1966.

16. Degelman, L. O., "The Mathematical Model for Predicting Solar Heat Gains through Building Walls and Roofs," Better Building Report No. 6, Pennsylvania State University, Institute for Building Research, June 1966.

17. Desai, C. S., and J. F. Abel, Introduction to the Finite Element Method, Van Nostrand Reinhold Company, 1972.

18. Doherty, W. P., E. L. Wilson, and R. L. Taylor, "Stress Analysis of Axisymmetric Solids Utilizing Higher Order Quadrilateral Finite Elements," SESM Report No. 69-3, University of California, Berkeley, 1966.

19. Emerson, M., "Bridge Temperatures and Movements in the British Isles," RRL Report LR 228, Road Research Laboratory, Ministry of Transport, Crowthorne, 1968.

20. Emerson, M., "The Calculations of the Distribution of Temperatures in Bridges," TRRL Report LR 561, Transport and Road Research Laboratory, Crowthorne, 1973.

21. Gloyne, R. W., "The Diurnal Variation of Global Radiation on a Horizontal Surface - With Special Reference to Aberdeen," Meteorological Magazine 101, 1972.

22. Irons, B. M., "A Frontal Solution for Finite Element Analysis," International Journal for Num. Math in Eng., Vol 2, 1970.

23. Johnson, C. P., "The Analysis of Thin Shells by a Finite Element Procedure," SEL Report No. 67-22, University of California, Berkeley, 1967.

24. Johnson, C. P., and H. Matlock, "Temperature Induced Stresses in Highway Bridges by Finite Element Analysis and Field Tests," Research Proposal, Project No. 3-5-73-23, Center for Highway Research, The University of Texas at Austin, 1973.

25. Johnson, C. P., T. Thepchatri, and K. Will, "Static and Buckling Analysis of Highway Bridges by Finite Element Procedures," Research Report No. 155-1F, Center for Highway Research, The University of Texas at Austin, 1973.

26. Jaber, M. M., D. W. Fowler, and D. R. Paul, "Repair of Concrete with Polymers," Research Report No. 114-3, Center for Highway Research, The University of Texas at Austin, 1975.

27. Khachaturian, N., and G. Gurfinkel, Prestressed Concrete, McGraw-Hill, 1969.

28. Krishnamurthy, N., "Temperature Effects on Continuous Reinforced Concrete Bridge," HPR Report No. 58, Alabama Highway Research, 1971.

29. Lin, T. Y., Design of Prestressed Concrete Structures, John Wiley & Sons, 1963.

30. Matlock, H., J. J. Panak, M. R. Vora, and J. H. C. Chan, "Field Investigation of a Skewed, Post-Stressed Continuous Slab Structure," Interim Study Report, Center for Highway Research, The University of Texas at Austin, 1970.

31. McCullough, B. F., A. Abou-Ayyash, R. Hudson, and J. Randall, "Design of Continuously Reinforced Concrete Pavements for Highways," Final Report, Research Project NCHRP 1-15, Center for Highway Research, The University of Texas at Austin, 1974.

32. "Polymer Impregnated Concrete: First Applications," Civil Engineering - ASCE, January 1974.

33. Proffitt, T. O., "Variations in Daily Solar Radiation at National Weather Service Observing Sites in Texas," ASG Report No. 27, The University of Texas at Austin, February 1971.

34. Radolli, M., and R. Green, "Thermal Stresses in Concrete Bridge Superstructures - Summer Conditions," Proceedings, 54th Annual Transportation Research Board Meeting, 1975.

35. Reynolds, J. C., and J. H. Emanuel, "Thermal Stresses and Movements in Bridges," Journal of the Structural Division, ASCE, January 1974.

36. Robinson, N., editor, Solar Radiation, Elsevier Publishing Company, 1966.

37. Rushing, H., and E. Leblanc, "Temperature Differential of Swingspan Bridges," Research Report No. 40, Louisiana Department of Highways, June 1969.

38. Strock, Clifford, editor, Handbook of Air Conditioning, Heating, and Ventilating, New York Industrial Press, 1965.

39. Thepchatri, Thaksin, C. Philip Johnson, and Hudson Matlock, "Prediction of Temperature and Stresses in Highway Bridges by a Numerical Procedure Using Daily Weather Reports," Research Report No. 23-1, Center for Highway Research, The University of Texas at Austin, February 1977.

40. Timoshenko, S., and J. N. Goodier, Theory of Elasticity, McGraw-Hill, 1970.

41. Wah, T., and R. E. Kirksey, "Thermal Characteristics of Highway Bridges," Final Report to Highway Research Board, Contract No. HR 12-4, Southwest Research Institute, San Antonio, Texas, July 1969.

42. Will, K. M., "Elastic Instability Analysis of Thin-Walled Structures by a Refined Element Procedure," CESM Report No. 71-2, The University of Texas at Austin, December 1971.

43. Will, Kenneth M., C. Philip Johnson, and Hudson Matlock, "Analytical and Experimental Investigation of the Thermal Response of Highway Bridges," Research Report No. 23-2, Center for Highway Research, The University of Texas at Austin, February 1977.

44. Willems, N., "Experimental Strain Analysis of Continuous Skew Slab Bridge Decks," Report No. HPR-SHC 71-3-F, State Highway Commission of Kansas, October 1973.

45. Wilson, E. L., "The Determination of Temperatures within Mass Concrete Structures," SEL Report No. 68-17, University of California, Berkeley, 1968.

46. Wilson, E. L., and R. E. Nickell, "Application of the Finite Element Method to Heat Conduction Analysis," Nuclear Engineering and Design, Vol 4, 1966.

47. Zienkiewicz, O. C., The Finite Element Method in Engineering Science, McGraw-Hill, 1971.

48. Zuk, W., "Thermal Behavior of Composite Bridges - Insulated and Uninsulated," Highway Research Record, No. 76, 1965.

49. Zuk, W., "Simplified Design Check of Thermal Stresses in Composite Highway Bridges," Highway Research Record, No. 103, 1965.

APPENDIX 1

APPENDIX 1. AN EXAMPLE PROBLEM FOR INPUT AND OUTPUT FOR PROGRAM TSAP

A one-span concrete slab and girder bridge subjected to daily temperature effects, as shown in Fig 47, was selected to illustrate the required input and the interpretation of output for program TSAP. The concrete was assumed to have a modulus of elasticity of 3,790,000 psi, a coefficient of thermal expansion of 0.000006, a density of 150 lb/cu.ft, a specific heat of 0.23 btu/lb/^{o}F, and a thermal conductivity of 0.81 btu/ft/hr/^{o}F.

By taking advantage of symmetry of the structure, only a small portion of the cross-section was used in the finite element idealization shown in Fig 48. This idealization included 34 elements and 49 nodal points.

Three sets of input data were used as shown in Tables 7, 8, and 9. The only change in the inputs appears on the transient boundary conditions for the nodal points with specified external heat flow or nodal temperature (fifth item of the second card). The first set of input data used the input option of external heat flow intensity. The second set used the input option of total solar radiation intensity in a day. In this case external heat flow intensity is internally computed by the program for each time increment. The third set of data used the option to input nodal temperatures for each time increment. Details of interpreting the resulting thermal stresses will be discussed later.

In preparing the input data it is advisable to use as many generation options as possible to minimize the coding time and reduce the coding errors.

With regard to the convective boundary cards, care must be exercised in specifying the correct boundary conditions. The element sides on the surface of the bridge transfer heat by air motion and therefore are convective boundaries. The effect of wind on the loss of heat by convection is included and the film coefficient as previously discussed in Chapter 2.

The transient information cards define the heat flow conditions at the nodal points with specified external heat flow or temperature. These cards need to be input for each time increment.

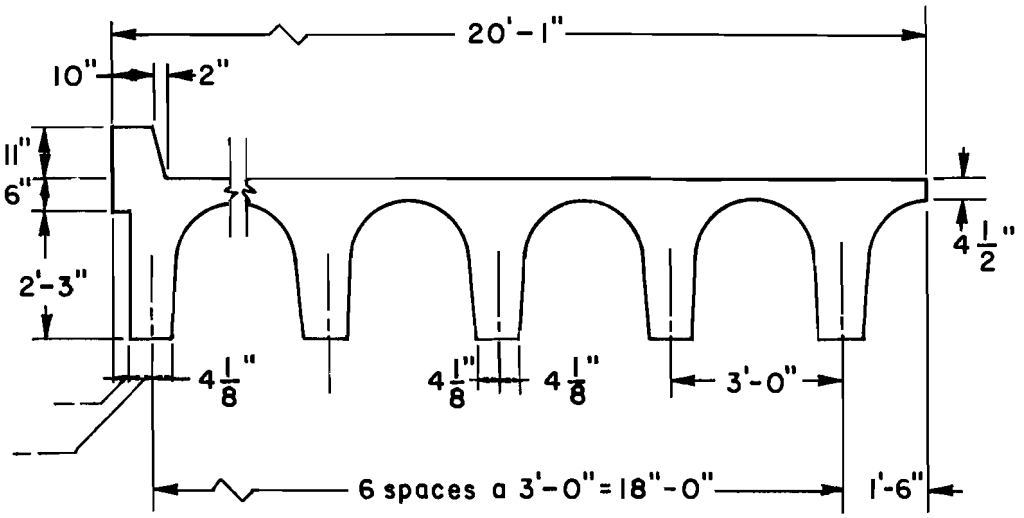

Fig 47. Typical cross-section of a concrete slab and girder bridge.

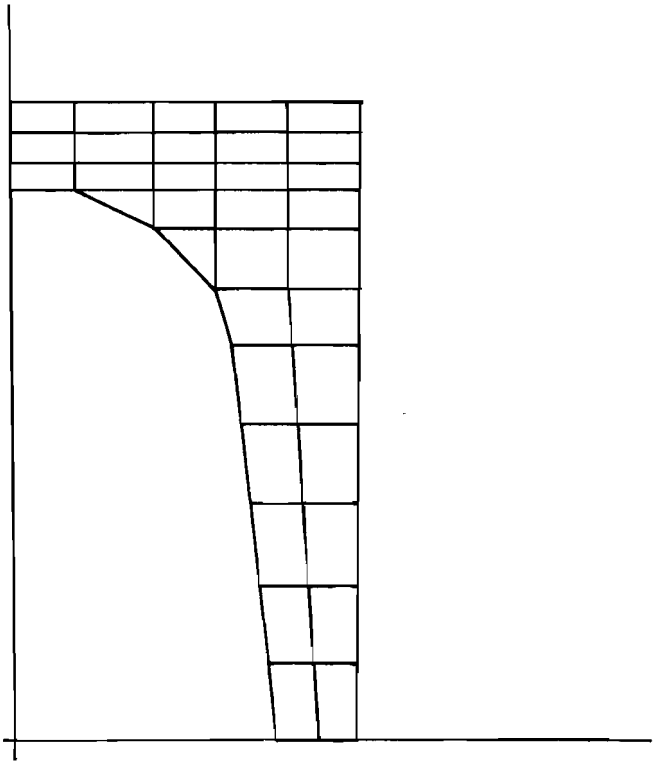

Fig 48. Finite element idealization of the bridge of Fig 47.

The output obtained by executing the first set of input data (Table 7) on the CDC 6600 at The University of Texas at Austin is contained in Tables 10 through 13. With regard to the second and third sets of input data, only the portions of the output relating to nodal temperatures and stresses is listed since the remaining output (except for the fifth and seventh items of the control card) would be identical to the first set of input data. These portions of output for the second and third sets of input data are contained in Tables 14 through 15 and 16 through 17 respectively.

The tenth item of the control card specifies the time interval for print of resulting nodal temperatures and stresses after each time step. If this item is input to be 1, then calculated nodal temperatures and stresses are printed at the end of each time step. If it is input to be 2, the print is obtained for every other time step. The output nodal stresses have the same units as the input modulus of elasticity. These stresses act on the cross-section in the direction parallel to the longitudinal axis of the bridge, i.e., normal to the cross-section. The sign conversion for stresses is (+) for tension and (-) for compression.

TABLE 7

```
&SAMPLE PROBLEM * TSAP * FT-BTU-FAHR-PSI * CODED BY A.YARGICOGLU
   49   34    1   16    0    6    5    1    0    1
 1.0        70.        0.5        0.9        -1.
    1
 0.81       0.81       0.0        0.23       150.0      0.0       3790000.    0.000006
    1    2   19    1    6
 0.0        2.75       0.25       2.75       0.0        2.375
    3    4   21    1    6
 0.5833     2.75       0.8333     2.75       0.5833     2.375
    5    6   23    1    6
 1.1667     2.75       1.5        2.75       1.1667     2.375
   25   25   25    0    0
 0.5833     2.2083
   26   28   29    1    3
 0.8333     2.2083     1.5        2.2083     0.8333     2.01247
   32   47   32    3    0
 0.9583     1.7083     1.3875     0.0        0.9583     1.7083
   33   48   33    3    0
 1.22915    1.7083     1.44375    0.0        1.22915    1.7083
   34   49   34    3    0
 1.5        1.7083     1.5        0.0        1.5        1.7083
    1    5   11    1    7    8    2    1    1    5    1    6
   16   16   16    1   25   21   20   25
   17   19   17    1   25   26   22   21    1    0    1
   20   20   20    1   29   26   25   29
   21   22   33    1   29   30   27   26    1    2    1    3
    1    6    1      229.5
    1    6    1      1.86
   19   20    1      1.86
   20   25    5      1.86
   25   29    4      1.86
   29   47    3      1.86
   47   49    1      1.86
 77.
 289.
 85.
 333.
 89.
 357.
 90.
357.
 92.
333.
&STOP
```

TABLE 8

```
SAMPLE PROBLEM * TSAP * FT-BTU-FAHR-PSI * CODED BY A.YARGICOGLU
   49   34    1   16    0    6    7    1    0    1
 1.0        70.        0.5        0.9        -1.
    1
 0.81       0.81       0.0        0.23       150.0      0.0       3790000.    0.000006
    1    2   19    1    6
 0.0        2.75       0.25       2.75       0.0        2.375
    3    4   21    1    6
 0.5833     2.75       0.8333     2.75       0.5833     2.375
    5    6   23    1    6
 1.1667     2.75       1.5        2.75       1.1667     2.375
   25   25   25    0    0
 0.5833     2.2083
   26   28   29    1    3
 0.8333     2.2083     1.5        2.2083     0.8333     2.01247
   32   47   32    3    0
 0.9583     1.7083     1.3875     0.0        0.9583     1.7083
   33   48   33    3    0
 1.22915    1.7083     1.44375    0.0        1.22915    1.7083
   34   49   34    3    3
 1.5        1.7083     1.5        0.0        1.5        1.7083
    1    5   11    1    7    8    2    1    1    5    1    6
   16   16   16    1   25   21   20   25
   17   19   17    1   25   26   22   21    1    0    1
   20   20   20    1   29   26   25   29
   21   22   33    1   29   30   27   26    1    2    1    3
    1    6    1      2962.0     5.5        19.5       8.0
    1    6    1      1.86
   19   20    1      1.86
   20   25    5      1.86
   25   29    4      1.86
   29   47    3      1.86
   47   49    1      1.86
 77.
 85.
 89.
 90.
 92.
 94.
 95.
&STOP
```

TABLE 9

```
SAMPLE PROBLEM * TSAP * FT-BTU-FAHR-PSI * CODED BY A.YARGICOGLU
   49    34     1    16     1     0     S     1     0     1
1.0          70.          0.5          0.9          -1.
   1
0.81         0.81         0.0          0.23         154.0        0.0        3700000.    0.000000
   1     2    19     1     6
0.0          2.75         0.25         2.75         0.0          2.375
   3     4    21     1     6
0.5833       2.75         0.8333       2.75         0.5833       2.375
   5     6    23     1     6
1.1667       2.75         1.5          2.75         1.1667       2.375
  25    25    25     2     0
0.5833       2.2083
  26    28    29     1     3
0.8333       2.2083       1.5          2.2083       0.8333       2.01247
  32    47    32     3     0
0.9583       1.7083       1.3675       0.0          0.9583       1.7083
  33    48    33     3     0
1.22915      1.7083       1.44375      0.0          1.22915      1.7083
  34    49    34     3     0
1.5          1.7083       1.5          0.0          1.5          1.7083
   1     5    11     1     7     8     2     1     1     5     1     6
  16    16    16     1    25    21    28    25
  17    19    17     1    25    26    22    21     3     0     1
  28    28    28     1    29    26    25    29
  21    22    33     1    29    30    27    26     1     2     1     3
   1     6     1      82.5
   1     6     1      1.86
  19    20     1      1.86
  20    25     5      1.86
  25    29     4      1.86
  29    47     3      1.86
  47    49     1      1.86
77.
   1     6     1      94.6
85.
   1     6     1      103.4
89.
   1     6     1      110.0
96.
   1     6     1      115.0
92.
   1     6     1      117.5
STOP
```

TABLE 10

```
SAMPLE PROBLEM * TSAP * FT-BTU-FAHR-PSI * CODED BY A.YARGICOGLU


NUMBER OF NODAL POINTS--          49
NUMBER OF ELEMENTS------          34
NUMBER OF CONVECTION BC=          16
NUMBER OF MATERIALS-----           1
NUMBER OF INCREMENTS----           7
OUTPUT INTERVAL---------           1
TIME INTERVAL------            1.00
INITIAL TEMPERATURE-----      70.00
ABSORPTIVITY                    .50
EMISSIVITY                      .90
STRESS OPTION                     1
SPAN RATIO                    -1.00

TWO DIMENSIONAL PLANE BODY

  M          KXX          KYY          KXY            C            D            Q           EM           AL
  1   8.100E-01    8.100E-01    0.       2.300E-01    1.500E+02    0.       3.790E+06    6.000E-06

 N.P. NO.     CODE          X            Y            T
        1        0    0.           2.750000E+00 1.615071E+02
        2        0    2.500000E-01 2.750000E+00 1.615071E+02
        3        0    5.833000E-01 2.750000E+00 1.615071E+02
        4        0    8.333000E-01 2.750000E+00 1.615071E+02
        5        0    1.166700E+00 2.750000E+00 1.615071E+02
        6        0    1.500000E+00 2.750000E+00 1.615071E+02
        7        0    0.           2.625000E+00 0.
        8        0    2.500000E-01 2.625000E+00 0.
        9        0    5.833000E-01 2.625000E+00 0.
       10        0    8.333000E-01 2.625000E+00 0.
       11        0    1.166700E+00 2.625000E+00 0.
       12        0    1.500000E+00 2.625000E+00 0.
       13        0    0.           2.500000E+00 0.
       14        0    2.500000E-01 2.500000E+00 0.
       15        0    5.833000E-01 2.500000E+00 0.
       16        0    8.333000E-01 2.500000E+00 0.
       17        0    1.166700E+00 2.500000E+00 0.
       18        0    1.500000E+00 2.500000E+00 0.
       19        0    0.           2.375000E+00 0.
       20        0    2.500000E-01 2.375000E+00 0.
       21        0    5.833000E-01 2.375000E+00 0.
       22        0    8.333000E-01 2.375000E+00 0.
       23        0    1.166700E+00 2.375000E+00 0.
       24        0    1.500000E+00 2.375000E+00 0.
       25        0   -0.          -0.           0.
       26        0    8.333000E-01 2.208300E+00 0.
       27        0    1.166650E+00 2.208300E+00 0.
       28        0    1.500000E+00 2.208300E+00 0.
       29        0    8.333000E-01 2.012470E+00 0.
       30        0    1.166650E+00 2.012470E+00 0.
       31        0    1.500000E+00 2.012470E+00 0.
       32        0    9.583000E-01 1.708300E+00 0.
       33        0    1.229150E+00 1.708300E+00 0.
       34        0    1.500000E+00 1.708300E+00 0.
       35        0    1.044140E+00 1.366640E+00 0.
       36        0    1.272070E+00 1.366640E+00 0.
       37        0    1.500000E+00 1.366640E+00 0.
       38        0    1.129980E+00 1.024980E+00 0.
       39        0    1.314990E+00 1.024980E+00 0.
       40        0    1.500000E+00 1.024980E+00 0.

       41        0    1.215820E+00 6.833200E-01 0.
       42        0    1.357910E+00 6.833200E-01 0.
       43        0    1.500000E+00 6.833200E-01 0.
       44        0    1.301660E+00 3.416600E-01 0.
       45        0    1.400830E+00 3.416600E-01 0.
       46        0    1.500000E+00 3.416600E-01 0.
       47        0    1.387500E+00 7.105427E-15 0.
       48        0    1.443750E+00 7.105427E-15 0.
       49        0    1.500000E+00 7.105427E-15 0.
```

TABLE 11

N	I	J	K	L	MATERIAL
1	7	8	2	1	1
2	8	9	3	2	1
3	9	10	4	3	1
4	10	11	5	4	1
5	11	12	6	5	1
6	13	14	8	7	1
7	14	15	9	8	1
8	15	16	10	9	1
9	16	17	11	10	1
10	17	18	12	11	1
11	19	20	14	13	1
12	20	21	15	14	1
13	21	22	16	15	1
14	22	23	17	16	1
15	23	24	18	17	1
16	25	21	20	25	1
17	25	26	22	21	1
18	26	27	23	22	1
19	27	28	24	23	1
20	29	26	25	29	1
21	29	30	27	26	1
22	30	31	28	27	1
23	32	33	30	29	1
24	33	34	31	30	1
25	35	36	33	32	1
26	36	37	34	33	1
27	38	39	36	35	1
28	39	40	37	36	1
29	41	42	39	38	1
30	42	43	40	39	1
31	44	45	42	41	1
32	45	46	43	42	1
33	47	48	45	44	1
34	48	49	46	45	1

I	J	K
1	2	1,868888E+00
2	3	1,868888E+00
3	4	1,868888E+00
4	5	1,868888E+00
5	6	1,868888E+00
19	20	1,868888E+00
20	25	1,868888E+00
25	29	1,868888E+00
29	32	1,868888E+00
32	35	1,868888E+00
35	38	1,868888E+00
38	41	1,868888E+00
41	44	1,868888E+00
44	47	1,868888E+00
47	48	1,868888E+00
48	49	1,868888E+00

TRANSIENT BOUNDARY CONDITIONS

AIR TEMPERATURE 77,00
HEAT FLOW INTENSITY 229,58

TEMPERATURES AT TIME= 1,000000E+00

1	8,2723E+01	2	8,2646E+01	3	8,2585E+01	4	8,2465E+01	5	8,2461E+01	6	8,2459E+01	7	7,6108E+01
8	7,5945E+01	9	7,5692E+01	10	7,5641E+01	11	7,5648E+01	12	7,5635E+01	13	7,3688E+01	14	7,3218E+01
15	7,2591E+01	16	7,2562E+01	17	7,2578E+01	18	7,2555E+01	19	7,4216E+01	20	7,2631E+01	21	7,0984E+01
22	7,1218E+01	23	7,1243E+01	24	7,1156E+01	25	7,3547E+01	26	7,1678E+01	27	7,0597E+01	28	7,0458E+01
29	7,2687E+01	30	7,0477E+01	31	7,0221E+01	32	7,2253E+01	33	7,0586F+01	34	7,0714E+01	35	7,2376E+01
36	7,0662E+01	37	7,0327E+01	38	7,2517E+01	39	7,0486E+01	40	7,0539E+01	41	7,2706E+01	42	7,1289E+01
43	7,0928E+01	44	7,3014E+01	45	7,1967E+01	46	7,1657E+01	47	7,4185E+01	48	7,3632E+01	49	7,5496E+01

TABLE 12

THERMAL INDUCED STRESSES

1	-1,95E+02	2	-1,95E+02	3	-1,98E+02	4	-1,89E+02	5	-1,89E+02	6	-1,89E+02	7	-0,91E+01
8	-4,56E+01	9	-3,99E+01	10	-3,87E+01	11	-3,87E+01	12	-3,86F+01	13	7,91E+01	14	1,15E+02
15	2,57E+01	16	2,84E+01	17	2,62F+01	18	2,66E+01	19	-1,61E+01	20	1,99E+01	21	5,78F+01
22	5,22E+01	23	5,15E+01	24	5,34E+01	25	-9,80E+01	26	3,52E+01	27	5,96F+01	28	6,28E+01
29	6,19E+01	30	5,46E+01	31	6,24E+01	32	2,26E+02	33	6,28E+01	34	4,86E+01	35	-1,49E+01
36	2,58E+01	37	3,26E+01	38	-3,88E+01	39	6,02E+02	40	1,44E+01	41	-4,82E+01	42	-1,61E+01
43	-7,74E+00	44	-6,88E+01	45	-4,50E+01	46	-3,79E+01	47	-1,89E+02	48	-9,63E+01	49	-9,25E+01

TRANSIENT BOUNDARY CONDITIONS

AIR TEMPERATURE 85,00
HEAT FLOW INTENSITY 288,98

TEMPERATURES AT TIME= 2,000000E+00

1	9,4597E+01	2	9,4354E+01	3	9,3897E+01	4	9,3776E+01	5	9,3764E+01	6	9,3754E+01	7	8,4316E+01
8	8,3847E+01	9	8,3973E+01	10	8,2919E+01	11	8,2914E+01	12	8,2892E+01	13	7,9919E+01	14	7,8644E+01
15	7,6957E+01	16	7,6883E+01	17	7,6918E+01	18	7,6881E+01	19	8,0662E+01	20	7,7802E+01	21	7,5226E+01
22	7,3774E+01	23	7,3845E+01	24	7,3583E+01	25	7,9636E+01	26	7,4786E+01	27	7,2872E+01	28	7,1664E+01
29	7,6579E+01	30	7,1644E+01	31	7,0895E+01	32	7,5893E+01	33	7,1687E+01	34	7,0864E+01	35	7,6140E+01
36	7,2142E+01	37	7,1221E+01	38	7,6423E+01	39	7,2838E+01	40	7,1903E+01	41	7,6844E+01	42	7,3889E+01
43	7,3036E+01	44	7,7638E+01	45	7,5638E+01	46	7,5410E+01	47	8,0329E+01	48	7,9415E+01	49	7,9128E+01

THERMAL INDUCED STRESSES

1	-3,44E+02	2	-3,39E+02	3	-3,28E+02	4	-3,26E+02	5	-3,25E+02	6	-3,25E+02	7	-1,28E+02
8	-1,84E+02	9	-9,15E+01	10	-8,68E+01	11	-8,79E+01	12	-8,74E+01	13	-2,98E+01	14	-2,65E+03
15	3,84E+01	16	4,88E+01	17	3,92E+01	18	4,18E+01	19	-5,97E+01	20	2,81E+01	21	1,14E+02
22	1,01E+02	23	9,99E+01	24	1,86E+02	25	-2,07E+02	26	4,88E+01	27	1,28E+02	28	1,37E+02
29	1,89E+01	30	1,23E+02	31	1,48E+02	32	4,96E+08	33	9,97E+01	34	1,19E+02	35	-2,68E+01
36	6,41E+01	37	8,51E+01	38	-9,85E+01	39	2,31E+01	40	6,43E+01	41	-9,33E+01	42	-2,61E+01
43	-6,69E+08	44	-1,36E+02	45	-9,11E+01	46	-7,68E+01	47	-2,23E+02	48	-2,02E+02	49	-1,96E+02

TRANSIENT BOUNDARY CONDITIONS

AIR TEMPERATURE 89,00
HEAT FLOW INTENSITY 333,14

TEMPERATURES AT TIME= 3,000000E+00

1	1,0456E+02	2	1,0413E+02	3	1,0331E+02	4	1,0312E+02	5	1,0311E+02	6	1,0310E+02	7	9,2511E+01
8	9,1692E+01	9	9,2361E+01	10	9,0126E+01	11	9,0143E+01	12	9,0104E+01	13	8,6608E+01	14	8,4515E+01
15	8,1955E+01	16	8,1891E+01	17	8,2014E+01	18	8,1862E+01	19	8,6994E+01	20	8,1827E+01	21	7,8215E+01
22	7,7039E+01	23	7,7355E+01	24	7,6917E+01	25	8,5082E+01	26	7,7853E+01	27	7,4278E+01	28	7,3597E+01
29	7,9081E+01	30	7,3337E+01	31	7,2089E+01	32	7,8998E+01	33	7,3261E+01	34	7,1898E+01	35	7,9262E+01
36	7,4898E+01	37	7,2591E+01	38	7,9611E+01	39	7,5139E+01	40	7,3822E+01	41	8,0229E+01	42	7,6795E+01
43	7,5713E+01	44	8,1618E+01	45	7,9355E+01	46	7,8669E+01	47	8,4875E+01	48	8,4889E+01	49	8,3834E+01

THERMAL INDUCED STRESSES

1	-4,47E+02	2	-4,37E+02	3	-4,18E+02	4	-4,14E+02	5	-4,14E+02	6	-4,13E+02	7	-1,86F+02
8	-1,68E+02	9	-1,36E+02	10	-1,32E+02	11	-1,33E+02	12	-1,32E+02	13	-6,58E+01	14	-1,84E+03
15	3,98E+01	16	4,12E+01	17	3,84E+01	18	4,14E+01	19	-8,86F+01	20	4,71E+01	21	1,56F+02
22	1,38E+02	23	1,31E+02	24	1,41E+02	25	-3,47E+02	26	1,81E+02	27	1,82E+02	28	1,98E+02
29	3,27E+01	30	1,82E+02	31	2,18F+02	32	1,96F+01	33	1,58E+02	34	1,81E+02	35	-2,41E+01
36	9,55E+01	37	1,24E+02	38	-6,98E+01	39	3,19E+01	40	8,19F+01	41	-1,22E+02	42	-4,35F+01
43	-1,08E+01	44	-1,86E+02	45	-1,39E+02	46	-1,24E+02	47	-3,03E+02	48	-2,85E+02	49	-2,79E+02

TABLE 13

TRANSIENT BOUNDARY CONDITIONS

AIR TEMPERATURE 94,00
HEAT FLOW INTENSITY 356,66

TEMPERATURES AT TIME= 0,0000E+00

1	1,11AAE+02	2	1,1105E+02	3	1,0995E+02	4	1,0975E+02	5	1,0979E+02	6	1,0974E+02	7	9,9296E+01
8	9,8188E+01	9	9,6465E+01	10	9,6223E+01	11	9,6323E+01	12	9,6286E+01	13	9,2361E+01	14	8,9641E+01
15	8,0672E+01	16	8,6699E+01	17	8,7825E+01	18	8,6874E+01	19	9,1643E+01	20	8,4035E+01	21	7,9366E+01
22	8,4377E+01	23	8,1288E+01	24	8,0668E+01	25	8,0538E+01	26	8,0581E+01	27	7,6916E+01	28	7,4066E+01
29	8,2266E+01	30	7,5296E+01	31	7,3720E+01	32	8,1863E+01	33	7,4934E+01	34	7,3258E+01	35	8,1244E+01
36	7,5836E+01	37	7,4198E+01	38	8,1634E+01	39	7,7285E+01	40	7,5874E+01	41	8,2420E+01	42	7,9323E+01
43	7,8281E+01	44	8,3866E+01	45	8,2229E+01	46	8,1663E+01	47	8,7243E+01	48	8,6745E+01	49	8,6585E+01

THERMAL INDUCED STRESSES

1	-4,97E+02	2	-4,84E+02	3	-4,59E+02	4	-4,54E+02	5	-4,55E+02	6	-4,55E+02	7	-2,35E+02
8	-2,19E+02	9	-1,71E+02	10	-1,65E+02	11	-1,67E+02	12	-1,66E+02	13	-9,56E+01	14	-3,37E+01
15	3,38E+01	16	3,32E+01	17	2,56E+01	18	2,92E+01	19	-9,74E+01	20	7,54E+01	21	1,02E+02
22	1,59E+02	23	1,48E+02	24	1,52E+02	25	-3,76E+02	26	1,29E+02	27	2,13E+02	28	7,32E+02
29	6,24E+01	30	2,21E+02	31	2,57E+02	32	6,55E+01	33	1,84E+02	34	2,23E+02	35	-6,15E+02
36	1,14E+02	37	1,51E+02	38	-6,83E+01	39	3,00E+01	40	6,27E+01	41	-1,36E+02	42	-6,59E+01
43	-4,22E+01	44	-2,19E+02	45	-1,02E+02	46	-1,69E+02	47	-3,46E+02	48	-3,35E+02	49	-3,31E+02

TRANSIENT BOUNDARY CONDITIONS

AIR TEMPERATURE 92,00
HEAT FLOW INTENSITY 356,66

TEMPERATURES AT TIME= 5,0000E+00

1	1,1681E+02	2	1,1618E+02	3	1,1483E+02	4	1,1465E+02	5	1,1477E+02	6	1,1478E+02	7	1,0478E+02
8	1,0338E+02	9	1,0142E+02	10	1,0122E+02	11	1,0145E+02	12	1,0143E+02	13	9,7247E+01	14	9,4844E+01
15	9,0897E+01	16	9,1035E+01	17	9,1623E+01	18	9,1484E+01	19	9,5826E+01	20	8,8968E+01	21	8,2552E+01
22	8,3699E+01	23	8,5069E+01	24	8,4666E+01	25	9,1332E+01	26	8,3376E+01	27	7,9803E+01	28	7,8453E+01
29	8,4851E+01	30	7,7489E+01	31	7,5715E+01	32	8,3056E+01	33	7,6726E+01	34	7,4853E+01	35	8,3149E+01
36	7,7694E+01	37	7,5939E+01	38	8,3681E+01	39	7,9383E+01	40	7,7955E+01	41	8,4658E+01	42	8,1712E+01
43	8,0711E+01	44	8,6369E+01	45	8,4817E+01	46	8,4318E+01	47	8,9585E+01	48	8,9096E+01	49	8,8950E+01

THERMAL INDUCED STRESSES

1	-5,10E+02	2	-5,02E+02	3	-4,73E+02	4	-4,69E+02	5	-4,72E+02	6	-4,72E+02	7	-2,65E+02
8	-2,34E+02	9	-1,90E+02	10	-1,85E+02	11	-1,91E+02	12	-1,90E+02	13	-1,17E+02	14	-4,44E+01
15	2,75E+01	16	2,44E+01	17	1,10E+01	18	1,42E+01	19	-1,86E+02	20	9,58E+01	21	1,95E+02
22	1,70E+02	23	1,36E+02	24	1,52E+02	25	-4,20E+02	26	1,47E+02	27	2,29E+02	28	2,59E+02
29	7,97E+01	30	2,47E+02	31	2,87E+02	32	6,72E+01	33	2,11E+02	34	2,56E+02	35	6,18E+02
36	1,29E+02	37	1,69E+02	38	-6,66E+01	39	3,11E+01	40	6,34E+01	41	-1,49E+02	42	-6,16E+01
43	-5,91E+01	44	-2,46E+02	45	-2,12E+02	46	-2,01E+02	47	-3,79E+02	48	-3,69E+02	49	-3,66E+02

TRANSIENT BOUNDARY CONDITIONS

AIR TEMPERATURE 90,00
HEAT FLOW INTENSITY 333,14

TEMPERATURES AT TIME= 6,0000E+00

1	1,1973E+02	2	1,1894E+02	3	1,1757E+02	4	1,1744E+02	5	1,1768E+02	6	1,1768E+02	7	1,0857E+02
8	1,0719E+02	9	1,0593E+02	10	1,0484E+02	11	1,0518E+02	12	1,0529E+02	13	1,0114E+02	14	9,7647E+01
15	9,4468E+01	16	9,4705E+01	17	9,5541E+01	18	9,5431E+01	19	9,9381E+01	20	8,9792E+01	21	8,5478E+01
22	8,6872E+01	23	8,8688E+01	24	8,8861E+01	25	9,3698E+01	26	8,6192E+01	27	8,2761E+01	28	8,1757E+01
29	8,7079E+01	30	8,0981E+01	31	7,7961E+01	32	8,5008E+01	33	7,8627E+01	34	7,6633E+01	35	8,5167E+01
36	7,9588E+01	37	7,7771E+01	38	8,5727E+01	39	8,1468E+01	40	8,0035E+01	41	8,6855E+01	42	8,4087E+01
43	8,3858E+01	44	8,8628E+01	45	8,7222E+01	46	8,6747E+01	47	9,1717E+01	48	9,1294E+01	49	9,1168E+01

THERMAL INDUCED STRESSES

1	-5,86E+02	2	-5,88E+02	3	-5,57E+02	4	-5,54E+02	5	-5,59E+02	6	-5,59E+02	7	-2,76E+02
8	-2,63E+02	9	-1,96E+02	10	-1,93E+02	11	-2,01E+02	12	-2,02E+02	13	-1,31E+02	14	-5,17E+01
15	2,96E+01	16	1,52E+01	17	-3,02E+00	18	-1,50E+00	19	-1,13E+02	20	1,03E+02	21	1,97E+02
22	1,69E+02	23	1,28E+02	24	1,42E+02	25	-4,40E+02	26	1,53E+02	27	2,31E+02	28	2,54E+02
29	6,63E+01	30	2,68E+02	31	3,03E+02	32	8,24E+01	33	2,29E+02	34	2,75E+02	35	1,58E+01
36	1,42E+02	37	1,83E+02	38	-6,28E+01	39	3,42E+01	40	6,67E+01	41	-1,50E+02	42	-8,99E+01
43	-6,73E+01	44	-2,59E+02	45	-2,27E+02	46	-2,17E+02	47	-3,95E+02	48	-3,85E+02	49	-3,82E+02

TRANSIENT BOUNDARY CONDITIONS

AIR TEMPERATURE 95,00
HEAT FLOW INTENSITY 288,98

TEMPERATURES AT TIME= 7,0000E+00

1	1,1992E+02	2	1,1910E+02	3	1,1773E+02	4	1,1765E+02	5	1,1795E+02	6	1,1808E+02	7	1,1056E+02
8	1,0985E+02	9	1,0893E+02	10	1,0803E+02	11	1,0743E+02	12	1,0748E+02	13	1,0371E+02	14	1,0016E+02
15	9,7140E+01	16	9,7457E+01	17	9,8403E+01	18	9,8888E+01	19	1,0155E+02	20	9,2497E+01	21	8,8516E+01
22	8,6788E+01	23	9,1780E+01	24	9,1179E+01	25	9,5250E+01	26	8,8716E+01	27	8,5587E+01	28	8,4576E+01
29	8,9698E+01	30	8,2211E+01	31	8,0275E+01	32	8,6823E+01	33	8,0547E+01	34	7,8523E+01	35	8,6771E+01
36	8,1412E+01	37	7,9621E+01	38	8,7395E+01	39	8,3191E+01	40	8,2828E+01	41	8,9689E+01	42	8,6868E+01
43	8,5165E+01	44	9,0886E+01	45	8,9211E+01	46	8,8803E+01	47	9,3199E+01	48	9,2874E+01	49	9,2778E+01

THERMAL INDUCED STRESSES

1	-6,57E+02	2	-6,39E+02	3	-6,08E+02	4	-6,06E+02	5	-6,13E+02	6	-6,14E+02	7	-2,69E+02
8	-2,35E+02	9	-1,88E+02	10	-1,86E+02	11	-1,98E+02	12	-1,99E+02	13	-1,38E+02	14	-5,69E+01
15	1,18E+01	16	9,63E+00	17	-1,87E+01	18	-1,79E+01	19	-1,13E+02	20	1,82E+02	21	1,64E+02
22	1,57E+02	23	1,09E+02	24	1,23E+02	25	-4,32E+02	26	1,47E+02	27	2,16E+02	28	2,41E+02
29	8,61E+01	30	2,56E+02	31	3,08E+02	32	9,23E+01	33	2,35E+02	34	2,61E+02	35	2,69E+01
36	1,40E+02	37	1,98E+02	38	-5,38E+01	39	5,72E+01	40	6,82E+01	41	-1,48E+02	42	-8,95E+01
43	-6,96E+01	44	-2,55E+02	45	-2,28E+02	46	-2,19E+02	47	-3,85E+02	48	-3,78E+02	49	-3,76E+02

TABLE 14

TRANSIENT BOUNDARY CONDITIONS

AIR TEMPERATURE 77,00
HEAT FLOW INTENSITY 280,00

TEMPERATURES AT TIME= 1,0000E+00

1	8,0924E+01	2	8,0635E+01	3	8,0686E+01	4	8,0654E+01	5	8,0664E+01	6	8,0660E+01	7	7,7992E+01
8	7,7610E+01	9	7,7544E+01	10	7,7506E+01	11	7,7538E+01	12	7,7532E+01	13	7,4561E+01	14	7,3992E+01
15	7,3337E+01	16	7,3342E+01	17	7,3487E+01	18	7,3419E+01	19	7,4776E+01	20	7,2776E+01	21	7,1147E+01
22	7,1415E+01	23	7,1014E+01	24	7,1538E+01	25	7,3532E+01	26	7,1755E+01	27	7,0714E+01	28	7,0506E+01
29	7,2669E+01	30	7,0511E+01	31	7,0257E+01	32	7,2259E+01	33	7,0513E+01	34	7,0229E+01	35	7,2376E+01
36	7,0663E+01	37	7,0327E+01	38	7,2517E+01	39	7,0966E+01	40	7,0539E+01	41	7,2700E+01	42	7,1289E+01
43	7,0926E+01	44	7,3914E+01	45	7,1657E+01	46	7,1657E+01	47	7,4185E+01	48	7,3632E+01	49	7,3456E+01

THERMAL INDUCED STRESSES

1	-2,66E+02	2	-2,58E+02	3	-2,55E+02	4	-2,54E+02	5	-2,54E+02	6	-2,54E+02	7	-6,40E+01
8	-6,85E+01	9	-5,45E+01	10	-5,36E+01	11	-5,41E+01	12	-5,42E+01	13	5,82E+00	14	1,88E+01
15	3,37E+01	16	3,35E+01	17	3,18E+01	18	3,21E+01	19	+6,62E+00	20	3,88E+01	21	7,66E+01
22	6,98E+01	23	6,53E+01	24	6,72E+01	25	-1,22E+02	26	5,28E+01	27	7,56E+01	28	7,96E+01
29	1,94E+01	30	6,85E+01	31	7,42E+01	32	1,83E+01	33	5,08E+01	34	5,67E+01	35	-1,30E+01
36	2,66E+01	37	3,36E+01	38	-3,68E+01	39	-2,11E-01	40	8,19E+00	41	+6,17E+01	42	-2,96E+01
43	-2,12E+01	44	-8,98E+01	45	-6,56E+01	46	-5,86E+01	47	-1,37E+02	48	-1,20E+02	49	-1,20E+02

TRANSIENT BOUNDARY CONDITIONS

AIR TEMPERATURE 85,00
HEAT FLOW INTENSITY 333,00

TEMPERATURES AT TIME= 2,0000E+00

1	9,0227E+01	2	9,0056E+01	3	9,0479E+01	4	9,0381E+01	5	9,0418E+01	6	9,0410E+01	7	8,7894E+01
8	8,7665E+01	9	8,7575E+01	10	8,7561E+01	11	8,7707E+01	12	8,7706E+01	13	8,4821E+01	14	8,4021E+01
15	7,9277E+01	16	7,9282E+01	17	7,9473E+01	18	7,9420E+01	19	8,1958E+01	20	7,7344E+01	21	7,3544E+01
22	7,4259E+01	23	7,4675E+01	24	7,4425E+01	25	7,9582E+01	26	7,4948E+01	27	7,2483E+01	28	7,2811E+01
29	7,6755E+01	30	7,1761E+01	31	7,1812E+01	32	7,5915E+01	33	7,1711E+01	34	7,1986E+01	35	7,6144E+01
36	7,2106E+01	37	7,1225E+01	38	7,6420E+01	39	7,2838E+01	40	7,1984E+01	41	7,6844E+01	42	7,3889E+01
43	7,3836E+01	44	7,7636E+01	45	7,5638E+01	46	7,5810E+01	47	8,0329E+01	48	7,9415E+01	49	7,9120E+01

THERMAL INDUCED STRESSES

1	-4,87E+02	2	-4,81E+02	3	-3,98E+02	4	-3,88E+02	5	-3,88E+02	6	-3,88E+02	7	-1,44E+02
8	-1,32E+02	9	-1,13E+02	10	-1,11E+02	11	-1,12E+02	12	-1,12E+02	13	-2,95E+01	14	4,19E+00
15	4,39E+01	16	4,37E+01	17	3,94E+01	18	4,05E+01	19	-5,27E+01	20	5,22E+01	21	1,30E+02
22	1,23E+02	23	1,13E+02	24	1,19E+02	25	-2,43E+02	26	8,97E+01	27	1,47E+02	28	1,58E+02
29	2,83E+01	30	1,42E+02	31	1,59E+02	32	1,61E+01	33	1,12E+02	34	1,31E+02	35	-2,42E+01
36	6,67E+01	37	8,76E+01	38	-6,57E+01	39	1,58E+01	40	3,78E+01	41	-1,19E+02	42	-6,32E+01
43	-2,39E+01	44	-1,63E+02	45	-1,18E+02	46	-1,08E+02	47	-2,68E+02	48	-2,39E+02	49	-2,32E+02

TRANSIENT BOUNDARY CONDITIONS

AIR TEMPERATURE 89,00
HEAT FLOW INTENSITY 357,00

TEMPERATURES AT TIME= 3,0000E+00

1	1,0036E+02	2	1,0788E+02	3	1,0703E+02	4	1,0608E+02	5	1,0695E+02	6	1,0696E+02	7	9,5248E+01
8	9,4383E+01	9	9,3990E+01	10	9,2837E+01	11	9,2972E+01	12	9,2970E+01	13	8,8440E+01	14	8,6899E+01
15	8,3677E+01	16	8,3533E+01	17	8,3886E+01	18	8,3794E+01	19	8,8319E+01	20	8,1527E+01	21	7,6719E+01
22	7,7732E+01	23	7,8512E+01	24	7,8098E+01	25	8,4078E+01	26	7,8245E+01	27	7,4825E+01	28	7,4177E+01
29	8,0291E+01	30	7,3555E+01	31	7,2310E+01	32	7,9842E+01	33	7,3316E+01	34	7,1953E+01	35	7,9278E+01
36	7,4811E+01	37	7,2682E+01	38	7,9612E+01	39	7,5141E+01	40	7,3824E+01	41	8,0238E+01	42	7,6795E+01
43	7,5713E+01	44	8,1016E+01	45	7,9356E+01	46	7,8669E+01	47	8,4075E+01	48	8,4089E+01	49	8,3834E+01

THERMAL INDUCED STRESSES

1	-4,89E+02	2	-4,77E+02	3	-4,59E+02	4	-4,56E+02	5	-4,57E+02	6	-4,57E+02	7	-2,89E+02
8	-1,89E+02	9	-1,57E+02	10	-1,53E+02	11	-1,57E+02	12	-1,57E+02	13	-7,89E+01	14	-1,77E+01
15	4,19E+01	16	4,07E+01	17	3,28E+01	18	3,47E+01	19	+8,56E+01	20	6,98E+01	21	1,70E+02
22	1,55E+02	23	1,37E+02	24	1,47E+02	25	-3,48E+02	26	1,28E+02	27	1,98E+02	28	2,13E+02
29	4,86E+01	30	2,08E+02	31	2,28E+02	32	3,26E+01	33	1,63E+02	34	1,98E+02	35	-2,81E+01
36	9,94E+01	37	1,31E+02	38	-7,55E+01	39	2,62E+01	40	5,62E+01	41	-1,37E+02	42	-5,98E+01
43	-3,44E+01	44	-2,12E+02	45	-1,65E+02	46	-1,49E+02	47	-3,38E+02	48	-3,28E+02	49	-3,16E+02

TRANSIENT BOUNDARY CONDITIONS

AIR TEMPERATURE 94,00
HEAT FLOW INTENSITY 357,00

TEMPERATURES AT TIME= 4,0000E+00

1	1,1349E+02	2	1,1325E+02	3	1,1213E+02	4	1,1198E+02	5	1,1211E+02	6	1,1213E+02	7	1,0142E+02
8	1,0022E+02	9	9,9840E+01	10	9,8552E+01	11	9,8562E+01	12	9,8562E+01	13	9,3997E+01	14	9,1851E+01
15	8,8446E+01	16	8,8197E+01	17	8,8708E+01	18	8,8687E+01	19	9,2856E+01	20	8,4008E+01	21	7,9998E+01
22	8,1169E+01	23	8,2463E+01	24	8,1952E+01	25	8,8364E+01	26	8,1806E+01	27	7,7611E+01	28	7,6803E+01
29	8,2661E+01	30	7,5619E+01	31	7,4867E+01	32	8,1115E+01	33	7,5829E+01	34	7,3352E+01	35	8,1255E+01
36	7,5855E+01	37	7,4219E+01	38	8,1637E+01	39	7,7289E+01	40	7,5078E+01	41	8,2421E+01	42	7,9324E+01
43	7,8282E+01	44	8,3866E+01	45	8,2229E+01	46	8,1663E+01	47	8,7243E+01	48	8,6745E+01	49	8,6585E+01

THERMAL INDUCED STRESSES

1	-5,12E+02	2	-4,99E+02	3	-4,72E+02	4	-4,69E+02	5	-4,72E+02	6	-4,72E+02	7	-2,50E+02
8	-2,23E+02	9	-1,83E+02	10	-1,79E+02	11	-1,85E+02	12	-1,85E+02	13	-1,02E+02	14	-3,53E+01
15	3,31E+01	16	2,96E+01	17	1,63E+01	18	1,84E+01	19	+0,75E+01	20	9,08E+01	21	1,95E+02
22	1,68E+02	23	1,39E+02	24	1,58E+02	25	-3,90E+02	26	1,42E+02	27	2,21E+02	28	2,39E+02
29	7,29E+01	30	2,53E+02	31	2,68E+02	32	5,66E+01	33	1,95E+02	34	2,33E+02	35	-4,49E+00
36	1,18E+02	37	1,56E+02	38	-7,18E+01	39	2,78E+01	40	5,99E+01	41	-1,47E+02	42	-7,63E+01
43	-5,26E+01	44	-2,37E+02	45	-2,09E+02	46	-1,97E+02	47	+3,72E+02	48	-3,61E+02	49	-3,57E+02

TABLE 15

TRANSIENT BOUNDARY CONDITIONS

AIR TEMPERATURE 92,00
HEAT FLOW INTENSITY 333,00

TEMPERATURES AT TIME= 5,0000E+00

1	1,1709E+02	2	1,1635E+02	3	1,1587E+02	4	1,1490E+02	5	1,1516E+02	6	1,1528E+02	7	1,8572E+02
8	1,4833E+02	9	1,4237E+02	10	1,8224E+02	11	1,8262E+02	12	1,8266E+02	13	8,8312E+01	14	9,4978E+01
15	9,1839E+01	16	9,2884E+01	17	9,2408E+01	18	9,2824E+01	19	9,6447E+01	20	8,7514E+01	21	8,3195E+01
22	8,4488E+01	23	8,6170E+01	24	8,5616E+01	25	9,1110E+01	26	8,3419E+01	27	8,0535E+01	28	7,9628E+01
29	8,5280E+01	30	7,7802E+01	31	7,6131E+01	32	8,3152E+01	33	7,6857E+01	34	7,4989E+01	35	8,3213E+01
36	7,7722E+01	37	7,5973E+01	38	8,3686E+01	39	7,9389E+01	40	7,7962E+01	41	8,4659E+01	42	8,1713E+01
43	8,4720E+01	44	8,6389E+01	45	8,4817E+01	46	8,4318E+01	47	8,9545E+01	48	8,9894E+01	49	8,8954E+01

THERMAL INDUCED STRESSES

1	-5,93E+02	2	-6,86E+02	3	-6,57E+02	4	-4,54E+02	5	-4,59E+02	6	-4,69E+02	7	-2,68E+02
8	-2,36E+02	9	-1,92E+02	10	-1,80E+02	11	-1,98E+02	12	-1,98E+02	13	-1,23E+02	14	-4,78E+01
15	2,04E+01	16	1,88E+01	17	1,94E+01	18	2,82E+00	19	-1,08E+02	20	9,95E+01	21	1,98E+02
22	1,69E+02	23	1,34E+02	24	1,43E+02	25	-4,26E+02	26	1,59E+02	27	2,27E+02	28	2,48E+02
29	8,25E+01	30	2,51E+02	31	2,91E+02	32	7,41E+01	33	2,17E+02	34	2,48E+02	35	8,88E+00
36	1,34E+02	37	1,74E+02	38	-6,57E+01	39	3,28E+01	40	6,45E+01	41	-1,52E+02	42	-8,67E+01
43	-8,21E+01	44	-2,55E+02	45	-2,19E+02	46	-2,88E+02	47	-3,98E+02	48	-3,88E+02	49	-3,77E+02

TABLE 16

TRANSIENT BOUNDARY CONDITIONS

AIR TEMPERATURE 77,00
FROM ITO 6INC ITREAD 90,68

TEMPERATURES AT TIME= 1,0000E+00

1	9,4688E+01	2	9,4688E+01	3	9,4688E+01	4	9,4688E+01	5	9,4688E+01	6	9,4688E+01	7	8,1338E+01
8	8,3144E+01	9	8,0998E+01	10	8,1012E+01	11	8,1009E+01	12	8,1104E+01	13	7,5814E+01	14	7,5131E+01
15	7,4628E+01	16	7,4748E+01	17	7,4981E+01	18	7,5005E+01	19	7,8957E+01	20	7,2539E+01	21	7,1131E+01
22	7,1681E+01	23	7,2267E+01	24	7,2219E+01	25	7,2291E+01	26	7,1838E+01	27	7,0869E+01	28	7,0883E+01
29	7,1965E+01	30	7,0807E+01	31	7,0284E+01	32	7,1514E+01	33	7,0368E+01	34	7,0169E+01	35	7,1575E+01
36	7,0842E+01	37	7,0228E+01	38	7,1668E+01	39	7,0860E+01	40	7,0357E+01	41	7,1787E+01	42	7,0655E+01
43	7,0609E+01	44	7,1904E+01	45	7,1382E+01	46	7,1896E+01	47	7,2749E+01	48	7,2603E+01	49	7,2267E+01

THERMAL INDUCED STRESSES

1	-3,88E+02	2	-5,88E+02	3	-3,88E+02	4	-3,88E+02	5	-5,88E+02	6	-3,88E+02	7	-9,15E+01
8	-8,76E+01	9	-8,36E+01	10	-8,41E+01	11	-8,59E+01	12	-8,82E+01	13	2,84E+01	14	3,61E+01
15	4,77E+01	16	4,58E+01	17	3,95E+01	18	3,98E+01	19	2,66E+01	20	8,69E+01	21	1,14E+02
22	1,83E+02	23	8,77E+01	24	8,48E+01	25	-1,69E+02	26	9,87E+01	27	1,02E+02	28	1,83E+02
29	5,54E+01	30	8,99E+01	31	9,37E+01	32	3,20E+01	33	5,91E+01	34	8,35E+01	35	-5,68E+00
36	2,83E+01	37	2,53E+01	38	-6,45E+01	39	-2,02E+01	40	-1,47E+01	41	-8,42E+01	42	-4,29E+01
43	-5,74E+01	44	-1,26E+02	45	-1,10E+02	46	-1,95E+02	47	-1,88E+02	48	-1,72E+02	49	-1,69E+02

TABLE 17

TRANSIENT BOUNDARY CONDITIONS

AIR TEMPERATURE 85,00
FROM ITO 6INC ITREAD 103,48

TEMPERATURES AT TIME= 2,0000E+00

1	1,0348E+02	2	1,0348E+02	3	1,0348E+02	4	1,0348E+02	5	1,0348E+02	6	1,0348E+02	7	8,9961E+01
8	8,6402E+01	9	8,0980E+01	10	8,0980E+01	11	8,0834E+01	12	8,0242E+01	13	8,0281E+01	14	8,1865E+01
15	7,9721E+01	16	7,9987E+01	17	8,0561E+01	18	8,0685E+01	19	8,1754E+01	20	7,6179E+01	21	7,5428E+01
22	7,9398E+01	23	7,5755E+01	24	7,5013E+01	25	7,6508E+01	26	7,4144E+01	27	7,2670E+01	28	7,2468E+01
29	7,5247E+01	30	7,1553E+01	31	7,1054E+01	32	7,4134E+01	33	7,1245E+01	34	7,0664E+01	35	7,4229E+01
36	7,1476E+01	37	7,0844E+01	38	7,4420E+01	39	7,1944E+01	40	7,1381E+01	41	7,4733E+01	42	7,2674E+01
43	7,2083E+01	44	7,5324E+01	45	7,3912E+01	46	7,5449E+01	47	7,7272E+01	48	7,6878E+01	49	7,6399E+01

THERMAL INDUCED STRESSES

1	-4,53E+02	2	-4,53E+02	3	-4,53E+02	4	-4,53E+02	5	-4,53E+02	6	-4,53E+02	7	-1,67E+02
8	-1,57E+02	9	-1,45E+02	10	-1,44E+02	11	-1,51E+02	12	-1,52E+02	13	-2,24E+01	14	1,52E+01
15	4,57E+01	16	3,97E+01	17	2,66E+01	18	2,56E+01	19	-2,02E+01	20	1,07E+02	21	1,69E+02
22	1,47E+02	23	1,16E+02	24	1,19E+02	25	-2,75E+02	26	1,27E+02	27	1,60E+02	28	1,65E+02
29	7,07E+01	30	1,55E+02	31	1,66E+02	32	4,48E+01	33	1,14E+02	34	1,27E+02	35	-7,95E+00
36	5,46E+01	37	4,49E+01	38	-4,63E+01	39	-9,81E+00	40	8,81E+00	41	-1,27E+02	42	-8,03E+01
43	-6,68E+01	44	-1,94E+02	45	-1,62E+02	46	-1,52E+02	47	-2,92E+02	48	-2,77E+02	49	-2,72E+02

TRANSIENT BOUNDARY CONDITIONS

AIR TEMPERATURE 80,00
FROM ITO 6INC ITREAD 118,00

TEMPERATURES AT TIME= 3,0000E+00

1	1,1088E+02	2	1,1088E+02	3	1,1088E+02	4	1,1088E+02	5	1,1088E+02	6	1,1088E+02	7	9,6868E+01
8	9,0128E+01	9	9,5280E+01	10	9,5374E+01	11	9,5718E+01	12	9,5779E+01	13	8,9871E+01	14	8,8572E+01
15	8,4522E+01	16	8,4925E+01	17	8,5824E+01	18	8,5882E+01	19	8,7831E+01	20	8,0876E+01	21	7,6349E+01
22	7,7702E+01	23	7,9667E+01	24	7,9429E+01	25	8,0720E+01	26	7,7208E+01	27	7,5116E+01	28	7,4741E+01
29	7,9448E+01	30	7,3191E+01	31	7,2332E+01	32	7,6634E+01	33	7,2511E+01	34	7,1534E+01	35	7,6643F+01
36	7,2859E+01	37	7,1856E+01	38	7,6923E+01	39	7,3264E+01	40	7,2698E+01	41	7,7417E+01	42	7,4866E+01
43	7,4879E+01	44	7,8423E+01	45	7,6824E+01	46	7,6897E+01	47	8,1198E+01	48	8,0539E+01	49	8,0324E+01

THERMAL INDUCED STRESSES

1	-4,91E+02	2	-4,91E+02	3	-4,91E+02	4	-4,91E+02	5	-4,91E+02	6	-4,91E+02	7	-2,17E+02
8	-1,99E+02	9	-1,88E+02	10	-1,82E+02	11	-1,98E+02	12	-1,91E+02	13	-4,29E+01	14	-6,13E+00
15	8,85E+01	16	3,13E+01	17	1,89E+01	18	4,58E+00	19	-9,69E+01	20	1,17E+02	21	2,61E+02
22	1,71E+02	23	1,27E+02	24	1,32E+02	25	-3,56E+02	26	1,58E+02	27	1,98E+02	28	2,07E+02
29	8,45E+01	30	2,84E+02	31	2,23E+02	32	6,66E+01	33	1,61E+02	34	1,83E+02	35	6,66E-02
36	8,46E+01	37	1,89E+02	38	-7,19E+01	39	2,54E+00	40	2,42E+01	41	-1,49E+02	42	-9,12E+01
43	-7,31E+01	44	-2,36E+02	45	-2,02E+02	46	-1,98E+02	47	-3,67E+02	48	-3,52E+02	49	-3,47E+02

TRANSIENT BOUNDARY CONDITIONS

AIR TEMPERATURE 90,00
FROM ITO 6INC ITREAD 115,00

TEMPERATURES AT TIME= 4,0000E+00

1	1,1588E+02	2	1,1588E+02	3	1,1588E+02	4	1,1588E+02	5	1,1588E+02	6	1,1588E+02	7	1,0216E+02
8	1,0143E+02	9	1,0936E+02	10	1,0858E+02	11	1,0897E+02	12	1,0906E+02	13	9,9327E+01	14	9,7245E+01
15	9,8803E+01	16	9,9353E+01	17	9,9552E+01	18	9,8627E+01	19	9,9525E+01	20	9,1337E+01	21	7,9558E+01
22	8,1854E+01	23	8,3594E+01	24	8,3271E+01	25	8,3896E+01	26	8,0108E+01	27	7,7884E+01	28	7,7388E+01
29	8,1118E+01	30	7,5147E+01	31	7,4822E+01	32	7,8563E+01	33	7,3961E+01	34	7,2788E+01	35	7,8442E+01
36	7,4824E+01	37	7,3144E+01	38	7,8746E+01	39	7,5357E+01	40	7,4283E+01	41	7,9416E+01	42	7,6942E+01
43	7,6123E+01	44	8,0763E+01	45	7,9352E+01	46	7,8872E+01	47	8,3818E+01	48	8,3318E+01	49	8,3153E+01

THERMAL INDUCED STRESSES

1	-5,05E+02	2	-5,05E+02	3	-5,05E+02	4	-5,05E+02	5	-5,05E+02	6	-5,05E+02	7	-2,47E+02
8	-2,24E+02	9	-2,08E+02	10	-2,03E+02	11	-2,14E+02	12	-2,16E+02	13	-9,88E+01	14	-2,97E+01
15	3,44E+01	16	2,23E+01	17	-4,94E+00	18	-6,66E+00	19	-7,78E+01	20	1,30E+02	21	2,17E+02
22	1,83E+02	23	1,26E+02	24	1,33E+02	25	-4,14E+02	26	1,67E+02	27	2,18E+02	28	2,29E+02
29	1,08E+02	30	2,36E+02	31	2,26E+02	32	9,84E+01	33	1,95E+02	34	2,24E+02	35	1,46E+01
36	1,18E+02	37	1,3RE+02	38	-6,67E+01	39	1,82E+01	40	3,46E+01	41	-1,59E+02	42	-1,22E+02
43	-8,37E+01	44	-2,68E+02	45	-2,34E+02	46	-2,23E+02	47	-4,12E+02	48	-4,00E+02	49	-3,97E+02

TRANSIENT BOUNDARY CONDITIONS

AIR TEMPERATURE 95,00
FROM ITO 6INC ITREAD 117,50

TEMPERATURES AT TIME= 5,0000E+00

1	1,1758E+02	2	1,1758E+02	3	1,1758E+02	4	1,1758E+02	5	1,1758E+02	6	1,1758E+02	7	1,0623E+02
8	1,0511E+02	9	1,0392E+02	10	1,0418E+02	11	1,0448E+02	12	1,0479E+02	13	9,8432E+01	14	9,5802E+01
15	9,2417E+01	16	9,3438E+01	17	9,4458E+01	18	9,4559E+01	19	9,6388E+01	20	8,6476E+01	21	8,2729E+01
22	8,4275E+01	23	8,7146E+01	24	8,6664E+01	25	8,6932E+01	26	8,2997E+01	27	8,0751E+01	28	8,0134E+01
29	8,3854E+01	30	7,7316E+01	31	7,6808E+01	32	8,0477E+01	33	7,5578E+01	34	7,4126E+01	35	8,0115E+01
36	7,7567F+01	37	7,4518E+01	38	8,0505E+01	39	7,7891E+01	40	7,5963E+01	41	8,1418E+01	42	7,8981E+01
43	7,8107E+01	44	8,3952E+01	45	8,1728E+01	46	8,1269E+01	47	8,6228E+01	48	8,5772E+01	49	8,5625E+01

THERMAL INDUCED STRESSES

1	-4,84E+02	2	-4,84E+02	3	-4,84E+02	4	-4,84E+02	5	-4,84E+02	6	-4,88E+02	7	-2,58E+02
8	-2,32E+02	9	-2,09E+02	10	-2,09E+02	11	-2,22E+02	12	-2,35E+02	13	-1,18E+02	14	-3,23E+01
15	2,05E+01	16	1,20E+01	17	+1,99E+01	18	-2,28E+01	19	+9,36E+01	20	1,12E+02	21	2,17E+02
22	1,82E+02	23	1,16E+02	24	1,23E+02	25	-4,43E+02	26	1,71E+02	27	2,22E+02	28	2,35E+02
29	1,84E+02	30	2,53E+02	31	2,43E+02	32	1,08E+02	33	2,19E+02	34	2,92E+02	35	3,23E+01
36	1,31E+02	37	1,61E+02	38	-5,79E+01	39	2,86E+01	40	4,63E+01	41	-1,68E+02	42	-1,04E+02
43	-8,59E+01	44	-2,79E+02	45	-2,49E+02	46	-2,39E+02	47	-4,33E+02	48	-4,23E+02	49	-4,28E+02

APPENDIX 2

APPENDIX 2. AN EXAMPLE PROBLEM FOR INPUT AND OUTPUT FOR PROGRAM SHELL8

A two-span skewed slab bridge subjected to a quartic temperature gradient through the thickness was selected to illustrate the required input and the interpretation of output for program SHELL8. The concrete slab was assumed to be isotropic with a modulus of elasticity of 4×10^6 psi and a Poisson's ratio of 0.167. The finite element idealization which is depicted in Fig 49 included 24 elements and 36 nodal points.

Two sets of input data were used as shown in Table 18. The only difference in the inputs appears on the second card (i.e., the value for ISIG of Sec. 5.1 of Chapter 4). The first set of input data of Table 18 used the option of ISIG = 1 to compute fiber stresses having the same units as that of the input modulus of elasticity. The second set of input data of Table 18 used the option of ISIG = 0 to compute membrane stress and bending resultants having the units of force and moment per unit length of mid-surface respectively. Details of interpreting the output will be discussed later.

In preparing the input data it is advisable to use as many generation options as possible to minimize the coding time and reduce coding errors. For example, with regard to the nodal coordinate cards (the third card in each set of input data of Table 18), Sec. 5.1 of the data input guide was used to generate nodal point coordinates along the X-axis (Fig 49). Then, on the fourth card, Sec. 5.6 was used to generate all the remaining nodal point coordinates.

With these mesh generation options, the surface coordinates, ξ_1 and ξ_2, were set to coincide with the X and Y-axes respectively. Since the support boundary constraints had directions other than the global ones (Fig 49), the surface coordinates for the nodal points on the support lines needed to be specified so that ξ_2 is normal to the skewed support in order to ensure zero rotation normal to that support. In order to be able to do this, IFLAG of Sec. 4.2 was set to be 1.

TABLE 18

```
SAMPLE PROBLEM-SHELL8- FAHR,PSI - CODED BY A,YARGICOGLU
   24   36   14    6    6    1    1    0    0    0    1    0    1    0    0    1
    1   33    4    1 0,0        0,0       0,0       800,0     0,0       0,0
    2   34    4   -3 57,735     100,0     0,0
    1    4    1       0,5       0,866025  0,0       -0,866025 0,5       0,0
   17   20    1       0,5       0,866025  0,0       -0,866025 0,5       0,0
   33   36    1       0,5       0,866025  0,0       -0,866025 0,5       0,0

    1    1    5    6    2    3    8
    1       4000000,0 1,0        0,167     0,167     0,0  0,0  0,000006  63,0
    1    1   20    1    1        18,0      18,0      18,0      18,0      0,0
    1   36    1
    1   36    1       114,6     84,6      71,7      71,5      82,3

    5 110000
   29 010000
    1 001010  4  1
   17 001010 20  1
   33 001010 36  1

    1
```

```
SAMPLE PROBLEM-SHELL8- FAHR,PSI - CODED BY A,YARGICOGLU
   24   36   14    6    6    1    1    0    0    0    0    0    0    0    0    1
    1   33    4    1 0,0        0,0       0,0       800,0     0,0       0,0
    2   34    4   -3 57,735     100,0     0,0
    1    4    1       0,5       0,866025  0,0       -0,866025 0,5       0,0
   17   20    1       0,5       0,866025  0,0       -0,866025 0,5       0,0
   33   36    1       0,5       0,866025  0,0       -0,866025 0,5       0,0

    1    1    5    6    2    3    8
    1       4000000,0 1,0        0,167     0,167     0,0  0,0  0,000006  63,0
    1    1   20    1    1        18,0      18,0      18,0      18,0      0,0
    1   36    1
    1   36    1       114,6     84,6      71,7      71,5      82,3

    5 110000
   29 010000
    1 001010  4  1
   17 001010 20  1
   33 001010 36  1

    1
```

TABLE 19

```
 SAMPLE PROBLEM-SHELL8- FAHR,PSI - CODED BY A,YARGICOGLU
NUMEL  =   24
NUPTS  =   36
NUSPTS =   14
IBANDP =    6
NDFRE  =    6
IFLAG  =    1
NUMAT  =    1
ISHEAR =    0
NRED   =    0
IRECT  =    0
LPROB  =    1
IGEN   =    0
ISIG   =    1
IROT   =    0
ITEMP  =    0
NLVT   =    1


DUPLICATION OF INPUT NODAL COORDINATE CARDS,
  1  33   4   1    0,          0,          0,
                  8,00000E+02 0,          0,
  2  34   4  -3    5,77350E+01 1,00000E+02 0,

DUPLICATION OF INPUT SURFACE DIRECTION COSINE CARDS,
  1   4   1        ,50000   ,86603  0,00000  -,86603   ,50000  0,00000
 17  20   1        ,50000   ,86603  0,00000  -,86603   ,50000  0,00000
 33  36   1        ,50000   ,86603  0,00000  -,86603   ,50000  0,00000
 -0  -0  -0     -0,00000 -0,00000 -0,00000 -0,00000 -0,00000 -0,00000

DUPLICATION OF ELEMENT NODAL POINT NUMBER CARDS,
   1   1   5   6   2   3   8  -0

DUPLICATION OF ELEMENT MATERIAL TABLE,
  1   0,00000E+00 1,00000E+00 1,67000E-01 1,67000E-01 0,          0,          6,00000E-06 6,30000E+01

DUPLICATION OF ELEMENT PROPERTY CARDS,
   1   1  24   1   1   1,00000E+01 1,00000E+01 1,00000E+01 1,00000E+01 0,

 ELEMENT DISTRIBUTED LOADS,
   1  36   1  -0,        -0,         -0,         -0,         -0,

DUBLICATION OF NODAL POINT TEMPERATURES FOR CASE    1

   1  36   1   1,14600E+02 8,46000E+01 7,17000E+01 7,15000E+01 8,23000E+01

NODAL COORDINATES
PT    X           Y           Z
  1   0,          0,          0,
  2   5,77350E+01 1,00000E+02 0,
  3   1,15470E+02 2,00000E+02 0,
  4   1,73205E+02 3,00000E+02 0,
  5   1,00000E+02 0,          0,
  6   1,57735E+02 1,00000E+02 0,
  7   2,15470E+02 2,00000E+02 0,
  8   2,73205E+02 3,00000E+02 0,
  9   2,00000E+02 0,          0,
 10   2,57735E+02 1,00000E+02 0,
 11   3,15470E+02 2,00000E+02 0,
 12   3,73205E+02 3,00000E+02 0,
 13   3,00000E+02 0,          0,
 14   3,57735E+02 1,00000E+02 0,
```

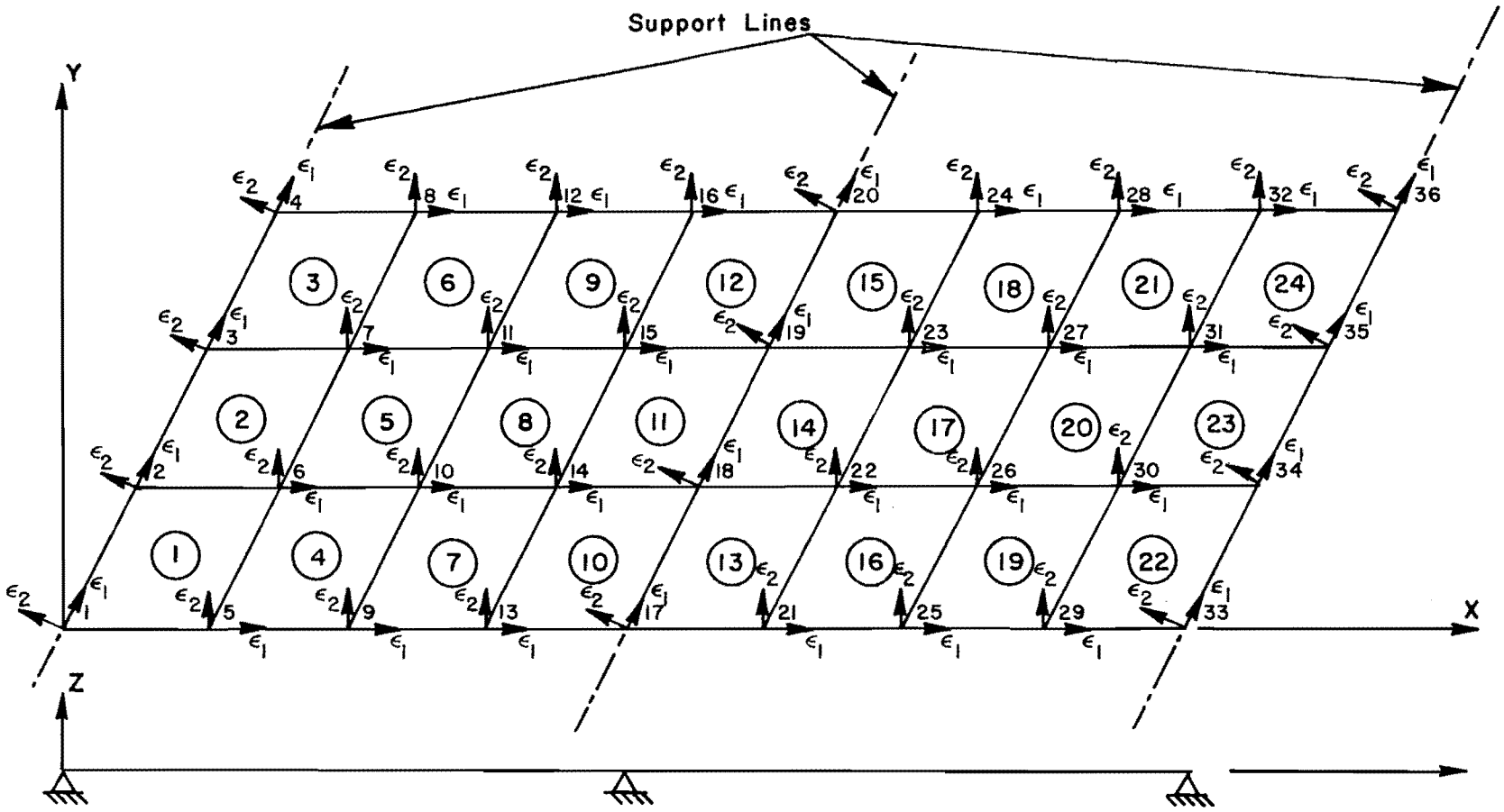

Fig 49. Two-span skewed slab bridge.

On the ninth card, only one data card was required to generate all 24 elements' nodal point number by following the description of Sec. 4.5 for a regular mesh. Again on the twelfth card, only one data card generated the temperature distribution along the thickness of the bridge at 36 nodal points.

With regard to the boundary condition cards, Sec. 4.10, care must be exercised in specifying the correct boundary conditions. Referring to Fig 49, for nodal points 1, 2, 3, 4, 17, 18, 19, 20, 33, 34, 35, and 36, which were on the top of the support, the vertical displacement, D3, and the rotation about ξ_2 , D5, are zero. With only these boundary restraints, the bridge would be free to move in space as a rigid body. In order to fix the bridge in space, the displacement in the ξ_1-direction at nodal point 5 and the displacements in both the ξ_1- and ξ_2-directions at nodal point 29 were arbitrarily set to be zero.

The output obtained by executing the first set of input data of Table 18 on the CDC 6600 at The University of Texas at Austin is contained in Tables 19 through 30. With regard to the second set of input data of Table 18, only the portion of the output relating to stress resultants is listed since the remaining output (except for ISIG) would be identical to the first set of input data. This portion of output is contained in Tables 31 through 33. Each section of input data is generally echo printed for check purposes followed by a complete listing in tabular form. For example, in Table 19 one line was used to echo print the input required to define nodal point temperatures while the complete listing of nodal point temperatures is printed in the lower portion of Table 20. All echo and complete listings are contained in Tables 19 through 22.

Nodal point displacements are listed in Table 30. Element displacements are listed in the lower portion of Tables 22 through 26. At each node six displacements are given. They consist of three translations (D1, D2, D3) and three rotations (D4, D5, D6). Both the translations and rotations are in surface coordinates since IFLAG = 1 was used on the control card of Sec. 4.2 in the data input guide.

As mentioned previously, there are two options available to the user in program SHELL for printing out the stresses, i.e.,

(a) stress resultants (force and moment per unit length of midsurface), ISIG = 0 , and

(b) stresses and principal stresses (force per unit area), ISIG = 1 .

TABLE 20

15	4.15470E+02	2.00000E+02	0.
16	4.73205E+02	3.00000E+02	0.
17	4.00000E+02	0.	0.
18	4.57735E+02	1.00000E+02	0.
19	5.15470E+02	2.00000E+02	0.
20	5.73205E+02	3.00000E+02	0.
21	5.00000E+02	0.	0.
22	5.57735E+02	1.00000E+02	0.
23	6.15470E+02	2.00000E+02	0.
24	6.73205E+02	3.00000E+02	0.
25	6.00000E+02	0.	0.
26	6.57735E+02	1.00000E+02	0.
27	7.15470E+02	2.00000E+02	0.
28	7.73205E+02	3.00000E+02	0.
29	7.00000E+02	0.	0.
30	7.57735E+02	1.00000E+02	0.
31	8.15470E+02	2.00000E+02	0.
32	8.73205E+02	3.00000E+02	0.
33	8.00000E+02	0.	0.
34	8.57735E+02	1.00000E+02	0.
35	9.15470E+02	2.00000E+02	0.
36	9.73205E+02	3.00000E+02	0.

NODAL POINT TEMPERATURES FOR CASE 1

1	1.14600E+02	8.46000E+01	7.17000E+01	7.15000E+01	8.23000E+01
2	1.14600E+02	8.46000E+01	7.17000E+01	7.15000E+01	8.23000E+01
3	1.14600E+02	8.46000E+01	7.17000E+01	7.15000E+01	8.23000E+01
4	1.14600E+02	8.46000E+01	7.17000E+01	7.15000E+01	8.23000E+01
5	1.14600E+02	8.46000E+01	7.17000E+01	7.15000E+01	8.23000E+01
6	1.14600E+02	8.46000E+01	7.17000E+01	7.15000E+01	8.23000E+01
7	1.14600E+02	8.46000E+01	7.17000E+01	7.15000E+01	8.23000E+01
8	1.14600E+02	8.46000E+01	7.17000E+01	7.15000E+01	8.23000E+01
9	1.14600E+02	8.46000E+01	7.17000E+01	7.15000E+01	8.23000E+01
10	1.14600E+02	8.46000E+01	7.17000E+01	7.15000E+01	8.23000E+01
11	1.14600E+02	8.46000E+01	7.17000E+01	7.15000E+01	8.23000E+01
12	1.14600E+02	8.46000E+01	7.17000E+01	7.15000E+01	8.23000E+01
13	1.14600E+02	8.46000E+01	7.17000E+01	7.15000E+01	8.23000E+01
14	1.14600E+02	8.46000E+01	7.17000E+01	7.15000E+01	8.23000E+01
15	1.14600E+02	8.46000E+01	7.17000E+01	7.15000E+01	8.23000E+01
16	1.14600E+02	8.46000E+01	7.17000E+01	7.15000E+01	8.23000E+01
17	1.14600E+02	8.46000E+01	7.17000E+01	7.15000E+01	8.23000E+01
18	1.14600E+02	8.46000E+01	7.17000E+01	7.15000E+01	8.23000E+01
19	1.14600E+02	8.46000E+01	7.17000E+01	7.15000E+01	8.23000E+01
20	1.14600E+02	8.46000E+01	7.17000E+01	7.15000E+01	8.23000E+01
21	1.14600E+02	8.46000E+01	7.17000E+01	7.15000E+01	8.23000E+01
22	1.14600E+02	8.46000E+01	7.17000E+01	7.15000E+01	8.23000E+01
23	1.14600E+02	8.46000E+01	7.17000E+01	7.15000E+01	8.23000E+01
24	1.14600E+02	8.46000E+01	7.17000E+01	7.15000E+01	8.23000E+01
25	1.14600E+02	8.46000E+01	7.17000E+01	7.15000E+01	8.23000E+01
26	1.14600E+02	8.46000E+01	7.17000E+01	7.15000E+01	8.23000E+01
27	1.14600E+02	8.46000E+01	7.17000E+01	7.15000E+01	8.23000E+01
28	1.14600E+02	8.46000E+01	7.17000E+01	7.15000E+01	8.23000E+01
29	1.14600E+02	8.46000E+01	7.17000E+01	7.15000E+01	8.23000E+01
30	1.14600E+02	8.46000E+01	7.17000E+01	7.15000E+01	8.23000E+01
31	1.14600E+02	8.46000E+01	7.17000E+01	7.15000E+01	8.23000E+01
32	1.14600E+02	8.46000E+01	7.17000E+01	7.15000E+01	8.23000E+01
33	1.14600E+02	8.46000E+01	7.17000E+01	7.15000E+01	8.23000E+01
34	1.14600E+02	8.46000E+01	7.17000E+01	7.15000E+01	8.23000E+01
35	1.14600E+02	8.46000E+01	7.17000E+01	7.15000E+01	8.23000E+01
36	1.14600E+02	8.46000E+01	7.17000E+01	7.15000E+01	8.23000E+01

TABLE 21

SURFACE DIRECTIONS COSINES.

PT.	E1X	E1Y	E1Z	E2X	E2Y	E2Z
1	.50060	.86603	0.00000	-.86603	.50000	0.00000
2	.50000	.86603	0.00000	-.86603	.50000	0.00000
3	.50000	.86603	0.00000	-.86603	.50000	0.00000
4	.50000	.86603	0.00000	-.86603	.50000	0.00000
5	1.00000	0.00000	0.00000	-0.00000	1.00000	0.00000
6	1.00000	0.00000	0.00000	-0.00000	1.00000	0.00000
7	1.00000	0.00000	0.00000	-0.00000	1.00000	0.00000
8	1.00000	0.00000	0.00000	-0.00000	1.00000	0.00000
9	1.00000	0.00000	0.00000	-0.00000	1.00000	0.00000
10	1.00000	0.00000	0.00000	-0.00000	1.00000	0.00000
11	1.00000	0.00000	0.00000	-0.00000	1.00000	0.00000
12	1.00000	0.00000	0.00000	-0.00000	1.00000	0.00000
13	1.00000	0.00000	0.00000	-0.00000	1.00000	0.00000
14	1.00000	0.00000	0.00000	-0.00000	1.00000	0.00000
15	1.00000	0.00000	0.00000	-0.00000	1.00000	0.00000
16	1.00000	0.00000	0.00000	-0.00000	1.00000	0.00000
17	.50000	.86603	0.00000	-.86603	.50000	0.00000
18	.50000	.86603	0.00000	-.86603	.50000	0.00000
19	.50000	.86603	0.00000	-.86603	.50000	0.00000
20	.50000	.86603	0.00000	-.86603	.50000	0.00000
21	1.00000	0.00000	0.00000	-0.00000	1.00000	0.00000
22	1.00000	0.00000	0.00000	-0.00000	1.00000	0.00000
23	1.00000	0.00000	0.00000	-0.00000	1.00000	0.00000
24	1.00000	0.00000	0.00000	-0.00000	1.00000	0.00000
25	1.00000	0.00000	0.00000	-0.00000	1.00000	0.00000
26	1.00000	0.00000	0.00000	-0.00000	1.00000	0.00000
27	1.00000	0.00000	0.00000	-0.00000	1.00000	0.00000
28	1.00000	0.00000	0.00000	-0.00000	1.00000	0.00000
29	1.00000	0.00000	0.00000	-0.00000	1.00000	0.00000
30	1.00000	0.00000	0.00000	-0.00000	1.00000	0.00000
31	1.00000	0.00000	0.00000	-0.00000	1.00000	0.00000
32	1.00000	0.00000	0.00000	-0.00000	1.00000	0.00000
33	.50000	.86603	0.00000	-.86603	.50000	0.00000
34	.50000	.86603	0.00000	-.86603	.50000	0.00000
35	.50000	.86603	0.00000	-.86603	.50000	0.00000
36	.50000	.86603	0.00000	-.86603	.50000	0.00000

EL. NO.,EL. NODE NOS.,MATL. TYPE=T,EL. TYPE=E,EL.THICKNESS,ANG.THER.COEF.

EL.	I	J	K	L	T	E	TI	TK	TL	ANG	ALPHA
1	1	5	6	2	1	1	1.800E+01	1.800E+01	1.800E+01	1.800E+01	0.0 6.000E-06
2	2	6	7	3	1	1	1.800E+01	1.800E+01	1.800E+01	1.800E+01	0.0 6.000E-06
3	3	7	8	4	1	1	1.800E+01	1.800E+01	1.800E+01	1.800E+01	0.0 6.000E-06
4	5	9	10	6	1	1	1.800E+01	1.800E+01	1.800E+01	1.800E+01	0.0 6.000E-06
5	6	10	11	7	1	1	1.800E+01	1.800E+01	1.800E+01	1.800E+01	0.0 6.000E-06
6	7	11	12	8	1	1	1.800E+01	1.800E+01	1.800E+01	1.800E+01	0.0 6.000E-06
7	9	13	14	10	1	1	1.800E+01	1.800E+01	1.800E+01	1.800E+01	0.0 6.000E-06
8	10	14	15	11	1	1	1.800E+01	1.800E+01	1.800E+01	1.800E+01	0.0 6.000E-06
9	11	15	16	12	1	1	1.800E+01	1.800E+01	1.800E+01	1.800E+01	0.0 6.000E-06
10	13	17	18	14	1	1	1.800E+01	1.800E+01	1.800E+01	1.800E+01	0.0 6.000E-06
11	14	18	19	15	1	1	1.800E+01	1.800E+01	1.800E+01	1.800E+01	0.0 6.000E-06
12	15	19	20	16	1	1	1.800E+01	1.800E+01	1.800E+01	1.800E+01	0.0 6.000E-06
13	17	21	22	18	1	1	1.800E+01	1.800E+01	1.800E+01	1.800E+01	0.0 6.000E-06
14	18	22	23	19	1	1	1.800E+01	1.800E+01	1.800E+01	1.800E+01	0.0 6.000E-06
15	19	23	24	20	1	1	1.800E+01	1.800E+01	1.800E+01	1.800E+01	0.0 6.000E-06
16	21	25	26	22	1	1	1.800E+01	1.800E+01	1.800E+01	1.800E+01	0.0 6.000E-06
17	22	26	27	23	1	1	1.800E+01	1.800E+01	1.800E+01	1.800E+01	0.0 6.000E-06
18	23	27	28	24	1	1	1.800E+01	1.800E+01	1.800E+01	1.800E+01	0.0 6.000E-06
19	25	29	30	26	1	1	1.800E+01	1.800E+01	1.800E+01	1.800E+01	0.0 6.000E-06

TABLE 22

```
  20   26   30   31   27 1 1 1.800E+01 1.800E+01 1.800E+01 1.800E+01    0.0 6.000E-06
  21   27   31   32   28 1 1 1.800E+01 1.800E+01 1.800E+01 1.800E+01    0.0 6.000E-06
  22   29   33   34   30 1 1 1.800E+01 1.800E+01 1.800E+01 1.800E+01    0.0 6.000E-06
  23   30   34   35   31 1 1 1.800E+01 1.800E+01 1.800E+01 1.800E+01    0.0 6.000E-06
  24   31   35   36   32 1 1 1.800E+01 1.800E+01 1.800E+01 1.800E+01    0.0 6.000E-06

 1 2 2 1 2 4 4 2 2 4 4 2 2 4 4 2 2 4 4 2 2 4 4 2 2 4 4 2 2 4 4 2 1 2 2 1

DUPLICATION OF INPUT BOUNDARY CONDITION CARDS,
D1,D2 AND D3 ARE TRANSLATIONS IN BASE COORDINATES,
D4,D5 AND D6 ARE ROTATIONS IN BASE COORDINATES,
PT, 123456  LIM MOD  D1          D2          D3          D4          D5          D6
  5 111000    -0  -0 -0.        -0.         -0.         -0.         -0.         -0.
 29 010000    -0  -0 -0.        -0.         -0.         -0.         -0.         -0.
  1 001010     4   1 -0.        -0.         -0.         -0.         -0.         -0.
 17 001010    20   1 -0.        -0.         -0.         -0.         -0.         -0.
 33 001010    36   1 -0.        -0.         -0.         -0.         -0.         -0.

BOUNDARY CONDITIONS OF POINTS HAVING SPECIFIED DISPLS,
PT, 1 2 3 4 5 6   D1          D2          D3          D4          D5          D6
  5 1 1 0 0 0 0 -0.         -0.         -0.         -0.         -0.         -0.
 29 0 1 0 0 0 0 -0.         -0.         -0.         -0.         -0.         -0.
  1 0 0 1 0 1 0 -0.         -0.         -0.         -0.         -0.         -0.
  2 0 0 1 0 1 0 -0.         -0.         -0.         -0.         -0.         -0.
  3 0 0 1 0 1 0 -0.         -0.         -0.         -0.         -0.         -0.
  4 0 0 1 0 1 0 -0.         -0.         -0.         -0.         -0.         -0.
 17 0 0 1 0 1 0 -0.         -0.         -0.         -0.         -0.         -0.
 18 0 0 1 0 1 0 -0.         -0.         -0.         -0.         -0.         -0.
 19 0 0 1 0 1 0 -0.         -0.         -0.         -0.         -0.         -0.
 20 0 0 1 0 1 0 -0.         -0.         -0.         -0.         -0.         -0.
 33 0 0 1 0 1 0 -0.         -0.         -0.         -0.         -0.         -0.
 34 0 0 1 0 1 0 -0.         -0.         -0.         -0.         -0.         -0.
 35 0 0 1 0 1 0 -0.         -0.         -0.         -0.         -0.         -0.
 36 0 0 1 0 1 0 -0.         -0.         -0.         -0.         -0.         -0.

NUMBER OF NODES WITH SPRINGS=   -0


NUMBER OF INDEPENDENT LOAD CASES        =    1
NUMBER OF LOADED NODES FOR LOAD CASE 1 =    -0
NUMBER OF LOADED NODES FOR LOAD CASE 2 =    -0
NUMBER OF LOADED NODES FOR LOAD CASE 3 =    -0
NUMBER OF LOADED NODES FOR LOAD CASE 4 =    -0
NUMBER OF LOADED NODES FOR LOAD CASE 5 =    -0
UNIFORM VERTICAL LOAD = -0.
 -0  -0

POINTS CONTAINED IN EQUIL,EQS,,RIGHT OF DIAGONAL,
   EQ,

       ELEMENT    24

  7.459E-02   2.085E-02   7.590E-02   1.504E-04
  4.511E-04   0.          6.057E-02  -6.320E-02
  6.173E-27   1.267E-03   1.778E-26   0.
  7.261E-02  -6.320E-02  -1.861E-26   4.691E-04
 -5.586E-25   0.          8.061E-02   3.128E-02
  4.383E-02  -3.913E-04   3.167E-04   0.

       ELEMENT    23
```

TABLE 23

```
  6.858E-02   1.043E-02   6.689E-02   3.679E-04
  2.424E-04   0.          4.853E-02  -6.320E-02
  2.978E-27   1.358E-03   1.061E-25   0.
  6.057E-02  -6.320E-02   6.173E-27   1.267E-03
  1.778E-26   0.          7.459E-02   2.085E-02
  7.590E-02   1.504E-04   4.511E-04   0.

       ELEMENT    22

  6.256E-02   4.506E-25   2.736E-03   9.345E-04
 -4.462E-04   0.          3.649E-02  -6.320E-02
 -2.539E-26   8.014E-04  -1.101E-24   0.
  4.853E-02  -6.320E-02   2.978E-27   1.358E-03
  1.061E-25   0.          6.858E-02   1.043E-02
  6.689E-02   3.679E-04   2.424E-04   0.

       ELEMENT    21

  6.417E-02   2.085E-02   8.829E-02  -2.025E-05
 -1.426E-04   0.          7.459E-02   2.085E-02
  7.590E-02   1.504E-04   4.511E-04   0.
  8.061E-02   3.128E-02   4.383E-02  -3.913E-04
  3.167E-04   0.          7.819E-02   3.128E-02
  5.826E-02  -7.319E-04   1.419E-05   0.

       ELEMENT    20

  5.815E-02   1.043E-02   5.347E-02   3.619E-04
 -4.501E-04   0.          6.858E-02   1.043E-02
  6.689E-02   3.679E-04   2.424E-04   0.
  7.459E-02   2.085E-02   7.590E-02   1.504E-04
  4.511E-04   0.          6.417E-02   2.085E-02
  8.829E-02  -2.025E-05  -1.426E-04   0.

       ELEMENT    19

  5.213E-02   1.076E-14  -4.466E-02   1.159E-03
 -4.271E-04   0.          6.256E-02   4.506E-25
  2.736E-03   9.345E-04  -4.462E-04   0.
  6.858E-02   1.043E-02   6.689E-02   3.679E-04
  2.424E-04   0.          5.815E-02   1.043E-02
  5.347E-02   3.619E-04  -4.501E-04   0.

       ELEMENT    18

  5.374E-02   2.085E-02   4.863E-02  -2.562E-05
 -6.156E-04   0.          6.417E-02   2.085E-02
  8.829E-02  -2.025E-05  -1.426E-04   0.
  7.819E-02   3.128E-02   5.826E-02  -7.319E-04
  1.419E-05   0.          5.976E-02   3.128E-02
  4.557E-02  -6.505E-04  -2.379E-04   0.

       ELEMENT    17

  4.772E-02   1.043E-02   8.597E-03   2.520E-04
```

TABLE 24

-4,077E-04	0,	5,815E-02	1,043E-02
5,347E-02	3,619E-04	-4,501E-04	0,
6,417E-02	2,085E-02	8,829E-02	-2,025E-05
-1,426E-04	0,	5,374E-02	2,085E-02
4,863E-02	-2,562E-05	-6,156E-04	0,

ELEMENT 16

4,170E-02	1,421E-14	-5,537E-02	9,265E-04
2,615E-04	0,	5,213E-02	1,076E-14
-4,466E-02	1,159E-03	-4,271E-04	0,
5,815E-02	1,043E-02	5,347E-02	3,619E-04
-4,501E-04	0,	4,772E-02	1,043E-02
8,597E-03	2,520E-04	-4,077E-04	0,

ELEMENT 15

3,972E-02	-2,709E-02	1,398E-26	-3,097E-04
2,940E-26	0,	5,374E-02	2,085E-02
4,863E-02	-2,562E-05	-6,156E-04	0,
5,976E-02	3,128E-02	4,557E-02	-6,505E-04
-2,379E-04	0,	5,176E-02	-2,709E-02
-1,511E-26	-8,379E-04	2,033E-25	0,

ELEMENT 14

2,768E-02	-2,709E-02	1,398E-26	3,097E-04
-2,940E-26	0,	4,772E-02	1,043E-02
8,597E-03	2,520E-04	-4,077E-04	0,
5,374E-02	2,085E-02	4,863E-02	-2,562E-05
-6,156E-04	0,	3,972E-02	-2,709E-02
1,398E-26	-3,097E-04	2,940E-26	0,

ELEMENT 13

1,564E-02	-2,709E-02	-1,511E-26	8,379E-04
-2,033E-25	0,	4,170E-02	1,421E-14
-5,537E-02	9,265E-04	2,615E-04	0,
4,772E-02	1,043E-02	8,597E-03	2,520E-04
-4,077E-04	0,	2,768E-02	-2,709E-02
1,398E-26	3,097E-04	-2,940E-26	0,

ELEMENT 12

3,289E-02	2,085E-02	8,597E-03	-2,520E-04
4,077E-04	0,	3,972E-02	-2,709E-02
1,398E-26	-3,097E-04	2,940E-26	0,
5,176E-02	-2,709E-02	-1,511E-26	-8,379E-04
2,033E-25	0,	3,891E-02	3,128E-02
-5,537E-02	-9,265E-04	-2,615E-04	0,

ELEMENT 11

2,687E-02	1,043E-02	4,863E-02	2,562E-05
6,156E-04	0,	2,768E-02	-2,709E-02
1,398E-26	3,097E-04	-2,940E-26	0,

TABLE 25

3,972E-02	-2,709E-02	1,398E-26	-3,097E-04
2,940E-26	0,	3,289E-02	2,085E-02
8,597E-03	-2,520E-04	4,077E-04	0,

ELEMENT 10

2,085E-02	1,605E-14	4,557E-02	6,505E-04
2,379E-04	0,	1,564E-02	-2,709E-02
-1,511E-26	8,379E-04	-2,033E-25	0,
2,768E-02	-2,709E-02	1,398E-26	3,097E-04
-2,940E-26	0,	2,687E-02	1,043E-02
4,863E-02	2,562E-05	6,156E-04	0,

ELEMENT 9

2,246E-02	2,085E-02	5,347E-02	-3,619E-04
4,501E-04	0,	3,289E-02	2,085E-02
8,597E-03	-2,520E-04	4,077E-04	0,
3,891E-02	3,128E-02	-5,537E-02	-9,265E-04
-2,615E-04	0,	2,848E-02	3,128E-02
-4,466E-02	-1,159E-03	4,271E-04	0,

ELEMENT 8

1,645E-02	1,043E-02	8,829E-02	2,025E-05
1,426E-04	0,	2,687E-02	1,043E-02
4,863E-02	2,562E-05	6,156E-04	0,
3,289E-02	2,085E-02	8,597E-03	-2,520E-04
4,077E-04	0,	2,246E-02	2,085E-02
5,347E-02	-3,619E-04	4,501E-04	0,

ELEMENT 7

1,043E-02	1,133E-14	5,826E-02	7,319E-04
-1,419E-05	0,	2,085E-02	1,605E-14
4,557E-02	6,505E-04	2,379E-04	0,
2,687E-02	1,043E-02	4,863E-02	2,562E-05
6,156E-04	0,	1,645E-02	1,043E-02
8,829E-02	2,025E-05	1,426E-04	0,

ELEMENT 6

1,204E-02	2,085E-02	6,689E-02	-3,679E-04
-2,424E-04	0,	2,246E-02	2,085E-02
5,347E-02	-3,619E-04	4,501E-04	0,
2,848E-02	3,128E-02	-4,466E-02	-1,159E-03
4,271E-04	0,	1,806E-02	3,128E-02
2,736E-03	-9,345E-04	4,462E-04	0,

ELEMENT 5

6,819E-03	1,043E-02	7,590E-02	-1,504E-04
-4,511E-04	0,	1,645E-02	1,043E-02
8,829E-02	2,025E-05	1,426E-04	0,
2,246E-02	2,085E-02	5,347E-02	-3,619E-04
4,501E-04	0,	1,204E-02	2,085E-02

TABLE 26

```
 6,689E-02  -3,679E-04  -2,424E-04   0.

      ELEMENT     4

-3,760E-37   4,506E-25   4,383E-02   3,913E-04
-3,167E-04   0.          1,043E-02   1,133E-14
 5,826E-02   7,319E-04  -1,419E-05   0.
 1,645E-02   1,043E-02   8,829E-02   2,025E-05
 1,426E-04   0.          6,019E-03   1,043E-02
 7,590E-02  -1,504E-04  -4,511E-04   0.

      ELEMENT     3

 1,886E-02   9,029E-03   2,978E-27  -1,358E-03
-1,061E-25   0.          1,204E-02   2,085E-02
 6,689E-02  -3,679E-04  -2,424E-04   0.
 1,806E-02   3,128E-02   2,736E-03  -9,345E-04
 4,462E-04   0.          3,094E-02   9,029E-03
-2,539E-26  -8,014E-04   1,101E-24   0.

      ELEMENT     2

 6,826E-03   9,029E-03   6,173E-27  -1,267E-03
-1,778E-26   0.          6,019E-03   1,043E-02
 7,590E-02  -1,504E-04  -4,511E-04   0.
 1,204E-02   2,085E-02   6,689E-02  -3,679E-04
-2,424E-04   0.          1,886E-02   9,029E-03
 2,978E-27  -1,358E-03  -1,061E-25   0.

      ELEMENT     1

-5,213E-03   9,029E-03  -1,861E-26  -6,691E-04
 5,586E-25   0.         -3,760E-37   4,506E-25
 4,383E-02   3,913E-04  -3,167E-04   0.
 6,019E-03   1,043E-02   7,590E-02  -1,504E-04
-4,511E-04   0.          6,826E-03   9,029E-03
 6,173E-27  -1,267E-03  -1,778E-26   0.
```

TABLE 27

ELEMENT STRESSES (TOP-BOTTOM) FOR LOAD CASE 1

N1	N2	S	N1	N2	S				
ELEMENT NO. 1						NODE			
-8,362E+02	-7,015E+02	-2,217E+02	2,500E+02	2,500E+02	-5,128E-11	-2,052E+02	-3,399E+02	2,217E+02	1
-7,535E+02	-6,225E+02	-1,936E+02	2,500E+02	2,500E+02	-5,128E-11	-2,879E+02	-4,189E+02	1,936E+02	5
-7,238E+02	-6,836E+02	-1,534E+02	2,500E+02	2,500E+02	-5,128E-11	-3,177E+02	-3,578E+02	1,534E+02	6
-7,618E+02	-6,998E+02	-1,712E+02	2,500E+02	2,500E+02	-5,128E-11	-2,797E+02	-3,417E+02	1,712E+02	2
-7,628E+02	-6,771E+02	-1,757E+02	2,500E+02	2,500E+02	-5,128E-11	-2,787E+02	-3,644E+02	1,757E+02	0
ELEMENT NO. 2						NODE			
-7,008E+02	-8,259E+02	-1,578E+02	2,500E+02	2,500E+02	5,723E-11	-3,406E+02	-2,155E+02	1,578E+02	2
-6,629E+02	-7,509E+02	-1,229E+02	2,500E+02	2,500E+02	5,723E-11	-3,786E+02	-2,905E+02	1,229E+02	6
-7,124E+02	-8,418E+02	-8,361E+01	2,500E+02	2,500E+02	5,723E-11	-3,291E+02	-1,996E+02	8,361E+01	7
-6,176E+02	-8,023E+02	-1,183E+02	2,500E+02	2,500E+02	5,723E-11	-4,239E+02	-2,392E+02	1,183E+02	3
-6,564E+02	-8,136E+02	-1,036E+02	2,500E+02	2,500E+02	5,723E-11	-3,851E+02	-2,279E+02	1,036E+02	0
ELEMENT NO. 3						NODE			
-5,818E+02	-9,414E+02	-7,026E+01	2,500E+02	2,500E+02	3,716E-11	-4,597E+02	-1,001E+02	7,026E+01	3
-5,686E+02	-8,989E+02	-1,284E+02	2,500E+02	2,500E+02	3,716E-11	-4,728E+02	-3,425E+02	1,284E+02	7
-7,239E+02	-7,337E+02	1,740E+02	2,500E+02	2,500E+02	3,716E-11	-3,175E+02	-3,078E+02	-1,740E+02	8
-6,019E+02	-1,084E+03	1,379E+02	2,500E+02	2,500E+02	3,716E-11	-4,395E+02	4,228E+01	-1,379E+02	4
-6,047E+02	-8,967E+02	1,282E+01	2,500E+02	2,500E+02	3,716E-11	-4,368E+02	-1,447E+02	-1,282E+01	0
ELEMENT NO. 4						NODE			
-7,880E+02	-6,526E+02	-1,051E+02	2,500E+02	2,500E+02	-1,453E-10	-2,535E+02	-3,889E+02	1,051E+02	5
-7,678E+02	-6,119E+02	-7,683E+01	2,500E+02	2,500E+02	-1,453E-10	-2,736E+02	-4,296E+02	7,683E+01	9
-7,842E+02	-7,233E+02	-5,242E+01	2,500E+02	2,500E+02	-1,453E-10	-2,572E+02	-3,182E+02	5,242E+01	10
-7,490E+02	-7,065E+02	-7,657E+01	2,500E+02	2,500E+02	-1,453E-10	-2,925E+02	-3,349E+02	7,657E+01	6
-7,650E+02	-6,760E+02	-6,922E+01	2,500E+02	2,500E+02	-1,453E-10	-2,764E+02	-3,654E+02	6,922E+01	0
ELEMENT NO. 5						NODE			
-6,773E+02	-7,695E+02	-5,121E+01	2,500E+02	2,500E+02	-4,162E-11	-3,642E+02	-2,720E+02	5,121E+01	6
-7,464E+02	-7,725E+02	-4,845E+01	2,500E+02	2,500E+02	-4,162E-11	-2,951E+02	-2,709E+02	4,845E+01	10
-7,667E+02	-8,190E+02	1,611E+00	2,500E+02	2,500E+02	-4,162E-11	-2,747E+02	-2,224E+02	-1,611E+00	11
-7,268E+02	-8,836E+02	-1,823E+01	2,500E+02	2,500E+02	-4,162E-11	-3,147E+02	-1,579E+02	1,823E+01	7
-7,335E+02	-8,131E+02	-3,873E+01	2,500E+02	2,500E+02	-4,162E-11	-3,079E+02	-2,283E+02	3,873E+01	0
ELEMENT NO. 6						NODE			
-6,431E+02	-8,323E+02	2,729E+00	2,500E+02	2,500E+02	2,973E-12	-3,983E+02	-2,092E+02	-2,729E+00	7
-7,877E+02	-6,119E+02	-5,889E+01	2,500E+02	2,500E+02	2,973E-12	-2,537E+02	-4,296E+02	5,889E+01	11
-1,032E+03	-7,059E+02	6,007E+01	2,500E+02	2,500E+02	2,973E-12	-9,566E+00	-3,355E+02	-6,007E+01	12
-8,182E+02	-8,216E+02	1,408E+02	2,500E+02	2,500E+02	2,973E-12	-2,232E+02	-2,199E+02	-1,408E+02	8
-8,198E+02	-7,425E+02	5,165E+01	2,500E+02	2,500E+02	2,973E-12	-2,307E+02	-2,990E+02	-5,165E+01	0
ELEMENT NO. 7						NODE			
-8,121E+02	-6,591E+02	1,686E+01	2,500E+02	2,500E+02	-4,348E-11	-2,293E+02	-3,823E+02	-1,686E+01	9
-8,257E+02	-7,157E+02	5,957E+01	2,500E+02	2,500E+02	-4,348E-11	-2,157E+02	-3,257E+02	-5,957E+01	13
-8,247E+02	-8,296E+02	3,120E+00	2,500E+02	2,500E+02	-4,348E-11	-2,167E+02	-2,118E+02	-3,120E+00	14
-7,759E+02	-7,111E+02	-2,624E+01	2,500E+02	2,500E+02	-4,348E-11	-2,656E+02	-3,304E+02	2,624E+01	10
-8,047E+02	-7,277E+02	2,246E+01	2,500E+02	2,500E+02	-4,348E-11	-2,368E+02	-3,137E+02	-2,246E+01	0
ELEMENT NO. 8						NODE			
-7,386E+02	-7,953E+02	-4,463E+01	2,500E+02	2,500E+02	-5,351E-11	-3,028E+02	-2,462E+02	4,463E+01	10
-8,957E+02	-8,122E+02	-4,026E+01	2,500E+02	2,500E+02	-5,351E-11	-1,458E+02	-2,292E+02	4,026E+01	14
-1,038E+03	-8,559E+02	-3,138E+01	2,500E+02	2,500E+02	-5,351E-11	-1,169E+01	-1,856E+02	3,138E+01	15
-8,808E+02	-8,742E+02	-3,478E+00	2,500E+02	2,500E+02	-5,351E-11	-1,606E+02	-1,673E+02	3,478E+00	11
-8,876E+02	-8,369E+02	-2,407E+01	2,500E+02	2,500E+02	-5,351E-11	-1,538E+02	-2,046E+02	2,407E+01	0
ELEMENT NO. 9						NODE			
-9,020E+02	-7,185E+02	-4,224E+01	2,500E+02	2,500E+02	-1,338E-11	-1,394E+02	-3,229E+02	4,224E+01	11
-1,063E+03	-6,531E+02	-7,021E+01	2,500E+02	2,500E+02	-1,338E-11	2,178E+01	-3,883E+02	7,021E+01	15
-1,261E+03	-7,532E+02	-6,945E+01	2,500E+02	2,500E+02	-1,338E-11	2,200E+02	-2,882E+02	6,945E+01	16
-1,037E+03	-7,078E+02	-1,752E+01	2,500E+02	2,500E+02	-1,338E-11	-4,876E+00	-3,345E+02	1,752E+01	12
-1,057E+03	-7,060E+02	-3,339E+01	2,500E+02	2,500E+02	-1,338E-11	1,546E+01	-3,355E+02	3,339E+01	0
ELEMENT NO. 10						NODE			
-8,149E+02	-6,647E+02	1,056E+02	2,500E+02	2,500E+02	-2,267E-11	-2,265E+02	-3,767E+02	-1,056E+02	13
-9,018E+02	-7,769E+02	-9,015E+00	2,500E+02	2,500E+02	-2,267E-11	-1,396E+02	-2,645E+02	9,015E+00	17
-1,202E+03	-8,978E+02	-3,525E+01	2,500E+02	2,500E+02	-2,267E-11	1,603E+02	-1,436E+02	3,525E+01	18

TABLE 28

-9,168E+02	-8,554E+02	-2,151E+01	2,500E+02	2,500E+02	-2,267E-11	-1,246E+02	-1,486E+02	2,151E+01	14
-9,366E+02	-8,368E+02	2,025E-01	2,500E+02	2,500E+02	-2,267E-11	-1,049E+02	-2,047E+02	-2,025E-01	0
ELEMENT NO, 11					NODE				
-9,887E+02	-8,797E+02	-5,319E+01	2,500E+02	2,500E+02	-5,454E-11	-5,274E+01	-1,618E+02	5,319E+01	14
-1,187E+03	-8,556E+02	-5,381E+01	2,500E+02	2,500E+02	-5,454E-11	1,455E+02	-1,859E+02	5,381E+01	18
-1,253E+03	-8,986E+02	-2,997E+01	2,500E+02	2,500E+02	-5,454E-11	1,120E+02	-1,429E+02	2,997E+01	19
-1,153E+03	-9,371E+02	8,718E-01	2,500E+02	2,500E+02	-5,454E-11	1,116E+02	-1,043E+02	-8,718E-01	15
-1,157E+03	-8,791E+02	-3,612E+01	2,500E+02	2,500E+02	-5,454E-11	1,157E+02	-1,623E+02	3,612E+01	0
ELEMENT NO, 12					NODE				
-1,120E+03	-7,587E+02	-8,377E+01	2,500E+02	2,500E+02	-2,973E-11	7,887E+01	-2,827E+02	8,377E+01	15
-1,277E+03	-9,964E+02	1,185E+01	2,500E+02	2,500E+02	-2,973E-11	2,360E+02	-4,505E+01	-1,185E+01	19
-1,014E+03	-7,765E+02	-1,304E+02	2,500E+02	2,500E+02	-2,973E-11	-3,185E+01	-2,650E+02	1,304E+02	24
-1,153E+03	-8,585E+02	-1,677E+02	2,500E+02	2,500E+02	-2,973E-11	1,117E+02	-3,829E+02	1,677E+02	16
-1,177E+03	-7,638E+02	-1,196E+02	2,500E+02	2,500E+02	-2,973E-11	1,354E+02	-2,777E+02	1,196E+02	0
ELEMENT NO, 13					NODE				
-1,018E+03	-7,765E+02	-1,304E+02	2,500E+02	2,500E+02	-2,007E-11	-3,185E+01	-2,650E+02	1,304E+02	17
-1,153E+03	-8,585E+02	-1,677E+02	2,500E+02	2,500E+02	-2,007E-11	1,117E+02	-3,829E+02	1,677E+02	21
-1,124E+03	-7,587E+02	-8,377E+01	2,500E+02	2,500E+02	-2,007E-11	7,887E+01	-2,827E+02	8,377E+01	22
-1,277E+03	-9,964E+02	1,185E+01	2,500E+02	2,500E+02	-2,007E-11	2,360E+02	-4,505E+01	-1,185E+01	18
-1,177E+03	-7,638E+02	-1,196E+02	2,500E+02	2,500E+02	-2,007E-11	1,354E+02	-2,777E+02	1,196E+02	0
ELEMENT NO, 14					NODE				
-1,253E+03	-8,986E+02	-2,997E+01	2,500E+02	2,500E+02	-4,088E-11	2,120E+02	-1,429E+02	2,997E+01	18
-1,153E+03	-9,371E+02	8,718E+01	2,500E+02	2,500E+02	-4,088E-11	1,116E+02	-1,043E+02	-8,718E+01	22
-9,887E+02	-8,797E+02	-5,319E+01	2,500E+02	2,500E+02	-4,088E-11	-5,274E+01	-1,618E+02	5,319E+01	23
-1,187E+03	-8,556E+02	-5,381E+01	2,500E+02	2,500E+02	-4,088E-11	1,455E+02	-1,859E+02	5,381E+01	19
-1,157E+03	-8,791E+02	-3,612E+01	2,500E+02	2,500E+02	-4,088E-11	1,157E+02	-1,623E+02	3,612E+01	0
ELEMENT NO, 15					NODE				
-1,292E+03	-8,978E+02	-3,525E+01	2,500E+02	2,500E+02	-3,270E-11	1,603E+02	-1,436E+02	3,525E+01	19
-9,168E+02	-8,554E+02	-2,151E+01	2,500E+02	2,500E+02	-3,270E-11	-1,246E+02	-1,860E+02	2,151E+01	23
-8,149E+02	-6,647E+02	1,058E+02	2,500E+02	2,500E+02	-3,270E-11	-2,265E+02	-3,767E+02	-1,058E+02	24
-9,018E+02	-7,769E+02	-9,015E+00	2,500E+02	2,500E+02	-3,270E-11	-1,396E+02	-2,645E+02	9,015E+00	20
-9,366E+02	-8,368E+02	2,025E-01	2,500E+02	2,500E+02	-3,270E-11	-1,049E+02	-2,047E+02	-2,025E-01	0
ELEMENT NO, 16					NODE				
-1,261E+03	-7,532E+02	-6,945E+01	2,500E+02	2,500E+02	-3,047E-11	2,208E+02	-2,882E+02	6,945E+01	21
-1,037E+03	-7,947E+02	-1,752E+01	2,500E+02	2,500E+02	-3,047E-11	-8,476E+00	-3,345E+02	1,752E+01	25
-9,029E+02	-7,185E+02	-4,224E+01	2,500E+02	2,500E+02	-3,047E-11	-1,394E+02	-3,229E+02	4,224E+01	26
-1,063E+03	-8,531E+02	-7,021E+01	2,500E+02	2,500E+02	-3,047E-11	2,178E+01	-3,883E+02	7,021E+01	22
-1,057E+03	-7,660E+02	-3,339E+01	2,500E+02	2,500E+02	-3,047E-11	1,546E+01	-3,355E+02	3,339E+01	0
ELEMENT NO, 17					NODE				
-1,038E+03	-8,559E+02	-3,138E+01	2,500E+02	2,500E+02	-4,088E-11	-1,169E+01	-1,856E+02	3,138E+01	22
-8,848E+02	-8,742E+02	-3,478E+00	2,500E+02	2,500E+02	-4,088E-11	-1,696E+02	-1,673E+02	3,478E+00	26
-7,386E+02	-7,953E+02	-4,463E-01	2,500E+02	2,500E+02	-4,088E-11	-3,028E+02	-2,462E+02	4,463E-01	27
-8,957E+02	-8,122E+02	-4,026E+01	2,500E+02	2,500E+02	-4,088E-11	-1,458E+02	-2,292E+02	4,026E+01	23
-8,876E+02	-8,369E+02	-2,447E+01	2,500E+02	2,500E+02	-4,088E-11	-1,538E+02	-2,446E+02	2,447E+01	0
ELEMENT NO, 18					NODE				
-8,247E+02	-8,296E+02	3,124E+00	2,500E+02	2,500E+02	5,946E-12	-2,167E+02	-2,118E+02	-3,124E+00	23
-7,759E+02	-7,111E+02	-2,624E+01	2,500E+02	2,500E+02	5,946E-12	-2,656E+02	-3,308E+02	2,624E+01	27
-8,121E+02	-6,591E+02	1,686E+01	2,500E+02	2,500E+02	5,946E-12	-2,293E+02	-3,823E+02	-1,686E+01	24
-8,257E+02	-7,157E+02	5,957E+01	2,500E+02	2,500E+02	5,946E-12	-2,157E+02	-3,257E+02	-5,957E+01	24
-8,447E+02	-7,277E+02	2,246E+01	2,500E+02	2,500E+02	5,946E-12	-2,368E+02	-3,137E+02	-2,246E+01	0
ELEMENT NO, 19					NODE				
-1,032E+03	-7,059E+02	6,007E+01	2,500E+02	2,500E+02	-3,493E-11	-9,566E+00	-3,355E+02	-6,007E+01	25
-8,192E+02	-8,216E+02	1,408E+02	2,500E+02	2,500E+02	-3,493E-11	-2,232E+02	-2,199E+02	1,498E+02	29
-6,431E+02	-8,323E+02	2,729E+00	2,500E+02	2,500E+02	-3,493E-11	-3,983E+02	-2,092E+02	-2,729E+00	30
-7,877E+02	-6,119E+02	-5,889E+01	2,500E+02	2,500E+02	-3,493E-11	-2,537E+02	-4,296E+02	5,889E+01	26
-8,108E+02	-7,425E+02	5,165E+01	2,500E+02	2,500E+02	-3,493E-11	-2,307E+02	-2,990E+02	-5,165E+01	0
ELEMENT NO, 20					NODE				
-7,667E+02	-8,190E+02	1,611E+00	2,500E+02	2,500E+02	2,378E-11	-2,747E+02	-2,224E+02	-1,611E+00	26
-7,268E+02	-8,836E+02	-1,823E+01	2,500E+02	2,500E+02	2,378E-11	-3,147E+02	-1,579E+02	1,823E+01	30
-6,773E+02	-7,695E+02	-5,121E+01	2,500E+02	2,500E+02	2,378E-11	-3,642E+02	-2,728E+02	5,121E+01	31
-7,444E+02	-7,705E+02	-4,845E+01	2,500E+02	2,500E+02	2,378E-11	-2,951E+02	-2,709E+02	4,845E+01	27
-7,335E+02	-8,131E+02	-3,873E+01	2,500E+02	2,500E+02	2,378E-11	-3,079E+02	-2,283E+02	3,873E+01	0

TABLE 29

ELEMENT NO, 21					NODE				
-7,842E+02	-7,233E+02	-5,242E+01	2,500E+02	2,500E+02	-1,486E-12	-2,572E+02	-3,182E+02	5,242E+01	27
-7,499E+02	-7,965E+02	-7,657E+01	2,500E+02	2,500E+02	-1,486E-12	-2,925E+02	-3,349E+02	7,657E+01	31
-7,894E+02	-6,526E+02	-1,051E+02	2,500E+02	2,500E+02	-1,486E-12	-2,535E+02	-3,689E+02	1,051E+02	32
-7,678E+02	-6,119E+02	-7,683E+01	2,500E+02	2,500E+02	-1,486E-12	-2,736E+02	-4,296E+02	7,683E+01	28
-7,659E+02	-6,760E+02	-6,922E+01	2,500E+02	2,500E+02	-1,486E-12	-2,764E+02	-3,654E+02	6,922E+01	0
ELEMENT NO, 22					NODE				
-7,239E+02	-7,337E+02	1,740E+02	2,500E+02	2,500E+02	6,615E-11	-3,175E+02	-3,078E+02	-1,740E+02	29
-6,019E+02	-1,984E+03	1,379E+02	2,500E+02	2,500E+02	6,615E-11	-4,395E+02	4,228E+01	-1,379E+02	33
-5,814E+02	-9,414E+02	-7,026E+01	2,500E+02	2,500E+02	6,615E-11	-4,597E+02	-1,001E+02	7,026E+01	34
-5,686E+02	-6,989E+02	-1,284E+02	2,500E+02	2,500E+02	6,615E-11	-4,728E+02	-3,425E+02	1,284E+02	30
-6,047E+02	-8,967E+02	1,282E+01	2,500E+02	2,500E+02	6,615E-11	-4,368E+02	-1,447E+02	-1,282E+01	0
ELEMENT NO, 23					NODE				
-7,124E+02	-8,418E+02	-8,361E+01	2,500E+02	2,500E+02	1,561E-11	-3,291E+02	-1,996E+02	8,361E+01	30
-6,176E+02	-9,023E+02	-1,183E+02	2,500E+02	2,500E+02	1,561E-11	-4,239E+02	-2,392E+02	1,183E+02	34
-7,008E+02	-8,259E+02	-1,578E+02	2,500E+02	2,500E+02	1,561E-11	-3,406E+02	-2,155E+02	1,578E+02	35
-6,629E+02	-7,509E+02	-1,229E+02	2,500E+02	2,500E+02	1,561E-11	-3,786E+02	-2,905E+02	1,229E+02	31
-6,544E+02	-8,136E+02	-1,036E+02	2,500E+02	2,500E+02	1,561E-11	-3,851E+02	-2,279E+02	1,036E+02	0
ELEMENT NO, 24					NODE				
-7,238E+02	-6,836E+02	-1,534E+02	2,500E+02	2,500E+02	8,919E-12	-3,177E+02	-3,578E+02	1,534E+02	31
-7,618E+02	-6,998E+02	-1,712E+02	2,500E+02	2,500E+02	8,919E-12	-2,797E+02	-3,417E+02	1,712E+02	35
-8,362E+02	-7,815E+02	-2,217E+02	2,500E+02	2,500E+02	8,919E-12	-2,052E+02	-3,399E+02	2,217E+02	36
-7,535E+02	-6,225E+02	-1,936E+02	2,500E+02	2,500E+02	8,919E-12	-2,879E+02	-4,189E+02	1,936E+02	32
-7,628E+02	-6,771E+02	-1,757E+02	2,500E+02	2,500E+02	8,919E-12	-2,747E+02	-3,644E+02	1,757E+02	0

PRINCIPAL STRESSES (TOP-BOTTOM) FOR LOAD CASE 1

ELEM	SMAX	SMIN	TMAX	ANG	SMAX	SMIN	TMAX	ANG
1	-5,391E+02	-9,007E+02	1,808E+02	3,813E+01	-1,487E+02	-5,023E+02	1,808E+02	-5,183E+01
2	-8,449E+02	-8,659E+02	1,301E+02	6,357E+01	-1,764E+02	-4,365E+02	1,301E+02	-2,639E+01
3	-8,041E+02	-8,973E+02	1,466E+02	-8,746E+01	-1,441E+02	-4,373E+02	1,466E+02	2,508E+00
4	-6,382E+02	-8,028E+02	8,229E+01	2,862E+01	-2,386E+02	-4,032E+02	8,229E+01	-6,134E+01
5	-7,178E+02	-8,288E+02	5,552E+01	6,786E+01	-2,126E+02	-3,236E+02	5,552E+01	-2,211E+01
6	-7,147E+02	-8,385E+02	6,192E+01	-2,825E+01	-2,829E+02	-3,267E+02	6,192E+01	6,171E+01
7	-7,217E+02	-8,107E+02	4,454E+01	-1,514E+01	-2,307E+02	-3,198E+02	4,454E+01	7,483E+01
8	-8,273E+02	-8,972E+02	3,497E+01	2,174E+01	-1,442E+02	-2,142E+02	3,497E+01	-6,823E+01
9	-7,028E+02	-1,068E+03	1,786E+02	5,385E+00	1,861E+01	-3,386E+02	1,786E+02	-8,458E+01
10	-8,368E+02	-9,366E+02	8,998E+01	-1,162E+01	-1,049E+02	-2,047E+02	8,998E+01	8,985E+01
11	-8,745E+02	-1,162E+03	1,436E+02	7,288E+00	1,203E+02	-1,669E+02	1,436E+02	-8,268E+01
12	-7,360E+02	-1,205E+03	2,343E+02	1,408E+01	1,631E+02	-3,055E+02	2,343E+02	-7,588E+01
13	-7,360E+02	-1,205E+03	2,343E+02	1,408E+01	1,631E+02	-3,055E+02	2,343E+02	-7,588E+01
14	-8,745E+02	-1,162E+03	1,436E+02	7,288E+00	1,203E+02	-1,669E+02	1,436E+02	-8,268E+01
15	-8,368E+02	-9,366E+02	8,998E+01	-1,162E+01	-1,049E+02	-2,047E+02	8,998E+01	8,985E+01
16	-7,028E+02	-1,068E+03	1,786E+02	-2,232E+02	-2,199E+02	-1,498E+02	1,786E+02	-8,458E+01
17	-8,273E+02	-8,972E+02	3,497E+01	2,174E+01	-1,442E+02	-2,142E+02	3,497E+01	-6,823E+01
18	-7,217E+02	-8,107E+02	4,454E+01	-1,514E+01	-2,307E+02	-3,198E+02	4,454E+01	7,483E+01
19	-7,147E+02	-8,385E+02	6,192E+01	-2,825E+01	-2,829E+02	-3,267E+02	6,192E+01	6,171E+01
20	-7,178E+02	-8,288E+02	5,552E+01	6,786E+01	-2,126E+02	-3,236E+02	5,552E+01	-2,211E+01
21	-6,382E+02	-8,028E+02	8,229E+01	2,862E+01	-2,386E+02	-4,032E+02	8,229E+01	-6,134E+01
22	-8,041E+02	-8,973E+02	1,466E+02	-8,746E+01	-1,441E+02	-4,373E+02	1,466E+02	2,508E+00
23	-8,449E+02	-8,659E+02	1,301E+02	6,357E+01	-1,764E+02	-4,365E+02	1,301E+02	-2,639E+01
24	-5,391E+02	-9,007E+02	1,808E+02	3,813E+01	-1,487E+02	-5,023E+02	1,808E+02	-5,183E+01

TABLE 30

NODAL POINT DISPLACEMENTS

1	-5,21300E-03	9,02918E-03	-1,86100E-26	-6,69070E-04	5,58600E-25	0,
2	6,02590E-03	9,02918E-03	6,17298E-27	-1,26662E-03	-1,77792E-26	0,
3	1,88648E-02	9,02919E-03	2,97763E-27	-1,35800E-03	-1,06135E-25	0,
4	3,09037E-02	9,02919E-03	-2,53920E-26	-8,01386E-04	1,10140E-24	0,
5	-3,75963E-37	4,50583E-25	4,38302E-02	3,91300E-04	-3,16692E-04	0,
6	6,01945E-03	1,04260E-02	7,59026E-02	-1,50409E-04	-4,51109E-04	0,
7	1,20389E-02	2,08520E-02	6,68886E-02	-3,67868E-04	-2,42354E-04	0,
8	1,80584E-02	3,12780E-02	2,73593E-03	-9,34504E-04	4,46187E-04	0,
9	1,04260E-02	1,13310E-14	5,82645E-02	7,31854E-04	-1,41902E-05	0,
10	1,64455E-02	1,04260E-02	8,82920E-02	2,02481E-05	1,42621E-04	0,
11	2,24649E-02	2,08520E-02	5,34724E-02	-3,61913E-04	4,50111E-04	0,
12	2,84844E-02	3,12780E-02	-4,46603E-02	-1,15850E-03	4,27067E-04	0,
13	2,08520E-02	1,60459E-14	4,55684E-02	6,50455E-04	2,37861E-04	0,
14	2,68715E-02	1,04260E-02	4,86276E-02	2,56172E-05	6,15559E-04	0,
15	3,28909E-02	2,08520E-02	8,59728E-03	-2,52011E-04	4,07705E-04	0,
16	3,89104E-02	3,12780E-02	-5,53678E-02	-9,26492E-04	-2,61523E-04	0,
17	1,56390E-02	-2,70875E-02	-1,51125E-26	8,37916E-04	-2,03309E-25	0,
18	2,76779E-02	-2,70875E-02	1,39814E-26	3,09682E-04	-2,93996E-26	0,
19	3,97168E-02	-2,70875E-02	1,39814E-26	-3,09682E-04	2,93996E-26	0,
20	5,17557E-02	-2,70875E-02	-1,51125E-26	-8,37916E-04	2,03309E-25	0,
21	4,17040E-02	1,42092E-14	-5,53678E-02	9,26492E-04	2,61523E-04	0,
22	4,77235E-02	1,04260E-02	8,59728E-03	2,52011E-04	-4,07705E-04	0,
23	5,37429E-02	2,08520E-02	4,86276E-02	-2,56172E-05	-6,15559E-04	0,
24	5,97624E-02	3,12780E-02	4,55684E-02	-6,50455E-04	-2,37861E-04	0,
25	5,21300E-02	1,07554E-14	-4,46603E-02	1,15850E-03	-4,27067E-04	0,
26	5,81495E-02	1,04260E-02	5,34724E-02	3,61913E-04	-4,50111E-04	0,
27	6,41689E-02	2,08520E-02	8,82920E-02	-2,02481E-05	-1,42621E-04	0,
28	7,01884E-02	3,12780E-02	5,82645E-02	-7,31854E-04	1,41902E-05	0,
29	6,25560E-02	4,50583E-25	2,73593E-03	9,34504E-04	-4,46187E-04	0,
30	6,85755E-02	1,04260E-02	6,68886E-02	3,67868E-04	2,42354E-04	0,
31	7,45949E-02	2,08520E-02	7,59026E-02	1,50409E-04	4,51109E-04	0,
32	8,06144E-02	3,12780E-02	4,38302E-02	-3,91300E-04	3,16692E-04	0,
33	3,64910E-02	-6,32043E-02	-2,53920E-26	8,01386E-04	-1,10140E-24	0,
34	4,85299E-02	-6,32043E-02	2,97763E-27	1,35800E-03	1,06135E-25	0,
35	6,05688E-02	-6,32042E-02	6,17298E-27	1,26662E-03	1,77792E-26	0,
36	7,26077E-02	-6,32042E-02	-1,86100E-26	6,69070E-04	-5,58600E-25	0,

TABLE 31

ELEMENT STRESS RESULANTS FOR LOAD CASE 1

M2	M1	M12	N1	N2	S	
ELEMENT NO. 1						NODE
-2,528E+04	-1,801E+04	-1,197E+04	-5,145E+03	-5,145E+03	-9,231E-10	1
-2,082E+04	-1,374E+04	-1,045E+04	-5,145E+03	-5,145E+03	-9,231E-10	5
-1,921E+04	-1,704E+04	-8,282E+03	-5,145E+03	-5,145E+03	-9,231E-10	6
-2,126E+04	-1,791E+04	-9,244E+03	-5,145E+03	-5,145E+03	-9,231E-10	2
-2,132E+04	-1,669E+04	-9,486E+03	-5,145E+03	-5,145E+03	-9,231E-10	0
ELEMENT NO. 2						NODE
-1,797E+04	-2,473E+04	-8,520E+03	-5,145E+03	-5,145E+03	1,030E-09	2
-1,592E+04	-2,068E+04	-6,635E+03	-5,145E+03	-5,145E+03	1,030E-09	6
-1,859E+04	-2,558E+04	-4,515E+03	-5,145E+03	-5,145E+03	1,030E-09	7
-1,347E+04	-2,345E+04	-6,389E+03	-5,145E+03	-5,145E+03	1,030E-09	3
-1,557E+04	-2,406E+04	-5,595E+03	-5,145E+03	-5,145E+03	1,030E-09	0
ELEMENT NO. 3						NODE
-1,154E+04	-3,096E+04	-3,794E+03	-5,145E+03	-5,145E+03	6,689E-10	3
-1,083E+04	-1,787E+04	-6,935E+03	-5,145E+03	-5,145E+03	6,689E-10	7
-1,922E+04	-1,974E+04	9,394E+03	-5,145E+03	-5,145E+03	6,689E-10	8
-1,263E+04	-3,865E+04	7,446E+03	-5,145E+03	-5,145E+03	6,689E-10	4
-1,278E+04	-2,855E+04	6,925E+02	-5,145E+03	-5,145E+03	6,689E-10	0
ELEMENT NO. 4						NODE
-2,268E+04	-1,537E+04	-5,678E+03	-5,145E+03	-5,145E+03	-2,615E-09	5
-2,159E+04	-1,317E+04	-4,149E+03	-5,145E+03	-5,145E+03	-2,615E-09	9
-2,247E+04	-1,918E+04	-2,831E+03	-5,145E+03	-5,145E+03	-2,615E-09	10
-2,057E+04	-1,828E+04	-4,135E+03	-5,145E+03	-5,145E+03	-2,615E-09	6
-2,144E+04	-1,663E+04	-3,738E+03	-5,145E+03	-5,145E+03	-2,615E-09	0
ELEMENT NO. 5						NODE
-1,670E+04	-2,168E+04	-2,766E+03	-5,145E+03	-5,145E+03	-7,492E-10	6
-2,043E+04	-2,174E+04	-2,617E+03	-5,145E+03	-5,145E+03	-7,492E-10	10
-2,153E+04	-2,435E+04	8,697E+01	-5,145E+03	-5,145E+03	-7,492E-10	11
-1,937E+04	-2,784E+04	-9,805E+02	-5,145E+03	-5,145E+03	-7,492E-10	7
-1,974E+04	-2,403E+04	-2,091E+03	-5,145E+03	-5,145E+03	-7,492E-10	0
ELEMENT NO. 6						NODE
-1,485E+04	-2,507E+04	1,474E+02	-5,145E+03	-5,145E+03	5,351E-11	7
-2,266E+04	-1,317E+04	-3,180E+03	-5,145E+03	-5,145E+03	5,351E-11	11
-3,585E+04	-1,825E+04	3,244E+03	-5,145E+03	-5,145E+03	5,351E-11	12
-2,431E+04	-2,449E+04	7,603E+03	-5,145E+03	-5,145E+03	5,351E-11	8
-2,391E+04	-2,022E+04	2,789E+03	-5,145E+03	-5,145E+03	5,351E-11	0
ELEMENT NO. 7						NODE
-2,398E+04	-1,572E+04	9,105E+02	-5,145E+03	-5,145E+03	-7,826E-10	9
-2,472E+04	-1,877E+04	3,217E+03	-5,145E+03	-5,145E+03	-7,826E-10	13
-2,466E+04	-2,493E+04	1,685E+02	-5,145E+03	-5,145E+03	-7,826E-10	14
-2,202E+04	-1,853E+04	-1,417E+03	-5,145E+03	-5,145E+03	-7,826E-10	10
-2,358E+04	-1,942E+04	1,213E+03	-5,145E+03	-5,145E+03	-7,826E-10	0
ELEMENT NO. 8						NODE
-2,001E+04	-2,307E+04	-2,410E+01	-5,145E+03	-5,145E+03	-9,632E-10	10
-2,849E+04	-2,399E+04	-2,174E+03	-5,145E+03	-5,145E+03	-9,632E-10	14
-3,573E+04	-2,634E+04	-1,694E+03	-5,145E+03	-5,145E+03	-9,632E-10	15
-2,769E+04	-2,733E+04	-1,878E+02	-5,145E+03	-5,145E+03	-9,632E-10	11
-2,806E+04	-2,532E+04	-1,300E+03	-5,145E+03	-5,145E+03	-9,632E-10	0
ELEMENT NO. 9						NODE
-2,884E+04	-1,893E+04	-2,281E+03	-5,145E+03	-5,145E+03	-2,408E-10	11
-3,754E+04	-1,540E+04	-3,791E+03	-5,145E+03	-5,145E+03	-2,408E-10	15
-4,824E+04	-2,088E+04	-3,750E+03	-5,145E+03	-5,145E+03	-2,408E-10	16
-3,610E+04	-1,830E+04	-9,461E+02	-5,145E+03	-5,145E+03	-2,408E-10	12
-3,720E+04	-1,825E+04	-1,803E+03	-5,145E+03	-5,145E+03	-2,408E-10	0
ELEMENT NO. 10						NODE
-2,413E+04	-1,602E+04	5,713E+03	-5,145E+03	-5,145E+03	-4,080E-10	13
-2,882E+04	-2,208E+04	-4,868E+02	-5,145E+03	-5,145E+03	-4,080E-10	17
-4,592E+04	-2,861E+04	-1,904E+03	-5,145E+03	-5,145E+03	-4,080E-10	18

(A) Stress Resultants

At a typical point the output stress resultants are as shown in Fig 50 and they are in the form of the two in-plane axial forces (N1,N2), the in-plane shearing force (S), the two bending moment components (M1,M2) and the twisting moment (M12). Stress resultants are referenced to element coordinates (η_1, η_2, and η_3). Positive directions are shown in Fig 50.

(B) Stresses and Principal Stresses

At a typical point the output stresses are shown in Fig 51 and are in the form of the two in-plane normal stresses (σ_1,σ_2), and an in-plane shearing stress (τ). These stresses are also referenced to the element coordinates (η_1, η_2, and η_3) with positive directions shown in Fig 51. These stresses are printed at the top (upper surface in the η_3 direction), middle, and bottom fiber of the element as shown in Tables 27, 28, and 29. In the computer output, the symbols of N1, N2 and S are used instead of σ_1, σ_2 and τ. Principal stresses are computed only at the central interior node of the quadrilateral element and printed as shown in Table 29. This orientation is given in terms of the angle between the minimum stress and η_1-direction, as shown in Fig 52.

With regard to the first set of input data of Table 18 (ISIG = 1), output stresses have the unit of forces per unit area. Two sets of stresses are given. The first set (Tables 27, 28, and 29) represents stresses acting at the top, middle, and bottom surfaces printed element by element. The second set (lower portion of Table 29) represents principal stresses computed at the centroid of each element at both the top and bottom surfaces.

Stress resultants in the computer output (Tables 31, 32, and 33) using the second set of input data from Table 18 (ISIG = 0) are forces and moments per unit length at the locations defined by the nodal point numbers since ISIG = 0 was used on the control card (Sec. 4.2 in the input guide). Two sets of stress resultants are given. The first set (Tables 31, 32, and 33) represents stress resultants printed element by element. Node 0 defines the location at the centroid of the element. The second set (lower portion of Table 33) represents the average value of nodal stress resultants. It should be noted that they are referenced to surface coordinates (η_1 and η_2).

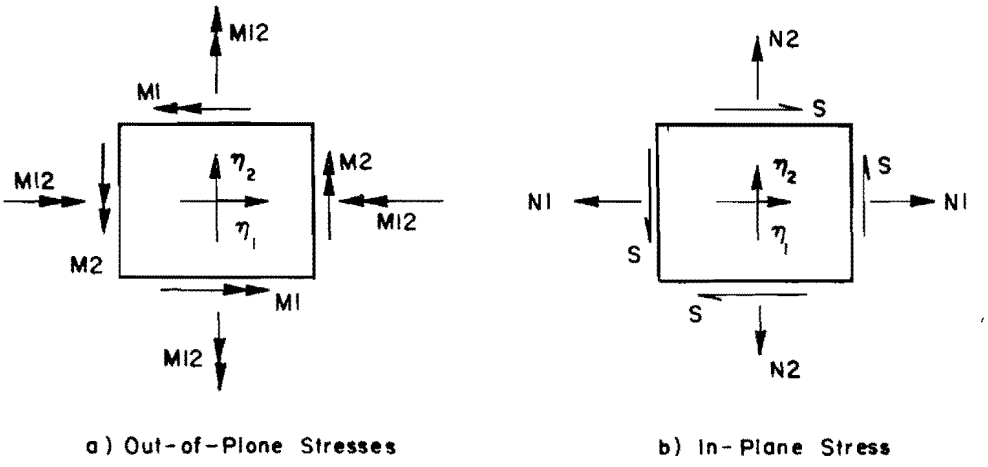

Fig 50. Positive direction of stress resultants.

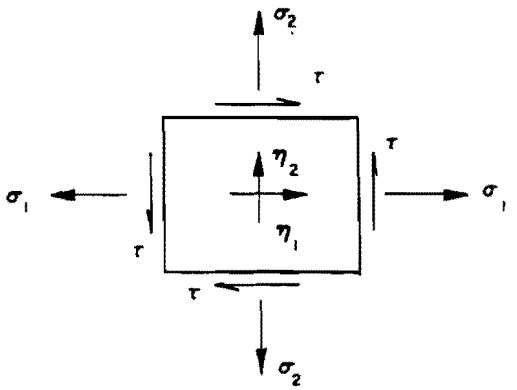

Fig 51. Positive direction of stresses.

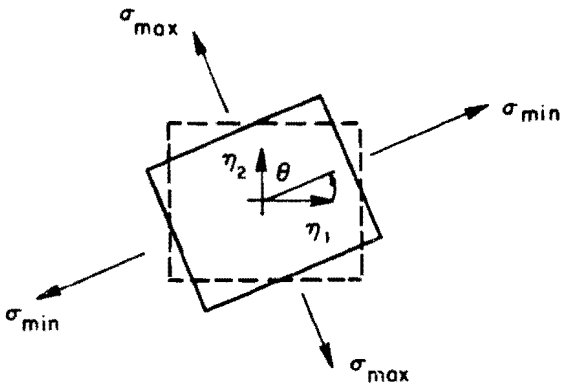

Fig 52. Positive direction of principal stresses.

TABLE 32

-2,963E+04	-2,632E+04	-1,162E+03	-5,145E+03	-5,145E+03	-4,080E-10	14
-3,070E+04	-2,531E+04	1,094E+01	-5,145E+03	-5,145E+03	-4,080E-10	0
ELEMENT NO, 11						NODE
-3,352E+04	-2,763E+04	-2,872E+03	-5,145E+03	-5,145E+03	-9,097E-10	14
-4,422E+04	-2,633E+04	-2,906E+03	-5,145E+03	-5,145E+03	-9,097E-10	18
-4,781E+04	-2,865E+04	-1,570E+03	-5,145E+03	-5,145E+03	-9,097E-10	19
-4,239E+04	-3,873E+04	4,708E+01	-5,145E+03	-5,145E+03	-9,097E-10	15
-4,261E+04	-2,760E+04	-1,951E+03	-5,145E+03	-5,145E+03	-9,097E-10	0
ELEMENT NO, 12						NODE
-4,862E+04	-2,110E+04	-4,524E+03	-5,145E+03	-5,145E+03	-5,351E-10	15
-4,911E+04	-3,393E+04	6,397E+02	-5,145E+03	-5,145E+03	-5,351E-10	19
-3,464E+04	-2,206E+04	-7,040E+03	-5,145E+03	-5,145E+03	-5,351E-10	20
-4,239E+04	-1,569E+04	-9,053E+03	-5,145E+03	-5,145E+03	-5,351E-10	16
-4,368E+04	-2,137E+04	-5,974E+03	-5,145E+03	-5,145E+03	-5,351E-10	0
ELEMENT NO, 13						NODE
-3,464E+04	-2,206E+04	-7,040E+03	-5,145E+03	-5,145E+03	-3,612E-10	17
-4,239E+04	-1,569E+04	-9,053E+03	-5,145E+03	-5,145E+03	-3,612E-10	21
-4,862E+04	-2,110E+04	-4,524E+03	-5,145E+03	-5,145E+03	-3,612E-10	22
-4,911E+04	-3,393E+04	6,397E+02	-5,145E+03	-5,145E+03	-3,612E-10	18
-4,368E+04	-2,137E+04	-5,974E+03	-5,145E+03	-5,145E+03	-3,612E-10	0
ELEMENT NO, 14						NODE
-4,781E+04	-2,865E+04	-1,570E+03	-5,145E+03	-5,145E+03	-7,358E-10	18
-4,239E+04	-3,873E+04	4,708E+01	-5,145E+03	-5,145E+03	-7,358E-10	23
-3,352E+04	-2,763E+04	-2,872E+03	-5,145E+03	-5,145E+03	-7,358E-10	24
-4,422E+04	-2,633E+04	-2,906E+03	-5,145E+03	-5,145E+03	-7,358E-10	19
-4,261E+04	-2,760E+04	-1,951E+03	-5,145E+03	-5,145E+03	-7,358E-10	0
ELEMENT NO, 15						NODE
-4,502E+04	-2,861E+04	-1,904E+03	-5,145E+03	-5,145E+03	-5,886E-10	19
-2,963E+04	-2,632E+04	-1,162E+03	-5,145E+03	-5,145E+03	-5,886E-10	23
-2,413E+04	-1,602E+04	5,713E+03	-5,145E+03	-5,145E+03	-5,886E-10	24
-2,882E+04	-2,208E+04	-4,868E+02	-5,145E+03	-5,145E+03	-5,886E-10	20
-3,070E+04	-2,531E+04	1,094E+01	-5,145E+03	-5,145E+03	-5,886E-10	0
ELEMENT NO, 16						NODE
-4,824E+04	-2,880E+04	-3,750E+03	-5,145E+03	-5,145E+03	-5,485E-10	21
-3,610E+04	-1,830E+04	-9,461E+02	-5,145E+03	-5,145E+03	-5,485E-10	25
-2,884E+04	-1,893E+04	-2,281E+03	-5,145E+03	-5,145E+03	-5,485E-10	26
-3,754E+04	-1,540E+04	-3,791E+03	-5,145E+03	-5,145E+03	-5,485E-10	22
-3,720E+04	-1,825E+04	-1,803E+03	-5,145E+03	-5,145E+03	-5,485E-10	0
ELEMENT NO, 17						NODE
-3,573E+04	-2,634E+04	-1,694E+03	-5,145E+03	-5,145E+03	-7,358E-10	22
-2,769E+04	-2,733E+04	-1,878E+02	-5,145E+03	-5,145E+03	-7,358E-10	26
-2,001E+04	-2,307E+04	-2,410E+01	-5,145E+03	-5,145E+03	-7,358E-10	27
-2,849E+04	-2,399E+04	-2,174E+03	-5,145E+03	-5,145E+03	-7,358E-10	23
-2,806E+04	-2,532E+04	-1,300E+03	-5,145E+03	-5,145E+03	-7,358E-10	0
ELEMENT NO, 18						NODE
-2,466E+04	-2,493E+04	1,685E+02	-5,145E+03	-5,145E+03	1,070E-10	23
-2,202E+04	-1,853E+04	-1,417E+03	-5,145E+03	-5,145E+03	1,070E-10	27
-2,398E+04	-1,572E+04	9,105E+02	-5,145E+03	-5,145E+03	1,070E-10	28
-2,472E+04	-1,877E+04	3,217E+03	-5,145E+03	-5,145E+03	1,070E-10	24
-2,358E+04	-1,942E+04	1,213E+03	-5,145E+03	-5,145E+03	1,070E-10	0
ELEMENT NO, 19						NODE
-3,585E+04	-1,825E+04	3,244E+03	-5,145E+03	-5,145E+03	-6,288E-10	25
-2,431E+04	-2,449E+04	7,603E+03	-5,145E+03	-5,145E+03	-6,288E-10	29
-1,485E+04	-2,507E+04	1,474E+02	-5,145E+03	-5,145E+03	-6,288E-10	30
-2,266E+04	-1,317E+04	-3,180E+03	-5,145E+03	-5,145E+03	-6,288E-10	26
-2,391E+04	-2,022E+04	2,789E+03	-5,145E+03	-5,145E+03	-6,288E-10	0
ELEMENT NO, 20						NODE
-2,153E+04	-2,435E+04	8,697E+01	-5,145E+03	-5,145E+03	4,281E-10	26
-1,937E+04	-2,784E+04	-9,845E+02	-5,145E+03	-5,145E+03	4,281E-10	30
-1,670E+04	-2,168E+04	-2,766E+03	-5,145E+03	-5,145E+03	4,281E-10	31
-2,043E+04	-2,174E+04	-2,617E+03	-5,145E+03	-5,145E+03	4,281E-10	27
-1,974E+04	-2,403E+04	-2,091E+03	-5,145E+03	-5,145E+03	4,281E-10	0

TABLE 33

ELEMENT NO, 21						NODE
-2,247E+04	-1,918E+04	-2,831E+03	-5,145E+03	-5,145E+03	-2,676E-11	27
-2,057E+04	-1,828E+04	-4,135E+03	-5,145E+03	-5,145E+03	-2,676E-11	31
-2,268E+04	-1,537E+04	-5,678E+03	-5,145E+03	-5,145E+03	-2,676E-11	32
-2,159E+04	-1,317E+04	-4,149E+03	-5,145E+03	-5,145E+03	-2,676E-11	28
-2,144E+04	-1,663E+04	-3,738E+03	-5,145E+03	-5,145E+03	-2,676E-11	0
ELEMENT NO, 22						NODE
-1,922E+04	-1,974E+04	9,394E+03	-5,145E+03	-5,145E+03	1,191E-09	29
-1,263E+04	-3,865E+04	7,446E+03	-5,145E+03	-5,145E+03	1,191E-09	33
-1,154E+04	-3,096E+04	-3,794E+03	-5,145E+03	-5,145E+03	1,191E-09	34
-1,883E+04	-1,787E+04	-6,935E+03	-5,145E+03	-5,145E+03	1,191E-09	30
-1,278E+04	-2,855E+04	6,925E+02	-5,145E+03	-5,145E+03	1,191E-09	0
ELEMENT NO, 23						NODE
-1,859E+04	-2,558E+04	-4,515E+03	-5,145E+03	-5,145E+03	2,809E-10	30
-1,347E+04	-2,345E+04	-6,389E+03	-5,145E+03	-5,145E+03	2,809E-10	34
-1,797E+04	-2,473E+04	-8,520E+03	-5,145E+03	-5,145E+03	2,809E-10	35
-1,592E+04	-2,068E+04	-6,635E+03	-5,145E+03	-5,145E+03	2,809E-10	31
-1,557E+04	-2,406E+04	-5,595E+03	-5,145E+03	-5,145E+03	2,809E-10	0
ELEMENT NO, 24						NODE
-1,921E+04	-1,784E+04	-8,282E+03	-5,145E+03	-5,145E+03	1,605E-10	31
-2,126E+04	-1,791E+04	-9,244E+03	-5,145E+03	-5,145E+03	1,605E-10	35
-2,528E+04	-1,801E+04	-1,197E+04	-5,145E+03	-5,145E+03	1,605E-10	36
-2,082E+04	-1,374E+04	-1,045E+04	-5,145E+03	-5,145E+03	1,605E-10	32
-2,132E+04	-1,669E+04	-9,486E+03	-5,145E+03	-5,145E+03	1,605E-10	0

AVERAGED NODAL STRESS RESULTANTS,M,R,T,,SURFACE COORDINATES,LOAD CASE 1

NODE	M2	M1	M12	N1	N2	S	
1	-2,528E+04	-1,801E+04	-1,197E+04	-5,145E+03	-5,145E+03	-9,231E-10	
2	-1,962E+04	-2,132E+04	-8,882E+03	-5,145E+03	-5,145E+03	5,351E-11	
3	-1,251E+04	-2,720E+04	-5,091E+03	-5,145E+03	-5,145E+03	8,495E-10	
4	-1,263E+04	-3,865E+04	7,446E+03	-5,145E+03	-5,145E+03	6,689E-10	
5	-2,175E+04	-1,455E+04	-8,066E+03	-5,145E+03	-5,145E+03	-1,769E-09	
6	-1,810E+04	-1,942E+04	-5,454E+03	-5,145E+03	-5,145E+03	-8,144E-10	
7	-1,591E+04	-2,409E+04	-3,072E+03	-5,145E+03	-5,145E+03	2,508E-10	
8	-2,176E+04	-2,212E+04	8,498E+03	-5,145E+03	-5,145E+03	3,612E-10	
9	-2,278E+04	-1,444E+04	-1,619E+03	-5,145E+03	-5,145E+03	-1,699E-09	
10	-2,123E+04	-2,063E+04	-1,722E+03	-5,145E+03	-5,145E+03	-1,278E-09	
11	-2,518E+04	-2,094E+04	-1,390E+03	-5,145E+03	-5,145E+03	-4,749E-10	
12	-3,597E+04	-1,827E+04	1,149E+03	-5,145E+03	-5,145E+03	-9,365E-11	
13	-2,442E+04	-1,740E+04	4,465E+03	-5,145E+03	-5,145E+03	-5,953E-10	
14	-2,988E+04	-2,571E+04	-1,510E+03	-5,145E+03	-5,145E+03	-7,659E-10	
15	-3,907E+04	-2,339E+04	-2,491E+03	-5,145E+03	-5,145E+03	-6,622E-10	
16	-4,532E+04	-1,824E+04	-6,402E+03	-5,145E+03	-5,145E+03	-3,880E-10	
17	-3,173E+04	-2,207E+04	-3,763E+03	-5,145E+03	-5,145E+03	-3,846E-10	
18	-4,654E+04	-2,938E+04	-1,435E+03	-5,145E+03	-5,145E+03	-6,037E-10	
19	-4,654E+04	-2,938E+04	-1,435E+03	-5,145E+03	-5,145E+03	-6,923E-10	
20	-3,173E+04	-2,207E+04	-3,763E+03	-5,145E+03	-5,145E+03	-5,619E-10	
21	-4,532E+04	-1,824E+04	-6,402E+03	-5,145E+03	-5,145E+03	-4,549E-10	
22	-3,907E+04	-2,339E+04	-2,491E+03	-5,145E+03	-5,145E+03	-5,953E-10	
23	-2,988E+04	-2,571E+04	-1,510E+03	-5,145E+03	-5,145E+03	-4,883E-10	
24	-2,442E+04	-1,740E+04	4,465E+03	-5,145E+03	-5,145E+03	-2,408E-10	
25	-3,597E+04	-1,827E+04	1,149E+03	-5,145E+03	-5,145E+03	-5,886E-12	
26	-2,518E+04	-2,094E+04	-1,390E+03	-5,145E+03	-5,145E+03	-3,712E-10	
27	-2,123E+04	-2,063E+04	-1,722E+03	-5,145E+03	-5,145E+03	-5,686E-11	
28	-2,278E+04	-1,444E+04	-1,619E+03	-5,145E+03	-5,145E+03	4,013E-11	
29	-2,176E+04	-2,212E+04	8,498E+03	-5,145E+03	-5,145E+03	2,809E-10	
30	-1,591E+04	-2,409E+04	-3,072E+03	-5,145E+03	-5,145E+03	3,177E-10	
31	-1,810E+04	-1,942E+04	-5,454E+03	-5,145E+03	-5,145E+03	2,107E-10	
32	-2,175E+04	-1,455E+04	-8,066E+03	-5,145E+03	-5,145E+03	6,689E-11	
33	-1,263E+04	-3,865E+04	7,446E+03	-5,145E+03	-5,145E+03	1,191E-09	
34	-1,251E+04	-2,720E+04	-5,091E+03	-5,145E+03	-5,145E+03	7,358E-10	
35	-1,962E+04	-2,132E+04	-8,882E+03	-5,145E+03	-5,145E+03	2,207E-10	
36	-2,528E+04	-1,801E+04	-1,197E+04	-5,145E+03	-5,145E+03	1,605E-10	

The relationships between stress resultants, stresses and principal stresses are demonstrated by an example problem in Appendix 1 of Ref 25.

APPENDIX 3

```
      C     PROGRAM TSAP     % INPUT,OUTPUT,TAPE5#INPUT,TAPE6#OUTPUT L
      C
      C ... TRANSIENT TEMPERATURE AND STRESS IN HIGHWAY BRIDGE
      C ... 2-D TEMPERATURE DISTRIBUTION
      C ... 1-D TEMPERATURE INDUCED STRESS
      C
            IMPLICIT  REAL*8  ( A-H, O-Z )
            COMMON/XY/ X(400),Y(400),IQ(4,300),NTYPE(300),EM(5),AL(5),AR(300),
           .           NOSP(400)
            COMMON/SS/ NUMNP,MBAND,A(400,20),TP(400)
            DIMENSION
           .       T(400),B(400),D(400),HED(12),LM(5),IX(3),E(3,3),P(5),SIG(5)
           .       ,DD(5),XCOND(5),YCOND(5),XYCOND(5),SPHT(5),DENS(5),QX(5),
           .       KX(4),EE(3,3),XVAL(20),TREAD(400),CGY(300),CGX(300),
           .       NHT(200),BE(400),IC(201),JC(201),CL(201),HH(201)
            DATA   EE/2.,3*1.,2.,3*1.,2./, MDIM/20/,KAT/0/
            DATA  DSTOP/4HSTOP/
      C
      C*****    READ AND PRINT OF CONTROL INFORMATION
      C
         50 READ (5,1100) HED
            IF( HED(1).EQ.DSTOP)  STOP
            READ(5,5001) NUMNP,NUMEL,NUMMAT,NUMCBC,KODE,
           1             NHPI,NDT,ISIG,IFLAG,INTER
       5001 FORMAT(15I5)
            READ(5,5002) DT,TO,ABS,EMIS,RL
       5002 FORMAT(8F10.0)
            WRITE (6,2000)  HED,NUMNP,NUMEL,NUMCBC,NUMMAT,NDT,INTER,DT,TO
           .               ,ABS,EMIS,ISIG,RL
            NDT = -NDT
            IBCA=0
            IF (NDT.LT.0) IBCA=1
            NDT=IABS(NDT)
            IF (DT.EQ.0.0) DT=1.E+20
            IF (KAT.EQ.0) WRITE (6,2011)
            IF (KAT.NE.0) WRITE (6,2010)
      C
      C ... READ MATERIAL PROPERTIES
      C
            DO 1 N=1,NUMMAT
            READ(5,5001) M
         1  READ(5,5002) XCOND(M),YCOND(M),XYCOND(M),SPHT(M),
           1             DENS(M),QX(M),EM(M),AL(M)
            WRITE (6,2009) (M, XCOND(M),YCOND(M),XYCOND(M),SPHT(M),DENS(M),
           1QX(M),EM(M),AL(M), M=1, NUMMAT)
      C
      C.....INITIALIZE  EXTERNAL TEMP VECTOR T
      C
            DO 2 I=1,NUMNP
            TREAD(I)=0.0
         2 T(I)=0.0
      C
      C*****    READ OR GENERATE NODAL POINT INFORMATION
      C
            IF(KAT.EQ.0) WRITE (6,2001)
            IF(KAT.NE.0) WRITE (6,2008)
         6  READ(5,5001) I,J,K,NINCX,NINCY
            READ(5,5002) X(I),Y(I),X(J),Y(J),X(K),Y(K)
```



```
            IF (J.EQ.I .AND. K.EQ.I)  GOTO 3
            IF (J.EQ.I)  NINCX = I
           XINC  = 1
            IF (J.NE.I)  XINC = (J-I)/NINCX
           XJ    = (X(J)-X(I))/XINC
           YJ    = (Y(J)-Y(I))/XINC
            IF (K.EQ.I)  GOTO 13
           IK    = K-I
           YINC  = (K-I)/NINCY
           XK    = (X(K)-X(I))/YINC
           YK    = (Y(K)-Y(I))/YINC
        13 CONTINUE
           DO 12 II = I,J,NINCX
             XN    = (II-I)/NINCX
             X(II) = X(I)+XN*XJ
             Y(II) = Y(I)+XN*YJ
              IF (K.EQ.I)  GOTO 12
             L     = II+NINCY
             K     = II+IK
           DO 20 JJ = L,K,NINCY
             YN    = (JJ-II)/NINCY
             X(JJ) = X(II)+YN*XK
        20   Y(JJ) = Y(II)+YN*YK
        12 CONTINUE
         3    IF (I.EQ.NUMNP.OR.J.EQ.NUMNP.OR.K.EQ.NUMNP) GOTO 16
           GOTO 6
        16   CONTINUE
      C
      C*****    READ OR GENERATE ELEMENT PROPERTIES
      C
         9  READ(5,5001) I,J,K,NTYPE(I),(IQ(N,I),N=1,4),
           1             INCX,INCY,NODX,NODY
              IF (J.EQ.I .AND. K.EQ.I)  GOTO 99
             NK    = K-I
             IF (INCX.EQ.0)  INCX = I
           DO 81 II = I,J,INCX
             NTYPE(II) = NTYPE(I)
             IJ = (II-I)/INCX
           DO 82 N = 1,4
        82   IQ(N,II) = IQ(N,I)+IJ*NODX
             IF (K.EQ.I)  GOTO 81
             IK = II+INCY
             K  = II+NK
           DO 83 JJ = IK,K,INCY
             NTYPE(JJ) =NTYPE(I)
             IJ = (JJ-II)/INCY
           DO 83 N = 1,4
        83   IQ(N,JJ) = IQ(N,II)+IJ*NODY
        81 CONTINUE
        99   IF (I.EQ.NUMEL.OR.J.EQ.NUMEL.OR.K.EQ.NUMEL) GOTO 84
           GOTO 9
        84 CONTINUE
      C
      C ... READ OR GENERATE SPECIFIED HEAT OR TEMPERATURE
      C
            ICOUNT=0
         7  READ(5,5003) I,J,INC,TR,TAM,TPM,TST
       5003 FORMAT(3I5,5X,6F10.0)
```

```
            IF ( TAM.LE.0. )  GOTO 32
            IF ( TST.LT.TAM .OR. TST.GT.TPM )  GOTO 34
            CALL SOLAR ( TAM,TPM,TST,TR,SR )
          GOTO 35
       34 SR = 0.0
       35 CONTINUE
          TREAD(I) = SR
          GOTO 33
       32 TREAD(I) = TR
       33 CONTINUE
          IF(INC.LE.0) INC=1
          IF(J.LE.0) J=I
          DO 11 II=I,J,INC
          ICOUNT=ICOUNT+1
          NHT(ICOUNT)=II
       11 TREAD(II)=TREAD(I)
          IF(ICOUNT .LT. NHP1) GO TO 7
          DO 5 L=1,NUMNP
        5 WRITE(6,2002) L,KODE,X(L),Y(L),TREAD(L)
          IF(KODE.GT.0)  GOTO 351
          NHP1M = NHP1-1
          DO 350 I = 1,NHP1M
            J = NHT(I)
            K = NHT(I+1)
           XJ = X(K)-X(J)
           YJ = Y(K)-Y(J)
          XL=DSQRT(XJ*XJ+YJ*YJ)
           IF ( KAT.NE.0 ) XL = XL*(X(J)+X(K))*0.5
           T(J) = TREAD(J)*XL*0.5*ABS + T(J)
           T(K) = TREAD(K)*XL*0.5*ABS + T(K)
      350 CONTINUE
          GOTO 352
      351 CONTINUE
           DO 353 I = 1,NUMNP
      353 T(I) = TREAD(I)
      352 CONTINUE
C
C ... INITIALIZE VECTORS AND MATRICES
C
          DO 110 I=1,NUMNP
          B(I)=0.0
          TP(I)=TO
          D(I)=0.0
          DO 110 J=1,MDIM
      110 A(I,J)=0.0
          MBAND=0
C
C*****    FORM CONDUCTIVITY AND HEAT CAPACITY MATRICES FOR COMPLETE BODY
C
          WRITE (6,2003)
          DO 200 N=1,NUMEL
          DO 125 I=1,4
      125 LM(I)=IQ(I,N)
          MTYPE=NTYPE(N)
          CONDI=XCOND(MTYPE)
          CONDJ=YCOND(MTYPE)
          CONDK=XYCOND(MTYPE)
          WRITE (6,2004) N,LM(1),LM(2),LM(3),LM(4),MTYPE
          DO 150 I=1,5
          P(I)=0.0
          DD(I)=0.0
          DO 150 J=1,5
      150 S(I,J)=0.0
          I=LM(1)
          J=LM(2)
          K=LM(3)
          L=LM(4)
          LM(5)=I
          XX=(X(I)+X(J)+X(K)+X(L))/4.
          YY=(Y(I)+Y(J)+Y(K)+Y(L))/4.
            AR(N) = 0.0
C
C*****    FORM QUADRILATERAL HEAT CAPACITY AND CONDUCTIVITY MATRICES
C
          DO 152 K=1,4
          I=LM(K)
          J=LM(K+1)
          IF (I-J) 135,152,135
      135 AJ=X(J)-X(I)
          AK=XX-X(I)
          BJ=Y(J)-Y(I)
          BK=YY-Y(I)
          C=BJ-BK
          DX=AK-AJ
          XMUL=1.0
          IF (KAT.NE.0)
         1XMUL=XMUL*(X(I)+X(J)+XX)/3.0
          XLAM=AJ*BK-AK*BJ
            AR(N) = AR(N)+0.5*XLAM
          COMM=.5*XMUL/XLAM
          QQ=XLAM*XMUL*QX(MTYPE)/4.0
          QSTORE=XLAM*XMUL*SPHT(MTYPE)*DENS(MTYPE)/4.0
C
C***** FORM CONDUCTIVITY TENSOR FOR ANISOTROPIC BODIES
C
          E(1,1)=C*C*CONDI+DX*DX*CONDJ+2.*C*DX*CONDK
          E(1,2)=C*BK*CONDI-DX*AK*CONDJ+CONDK*(DX*BK-C*AK)
          E(1,3)=-C*BJ*CONDI+DX*AJ*CONDJ+CONDK*(C*AJ-DX*BJ)
          E(2,1)=E(1,2)
          E(2,2)=BK*BK*CONDI+AK*AK*CONDJ-2.*AK*BK*CONDK
          E(2,3)=-BK*BJ*CONDI-AJ*AK*CONDJ+CONDK*(AJ*BK+BJ*AK)
          E(3,1)=E(1,3)
          E(3,2)=E(2,3)
          E(3,3)=BJ*BJ*CONDI+AJ*AJ*CONDJ-2.*AJ*BJ*CONDK
          IX(1)=K
          IX(2)=K+1
          IF (K-4) 145,140,145
      140 IX(2)=1
      145 IX(3)=5
          DO 151 I=1,3
          II=IX(I)
          P(II)=P(II)+QQ
          DD(II)=DD(II)+QSTORE
          DO 151 J=1,3
          JJ=IX(J)
      151 S(II,JJ)=S(II,JJ)+E(I,J)*COMM
```

```
  152 CONTINUE
C
C*****    ELIMINATE CENTER NODAL POINT
C
      DO 143 I=1,4
      DO 143 J=1,4
  143 S(I,J)=S(I,J)-S(I,5)*S(J,5)/S(5,5)
C
C*****    ADD ELEMENT MATRICES TO COMPLETE MATRICES
C
      DO 175 L=1,4
      I=LM(L)
      B(I)=B(I)+P(L)
      D(I)=D(I)+DD(L)
      DO 175 M=1,4
      J=LM(M)-I+1
      IF(MBAND-J) 160,165,165
  160 MBAND=J
  165 IF(J) 175,175,170
  170 A(I,J)=A(I,J)+S(L,M)
  175 CONTINUE
  200 CONTINUE
        IF ( ISIG.LE.0 )  GOTO 201
C
C ... COMPUTE CENTER OF GRAVITY AND MOMENT OF INERTIA
C
        AREAX = 0.0
        AREAY = 0.0
        AREA  = 0.0
        XI    = 0.0
        YI    = 0.0
      DO 22 N = 1,NUMEL
        I = IQ(1,N)
        J = IQ(2,N)
        K = IQ(3,N)
        L = IQ(4,N)
        MTYPE = NTYPE(N)
      EAY= EM(MTYPE)
        AJ = X(J)-X(I)
        AK = X(J)-X(K)
        BJ = Y(J)-Y(I)
        BK = Y(K)-Y(J)
        AREA = AREA+AR(N)*EAY
C
C ... COMPUTE ELEMENT MOMENT OF INERTIA ABOUT X-AXIS
C ... ASSUME SIDES PARALLEL TO THE AXES
C
        IF (I.EQ.L ) CGY(N) = (Y(I)+Y(J)+Y(K))/3.
        IF (I.NE.L ) CGY(N) = 0.25*(Y(I)+Y(J)+Y(K)+Y(L))
      AREAX= AREAX+AR(N)*EAY*CGY(N)
        IF ( I.NE.L )  XI = XI+(AJ*BK**3.)/12.*EAY
        IF ( I.EQ.L .AND. AJ.NE.0. ) XI = XI+(AJ*BK**3.)/36.*EAY
        IF ( I.EQ.L .AND. AJ.EQ.0. ) XI = XI+(AK*BJ**3.)/36.*EAY
        IF ( IFLAG.LE.0 )  GOTO 22
C
C ... COMPUTE ELEMENT MOMENT OF INERTIA ABOUT Y-AXIS
C
        IF ( I.EQ.L )  CGX(N) = (X(I)+X(J)+X(K))/3.
```



```
        IF ( I.NE.L )  CGX(N) = 0.25*(X(I)+X(J)+X(K)+X(L))
      AREAY= AREAY+AR(N)*EAY*CGX(N)
        IF ( I.NE.L )  YI = YI+(BK*AJ**3.)/12.*EAY
        IF ( I.EQ.L.AND.AJ.NE.0. )  YI = YI+(BK*AJ**3.)/36.*EAY
        IF ( I.EQ.L.AND.AJ.EQ.0. )  YI = YI+(BJ*AK**3.)/36.*EAY
   22 CONTINUE
        CG1 = AREAX/AREA
        IF ( IFLAG.GT.0 ) CG2 = AREAY/AREA
      DO 25 N = 1,NUMEL
        DCG = CGY(N)-CG1
        M   = NTYPE(N)
        XI = XI+AR(N)*EM(M)*DCG*DCG
        IF ( IFLAG.LE.0 ) GOTO 25
        DCG = CGX(N)-CG2
        YI  = YI+AR(N)*EM(M)*DCG*DCG
   25 CONTINUE
      DO 203 I = 1,NUMEL
      DO 203 J = 1,4
            N = IQ(J,I)
     NOSP(N) = NTYPE(I)
  203 CONTINUE
  201   IF ( NUMCBC.EQ.0 )  GOTO 220
        WRITE ( 6,2006)
        ICOUNT = 0
C
C ... READ OR GENERATE CONVECTION COEFFICIENT
C
  213 READ(5,5003) I,J,INC,HC
      DO 215 K = I,J,INC
        L = K+INC
        ICOUNT = ICOUNT+1
        WRITE (6,2007) K,L,HC
        XJ = X(L)-X(K)
        YJ = Y(L)-Y(K)
      XL=DSQRT(XJ*XJ+YJ*YJ)
        IF ( KAT.NE.0 ) XL = XL*(X(L)+X(K))*0.5
        IC(ICOUNT) = K
        JC(ICOUNT) = L
        HH(ICOUNT) = HC
        CL(ICOUNT) = XL
C
C .. MODIFY FOR CONVECTION BOUNDARY CONDITIONS
C
        H = HC*XL/6.
        A(K,1) = A(K,1) + 2.*H
        A(L,1) = A(L,1) + 2.*H
        KK     = L-K+1
        IF ( KK.GT.0 )  A(K,KK) = A(K,KK)+H
        KK = K-L+1
        IF ( KK.GT.0 )  A(L,KK) = A(L,KK) + H
        IF ( L.EQ.J )  GOTO 214
  215   CONTINUE
  214   IF ( ICOUNT.LT.NUMCBC )  GOTO 213
C
C ... MODIFY FOR TEMP. BC AND FORM EFFECTIVE CONDUCTIVITY MATRIX
C
  220   IF ( KODE.LE.0 )  GOTO 301
      DO 302 N = 1,NHP1
```

```
          I = NHT(N)
          A(I,1) = 1.E+40
  302     D(I)   = 0.0
  301 DO 300 N = 1,NUMNP
  300     A(N,1) = A(N,1)+D(N)/DT
C
C.....    TRIANGULARIZED EFFECTIVE CONDUCTIVITY MATRIX
C
      CALL SYMSOL(1)
        TIME = 0.0
        LL   = 0
C
C ... BEGIN TRANSIENT CALCULATIONS
C
      DO 600 LNDT = 1,NDT
      PRINT 2040
 2040 FORMAT (// 34H      TRANSIENT BOUNDARY CONDITIONS,/)
        IF ( NUMCBC.LE.0 )  GOTO 221
C
C ... READ IN THE TEMPERATURE OF EXTERNAL ENVIRONMENT
C
      READ(5,5002) TEMPR
      WRITE ( 6,2028) TEMPR
C
C ... CALCULATE EFFECTIVE LOAD VECTOR
C
      DO 236 N = 1,NUMNP
  236   BE(N)  = B(N)
      DO 235 N = 1,NUMCBC
        K = IC(N)
        L = JC(N)
        TEMP = HH(N)*CL(N)*TEMPR*0.5
        QLN = 0.0
        IF ( KODE.GT.0 )  GOTO 237
      DO 239 M = 1,NHP1
        IF ( K.EQ.NHT(M) )  GOTO 240
  239   CONTINUE
        TSA = (((TP(K)+TP(L))*0.5+460.)*.01)**4.
        TAA = ((TEMPR+460.)*.01)**4.
        QLN = CL(N)*0.5*EMIS*.174*(TSA-TAA)
        GOTO 237
  240   TSA = (((TP(K)+TP(L))*0.5+460.)*.01)**4.
        TAA = ((TEMPR+460.)*.01)**6.
        QLN = CL(N)*0.5*EMIS*(.174*TSA-.00496*TAA)
  237   CONTINUE
        BE(K) = BE(K)+TEMP-QLN
  235   BE(L) = BE(L)+TEMP-QLN
  221 DO 219 II = 1,NUMNP
  219 TREAD(II)=0.0
        IF ( KODE.LE.0 )  GOTO 36
      ICOUNT=0
C
C ... READ OR GENERATE BOUNDARY CONDITIONS
C
  218 READ(5,5003) I,J,INC,TREAD(I)
      PRINT 2050,I,J,INC,TREAD(I)
      IF(J .EQ. I .OR. J .EQ. 0) ICOUNT=ICOUNT+1
      IF(J .EQ. I .OR. J .EQ. 0) GO TO 217
```



```
      DO 216 K=I,J,INC
      ICOUNT=ICOUNT + 1
  216 TREAD(K)=TREAD(I)
  217 CONTINUE
      IF(ICOUNT .LT. NHP1) GO TO 218
        GOTO 305
   36 IF ( TAM.LE.0 )  GOTO 230
        TST = TST+DT
        IF ( TST.EQ.24. )  TAM = TAM+24.
        IF ( TST.EQ.24. )  TPM = TPM+24.
        IF ( TST.EQ.48. )  TAM = TAM+48.
        IF ( TST.EQ.48. )  TPM = TPM+48.
        IF ( TST.LT.TAM .OR. TST.GT.TPM )  GOTO 37
        CALL SOLAR ( TAM,TPM,TST,TR,HF )
      GOTO 39
   37 HF = 0.0
      GOTO 39
C
C ... READ HEAT FLOW INTENSITIES
C
  230  READ(5,5002) HF
   39 WRITE ( 6,2029 ) HF
      DO 231 N = 1,NHP1M
        J = NHT(N)
        K = NHT(N+1)
        XJ = X(K)-X(J)
        YJ = Y(K)-Y(J)
      XL=DSQRT(XJ*XJ+YJ*YJ)
        IF ( KAT.NE.0 ) XL = XL*(X(J)+X(K))*0.5
        TREAD(J) = HF*XL*0.5*A8S + TREAD(J)
        TREAD(K) = HF*XL*0.5*A8S + TREAD(K)
  231 CONTINUE
  305 DO 400 N=1,NUMNP
      QEFF=BE(N)+0.5*T(N)+D(N)*TP(N)/DT
      IF (18CA.EQ.0) GO TO 330
      T(N)=TREAD(N)
  330 TP(N)=QEFF+0.5*T(N)
  400 CONTINUE
        IF ( KODE.LE.0 )  GOTO 401
      DO 238 N = 1,NHP1
        I = NHT(N)
  238   TP(I) = (1.E+40)*T(I)
  401   CONTINUE
C
C.....    SOLVE FOR NEW TEMPERATURES
C
      CALL SYMSOL(2)
      TIME=TIME+DT
      LL=LL+1
C
C*****    PRINT TEMPERATURES
C
      IF (NDT.EQ.1.AND.DT.EQ.1.E+20) TIME=0.0
      IF (LL.LT.INTER) GO TO 600
      WRITE (6,2005) TIME,(N,TP(N),N=1,NUMNP)
      LL=0
      IF(ISIG.GT.0)CALL STRESS ( NUMEL,TO,XI,YI,CG1,CG2,AREA,RL,IFLAG )
  600 CONTINUE
```

```
      GO TO 50
C
C*****    FORMAT STATEMENTS
C
 1100 FORMAT (12A6)
 2000 FORMAT (1H1 12A6// 25HONUMBER OF NODAL POINTS-- ,6X,I4/
     1 25H NUMBER OF ELEMENTS------I10/25H NUMBER OF CONVECTION BC-I10/
     2 25H NUMBER OF MATERIALS-----I10/25H NUMBER OF INCREMENTS----I10/
     3 25H OUTPUT INTERVAL---------I10/20H TIME INTERVAL------5X,F10.2/
     4 25H INITIAL TEMPERATURE----- F10.2/13H ABSORBTIVITY,12X,F10.2/
     5 11H EMISSIVITY,14X,F10.2/ 14H STRESS OPTION,11X,I10/
     6 11H SPAN RATIO,14X,F10.2 )
 2001 FORMAT (20HO N.P. NO.       CODE 14X,1HX,14X,1HY,14X,1HT)
 2002 FORMAT (2I10,3E15.6)
 2003 FORMAT (35HO    N     I     J     K     L   MATERIAL )
 2004 FORMAT (5I5,I10)
 2005 FORMAT (22HOTEMPERATURES AT TIME# E13.5/(7(I5,E12.4)))
 2006 FORMAT (25HO    I     J                H      )
 2007 FORMAT (2I5,2E15.6)
 2008 FORMAT (20HO N.P. NO.       CODE 14X,1HR,14X,1HZ,14X,1HT)
 2009 FORMAT (I4,8E12.3)
 2010 FORMAT (24HOAXISYMMETRIC SOLID BODY /
     1 4HO  M 9X 3HKRR 9X 3HKZZ 9X 3HKRZ 11X 1HC 11X 1HD 11X 1HQ
     2 10X,2HEM,10X,2HAL)
 2011 FORMAT (27HOTWO DIMENSIONAL PLANE BODY /
     1 4HO  M 9X 3HKXX 9X 3HKYY 9X 3HKXY 11X 1HC 11X 1HD 11X 1HQ
     2 10X,2HEM,10X,2HAL)
 2020 FORMAT (10HOCARD NO. I4, 13H OUT OF ORDER )
 2021 FORMAT (13HOBAD CARD NO. I4)
 2028 FORMAT (  20H      AIR TEMPERATURE,5X,F10.2)
 2029 FORMAT (    24H      HEAT FLOW INTENSITY,F10.2)
 2050 FORMAT (5X, 4HFROM,I5,2HTO,I5,3HINC,I5,5HTREAD,F10.2)
      END
```

```
      SUBROUTINE SOLAR ( TAM,TPM,TST,TR,SR )
C
C ... COMPUTE THE INTENSITIES OF SOLAR RADIATION ON HORIZONTAL SURFACE
C
      IMPLICIT  REAL*8  ( A-H, O-Z )
        TIME = TPM-TAM
        T    = TST-TAM
        AL   = T*3.141592654/TIME
         SR=1.7*TR*DSIN(AL)*(DSIN(AL)+2.1)/(3.*TIME)
        RETURN
        END
```



```
      SUBROUTINE SYMSOL (KKK)
C
      IMPLICIT  REAL*8  ( A-H, O-Z )
      COMMON/SS/ NN,MM,A(400,20),B(400)
C
      GO TO (1000,2000),KKK
C
C     REDUCE MATRIX
C
 1000 DO 280 N=1,NN
      DO 260 L=2,MM
      C=A(N,L)/A(N,1)
      I = N+L-1
      IF(NN-I) 260,240,240
  240 J=0
      DO 250 K=L,MM
      J=J+1
  250 A(I,J)=A(I,J)-C*A(N,K)
  260 A(N,L)=C
  280 CONTINUE
      GO TO 500
C
C     REDUCE VECTOR
C
 2000 DO 290 N=1,NN
      DO 285 L=2,MM
      I=N+L-1
      IF(NN-I) 290,285,285
  285 B(I)=B(I)-A(N,L)*B(N)
  290 B(N)=B(N)/A(N,1)
C
C     BACK SUBSTITUTION
C
      N=NN
  300 N = N-1
      IF(N) 350,500,350
  350 DO 400 K=2,MM
      L = N+K-1
      IF(NN-L) 400,370,370
  370 B(N) = B(N) - A(N,K) * B(L)
  400 CONTINUE
      GO TO 300
C
  500 RETURN
C
      END
```

```
      SUBROUTINE STRESS ( NUMEL,TREF,XI,YI,CG1,CG2,AREA,RL,IFLAG )
      IMPLICIT  REAL*8  ( A-H, O-Z )
      COMMON/XY/ X(400),Y(400),IQ(4,300),NTYPE(300),EM(5),AL(5),AR(300),
     1           NOSP(400)
      COMMON/SS/ NUMNP,MBAND,A(400,20),TP(400)
      DIMENSION TD(400)
C
C ... COMPUTE TEMPERATURE DIFFERENCE
C
      DO 1 N = 1,NUMNP
    1   TD(N) = TP(N) - TREF
        PT  = 0.0
        CTX = 0.0
        CTY = 0.0
      DO 2 N = 1,NUMEL
        I = IQ(1,N)
        J = IQ(2,N)
        K = IQ(3,N)
        L = IQ(4,N)
C
C ... COMPUTE THERMAL FORCE AND MOMENT
C
        IF ( I.NE.L ) TAV = 0.25*(TD(I)+TD(J)+TD(K)+TD(L))
        IF ( I.EQ.L ) TAV = (TD(I)+TD(J)+TD(K))/3.
        IF ( I.EQ.L )  GOTO 11
        T1 = (TD(I)+TD(J))*0.5
        T2 = (TD(K)+TD(L))*0.5
        Y1 = (Y(I)+Y(J))*0.5
        Y2 = (Y(K)+Y(L))*0.5
        DY = Y2-Y1
        CGY = Y1+DY*((T1+2.*T2)/(3.*(T2+T1)))
        IF ( IFLAG.LE.0 )  GOTO 12
        T1  = (TD(L)+TD(I))*0.5
        T2  = (TD(K)+TD(J))*0.5
        X1  = (X(L)+X(I))*0.5
        X2  = (X(K)+X(J))*0.5
        DX  = X2-X1
        CGX = X1+DX*((T1+2.*T2)/(3.*(T2+T1)))
        GOTO 12
   11   CGY = (Y(I)+Y(J)+Y(K))/3.
        IF ( IFLAG.GT.0 )  CGX = (X(I)+X(J)+X(K))/3.
   12   CONTINUE
        MTYPE = NTYPE(N)
        EL = EM(MTYPE)*AL(MTYPE)
        P  = EL*AR(N)*TAV
        C1 = P*(CGY-CG1)
        PT = PT+P
        CTX= CTX+C1
        IF ( IFLAG.LE.0 )  GOTO 2
        C2 = P*(CGX-CG2)
        CTY= CTY+C2
    2   CONTINUE
C
C ... CALCULATE STRESS AT LOCATION OF MAXIMUN MOMENT
C ... STRP    IS STRAIN DUE TO AXIAL THERMAL FORCE
C ... STRCB   IS STRAIN DUE TO THERMAL MOMENT
C
        CMX = CTX/(3.*RL+2.)
```



```
        STRP = PT/AREA
        IF ( IFLAG.GT.0 )  CMY = CTY/(3.*RL+2.)
      DO 3 N = 1,NUMNP
        MP = NOSP(N)
        DY = CG1-Y(N)
        STRM1 = CMX*DY/XI
        STRM2 = 0.0
        IF ( IFLAG.LE.0 )  GOTO 4
        DX    = CG2-X(N)
        STRM2 = CMY*DX/YI
    4 CONTINUE
        TD(N) = EM(MP)*(STRP+STRM1+STRM2-AL(MP)*TD(N))
    3   CONTINUE
        WRITE (6,2000) (N,TD(N),N=1,NUMNP)
 2000 FORMAT (25HOTHERMAL INDUCED STRESSES/(7(I5,E12.2)))
      RETURN
      END
```

APPENDIX 4

```
C     PROGRAM SHELL 8          IBM 360 VERSION    21 MAR 1977      ATALAY AND JJP
CNULL PROGRAM MAIN(INPUT,OUTPUT,TAPE1,TAPE2,TAPE3,TAPE4,TAPE8,TAPE9)
C.....THIS VERSION OF THE SHELL PROGRAM HAS BEEN MODIFIED TO RUN
C.....ON THE IBM 370 AT THE TEXAS STATE HIGHWAY DEPARTMENT.
C.....ALL REAL VARIABLES ARE DOUBLE LENGTH AND INTEGER VARIABLES
C.....STANDARD LENGTH.
      IMPLICIT REAL*8 (A-H,O-Z)
      COMMON/CV/NUMEL,NUPTS,NUBPTS,IBANDP,MBAND,NBLOC,NDFRE,IFLAG,NUMAT
     1      ,ITEMP,NLVT,ISTRAN
      COMMON/SS/IGEN,ISHEAR,JSHEAR,NRED,IREACT,NTRUSS,ISIG,IROT
      DIMENSION ITITLE(20),C(5),XV(20)
      EQUIVALENCE (ISHEAR,N1)            , (NRED,N2), (IREACT,N3)
    1 READ 1002, ITITLE
      PRINT 1003, ITITLE
 1002 FORMAT (20A4)
 1003 FORMAT (1H1,4X,20A4)
      READ 30,NUMEL,NUPTS,NUBPTS,IBANDP,NDFRE,IFLAG,NUMAT,N1,N2,N3,N4,
     .    IGEN,ISIG,IROT,ITEMP,NLVT
   30 FORMAT(16I5)
              JSHEAR = N1
      PRINT 31,NUMEL,NUPTS,NUBPTS,IBANDP,NDFRE,IFLAG,NUMAT,N1,N2,N3,N4,
     .    IGEN,ISIG,IROT,ITEMP,NLVT
      MBAND=IBANDP*NDFRE
      NBLOC =(NUPTS*NDFRE)/MBAND
      IF((MBAND*NBLOC-NUPTS*NDFRE).NE.0)  NBLOC=NBLOC+1
      REWIND1
      REWIND2
      REWIND3
      REWIND4
      CALL OVER1
      CALL OVER2
      CALL OVER3
          IF(IGEN.GT.3)     GO TO 3
      CALL OVER4
    3 CONTINUE
   31 FORMAT ( 9H NUMEL  =,I5/9H NUPTS  =,I5/9H NUBPTS =,I5/9H IBANDP =,
     .       I5/9H NDFRE  =,I5/9H IFLAG  =,I5/9H NUMAT  =,I5/9H ISHEAR =,
     .       I5/9H NRED   =,I5/9H IRECT  =,I5/9H LPROB  =,I5/9H IGEN   =,
     .       I5/9H ISIG   =,I5/9H IROT   =,I5/9H ITEMP  =,I5/9H NLVT   =,
     .       I5/)
   90 FORMAT ( F13.4 )
          IF ( N4.GT.0 )      GO TO 1
    2 STOP
      END
```

```
      SUBROUTINE OVER1
      IMPLICIT REAL*8 (A-H,O-Z)
      COMMON/CV/NUMEL,NUPTS,NUBPTS,IBANDP,MBAND,NBLOC,NDFRE,IFLAG,NUMAT
     .      ,ITEMP,NLVT
      COMMON/SS/IGEN,ISHEAR,JSHEAR,NRED,IREACT,NTRUSS,ISIG,IROT
      COMMON  KQ(4),NODES,QUADT,SMAT(7,30),EM,RM,VM,GM,O1,O2,
     1        XQ(3,400),DIR(6,401),U(9),S(201),T(3,3),E1(3),
     2 E2(3),TH(5),TPC(5,4,5),TP1,TP2,X(4),Y(4),Z(4),D11,D12,D22,D33,
     3 EM1,G1,G2,D1(3,4),D2(3,4),ELOAD(5),IB(401),IDUMMY,TEMP(5,400,12)
      DIMENSION  DMAT(6),XV(20),TH155(155)
      DIMENSION  IQ(4,2000),ITYPE(2000),QTYPE(2000),
     1            TMAT(5,2000),DISTLD(5,2000),TEMPIN(30)
      EQUIVALENCE  (SMAT(1),IQ(1)),(XQ(1),ITYPE(1),DISTLD(1)),
     1  ( DIR(801),QTYPE(1)),(TMAT(1),TEMP(1,1,1))
      EQUIVALENCE (TH155(1),TH(1))
      EQUIVALENCE   (EM,DMAT(1)),
     1 (U(1),XI),(U(2),YI),(U(3),ZI),(U(4),XJ),(U(5),YJ),(U(6),ZJ),
     2 (U(7),XK),(U(8),YK),(U(9),ZK),(U(1),XO),(U(2),YO),(U(3),ZO),
     3 (U(4),BI),(U(5),BJ),(U(7), W),(U(6), A),(U(7), B),(U(8), O)
      LOGICAL TEST1,TEST2
      INTEGER QTYPE,QUADT
      DO 80 I=1,401
   80 DIR(6,I)=0.
      PI=3.14159265358980
C.....GENERATE NODAL COORDINATES AND DIRECTION COSINES.
      PRINT 900
    1 READ 521,II,JJ,IJ,IGO,(U(I),I=1,6)
  521 FORMAT(4I5,6F10.0)
      IF(IGO.GT.1) READ 519,(U(I),I=7,9)
  519 FORMAT(20X,3F10.0)
      IF ( IGO.LE.0 ) PRINT 30,II,JJ,IJ,IGO,(U(I),I=1,3)
      IF ( IGO.EQ.1 ) PRINT 31,II,JJ,IJ,IGO,(U(I),I=1,6)
      IF ( IGO.GT.1 ) PRINT 91,II,JJ,IJ,IGO,U
      IF(IGO.LT.0)  GOTO  17
      IGO=IGO+1
      IF (IJ.GT.0) XINC = (JJ-II)/IJ
      GOTO ( 2, 4, 8,10,12),IGO
    2 DO 3 I=1,3
    3 XQ(I,II)=U(I)
      IF(II-NUPTS)  1,51,51
C.....STRAIGHT LINE.
    4 XJ=XJ-XI
      YJ=YJ-YI
      ZJ=ZJ-ZI
      XL=DSQRT(XJ**2+YJ**2+ZJ**2)
      XD=XJ/XINC
      YD=YJ/XINC
      ZD=ZJ/XINC
      DO 5 I=II,JJ,IJ
      XINC=(I-II)/IJ
      XQ(1,I)=XI+XD*XINC
      XQ(2,I)=YI+YD*XINC
    5 XQ(3,I)=ZI+ZD*XINC
      SQ=DSQRT(XJ*XJ+YJ*YJ)
      DO 7 I=II,JJ,IJ
      DIR(1,I)=XJ/XL
      DIR(2,I)=YJ/XL
      DIR(3,I)=ZJ/XL
      IF(SQ.EQ..0)  GOTO 6
      DIR(4,I)=-YJ/SQ
      DIR(5,I)= XJ/SQ
      GOTO 7
    6 DIR(4,I)=0.
      DIR(5,I)=1.
    7 CONTINUE
      GOTO  19
```

```
C.....CIRCULAR CURVE.
    8 DIJ=DSQRT((XI-XJ)**2+(YI-YJ)**2+(ZI-ZJ)**2)
      DIL=DSQRT((XI-XK)**2+(YI-YK)**2+(ZI-ZK)**2)/2.
      DJL=DSQRT(DIJ**2-DIL**2)
      DEL=PI        -2.*DATAN(DIL/DJL)
      XL=(XI+XK)/2.
      YL=(YI+YK)/2.
      ZL=(ZI+ZK)/2.
      R=    DIJ/DSIN(DEL/2.)
      T(1,1)=(XK-XL)/DIL
      T(2,1)=(YK-YL)/DIL
      T(3,1)=(ZK-ZL)/DIL
      T(1,2)=(XJ-XL)/DJL
      T(2,2)=(YJ-YL)/DJL
      T(3,2)=(ZJ-ZL)/DJL
      T(1,3)= T(2,1)*T(3,2)-T(2,2)*T(3,1)
      T(2,3)=-T(1,1)*T(3,2)+T(1,2)*T(3,1)
      T(3,3)= T(1,1)*T(2,2)-T(1,2)*T(2,1)
      CONST=DSQRT(T(1,3)**2+T(2,3)**2+T(3,3)**2)
      AINC=DEL/XINC
      DO 9 I=II,JJ,IJ
      XINC=(I-II)/IJ
      ANG=AINC*XINC
      DX=R*DSIN(ANG)*DCOS(DEL-ANG)
      DY=R*DSIN(ANG)*DSIN(DEL-ANG)
      XQ(1,I)=XI+T(1,1)*DX+T(1,2)*DY
      XQ(2,I)=YI+T(2,1)*DX+T(2,2)*DY
      XQ(3,I)=ZI+T(3,1)*DX+T(3,2)*DY
      C=DCOS(DEL-2.*ANG)
      D=DSIN(DEL-2.*ANG)
      DIR(1,I)=T(1,1)*C+T(1,2)*D
      DIR(2,I)=T(2,1)*C+T(2,2)*D
      DIR(3,I)=T(3,1)*C+T(3,2)*D
      DIR(4,I)=-T(1,3)/CONST
      DIR(5,I)=-T(2,3)/CONST
    9 DIR(6,I)=-T(3,3)/CONST
      GOTO  19
C.....PARABOLA.
   10 IF(DABS(BI).GT.DABS(BJ))  CONST=ZJ/BI**2
      IF(DABS(BJ).GE.DABS(BI))  CONST=ZJ/BJ**2
      DIJ=DABS(BI)+DABS(BJ)
      W=W*PI/180.
      CW=DCOS(W)
      SW=DSIN(W)
      DINC=DIJ/XINC
      DO 11 I=II,JJ,IJ
      XINC=(I-II)/IJ
      DX=BI*DINC*XINC
      XQ(1,I)=XO+DX*CW
      XQ(2,I)=YO+DX*SW
      XQ(3,I)=ZO+CONST*DX*DX
      ANG=DATAN(2.*CONST*DX)
      DIR(1,I)=CW*DCOS(ANG)
      DIR(2,I)=SW*DCOS(ANG)
      DIR(3,I)= DSIN(ANG)
      DIR(4,I)=-SW
   11 DIR(5,I)= CW
      GOTO  19
C.....ELLIPSE.
   12 A2=A*A
      B2=B*B
      AB=A/B
      BA=B/A
      ATB=A*B
      W=O*PI/180.
      SW=DSIN(W)
      CW=DCOS(W)
      IFAC=200
      FAC=IFAC
      XK=B2/DSQRT(A2+B2)
      Z1=AB*DSQRT(B2-BI*BI)
      ZJ=AB*DSQRT(B2-BJ*BJ)
      WI=-PI/2.
      WJ= PI/2.
      IF(Z1.GT..0) WI=DATAN(BI/Z1)
      IF(ZJ.GT..0) WJ=DATAN(BJ/ZJ)
      DW=(WJ-WI)/FAC
      WC=PI/2.  -WI-DW
      S(1)=0.
      DO 13 I=1,IFAC
      SWC=DSIN(WC)
      CWC=DCOS(WC)
      R=    ATB/DSQRT(B2*SWC*SWC+A2*CWC*CWC)
      DX=R*CWC-BI
      DZ=R*SWC-Z1
      S(I+1)=S(I)+DSQRT(DX*DX+DZ*DZ)
      BI=BI+DX
      Z1=Z1+DZ
   13 WC=WC-DW
      DS=S(IFAC+1)/XINC
      ST=0.
      WC=PI/2.  -WI
   14 DO 15 K=1,IFAC
      J=K+1
      IF(S(J).GE.ST)  GOTO 16
   15 CONTINUE
   16 AINC=J-2
      AINC=AINC*DW
      ANG=WC-AINC-((ST-S(J-1))/(S(J)-S(J-1)))*DW
      SS=DSIN(ANG)
      CC=DCOS(ANG)
      R=    ATB/DSQRT(B2*SS*SS+A2*CC*CC)
      XR=DABS(R*CC)
      ZR=DABS(R*SS)
      Q=DSIGN(1.DO,CC)
      IF(XR.LE.XK)  ANGT=-Q*DATAN((AB*XR)/DSQRT(B2-XR*XR))
      IF(XR.GT.XK)  ANGT=-Q*(PI/2.  -DATAN(BA*ZR/DSQRT(A2-ZR*ZR)))
      SA=DSIGN(1.DO,A)
      XQ(1,II)=XO+XR*CW*Q
      XQ(2,II)=YO+XR*SW*Q
      XQ(3,II)=ZO+ZR*SA
      DIR(1,II)=DCOS(ANGT)*CW*SA
      DIR(2,II)=DCOS(ANGT)*SW*SA
      DIR(3,II)=DSIN(ANGT)*SA
      DIR(4,II)=-SW
      DIR(5,II)= CW
      IF(II.EQ.JJ)  GOTO 19
      II=II+IJ
      ST=ST+DS
      GOTO  14
C.....REPEATED NODAL COORDINATES,AND EI COSINES.
   17 IGO=IABS(IGO)
      IF ( IJ.LE.1 )  I=IABS(IJ)
      IF ( IJ.LE.1 )  IJ=1
      IF ( IJ.GT.1 )  I=1
      JI=0
   20 DO 18 J=II,JJ,IJ
      DO 18 L=1,3
```

```
      DIR(L  ,J)=DIR(L  ,J-I)
      DIR(L+3,J)=DIR(L+3,J-I)
18    XQ(L,J)=XQ(L,J-I)+U(L)
      JI=JI+1
      IF ( JI.GE.IGO )  GO TO 19
      II=II+I
      JJ=JJ+I
      GOTO 20
19    IF((JJ.LT.NUPTS).AND.(II.LT.NUPTS))GOTO 1
C.....INPUT DIRECTION COSINES FOR ARBITARY NODAL POINTS.
   51 PRINT 901
   53 READ 522,M,LIM,MOP,(E1(I),I=1,3),(E2(J),J=1,3)
  522 FORMAT(3I5,5X,6F10.0)
      PRINT 33, M, LIM, MOP, E1, E2
      IF( M.LE.0)  GOTO 57
      TEST1=DABS(E1(1))+DABS(E1(2))+DABS(E1(3)).GT..0
      TEST2=DABS(E2(1))+DABS(E2(2))+DABS(E2(3)).GT..0
      IF(MOP.LE.0)  LIM=M
      IF(MOP.LE.0)  MOP=1
      DO 52 L=M,LIM,MOP
      DO 52 K=1,3
      IF(TEST1)  DIR(K  , L)=E1(K)
   52 IF(TEST2)  DIR(K+3, L)=E2(K)
      GOTO 53
   57 L = 3 * NUPTS
         IF ( IFLAG .EQ. 1 )  GO TO 58
         DO  56  L = 1, NUPTS
              DIR(1,L) = 1.000
              DIR(2,L) = 0.000
              DIR(3,L) = 0.000
              DIR(4,L) = 0.000
              DIR(5,L) = 1.000
              DIR(6,L) = 0.000
   56    CONTINUE
   58    CONTINUE
      WRITE(3) XQ
      L = 6 * NUPTS + 6
      WRITE(3) DIR
C.....INPUT MESH.
      PRINT 902
   59 READ 523,JJ,((IQ(I,JJ),I=1,4),MODL,NLAY,LASTEL
  523 FORMAT(1615)
      PRINT 193,JJ, ((IQ(I,JJ),I=1,4),MODL,NLAY,LASTEL
  193 FORMAT(8(1X,I4))
      IF ( JJ .EQ. NUMEL )  GOTO 66
      IF ( NLAY .EQ. 0 )  GO TO 59
   62 II=JJ
      IF( MODL )  69,60,64
   60 IF(II.EQ.NUMEL)  GOTO 66
      READ 523,JJ,((IQ(I,JJ),I=1,4),MODL,NLAY,LASTEL
      PRINT193,JJ,((IQ(I,JJ),I=1,4),MODL,NLAY,LASTEL
      IF(II+1.EQ.JJ)  GOTO 62
      JK=JJ-2
      DO 63 J=II,JK
      DO 63 K=1,4
   63 IQ(K,J+1)=IQ(K,J)+1
      IF(JJ  -NUMEL )  62,66,66
   64 IFAC=IQ(1,II)-1
      DO 65 I=1,NLAY
      M=(MODL+1)*(I-1)
      DO 65 J=1,MODL
      IQ(1,II)=M+J+IFAC
      IQ(4,II)=IQ(1,II)+1
      IQ(2,II)=IQ(4,II)+MODL
      IQ(3,II)=IQ(2,II)+1
   65 II=II+1
      IF(II-1  - NUMEL)  59,66,66
   69 II=JJ+NLAY
      DO 72 J=II,LASTEL,NLAY
      L=J-NLAY
      DO 70 K=1,4
   70 IQ(K,J)=IQ(K,L)-MODL
      IF ( IQ(3,L).LE.0)  IQ(3,J)=0
      IF ( IQ(4,L).LE.0 )  IQ(4,J)=0
   72 CONTINUE
      IF(LASTEL.LT.NUMEL)  GOTO 59
   66 PRINT 903
      DO 1100 I = 1, NUMEL
      DO 1000 J = 1, 4
 1000 KQ(J) = IQ(J,I)
 1100 WRITE(1) KQ
C.....INPUT MATERIAL TABLE.
      DO 67 II=1,NUMAT
      READ 524,I,(SMAT(J,I),J=1,7),TEMPIN(I)
  524 FORMAT(I5,5X,4F10.0,2F5.0,2F10.0)
21MR77   67  PRINT 96,I,(SMAT(J,I),J=1,7),TEMPIN(I)
21MR77 C.....INPUT ELEMENT PROPERTY CARDS.
21MR77       PRINT 906
21MR77    75 READ 525,II,JJ,LIM,MODL,KK,(DMAT(I),I=1,5)
21MR77   525 FORMAT(5I5,5X,5F10.0)
21MR77       PRINT 98,II,JJ,LIM,MODL,KK,(DMAT(I),I=1,5)
21MR77       IF(LIM.LE.0)  LIM=II
21MR77       IF(MODL.LE.0)  MODL=1
21MR77       DO 71 I=II,LIM,MODL
21MR77       ITYPE(I)=JJ
21MR77       QTYPE(I)=KK
21MR77       DO 71 J=1,5
21MR77    71 TMAT(J,I)=DMAT(J)
21MR77       IF(LIM.LT.NUMEL)  GOTO 75
21MR77       DO 2200 I = 1, NUMEL
21MR77       MTYPE = ITYPE(I)
21MR77       QUADT = QTYPE(I)
21MR77       WRITE(2) MTYPE,QUADT
21MR77       DO 2000 J = 1, 5
21MR77  2000 DMAT(J) = TMAT(J,I)
21MR77  2200 WRITE(2) ( DMAT(J),J=1,5)
21MR77 C.....INPUT DISTRIBUTED LOADS ON ELEMENTS.
21MR77       PRINT 35
21MR77    40 READ 526,II,LIM,MODL,(DMAT(I),I=1,5)
21MR77   526 FORMAT(3I5,5X,5F10.0)
21MR77       PRINT 37,II,   LIM,MODL,(DMAT(I),I=1,5)
21MR77       IF(LIM.LE.0)  LIM=II
21MR77       IF(MODL.LE.0)  MODL=1
21MR77       DO 41 I=II,LIM,MODL
21MR77       DO 41 J=1,5
21MR77    41 DISTLD(J,I)=DMAT(J)
21MR77       IF(LIM.LT.NUMEL)  GOTO 40
21MR77       DO 4400 I = 1, NUMEL
21MR77       DO 4000 J = 1, 5
21MR77  4000 DMAT(J) = DISTLD(J,I)
```

```
 4400 WRITE(4) (DMAT(J),J=1,5)
      REWIND3
      REWIND1
      REWIND2
      REWIND4
      L = 3 * NUPTS
      READ(3) XQ
      L = 6 * NUPTS + 6
      READ(3) DIR
      REWIND3
      DO 5000 I = 1, 401
 5000 IB(I) = 0
      IF ( NLVT.EQ.0 ) NLVT=1
      IF (ITEMP .EQ. 1) CALL INTEMP
      IF (ITEMP .EQ. 1) GO TO 299
C.....
C.....INPUT TEMPERATURES BY NODAL POINT NUMBERS IF ITEMP .NE. 1
C.....
      DO 305 ILV = 1,NLVT
      DO 907 I = 1,5
      DO 907 J = 1,NUPTS
  907 TEMP(I,J,ILV) = 0.0
      PRINT 300,ILV
  300 FORMAT(49HODUBLICATION OF NODAL POINT TEMPERATURES FOR CASE,I5,/)
  301 READ 526,M,LIM,MOP,TEMT,TT4,TEMM,TB4,TEMB
      IF(M .LE. 0) GO TO 305
      PRINT 303,M,LIM,MOP,TEMT,TT4,TEMM,TB4,TEMB
      IF(MOP.LE.0)LIM=M
      IF(MOP.LE.0)MOP=1
      IF(TEMM .NE. 0.0 .OR.  TEMB .NE. 0.0) GO TO 999
      IF(TT4 .NE. 0.0 .OR. TB4 .NE. 0.0) GO TO 999
      TEMM=TEMT
      TEMB=TEMT
      TT4=TEMT
      TB4=TEMT
  999 CONTINUE
      DO 304 L=M,LIM,MOP
      TEMP(1,L,ILV)=TEMT
      TEMP(2,L,ILV)=TT4
      TEMP(4,L,ILV)=TB4
      TEMP(3,L,ILV)=TEMM
  304 TEMP(5,L,ILV)=TEMB
      GO TO 301
  305 CONTINUE
  299 CONTINUE
  777      IF (IGEN.GT.0)    GOTO 77
   73 PRINT 904
      PRINT 700
      DO 74 I=1,NUPTS
   74 PRINT 92,I,(XQ(J,I),J=1,3)
      IF (ITEMP .EQ. 1) GO TO 307
C.....
C.....OUTPUT TEMPERATURES BY NODAL POINT NUMBERS
C.....
      DO 306 ILV = 1,NLVT
      PRINT 800,ILV
  800 FORMAT(/34H NODAL POINT TEMPERATURES FOR CASE,I5/)
      DO 306 I = 1,NUPTS
  306 PRINT 801,I,(TEMP(J,I,ILV),J=1,5)
  801 FORMAT ( I4,2X,5E12.5 )
  307 CONTINUE
      PRINT 701
      PRINT 702
      DO 76 I=1,NUPTS
   76 PRINT 32,I,(DIR(J,I),J=1,6)
      PRINT 905
      PRINT 703
   77 DO 83 M=1,NUMEL
      READ(1) KQ
      READ(2) MTYPE,QUADT
      DO 85 I=1,4
   85 DMAT(I)=SMAT(I,MTYPE)
                EM1 = SMAT(1,MTYPE)
                G1 = SMAT(5,MTYPE)
                G2 = SMAT(6,MTYPE)
                TP1=(SMAT(7,MTYPE)*EM)/(24.*(1.-VM))
                TP2=SMAT(7,MTYPE)
      READ(2) TH
      READ(4) ELOAD
      NODES=4
      IF(KQ(4).LE.0)  NODES=3
      IF(KQ(3).LE.0.AND.KQ(4).LE.0)    NODES = 2
      II=0
      DO 82 J=1,NODES
      K=KQ(J)
      IF(NODES.EQ.2)      GO TO  600
      C1=DSQRT ( DIR(1,K)**2+DIR(2,K)**2+DIR(3,K)**2 )
      C2=DSQRT ( DIR(4,K)**2+DIR(5,K)**2+DIR(6,K)**2 )
      DO 81 L=1,3
      D1(L,J)=DIR(L,K)/C1
   81 D2(L,J)=DIR(L+3,K)/C2
  600 X(J)=XQ(1,K)
      Y(J)=XQ(2,K)
      Z(J)=XQ(3,K)
      IF(ITEMP .EQ. 1) CALL TEMSEL (J,M,II,MTYPE,TEMPIN)
      IF(ITEMP .EQ. 1) GO TO 82
      DO 313 ILV = 1,NLVT
      DO 313 I   = 1,5
  313 TPC(I,J,ILV)=TEMP(I,K,ILV)-TEMPIN(MTYPE)
   82 IB(K)=IB(K)+1
         IF (IGEN.GT.0)      GO TO 78
      PRINT 94,M,KQ,MTYPE,QUADT,TH,TP2
   78 IF(NODES.GT.2)      GO TO 610
      TH(2) = EM
      GO TO  620
  610 TH(5)=TH(5)*PI/180.
      D=EM/(1.-VM*VM)
      D11=D*DSQRT(RM)
      D22=D/DSQRT(RM)
      D33=D*(1.-VM*VM)*.5/(1.+GM)
      D12=D*VM
  620 WRITE(3) KQ,NODES,QUADT
   83 WRITE(3) TH155
      REWIND1
      REWIND2
      REWIND4
      REWIND3
         IF (IGEN.GT.1)      GO TO 79
      PRINT 84,(IB(I),I=1,NUPTS)
   79 CONTINUE
```

```
   84 FORMAT (1H0,60I2)
91     FORMAT ( 4I4,2X,3E12.5/18X,3E12.5/18X,3E12.5 )
   92 FORMAT(I4,2X,3E12.5)
   94  FORMAT (2X,5I4,2I2,1P4E10.3,F6.1,1PE10.3)
   96  FORMAT (I4,2X,1P8E12.5)
   98  FORMAT (2X,5I4,2X,1P5E12.5)
  900 FORMAT (45HODUPLICATION OF INPUT NODAL COORDINATE CARDS.)
901    FORMAT (53HODUPLICATION OF INPUT SURFACE DIRECTION COSINE CARDS.)
902    FORMAT (49HODUPLICATION OF ELEMENT NODAL POINT NUMBER CARDS.)
903    FORMAT (39HODUPLICATION OF ELEMENT MATERIAL TABLE.)
  904 FORMAT (18HONODAL COORDINATES )
  700 FORMAT( 31H PT    X           Y           Z         )
  701 FORMAT (28HOSURFACE DIRECTIONS COSINES.)
  702 FORMAT (/,2X,3HPT.,6X,3HE1X,6X,3HE1Y,6X,3HE1Z
     .         ,6X,3HE2X,6X,3HE2Y,6X,3HE2Z)
  905 FORMAT (57HO EL. NO.,EL. NODE NOS.,MATL. TYPE=T,EL. TYPE=E,EL.THICKN
     .  ,9HNESS,ANG.,10HTHER.COEF.)
  703 FORMAT (/,2X,3HEL.,3X,1HI,3X,1HJ,3X,1HK,3X,1HL,1X,1HT,1X,1HE
     .         ,3X,2HTI,8X,2HTK,8X,2HTL,8X,3HANG,3X,5HALPHA )
  906 FORMAT(39HODUPLICATION OF ELEMENT PROPERTY CARDS.)
30     FORMAT ( 4I4,2X,1P3E12.5 )
  31  FORMAT ( 4I4,2X,1P3E12.5,/,18X,1P3E12.5)
32     FORMAT ( I4,2X,6F9.5 )
   33 FORMAT ( 3I4,4X,6F9.5 )
   35 FORMAT (30HO ELEMENT DISTRIBUTED LOADS.
  37  FORMAT(2X,3I4,2X,1P5E11.4)
 303  FORMAT(2X,3I4,2X,1P5E12.5)
      RETURN
      END
```

```
      SUBROUTINE TEMSEL (J,M,II,MTYPE,TEMPIN)
      IMPLICIT REAL*8 (A-H,O-Z)
      COMMON/CV/NUMEL,NUPTS,NUBPTS,IBANDP,MBAND,NBLOC,NDFRE,IFLAG
     1         ,NUMAT,ITEMP,NLVT
      COMMON IX1(6),PX1(4052),TPC(5,4,5),PX2(50),IX2(402),
     1       TEMP(20,400,3)
      DIMENSION TEMPIN(30)
C.....THIS SUBROUTINE GETS EACH ELEMENTS TEMPERATURES FROM TEMP
C.....AND STORES THEM IN TPC.
      DO 312 I=1,5
      II=II+1
      DO 312 ILV=1,NLVT
  312 TPC(I,J,ILV)=TEMP(II,M,ILV) - TEMPIN(MTYPE)
      RETURN
      END
```

```
      SUBROUTINE INTEMP
C.....
C.....THIS SUBROUTINE GENERATES THE TEMPERATURES BY ELEMENT NUMBER. IT
C.....IS LIMITED TO 400 ELEMENTS AND 3 LOAD CASES FOR TEMPERATURE.
C.....
      IMPLICIT REAL*8 (A-H,O-Z)
      COMMON /SS/ IGEN,ISHEAR,JSHEAR,NRED,IREACT,NTRUSS,ISIG,IROT
      COMMON /CV/ NUMEL,NUPTS,NUBPTS,IBANDP,MBAND,NBLOC,NDFRE,IFLAG,
     1            NUMAT,ITEMP,NLVT
      COMMON IX1(6),PX1(4202),IX2(402),TEMP(20,400,3)
      DIMENSION XV(23),TEMPI(20)
      IF (NUMEL .GT. 400) PRINT 301
  301 FORMAT(/,4X,50HNUMEL GREATER THAN 400. INPUT OF TEMP BY ELEM EXCE
     1       ,11HEDS STORAGE,/)
      IF(NLVT .GT. 3) PRINT 302
  302 FORMAT(/,5X,46HNLVT GREATER THAN 3. STORAGE OF TEMP EXCEEDED.,/)
      DO 1 I=1,20
      DO 1 J=1,NUMEL
      DO 1 K=1,NLVT
    1 TEMP(I,J,K)=0.0
      DO 2 ILV=1,NLVT
      PRINT 300,ILV
  300 FORMAT(/////,5X,45HDUPLICATION OF ELEMENT TEMPERATURES FOR CASE
     .       ,I5,/)
    5 READ 526,M,LIM,MOP,(TEMPI(I),I=1,5)
  526 FORMAT(3I5,5X,5F10.0)
      IF (M .LE. 0) GO TO 2
      DO 6 I=1,3
      K1=I*5+1
      K2=K1+4
    6 READ 527,(TEMPI(L),L=K1,K2)
  527 FORMAT(20X,5F10.0)
      PRINT 303,M,LIM,MOP,(TEMPI(K),K=1,20)
  303 FORMAT(2X,3I4,1P5E12.5/13X,1P5E12.5/13X,1P5E12.5/13X,1P5E12.5)
      IF (MOP .LE. 0) LIM=M
      IF(MOP .LE. 0) MOP=1
      DO 4 L=M,LIM,MOP
      DO 4 J=1,20
    4 TEMP(J,L,ILV)=TEMPI(J)
      GO TO 5
    2 CONTINUE
C.....
C.....OUTPUT TEMPERATURES BY ELEMENT NUMBERS
C.....
      IF ( IGEN .GT. 0 ) GO TO 311
      DO 309 ILV=1,NLVT
      PRINT 802,ILV
  802 FORMAT(31HOELEMENT TEMPERATURES FOR CASE=,I5/)
      DO 310 I=1,NUMEL
      DO 310 J=1,4
      L=5*(J-1) + 1
      M=L+4
  310 PRINT 803,I,J,(TEMP(K,I,ILV),K=L,M)
  803 FORMAT(2I5,2X,1P5E12.5)
  309 CONTINUE
  311 CONTINUE
          RETURN
      END
```

```
      SUBROUTINE OVER2
      IMPLICIT REAL*8 (A-H,O-Z)
      COMMON/CV/NUMEL,NUPTS,NUBPTS,IBANDP,MBAND,NBLOC,NDFRE,IFLAG,LVECT
     1,ITEMP,NLVT
      COMMON/SS/IGEN,ISHEAR,JSHEAR,NRED,IREACT,NTRUSS,ISIG,IROT
      COMMON  IQ(4),NODES,QUADT,NTRI,IX1,IBD(200,7),
     1BC(200,6),S(37,37),PT(37,5),PX5(315)
     2    ,THQ(4),ANG,TPC(5,4,5),TP1,TP2,X(4),Y(4),Z(4)
     3,D11,    D12, D22, D33,EM, G1, G2, C(3,4), E(3,4), GM, QP(4),
     4        PX2(920), TG(3,3,4), PX3(96),ISPRNG(50),SPRING(6,50)
     5        ,NOPL(100,5)
      DIMENSION P(6,100,5), R(6), DX(6,6), CQ1(6220), LOADS(5),XV(20)
     1        ,THQ155(155)
      INTEGER Q,QUADT
      EQUIVALENCE (THQ(1),THQ155(1))
C     D(NDFRE**2,6,25),IBD(NUBPTS,NDFRE+1,)BC(NUBPTS,NDFRE),IBC(NUPTS)
C     IB(NUPTS),P(NUPTS,NDFRE),R(NDFRE),IQ,X,Y,Z(NODES).
      DATA GX/1.,5*0.,0.,1.,4*0.,2*0.,1.,3*0.,3*0.,1.,0.,0.,4*0.,1.,0.,
     1      5*0.,1./
C.....INITIALIZE BLANK COMMON (EXCEPT IB).
      DO 6 I=1,1408
    6 IQ(I)=0
      DO 561 I=1,37
      DO 562 K=1,5
  562 PT(I,K)=0.0
      DO 561 J=1,37
  561 S(I,J)=0.0
      DO 563 I=1,1522
  563 PX5(I)=0.0
      DO 564 I=1,50
  564 ISPRNG(I)=0
      DO 566 I=1,6
      DO 566 J=1,100
      DO 566 K=1,5
  566 P(I,J,K)=0.000
      DO 567 I=1,6
      DO 568 J=1,200
  568 BC(J,I)=0.000
      DO 569 K=1,50
  569 SPRING(I,K)=0.000
  567 CONTINUE
      DO 571 I=1,100
      DO 571 J=1,5
  571 NOPL(I,J)=0
      IK=1
      PRINT 82
      PRINT 83
      L=0
    7 L=L+1
      READ 528,(IBD(L,K),K=1,7),LIM,MOP,(BC(L,J),J=1,6)
  528 FORMAT(15,1X,6I1,2I3,2X,6F10.0)
      PRINT 81,(IBD(L,K),K=1,7),LIM,MOP,(BC(L,K),K=1,NDFRE)
      IF(L.EQ.NUBPTS)  GOTO 74
      IF(MOP) 7,7,8
    8 K=IBD(L,1)+MOP
      DO 70 I=K,LIM,MOP
      L=L+1
      IBD(L,1)=I
      DO 70 J=1,NDFRE
      IBD(L,J+1)=IBD(L-1,J+1)
   70 BC(L,J)=BC(L-1,J)
      IF(L.LT.NUBPTS)  GOTO 7
   74     IF (IGEN.GT.0)     GO TO 150
      PRINT 90
      PRINT 91
      DO 79 L=1,NUBPTS
   79 PRINT 89,(IBD(L,K),K=1,7),(BC(L,K),K=1,NDFRE)
  150 READ 529,NSPRNG
  529 FORMAT(16I5)
      PRINT 151,NSPRNG
  151 FORMAT(30HONUMBER OF NODES WITH SPRINGS=,I5,/)
      IF (NSPRNG.LE. 0)  GOTO 15
      PRINT 29
      L=0
   21 L=L+1
         NWDS=NDFRE+3
      READ 531,ISPRNG(L),LIM,MOP,(SPRING(K,L),K=1,6)
  531 FORMAT(3I5,5X,6F10.0)

      PRINT 23,ISPRNG(L),LIM,MOP,(SPRING(K,L),K=1,NDFRE)
      IF (L.EQ.NSPRNG)  GOTO 15
      IF (MOP) 21,21,24
   24 K=ISPRNG(L)+MOP
      DO 25 I = K,LIM,MOP
      L=L+1
      ISPRNG(L)=I
      DO 25 J = 1,NDFRE
   25 SPRING(J,L)=SPRING(J,L-1)
      IF(L.LT.NSPRNG)  GOTO 21
      IF (IGEN.GT.0)  GOTO 15
      PRINT 26
      PRINT 27
      DO 28 L = 1,NSPRNG
   28 PRINT 35,ISPRNG(L),(SPRING(K,L),K=1,NDFRE)
   15 READ 532,LVECT,(LOADS(K),K=1,5),UPL
  532 FORMAT(6I5,F10.0)
      PRINT 51,LVECT,LOADS,UPL
   51 FORMAT (/,1X,40HNUMBER OF INDEPENDENT LOAD CASES        =,I5/
     .        ,1X,40HNUMBER OF LOADED NODES FOR LOAD CASE 1 =,I5/
     .        ,1X,40HNUMBER OF LOADED NODES FOR LOAD CASE 2 =,I5/
     .        ,1X,40HNUMBER OF LOADED NODES FOR LOAD CASE 3 =,I5/
     .        ,1X,40HNUMBER OF LOADED NODES FOR LOAD CASE 4 =,I5/
     .        ,1X,40HNUMBER OF LOADED NODES FOR LOAD CASE 5 =,I5/
     .        ,1X,23HUNIFORM VERTICAL LOAD =,1PE12.4 )
```

```
      READ 529,ISKIP,JSKIP
      PRINT 85,ISKIP,JSKIP
          IF(IGEN.LT.2)      PRINT 87
      NTRUSS=0
      NQBLOC = 0
      REWIND9
C.....CONCENTRATED NODAL POINT LOAD GENERATION
      DO 73 I=1,LVECT
      II=1
      NLN=LOADS(I)
      IF(NLN.LE.0) GO TO 73
      PRINT 84,I
      PRINT 86
   71 READ 531,M,LIM,MOP,(R(K),K=1,6)
      PRINT 85,M,LIM,MOP,R
      IF(MOP.LE.0) LIM=M
      IF(MOP.LE.0) MOP=1
      DO 72 L=M,LIM,MOP
      NOPL(II,I)=L
      DO 75 K=1,NDFRE
   75 P(K,II,I)=R(K)
   72 II=II+1
      IF(II.LE.NLN) GO TO 71
   73 CONTINUE
      DO 14 LV=1,LVECT
         IF(IGEN.GT.2) GO TO 14
      NLN=LOADS(LV)
        IF(NLN.LE.0) GO TO 14
      PRINT 92,LV
      PRINT 86
      PRINT 88,(NOPL(L,LV),(P(J,L,LV),J=1,NDFRE),L=1,NLN)
   14 CONTINUE
      DO 10 LZ=1,NUMEL
      READ(3) IQ,NODES,QUADT
      READ(3) THQ155
      MD=NODES*NDFRE
      IF ( NODES.EQ.2 )  NTRUSS=NTRUSS+1
      IF(NODES.EQ.2)     GO TO  600
      DO 20 I=1,NODES
      TG(1,1,I)=C(1,I)
      TG(1,2,I)=C(2,I)
      TG(1,3,I)=C(3,I)
      TG(3,1,I)= C(2,I)*E(3,I)-C(3,I)*E(2,I)
      TG(3,2,I)=-C(1,I)*E(3,I)+C(3,I)*E(1,I)
      TG(3,3,I)= C(1,I)*E(2,I)-C(2,I)*E(1,I)
      CONST=DSQRT(TG(3,1,I)**2+TG(3,2,I)**2+TG(3,3,I)**2)
      TG(3,1,I)=TG(3,1,I)/CONST
      TG(3,2,I)=TG(3,2,I)/CONST
      TG(3,3,I)=TG(3,3,I)/CONST
      TG(2,1,I)= TG(1,3,I)*TG(3,2,I)-TG(1,2,I)*TG(3,3,I)
      TG(2,2,I)=-TG(1,3,I)*TG(3,1,I)+TG(1,1,I)*TG(3,3,I)
   20 TG(2,3,I)= TG(1,2,I)*TG(3,1,I)-TG(1,1,I)*TG(3,2,I)
  600 CALL QDSHEL  (        ISHEAR,JSHEAR,LZ,ISKIP,JSKIP )
      CALL MODIFY (NODES,NDFRE,LVECT,LOADS,NOPL,PT,P,IBD,S,BC,
     .             NSPRNG,ISPRNG,SPRING,IQ,NUBPTS)
      WRITE(1) NODES,MD,(IQ(L),L=1,NODES)
      WRITE(2) ((PT(I,J),I=1,MD),J=1,1),((S(I,J),J=1,MD),I=1,MD)
   10 CONTINUE
   81 FORMAT(14,1X,611,1X,214,1X,1P6E10.3)
   82 FORMAT (/,1X,46HDUPLICATION OF INPUT BOUNDARY CONDITION CARDS.,/
     .        ,1X,50HD1,D2 AND D3 ARE TRANSLATIONS IN BASE COORDINATES.,
     .         /,1X,47HD4,D5 AND D6 ARE ROTATIONS IN BASE COORDINATES.)
   83 FORMAT(1X,3HPT.,1X,6H123456,2X,11HLIM MOD  D1,8X,2HD2,8X,2HD3,
     1        8X,2HD4,8X,2HD5,8X,2HD6 )
   84 FORMAT(48HODUPLICATION OF INPUT NODAL FORCES,LOAD CASE NO.,I5)
   85 FORMAT ( 3I4,3X,1P6E11.4 )
   86 FORMAT(1X,11HPT. LIM MOD,4X,2HP1,9X,2HP2,9X,2HP3,9X,2HP4,
     1        9X,2HP5,9X,2HP6)
   87 FORMAT (50HOPOINTS CONTAINED IN EQUIL.EQS.,RIGHT OF DIAGONAL.,/
     .        7H    EQ.  )
   88 FORMAT(I4,11X,1P6E11.4)
   89 FORMAT ( I4,6I2,1X,1P6E11.4 )
   90 FORMAT(55H0BOUNDARY CONDITIONS OF POINTS HAVING SPECITIED DISPLS.)
   91 FORMAT(1X,17HPT. 1 2 3 4 5 6  ,2HD1,9X,2HD2,9X,2HD3,9X,2HD4,
     1        9X,2HD5,9X,2HD6)
   92 FORMAT(43HOTOTAL APPLIED NODAL POINT FORCES,LOAD CASE,I7)
   26 FORMAT(54H BOUNDARY CONDITIONS OF POINTS HAVING SPECIFIED SPRING
     .        1GHCONSTANTS. )
   27 FORMAT(1X,3HPT.,5X,2HD1,9X,2HD2,9X,2HD3,9X,2HD4,9X,2HD5,9X,2HD6)
   29 FORMAT(/,1X,38HDUPLICATION OF INPUT SPRING CONSTANTS.,/,
     .1X,3HPT.,2X,7HLIM MOD,2X,2HD1,8X,2HD2,8X,2HD3,8X,2HD4,8X,2HD5,
     . 8X,2HD6)
   23 FORMAT (I4,1X,214,1X,1P6E10.3)
   35 FORMAT (I4,4X,1P6E11.4)
      RETURN
      END




      SUBROUTINE MODIFY (NODES,NDFRE,LVECT,LOADS,NOPL,PT,P,IBD,S,BC,
     .NSPRNG,ISPRNG,SPRING,IQ,NUBPTS)
      IMPLICIT REAL*8 (A-H,O-Z)
      DIMENSION LOADS(5),NOPL(100,5),PT(37,5),P(6,100,5),IBD(20),7)
     .          ,S(37,37),BC(200,6),ISPRNG(50),SPRING(6,50),IQ(4)
C
C.....THIS SUBROUTINE MODIFIES ELEMENT STIFFNESS AND FORCE
C.....MATRICES FOR CONCENTRATED FORCES BOUNDARY CONDITIONS
C.....AND SPRINGS


      DO 50 J=1,NODES
C
C.....MODIFY ELEMENT FORCE VECTOR FOR CONCENTRATED FORCES
C
```

```
      DO 62 K=1,LVECT
      IF(LOADS(K).LE.0) GO TO 62
      LK=LOADS(K)
      DO 60 I=1,LK
      IF(NOPL(I,K).NE.IQ(J)) GO TO 60
       NOPL(I,K)=-NOPL(I,K)
      JJ=(J-1)*NDFRE
      DO 61 M=1,NDFRE
      JJ=JJ+1
      PT(JJ,K)=PT(JJ,K)+P(M,I,K)
   61   CONTINUE
   60 CONTINUE
   62 CONTINUE
C
C.....MODIFY STIFFNESS AND FORCE MATRICES FOR BOUNDARY CONDITIONS
C
      DO 63 I=1,NUBPTS
      IF(IBD(I,1).NE.IQ(J)) GO TO 63
      JJ=(J-1)*NDFRE
      DO 64 K=1,NDFRE
      JJ=JJ+1
      IF(IBD(1,K+1).LE.0) GO TO 64
              S(JJ,JJ) = 1.0D30                                    23FE77
      DO 65 M=1,LVECT
   65 PT(JJ,M)=1.0D30*BC(I,K)
   64 CONTINUE
   63 CONTINUE
C
C.....MODIFY STIFFNESS FOR SPRINGS
C
      IF(NSPRNG.LE.0) GO TO 50
      DO 66 I=1,NSPRNG
      IF(ISPRNG(1).NE.IQ(J)) GO TO 66
      JJ=(J-1)*NDFRE
      DO 67 K=1,NDFRE
      JJ=JJ+1
      IF(SPRING(K,1).LE.0) GO TO 67
      S(JJ,JJ)=SPRING(K,I)
   67 CONTINUE
      ISPRNG(I)=-ISPRNG(I)
   66 CONTINUE
   50 CONTINUE
      RETURN
      END



      SUBROUTINE QDSHEL (       ISHEAR,JSHEAR,LZ,ISKIP,JSKIP )
      IMPLICIT REAL*8 (A-H,O-Z)
      COMMON/CV/NUMEL,NUPTS,NUBPTS,IBANDP,MBAND,NBLOC,NDFRE,IFLAG,LVECT
     1,ITEMP,NLVT
      COMMON  IQ(4),NODES,QUADT, NTRI,IX1,IBD(200,7),BC(200,6),
     1        S(37,37), PT(37,5), TH(3), AD(3,4), BD(3,4),
     2        TD(3,36), TR(3,36), T(3,3,4), XMQ(3,3,4), THQ(4),ANG,
     3TPC(5,4,5),TP1,TP2,X(4),Y(4),Z(4),D11,D12,D22,D33,EM,G1,G2,
     4PX3(24),GM, QP(4), AREA, B(3), A(3), XM(3,3), ST(15,15),PX4(315),
     5        XS(2,2), SCOND(15,6,4), TG(3,3,4), TO(3,3), TDIS(3,3,3),
     6        TROT(3,3,3), X1, Y1, Z1, X2, Y2, Z2, X3, Y3, Z3,
     7 PE(3,5),P1,P2,P3,D1,D2,D3,Q1,Q2,Q3,IX2(50),PX5(300),IX3(500)
      DIMENSION LOC5(10),TX(3,3),IPERM(4),LOCB(15,4),LOCQ(3,5,4),
     1 LOCM(5),TP(9),TEMP(2,5)
     2 ,THQ119(119),TH437(437),S481(481),PT13(13),PT185(185)
      EQUIVALENCE                (X1,TX),(P1,TP)
      EQUIVALENCE (THQ(1),THQ119(1)),(TH(3),TH437(1)),(S(1,21),S481(1)),
     1           (PT(21,1),PT13(1)),(PT(1,1),PT185(1))
      DATA  LOCQ /
     1    1, 2, 3, 6, 7, 8,21,22,23,28,29,35,26,27,34,
     2    6, 7, 8,11,12,13,21,22,23,30,31,36,28,29,35,
     3   11,12,13,16,17,18,21,22,23,32,33,37,30,31,36,
     4   16,17,18, 1, 2, 3,21,22,23,26,27,34,32,33,37  /
      DATA  LOCB / 1, 2, 3, 4, 5, 6, 7, 8, 9,10,21,22,23,24,25,
     1             6, 7, 8, 9,10,11,12,13,14,15,21,22,23,24,25,
     2            11,12,13,14,15,16,17,18,19,20,21,22,23,24,25,
     3            16,17,18,19,20, 1, 2, 3, 4, 5,21,22,23,24,25 /
      DATA LOC5 / 1,2,6,7,11,12,16,17,21-22 /
      DATA  LOCM/1,3,5,7,9/, IPERM /2,3,4,1/
      REAL*8 NU,NORM
      INTEGER QUADT
C.....................................................................
C.....TRANSFORMATION MATRICES.........................................
C.....T(3,3,4).......FROM Z TO ZBAR...................................
C.....TO(3,3)........FROM Z TO ZO.....................................
C.....TG(3,3,4)......FROM Z TO Z'.....................................
C.....TROT(3,3,3)....FROM Z' TO ZBAR...................................
C.....TDIS(3,3,3)....FROM ZB TO ZBAR...................................
C.....T(3,3,4).......FROM ZB TO ZO.....................................
C.....COMPUTE INTERNAL MID POINT COORDINATES IF QUAD...................
      DO 160 I =1,37
      DO 162 K =1,5
  162 PT(I,K) = 0.0
      DO 160 J =1,37
  160 S(I,J) = 0.
      SAREA=0.
      IF ( NODES.GT.2 )  GOTO 500
      DO 161 I = 1,NLVT
      TEMP(1,I) = TPC(3,1,I)
  161 TEMP(2,I) = TPC(3,2,I)
      CALL TRUSS ( IQ,X,Y,Z,THQ(1),THQ(2),S,PT,GM,TEMP,TP2,NLVT)
      WRITE(9) IQ,NODES,QUADT,NTRI
      WRITE(9) THQ119
      GOTO 1001
  500 NTRI=4
      IF(IQ(4).LT.1)  NTRI=1
      IF(NTRI.EQ.1)  IADD=10
      IF(NTRI.EQ.4)  IADD=20
      IF(NTRI.EQ.1)  TH(3)=THQ(3)
      IF(NTRI.EQ.4)  TH(3)=(THQ(1)+THQ(2)+THQ(3)+THQ(4))/4.
      AVTH = (THQ(1)+THQ(2)+THQ(3))/3.
      IF ( NTRI .EQ. 4 )   AVTH = TH(3)
      DO 10 I=1,3
   10 LOCQ(I,3,1)=IADD+I
      DO 11 I=1,5
   11 LOCB(I+10,1)=IADD+I
      IF ( D11 .GE. .000001 ) GO TO 1101
      IF ( XMQ(1,1,1) .EQ.0. .AND. XMQ(2,2,1) .EQ.0. )  GOTO 1000
 1101 XC=X(3)
      YC=Y(3)
      ZC=Z(3)
```

```
      TP(3)=QP(3)
      IF(NTRI.EQ.1)  GOTO 700
      XC = 0.25*(X(1)+X(2)+X(3)+X(4))
      YC = 0.25*(Y(1)+Y(2)+Y(3)+Y(4))
      ZC = 0.25*(Z(1)+Z(2)+Z(3)+Z(4))
      TP(3)=.25*(QP(1)+QP(2)+QP(3)+QP(4))
C.....COMPUTE ELEMENT DIRECTION COSINES, T(I,J,4).....................
  700 DO 130  N = 1,NTRI
      M = IPERM(N)
      X1 = X(M)-X(N)
      Y1 = Y(M)-Y(N)
      Z1 = Z(M)-Z(N)
      X2 = XC - X(N)
      Y2 = YC - Y(N)
      Z2 = ZC - Z(N)
      S11 = X1*X1+Y1*Y1+Z1*Z1
      S12 = X1*X2+Y1*Y2+Z1*Z2
      S22 = X2*X2+Y2*Y2+Z2*Z2
      COS12 = -S12/S11
      X2 = X2 + X1*COS12
      Y2 = Y2 + Y1*COS12
      Z2 = Z2 + Z1*COS12
      S1 = DSQRT(S11)
      S2 = DSQRT(X2*X2+Y2*Y2+Z2*Z2)
      T(1,1,N) = X1/S1
      T(1,2,N) = Y1/S1
      T(1,3,N) = Z1/S1
      T(2,1,N) = X2/S2
      T(2,2,N) = Y2/S2
      T(2,3,N) = Z2/S2
      T(3,1,N) = T(1,2,N)*T(2,3,N) - T(1,3,N)*T(2,2,N)
      T(3,2,N) = T(1,3,N)*T(2,1,N) - T(1,1,N)*T(2,3,N)
  130 T(3,3,N) = T(1,1,N)*T(2,2,N) - T(1,2,N)*T(2,1,N)
      IF ( NTRI.EQ.1 )  GOTO 1100
C.....COMPUTE DIRECTION COSINES OF N1,N2 PLANE.......................
      CALL QDCOS(4,X,Y,Z,TO )
      DO 5002 I=1,4
      Q1 = X(I)
      Q2 = Y(I)
      Q3 = Z(I)
      X(I) = TO(1,1)*Q1+TO(1,2)*Q2+TO(1,3)*Q3
      Y(I) = TO(2,1)*Q1+TO(2,2)*Q2+TO(2,3)*Q3
 5002 Z(I)=0.0
      XC = 0.25*(X(1)+X(2)+X(3)+X(4))
      YC = 0.25*(Y(1)+Y(2)+Y(3)+Y(4))
      ZC = 0.25*(Z(1)+Z(2)+Z(3)+Z(4))
      TP(3)=.25*(QP(1)+QP(2)+QP(3)+QP(4))
C.....COMPUTE ELEMENT DIRECTION COSINES, T(I,J,4).....................
      DO 131  N = 1,NTRI
      M = IPERM(N)
      X1 = X(M)-X(N)
      Y1 = Y(M)-Y(N)
      Z1 = Z(M)-Z(N)
      X2 = XC - X(N)
      Y2 = YC - Y(N)
      Z2 = ZC - Z(N)
      S11 = X1*X1+Y1*Y1+Z1*Z1
      S12 = X1*X2+Y1*Y2+Z1*Z2
      S22 = X2*X2+Y2*Y2+Z2*Z2
      COS12 = -S12/S11
      X2 = X2 + X1*COS12
      Y2 = Y2 + Y1*COS12
      Z2 = Z2 + Z1*COS12
      S1 = DSQRT(S11)
      S2 = DSQRT(X2*X2+Y2*Y2+Z2*Z2)
C.....COMPUTE A'S AND B'S.............................................
 1100 AD(2,N) = S1*COS12
      AD(3,N) = S1
      AD(1,N) = -AD(3,N)-AD(2,N)
      BD(1,N) = -(S22+COS12*S12)/S2
      BD(2,N) = -BD(1,N)
  131 BD(3,N) = 0.
C.....DIRECTION COSINES FOR MID POINT IF ELEMENT IS A TRI.............
      DO 900 I=1,3
      DO 900 J=1,3
      XM(I,J)=0.
      IF (NTRI.EQ.1) TO(I,J)=T(I,J,1)
  900 CONTINUE
C.....SUM OVER 4 TRIS. IF QUAD OR 1 TRI. IF ELEMENT IS A TRI..........
  701 DO 301  NT = 1,NTRI
      N1 = NT
      N2 = IPERM(N1)
      TH(1)=THQ(N1)
      TH(2)=THQ(N2)
      TP(1)=QP(N1)
      TP(2)=QP(N2)
C.....COMPUTE TRANSFORMATIONS FOR EACH POINT OF TRIANGLE..............
      DO 200  I = 1,3
      TP(I+3)=TH(I)*GM
      TP(I+6)=T(I,3,NT)
      A(I) = AD(I,NT)
      B(I) = BD(I,NT)
      T1 = T(I,1,NT)
      T2 = T(I,2,NT)
      T3 = T(I,3,NT)
      DO 200  J = 1,3
      TROT(I,J,1) = T1*TO(J,1)    + T2*TO(J,2)    + T3*TO(J,3)
      TROT(I,J,2) = T1*TO(J,1)    + T2*TO(J,2)    + T3*TO(J,3)
      TROT(I,J,3) = T1*TO(J,1)    + T2*TO(J,2)    + T3*TO(J,3)
      TDIS(I,J,1) = TROT(I,J,1)
      TDIS(I,J,2) = TROT(I,J,2)
      TDIS(I,J,3) = TROT(I,J,3)
  200 CONTINUE
C.....STORE BASE TRANSFORMATION MATRICES..............................
      C= DCOS(ANG )
      R= DSIN ( ANG )
      IF(NTRI.EQ.1)  GOTO 201
      CC=TDIS(1,1,3)
      RR=TDIS(1,2,3)
      CS=DSQRT(CC*CC+RR*RR)
      CC=CC/CS
      RR=RR/CS
      C= CC*DCOS(ANG)-RR*DSIN(ANG)
      R= CC*DSIN(ANG)+RR*DCOS(ANG)
  201 CALL SSTQM5 ( C,R,D11,D12,D22,D33,XM )
      XS(1,1)=G1
      XS(2,2)=G2
      XS(1,2)=0.
      XS(2,1)=0.
      KK=(NT-1)*9
```

```
      DO 1 K=1,3
      L=KK+(K-1)*3
      DO 1 J=1,3
      XMQ(K,J,NT)=XM(K,J)
      JL=J+L
      DO 1 I=1,3
      TD(I,JL)=TDIS(I,J,K)
    1 TR(I,JL)=TROT(I,J,K)
C.....COMPUTE AREA OF TRIANGLE.....
    3 AREA = A(3)*B(2) - A(2)*B(3)
      SAREA = SAREA + AREA/2.
C.....FORM AND TRANSFORM MEMBRANE STIFFNESS TO BASE SYSTEM IF A TRI.....
C.....FORM AND TRANSFORM MEMBRANE STIFFNESS TO ZO   SYSTEM IF A QUAD....
      IF ( QUADT.GT.0 )  GOTO 5000
      IF(NTRI.EQ.1)  CALL CLST10  (3,3,TH,AREA,B,XM,ST)
      IF(NTRI.EQ.4)  CALL CLST10  (5,1,TH,AREA,B,XM,ST)
      IEND=3
      IF(NTRI.EQ.4)  IEND=5
      DO 27 II=1,IEND
      I=LOCM(II)
      IF(II.LT.4)  IL=II
      DO 27 JJ=1,II
      J=LOCM(JJ)
      IF(JJ.LT.4)  JL=JJ
      LS=1
      DO 27 K=1,3
      N=LOCQ(K,JJ,NT)
      H1=ST(I  ,J)*TDIS(1,K,JL)+ST(I  ,J+1)*TDIS(2,K,JL)
      H2=ST(I+1,J)*TDIS(1,K,JL)+ST(I+1,J+1)*TDIS(2,K,JL)
      IF(I.EQ.J)  LS=K
      DO 27 L=LS,3
      M=LOCQ(L,II,NT)
      S(M,N)=S(M,N)+TDIS(1,L,IL)*H1+TDIS(2,L,IL)*H2
   27 S(N,M)=S(M,N)
C.....FORM AND TRANSFORM PLATE STIFFNESS TO BASE SYSTEM IF A TRI.....
C.....FORM AND TRANSFORM PLATE STIFFNESS TO ZO   SYSTEM IF A QUAD.....
 5000 IF ( LZ.LT.ISKIP .OR. LZ.GT.JSKIP )  GOTO 6002
      GOTO 301
 6002 CALL SLCCT (9,ISHEAR,NT,0)
      DO 300  II = 1,3
      K = 3*II - 2
      KK = 5*(II-1)
      DO 300  JJ = II,3
      L = 3*JJ - 2
      LL = 5*(JJ-1)
      DO 300  M = 1,5
      J = LL + M
      JS = LOCB(J,NT)
      IF (M.GT.3)  GO TO 270
      T3 = TDIS(3,M,JJ)
      H1 = ST(K,  L)*T3
      H2 = ST(K+1,L)*T3
      H3 = ST(K+2,L)*T3
      GO TO 280
  270 T1 = TROT(1,M-3,JJ)
      T2 = TROT(2,M-3,JJ)
      H1 = ST(K,  L+1)*T1 + ST(K,  L+2)*T2
      H2 = ST(K+1,L+1)*T1 + ST(K+1,L+2)*T2
      H3 = ST(K+2,L+1)*T1 + ST(K+2,L+2)*T2
  280 DO 300  N = 1,5
      I = KK + N
      IF (I.GT.J)  GO TO 300
      IS = LOCB(I,NT)
      IF (N.GT.3)  GO TO 290
      S(IS,JS) = S(IS,JS) + H1*TDIS(3,N,II)
      GO TO 295
  290 S(IS,JS) = S(IS,JS) + H2*TROT(1,N-3,II) + H3*TROT(2,N-3,II)
  295 S(JS,IS) = S(IS,JS)
  300 CONTINUE
      CALL NLOAD (Q1,Q2,Q3,P1,P2,P3,D1,D2,D3,PE,AREA,A,B,TH)
      DO 800 I=1,3
      K=I
      IF(NTRI.EQ.4) K=3
      Q1=PE(1,I)
      Q2=PE(2,I)
      Q3=PE(3,I)
      DO 800 J=1,3
      L=LOCQ(J,I,NT)
  800 PT185(L)=PT185(L)+TDIS(I,J,K)*Q1+TDIS(2,J,K)*Q2+TDIS(3,J,K)*Q3
  301 CONTINUE
      IF(NTRI.EQ.1)  GOTO 1000
      IF ( QUADT.GT.0 )  GOTO 5001
C.....ELIMINATE TRANSL. COMPONENTS NORMAL TO N1,N2 PLANE OF MIDSIDE NODE
      DO 34 I=1,37
      S(I, 3)=S(1, 3)+S(I,34)/2.
      S(1, 8)=S(I, 8)+S(I,35)/2.
      S(I,13)=S(I,13)+S(I,36)/2.
      S(I,18)=S(1,18)+S(1,37)/2.
   34 S(I,23)=S(I,23)+(S(I,34)+S(I,35)+S(I,36)+S(I,37))/2.
      DO 35 J=1,37
      S( 3,J)=S( 3,J)+S(34,J)/2.
      S( 8,J)=S( 8,J)+S(35,J)/2.
      S(13,J)=S(13,J)+S(36,J)/2.
      S(18,J)=S(18,J)+S(37,J)/2.
   35 S(23,J)=S(23,J)+(S(34,J)+S(35,J)+S(36,J)+S(37,J))/2.
      GOTO 5004
 5001 CALL SSTQM5 ( DCOS(ANG),DSIN(ANG),D11,D12,D22,D33,XM )
      DO 5005 I=1,3
      DO 5005 J=1,3
 5005 XM(I,J)=XMQ(I,J,1)*TH(3)
      CALL QM5STF ( X,Y,XM,ST )
      DO 5003 I=1,10
      II=LOC5(I)
      DO 5003 J=1,10
      JJ=LOC5(J)
 5003 S(II,JJ)=S(II,JJ)+ST(I,J)
      DO 5500 I = 1, 16, 5
      PT185(I)=PT185(I)+PT185(21)/4.0
 5500 PT185(I+1)=PT185(I+1)+PT185(22)/4.0
      PT185(21)  = 0.0
      PT185(22)  = 0.0
C.....CONDENSE INTERNAL DEGREES OF FREEDOM.....
 5004 IF ( LZ.LT.ISKIP.OR.LZ.GT.JSKIP )  GOTO 6001
      DO 6000 J=23,25
      DO 6000 I= 1,33
      S(I,J)=0.
      S(J,I)=0.
      IF ( I.EQ.J )  S(I,J)=1.
 6000 CONTINUE
 6001 NDOFQ=33
```

```
      IF ( QUADT.GT.0 ) NDOFQ=25
      NDOFC=13
      IF ( QUADT.GT.0 ) NDOFC=5
      DO 400 N =1,NDOFC
      K=NDOFQ-N
      L = K + 1
      PIVOT = S(L,L)
      DO 400  I = 1,K
      C = S(I,L)/PIVOT
      PT185(I)=PT185(I)-C*PT185(L)
      S(I,L) = C
      DO 400  J = I,K
      S(I,J) = S(I,J) - C*S(L,J)
  400 S(J,I) = S(I,J)
C.....ESTABLISH TRANSFORMATION FROM BASE COORDS. TO N1,N2 PLANE.........
 1000 L2=3
      IF (NTRI.EQ.4) L2 = 4
      IF(IFLAG.EQ.1)  GOTO 39
      DO 38 L=1,L2
      DO 38 I=1,3
      DO 38 J=1,3
   38 T(I,J,L)=T0(I,J)
      GOTO 1002
   39 DO 40 L=1,L2
      DO 40 I=1,3
      DO 40 J=1,3
      T(I,J,L)=0.
      DO 40 K=1,3
   40 T(I,J,L)=T(I,J,L)+T0(I,K)*TG(J,K,L)
 1002 WRITE(9) IQ,NODES,QUADT,NTRI
      PR=C12/D11
      ALP=TP2
C.....FORM THERMAL FORCES
      CALL TRIPLT( PR,ALP,NLVT)
      WRITE(9) TH437
      IF ( QUADT.GT.0 ) WRITE(9) X,Y
      IF ( JSHEAR.EQ.6 ) WRITE(9) SCONO
      IF (NODES.EQ.4 ) WRITE(9) S481
      IF ( NODES.EQ.4 ) WRITE(9) PT13
      IF ( XMQ(1,1,1) .EQ. 0. .AND. XMQ(2,2,1) .EQ.0. )  GOTO 1001
      CALL ROTAS (NODES,NDFRE,EM,SAREA,AVTH,S,PT,NLVT)
      CALL TRANSF (NODES,NDFRE,T,S,PT,NLVT)
 1001 RETURN
      END
```

```
      SUBROUTINE ROTAS (NODES,NDFRE,EM,AREA,TH,S,PT,NLVT)
      IMPLICIT REAL*8 (A-H,O-Z)
      COMMON/SS/IGEN,ISHEAR,JSHEAR,NRED,IREACT,NTRUSS,ISIG,IROT
C.....THIS SUBROUTINE COMPUTES A FICTITIOUS ROTATIONAL STIFFNESS USED
C.....IN MODIFYING 5 DOF TO 6 DOF. ASSUMED CONSTANT IS 0.02
      DIMENSION S(37,37),PT(37,5),LOC6(20),LOCR(4),ST(24,24),P(24,5)
      DATA LOC6/1,2,3,4,5, 7,8,9,10,11, 13,14,15,16,17, 19,20,21,22,23/
      DATA LOCR/6,12,18,24/
      NDIM = NODES*NDFRE
      DO 10 I = 1,NDIM
      DO 1 ILVT = 1,NLVT
    1 P(I,ILVT)    = 0.
      DO 10 J = 1,NDIM
   10 ST(I,J) = 0.
      NSIZE   = 5*NODES
      DO 20 I = 1,NSIZE
      II      = LOC6(I)
      DO 11 ILVT = 1,NLVT
   11 P(II,ILVT) = PT(I,ILVT)
      DO 20 J = 1,NSIZE
      JJ      = LOC6(J)
   20 ST(II,JJ) = S(I,J)
      IF ( IROT.GT.0 )  GOTO 50
      FACT =0.02*EM*AREA*TH
      DO 30 I = 1,NODES
      II = LOCR(I)
      DO 30 J = 1,NODES
      JJ = LOCR(J)
      ST(II,JJ) = -0.5*FACT
      IF ( II.EQ.JJ .AND. NODES.EQ.3 )  ST(II,JJ) = 1.0*FACT
   30 IF ( II.EQ.JJ .AND. NODES.EQ.4 )  ST(II,JJ) = 1.5*FACT
   50 CONTINUE
      DO 40 I = 1,NDIM
      DO 51 ILVT = 1,NLVT
   51 PT(I,ILVT) = P(I,ILVT)
      DO 40 J = 1,NDIM
   40 S(I,J) = ST(I,J)
      RETURN
      END
```

```
      SUBROUTINE BASE (T,L)
      IMPLICIT REAL*8 (A-H,O-Z)
      COMMON /TB/ TX(3,3)
      DIMENSION T(3,3,4)
      L = L+1
      DO 1 I = 1,3
      DO 1 J = 1,3
    1 TX(I,J) = T(I,J,L)
      RETURN
      END
```

```
      SUBROUTINE TRANSF (NODES,NDFRE,T,S,PT,NLVT)
      IMPLICIT REAL*8 (A-H,O-Z)
C.....THIS SUBROUTINE TRANSFORMS MATRICES TO THE BASE SYSTEM
      COMMON /TB/ X1,Y1,Z1,X2,Y2,Z2,X3,Y3,Z3
      DIMENSION S(37,37),PT(37,5),T(3,3,4)
C.....TRANSFORM TRANSLATION COMPONENTS
      L = 0
      LIM = NDFRE*(NODES-1)+1
      NSIZE = NODES*NDFRE
      DO 1 II = 1,LIM,NDFRE
      CALL BASE (T,L)
      DO 10 ILVT = 1,NLVT
      Q1 = PT(II,ILVT   )
      Q2 = PT(II+1,ILVT)
      Q3 = PT(II+2,ILVT)
      PT(II,ILVT   ) = X1*Q1+Y1*Q2+Z1*Q3
      PT(II+1,ILVT) = X2*Q1+Y2*Q2+Z2*Q3
   10 PT(II+2,ILVT) = X3*Q1+Y3*Q2+Z3*Q3
      DO 1 I = II,NSIZE
      F = S(I,II   )
      G = S(I,II+1)
      H = S(I,II+2)
      S(I,II   ) = F*X1+G*Y1+H*Z1
      S(I,II+1) = F*X2+G*Y2+H*Z2
    1 S(I,II+2) = F*X3+G*Y3+H*Z3
      L = 0
      LIM = NSIZE-3
      DO 2 II = 3,LIM,NDFRE
      CALL BASE (T,L)
      DO 2 J = 1,II
      F = S(II-2,J)
      G = S(II-1,J)
      H = S(II   ,J)
      S(II-2,J) = F*X1+G*Y1+H*Z1
      S(II-1,J) = F*X2+G*Y2+H*Z2
    2 S(II   ,J) = F*X3+G*Y3+H*Z3
C.....TRANSFORM ROTATION COMPONENTS
      L = 0
      LIM = NDFRE*NODES-2
      DO 3 II = 4,LIM,NDFRE
      CALL BASE (T,L)
      DO 11 ILVT = 1,NLVT
      Q1 = PT(II,ILVT   )
      Q2 = PT(II+1,ILVT)
      Q3 = PT(II+2,ILVT)
      PT(II,ILVT   ) = X1*Q1+Y1*Q2+Z1*Q3
      PT(II+1,ILVT) = X2*Q1+Y2*Q2+Z2*Q3
   11 PT(II+2,ILVT) = X3*Q1+Y3*Q2+Z3*Q3
      DO 3 I = II,NSIZE
      F = S(I,II   )
      G = S(I,II+1)
      H = S(I,II+2)
      S(I,II   ) = F*X1+G*Y1+H*Z1
      S(I,II+1) = F*X2+G*Y2+H*Z2
    3 S(I,II+2) = F*X3+G*Y3+H*Z3
      L = 0
      DO 4 II = 6,NSIZE,NDFRE
      CALL BASE (T,L)
      DO 4 J = 1,II
      F = S(II-2,J)
      G = S(II-1,J)
      H = S(II   ,J)
      S(II-2,J) = F*X1+G*Y1+H*Z1
      S(II-1,J) = F*X2+G*Y2+H*Z2
    4 S(II   ,J) = F*X3+G*Y3+H*Z3
      DO 5 J = 1,NSIZE
      DO 5 I = 1,NSIZE
    5 S(J,I) = S(I,J)
      RETURN
      END
```

```
      SUBROUTINE TRUSS(IQ,X,Y,Z,AREA,E,S,PT,GM,TEMP,TP2,NLVT)
      IMPLICIT REAL*8 (A-H,O-Z)
      DIMENSION IQ(4), X(4), Y(4), Z(4), S(37,37),PT(37,5)
      DIMENSION A(3,3), LQ(6), TEMP(2,5)
      DATA LQ / 3*0,3*3 /
      EQUIVALENCE (A(1,1),X1),(A(2,1),Y1),(A(3,1),Z1),
     1            (A(1,2),X2),(A(2,2),Y2),(A(3,2),Z2),
     2            (A(1,3),X3),(A(2,3),Y3),(A(3,3),Z3)
      REAL*8  L,L1,L2,L3,LY,LZ
      DO 1 I=1,37
      DO 1 J=1,37
    1 S(I,J)=0.
      L=DSQRT((X(1)-X(2))**2+(Y(1)-Y(2))**2+(Z(1)-Z(2))**2)
      L1=E/L
      L2=E/L**2
      L3=E/L**3
      S( 1, 1)=AREA*L1
```

```
      S( 7, 1)=-AREA*L1
      S( 1, 7)=S( 7, 1)
      S( 7, 7)=AREA*L1
      L1=X(2)-X(1)
      L2=Y(2)-Y(1)
      L3=Z(2)-Z(1)
      H1=DSQRT(L1**2+L2**2)
      C1=1.
      S1=0.
      IF(H1.GT..000001)  C1=L1/H1
      IF(H1.GT..000001)  S1=L2/H1
      C2=H1/L
      S2=-L3/L
      A(1,1)=L1/L
      A(1,2)=L2/L
      A(1,3)=L3/L
      A(2,1)=-S1
      A(2,2)= C1
      A(2,3)= 0.
      A(3,1)=C1*S2
      A(3,2)= S1*S2
      A(3,3)=C2
      DO 4 II=1, 6,3
      N = II + LQ(II)
      DO 4 I=II, 6
      M = I  + LQ(1)
      F=S(M, N  )
      G=S(M, N+1)
      H=S(M, N+2)
      S(M, N  )=F*X1+G*Y1+H*Z1
      S(M, N+1)=F*X2+G*Y2+H*Z2
    4 S(M, N+2)=F*X3+G*Y3+H*Z3
      DO 5 II=3, 6,3
      M = II + LQ(II)
      DO 5 J=1,II
      N = J + LQ(J)
      F=S( M-2,N)
      G=S( M-1,N)
      H=S( M  ,N)
      S( M-2,N)=F*X1+G*Y1+H*Z1
      S( M-1,N)=F*X2+G*Y2+H*Z2
    5 S( M  ,N)=F*X3+G*Y3+H*Z3
      DO 6 J=1,12
      DO 6 I=J,12
    6 S(J,I)=S(I,J)
      DO 10 ILVT = 1,NLVT
      AVTP = 0.5*(TEMP(1,ILVT)+TEMP(2,ILVT))
      PP   = E*TP2*AREA*AVTP
      DO 10 I=1,7,6
      PP = -PP
      PT(I,ILVT) = PP*C2*C1
      PT(I+1,ILVT) = PP*C2*S1
   10 PT(I+2,ILVT) = -(PP*S2)+GM*L*AREA*0.5
    7 RETURN
      END
```

```
      SUBROUTINE SSTQM5 ( C,R,D11,D12,D22,D33,XM )
      IMPLICIT REAL*8 (A-H,O-Z)
      DIMENSION XM(3,3)
  201 S4=R**4
      C4=C**4
      S2C2=R*R*C*C
      SC3=R*C**3
      S3C=R**3*C
      XM(1,1)=C4*D11+S4*D22+S2C2*(2.*D12+4.*D33)
      XM(2,1)=(S4+C4)*D12+S2C2*(D11+D22-4.*D33)
      XM(3,1)=SC3*(-D11+D12+2.*D33)+S3C*(-D12+D22-2.*D33)
      XM(2,2)=S4*D11+C4*D22+S2C2*(2.*D12+4.*D33)
      XM(3,2)=SC3*(-D12+D22-2.*D33)+S3C*(-D11+D12+2.*D33)
      XM(3,3)=(C4+S4)*D33+S2C2*(D11-2.*D12+D22-2.*D33)
      XM(1,2)=XM(2,1)
      XM(1,3)=XM(3,1)
      XM(2,3)=XM(3,2)
      RETURN
      END
```

```
      SUBROUTINE QM5STF ( X,Y,DD,QQ )
      IMPLICIT REAL*8 (A-H,O-Z)
C
C.....    QM5 MEMBRANE STIFFNESS MATRIX FOR A GENERAL QUAD
C
      DIMENSION X(4),Y(4),DD(3,3),QQ(15,15)
      DIMENSION QC(3,10),SS(4),TT(4)
      DATA SS /-1.,1.,1.,-1./, TT /-1.,-1.,1.,1./
      DO 6 I=1,15
      DO 6 J=1,15
    6 QQ(I,J)=0.0
      R12 = X(1) - X(2)
      R13 = X(1) - X(3)
      R14 = X(1) - X(4)
      R23 = X(2) - X(3)
      R24 = X(2) - X(4)
      R34 = X(3) - X(4)
      Z12 = Y(1) - Y(2)
      Z13 = Y(1) - Y(3)
      Z14 = Y(1) - Y(4)
      Z23 = Y(2) - Y(3)
      Z24 = Y(2) - Y(4)
      Z34 = Y(3) - Y(4)
      VOL=R13*Z24-R24*Z13
      CALL QM5C2 ( R13,R24,Z13,Z24,VOL,X5,X6,X7,X8,Y5,Y6,Y7,Y8 )
      DO 30 II=1,4
      S=SS(II)*0.577350269189626
      T=TT(II)*0.577350269189626
      CALL QM5C1 ( S,T,R12,R13,R14,R23,R24,R34,Z12,Z13,Z14,Z23,Z24,Z34,
     .             VOL,X1,X2,X3,X4,XC,Y1,Y2,Y3,Y4,YC,XJAC,X(1),X(2),
     .             X(3),X(4),Y(1),Y(2),Y(3),Y(4) )
C.....    FORM STIFFNESS QQ
```

```
      DO  10  I = 1, 3
      D1 = DD(I,1)*XJAC
      D2 = DD(I,2)*XJAC
      D4 = DD(I,3)*XJAC
      QC(I,1)=          D1*Y1+D4*X5
      QC(I,3)=          D1*Y2+D4*X6
      QC(I,5)=          D1*Y3+D4*X7
      QC(I,7)=          D1*Y4+D4*X8
      QC(I,9)=          D1*YC
      QC(I,2)=          D2*X1+D4*Y5
      QC(I,4)=          D2*X2+D4*Y6
      QC(I,6)=          D2*X3+D4*Y7
      QC(I,8)=          D2*X4+D4*Y8
      QC(I,10)=         D2*XC
   10 CONTINUE
      DO 20 I=1,10
      D1=QC(1,I)
      D2=QC(2,I)
      D4=QC(3,I)
      QQ(1,I)=QQ(1,I)+D1*Y1+D4*X5
      QQ(3,I)=QQ(3,I)+D1*Y2+D4*X6
      QQ(5,I)=QQ(5,I)+D1*Y3+D4*X7
      QQ(7,I)=QQ(7,I)+D1*Y4+D4*X8
      QQ(9,I)=QQ(9,I)+D1*YC
      QQ(2,I)=QQ(2,I)+D2*X1+D4*Y5
      QQ(4,I)=QQ(4,I)+D2*X2+D4*Y6
      QQ(6,I)=QQ(6,I)+D2*X3+D4*Y7
      QQ(8,I)=QQ(8,I)+D2*X4+D4*Y8
      QQ(10,I)=QQ(10,I)+D2*XC
   20 CONTINUE
C
   30 CONTINUE
       RETURN
       END
```

```
      SUBROUTINE QM5C2 ( R13,R24,Z13,Z24,VOL,X5,X6,X7,X8,Y5,Y6,Y7,Y8 )
      IMPLICIT REAL*8 (A-H,O-Z)
C.....    THIS ROUTINE IS CALLED BY QM5 STIFFNESS AND STRESS ROUTINES
      Y5 = Z24/VOL
      X6 = R13/VOL
      X7 = R24/VOL
      Y8 = Z13/VOL
      X5 =-X7
      Y6 =-Y8
      Y7 =-Y5
      X8 =-X6
      RETURN
      END
```

```
      SUBROUTINE QM5C1 ( S,T,R12,R13,R14,R23,R24,R34,Z12,Z13,Z14,Z23,
     .           Z24,Z34,VOL,X1,X2,X3,X4,XC,Y1,Y2,Y3,Y4,YC,XJAC,R1,R2,
     .           R3,R4,Z1,Z2,Z3,Z4 )
      IMPLICIT REAL*8 (A-H,O-Z)
C.....    THIS ROUTINE IS CALLED BY QM5 STIFFNESS AND STRESS ROUTINES
      XJ =VOL+S*(R34*Z12-R12*Z34)+T*(R23*Z14-R14*Z23)
      XJAC=XJ/8.0
      SM=1.0-S
      SP=1.0+S
      TM=1.0-T
      TP=1.0+T
      X1=(-R24+R34*S+R23*T)/XJ
      X2=( R13-R34*S-R14*T)/XJ
      X3=( R24-R12*S+R14*T)/XJ
      X4=(-R13+R12*S-R23*T)/XJ
      Y1=( Z24-Z34*S-Z23*T)/XJ
      Y2=(-Z13+Z34*S+Z14*T)/XJ
      Y3=(-Z24+Z12*S-Z14*T)/XJ
      Y4=( Z13-Z12*S+Z23*T)/XJ
      RS=0.25*(-TM*R1+TM*R2+TP*R3-TP*R4)
      ZS=0.25*(-TM*Z1+TM*Z2+TP*Z3-TP*Z4)
      RT=0.25*(-SM*R1-SP*R2+SP*R3+SM*R4)
      ZT=0.25*(-SM*Z1-SP*Z2+SP*Z3+SM*Z4)
      XC=-2.0*(T*SM*SP*RS-S*TM*TP*RT)/XJAC
      YC= 2.0*(T*SM*SP*ZS-S*TM*TP*ZT)/XJAC
      RETURN
      END
```

```
      SUBROUTINE CLST10  (LNODES,LSIDES,TH,AREA,B,XM,S)
      IMPLICIT REAL*8 (A-H,O-Z)
      COMMON/CLS/ X(3,5),Y(3,5),X1,X2,X3,X4,X5,X6,X7,X8,X9,
     1            Y4,Y5,Y6,Y7,Y8,Y9,T(3,3),TU1(3,5),TU2(3,5)
      DIMENSION  XM(3,3),TH(3),S(15,15),B(3,2)
      DIMENSION U(3,5,2),V(9),W(6),LO(10),IPERM(3)
      EQUIVALENCE (X1,V),(Y4,W),(X,U)
      DATA  LO/1,3,5,7,9,2,4,6,8,10/,IPERM/2,3,1/
      T1=TH(1)
      T2=TH(2)
      T3=TH(3)
      FAC=1./(120.*AREA)
      T(1,1)=(6.*T1+2.*T2+2.*T3)*FAC
      T(1,2)=(2.*T1+2.*T2+   T3)*FAC
      T(1,3)=(2.*T1+   T2+2.*T3)*FAC
      T(2,2)=(2.*T1+6.*T2+2.*T3)*FAC
      T(2,3)=(   T1+2.*T2+2.*T3)*FAC
      T(3,3)=(2.*T1+2.*T2+6.*T3)*FAC
      T(2,1)=T(1,2)
      T(3,1)=T(1,3)
      T(3,2)=T(2,3)
      DO  1  I=1,2
      U(1,1,I)= B(1,1)-2.*B(3,I)
      U(2,1,I)= B(1,I)
      U(3,1,I)= -B(1,I)
      U(1,2,I)= B(2,I)
      U(2,2,I)= B(2,I)-2.*B(3,1)
      U(3,2,I)=-B(2,I)
      U(1,3,I)=-B(3,I)
      U(2,3,I)=-B(3,I)
      U(3,3,I)=3.*B(3,I)
      U(1,4,I)=0.
      U(2,4,I)=4.*B(3,1)
      U(3,4,I)=4.*B(2,I)
      U(1,5,I)=4.*B(3,I)
      U(2,5,I)=0.
    1 U(3,5,I)=4.*B(1,I)
      IF(LSIDES.EQ.1)  GOTO  11
      DO  10 M=2,LSIDES
      L=IPERM(M)
      DO  10  I=1,3
      DO  10 K=1,2
      U(I,M,K)=U(I,M,K)+U(I,M+2,K)*.5
   10 U(I,L,K)=U(I,L,K)+U(I,M+2,K)*.5
   11 DO  2  I=1,3
      DO  2 J=1,LNODES
      TU1(I,J)=0.
      TU2(I,J)=0.
      DO  2 K=1,3
      TU1(I,J)=TU1(I,J)+T(I,K)*X(K,J)
    2 TU2(I,J)=TU2(I,J)+T(I,K)*Y(K,J)
      DO  5 J=1,LNODES
      M=LO(J)
      L=LO(J+5)
      DO  3 N=1,3
      U1=TU1(N,J)
      U2=TU2(N,J)
      V(N   )=XM(1,1)*U1+XM(3,1)*U2
      V(N+3)=XM(2,1)*U1+XM(3,2)*U2
      V(N+6)=XM(3,1)*U1+XM(3,3)*U2
      W(N   )=XM(2,2)*U2+XM(3,2)*U1
    3 W(N+3)=XM(3,2)*U2+XM(3,3)*U1
      DO  4  I=J,LNODES
      N=LO(I)
      K=LO(I+5)
      S(N,M)=X(1,I)*X1+X(2,I)*X2+X(3,I)*X3+Y(1,I)*X7+Y(2,I)*X8+Y(3,I)*X9
      S(M,N)=S(N,M)
      S(K,L)=Y(1,I)*Y4+Y(2,I)*Y5+Y(3,I)*Y6+X(1,I)*Y7+X(2,I)*Y8+X(3,I)*Y9
    4 S(L,K)=S(K,L)
      DO  5  I=1,LNODES
      K=LO(I+5)
      S(K,M)=Y(1,I)*X4+Y(2,I)*X5+Y(3,I)*X6+X(1,I)*X7+X(2,I)*X8+X(3,I)*X9
    5 S(M,K)=S(K,M)
      RETURN
      END
```

```
      SUBROUTINE QDCOS (N,X,Y,Z,T)
      IMPLICIT REAL*8 (A-H,O-Z)
C
C     THIS SUBROUTINE COMPUTES THE DIRECTION COSINES OF THE LOCAL
C     ELEMENT SYSTEM OF A QUADRILATERAL (N=4) OR SINGLE TRIANGLE (N=1)
C
      DIMENSION X(1), Y(1), Z(1), T(1)
      X1 = X(2)+X(3)-X(N)-X(1)
      Y1 = Y(2)+Y(3)-Y(N)-Y(1)
      Z1 = Z(2)+Z(3)-Z(N)-Z(1)
      X2 = X(3)+X(N)-X(1)-X(2)
      Y2 = Y(3)+Y(N)-Y(1)-Y(2)
      Z2 = Z(3)+Z(N)-Z(1)-Z(2)
      S1 = X1**2+Y1**2+Z1**2
      C  = (X1*X2+Y1*Y2+Z1*Z2)/S1
      X2 = X2 - C*X1
      Y2 = Y2 - C*Y1
      Z2 = Z2 - C*Z1
      S1 = DSQRT (S1)
      S2 = DSQRT (X2**2+Y2**2+Z2**2)
      X1 = X1/S1
      Y1 = Y1/S1
      Z1 = Z1/S1
      X2 = X2/S2
      Y2 = Y2/S2
      Z2 = Z2/S2
      T(1) = X1
      T(2) = X2
      T(3) = Y1*Z2-Y2*Z1
      T(4) = Y1
      T(5) = Y2
      T(6) = Z1*X2-Z2*X1
      T(7) = Z1
      T(8) = Z2
      T(9) = X1*Y2-X2*Y1
      RETURN
      END
```

```
      SUBROUTINE SLCCT (NBF,NSF,NT,ITYPE)
      IMPLICIT REAL*8 (A-H,O-Z)
      COMMON/SLC/ H(21),U(21),Q(3,6),TX(3),TY(3),
     1HT(3),T(3,3,3),QS(3,3)
      COMMON IX5(1408),PX1(2754),TH(3),PX2(467),AREA,B(3),A(3),XM(3,3),
     1       ST(15,15),P(21,15),XS(2,2),
     2  SCOND(15,6,4),PX4(132),IX2(50),PX6(300),IX3(500)
      DIMENSION IPERM(3),NKN(4,3)
      DATA IPERM/2,3,1/, NKN/2,5,3,6, 8,2,9,3, 5,8,6,9/
      NDF=NBF+NSF
      TO = (TH  (1)+TH  (2)+TH  (3))/3.
      FAC = TO**3*AREA/15120.
      DO 150  I = 1,3
      J = IPERM(I)
      K=IPERM(J)
      X = A(I)**2+B(I)**2
      U(I) = -(A(I)*A(J)+B(I)*B(J))/X
      X = DSQRT(X)
      HT(I) =  4.0*AREA/X
      TY(I) = -0.5*B(I)/X
      TX(I) =  0.5*A(I)/X
      A1 = A(I)/AREA
      A2 = A(J)/AREA
      B1 = B(I)/AREA
      B2 = B(J)/AREA
      Q(1,I)   = B1*B1
      Q(2,I)   = A1*A1
      Q(3,I)   = 2.*A1*B1
      Q(1,I+3) = 2.*B1*B2
      Q(2,I+3) = 2.*A1*A2
      Q(3,I+3) = 2.*(A1*B2+A2*B1)
      QS(I,I) = TO/20.+TH  (I)/30.
      QS(J,K) = TO/20.-TH  (I)/120.
      QS(K,J) = QS(J,K)
      X=TH  (I)/TO
      Y=TH  (J)/TO
      X2=X**2
      Y2=Y**2
      XY=X*Y
      IF ( ITYPE .EQ. 1 ) GO TO 150
      T(1,1,I)=X2*(10.*X+6.*Y+6.)+Y2*(3.*X+Y+1.)+3.*X+Y+3.*XY+1.
      T(2,2,I)=X2*(X+3.*Y+1.)+Y2*(6.*X+10.*Y+6.)+X+3.*Y+3.*XY+1.
      T(3,3,I)=X2*(X+Y+3.)+Y2*(X+Y+3.)+6.*X+6.*Y+3.*XY+10.
      T(1,2,I)=X2*(2.*X+3.*Y+1.5)+Y2*(3.*X+2.*Y+1.5)+X+Y+2.*XY+.5
      T(1,3,I)=X2*(2.*X+1.5*Y+3.)+Y2*(X+.5*Y+1.)+3.*X+1.5*Y+2.*XY+2.
      T(2,3,I)=X2*(.5*X+Y+1.)+Y2*(1.5*X+2.*Y+3.)+1.5*X+3.*Y+2.*XY+2.
      T(2,1,I)=T(1,2,1)
      T(3,1,I)=T(1,3,I)
      T(3,2,I)=T(2,3,I)
  150 CONTINUE
      DO 200  I = 1,3
      J = IPERM(I)
      K = IPERM(J)
      II = 3*I
      JJ = 3*J
      KK = 3*K
      A1 = A(I)
      A2 = A(J)
      A3 = A(K)
      B1 = B(I)
      B2 = B(J)
      B3 = B(K)
      U1 = U(I)
      U2 = U(J)
      U3 = U(K)
      W1 = 1.-U1
      W2 = 1.-U2
      W3 = 1.-U3
      B1D = 2.*B1
      B2D = 2.*B2
      B3D = 2.*B3
      A1D = 2.*A1
      A2D = 2.*A2
      A3D = 2.*A3
      C21 = B1-B3*U3
      C22 = -B1D+B2*W2+B3*U3
      C31 = A1-A3*U3
      C32 = -A1D+A2*W2+A3*U3
      C51 = B3*W3-B2
      C52 = B2D-B3*W3-B1*U1
      C61 = A3*W3-A2
      C62 = A2D-A3*W3-A1*U1
      C81 = B3-B2D-B2*U2
      C82 = B1D-B3+B1*W1
      C91 = A3-A2D-A2*U2
      C92 = A1D-A3+A1*W1
      DO 200  N = 1,3
      L = 6*(I-1) + N
      Q11 = Q(N,I)
      Q22 = Q(N,J)
      Q33 = Q(N,K)
      Q12 = Q(N,I+3)
      Q23 = Q(N,J+3)
      Q31 = Q(N,K+3)
      Q2333 = Q23-Q33
      Q3133 = Q31-Q33
      P(L    ,II-2) = 6.*(-Q11+W2*Q33+U3*Q2333)
      P(L    ,II-1) = C21*Q23+C22*Q33-B3D*Q12+B2D*Q31
      P(L    ,II  ) = C31*Q23+C32*Q33-A3D*Q12+A2D*Q31
      P(L    ,JJ-2) = 6.*(Q22+W3*Q2333)
      P(L    ,JJ-1) = C51*Q2333+B3D*Q22
      P(L    ,JJ  ) = C61*Q2333+A3D*Q22
      P(L    ,KK-2) = 6.*(1.+U2)*Q33
      P(L    ,KK-1) = C81*Q33
      P(L    ,KK  ) = C91*Q33
      P(L    ,I+9 ) = 0.
      P(L    ,J+9 ) = HT(J)*Q33
      P(L    ,K+9 ) = HT(K)*Q2333
      P(L+3  ,II-2) = 6.*(Q11+U3*Q3133)
      P(L+3  ,II-1) = C21*Q3133-B3D*Q11
      P(L+3  ,II  ) = C31*Q3133-A3D*Q11
      P(L+3  ,JJ-2) = 6.*(-Q22+U1*Q33+W3*Q3133)
      P(L+3  ,JJ-1) = C51*Q31+C52*Q33+B3D*Q12-B1D*Q23
      P(L+3  ,JJ  ) = C61*Q31+C62*Q33+A3D*Q12-A1D*Q23
      P(L+3  ,KK-2) = 6.*(1.+W1)*Q33
      P(L+3  ,KK-1) = C82*Q33
      P(L+3  ,KK  ) = C92*Q33
      P(L+3  ,I+9 ) = HT(I)*Q33
      P(L+3  ,J+9 ) = 0.
      P(L+3  ,K+9 ) = HT(K)*Q3133
```

```
      P(N+18,II-2) = 2.*(Q11+U3*Q12+W2*Q31)
      P(N+18,KK-1) = ((B1D-B2D)*Q33+C82*Q23+C81*Q31)/3.
      P(N+18,KK   ) = ((A1O-A2D)*Q33+C92*Q23+C91*Q31)/3.
  200 P(N+18,K+9  ) = HT(K)*Q12/3.
      NK = 12 - NBF
      IF (NK.LE.0)  GO TO 240
      DO 220  N = 1,NK
      K = 13 - N
      DO 220  L = 1,4
      J = NKN(L,N)
      IF (L.LE.2)  C = TX(K-9)
      IF (L.GT.2)  C = TY(K-9)
      DO 220  I = 1,21
  220 P(I,J) = P(I,J) + C*PII,K)
      IF( ITYPE .EQ. 1 ) GO TO 1000
  240 IF(NSF.LE.0)  GOTO 300
      DO 260  K = 1,3
      J = K + NBF
      L = 3*K
      A1 = A(K)/AREA
      B1 = B(K)/AREA
      DO 260  I = 1,19,3
      P(I  ,J  ) =  P(I  ,L  ) + B1
      P(I+1,J  ) =  P(I+1,L  )
      P(I+2,J  ) =  P(I+2,L  ) + A1
      P(I  ,J+3) = -P(I  ,L-1)
      P(I+1,J+3) = -P(I+1,L-1) + A1
  260 P(I+2,J+3) = -P(I+2,L-1) + B1
  300 DO 400 J=1,NDF
      DO 340 L=19,21
      H(L)=0.
      DO 340 M=1,3
      N=(M-4)*6+L
      H(N  )=      T(1,1,M)*P(N,J)+T(1,2,M)*P(N+3,J)+T(1,3,M)*P(L,J)
      H(N+3)=      T(2,1,M)*P(N,J)+T(2,2,M)*P(N+3,J)+T(2,3,M)*P(L,J)
  340 H(L  )=H(L)+T(3,1,M)*P(N,J)+T(3,2,M)*P(N+3,J)+T(3,3,M)*P(L,J)
      DO 360  N = 1,19,3
      U(N  )=XM(1,1)*H(N)+XM(2,1)*H(N+1)+XM(3,1)*H(N+2)
      U(N+1)=XM(2,1)*H(N)+XM(2,2)*H(N+1)+XM(3,2)*H(N+2)
  360 U(N+2)=XM(3,1)*H(N)+XM(3,2)*H(N+1)+XM(3,3)*H(N+2)
      DO 400  I = 1,J
      X = 0.
      DO 380  N = 1,21
  380 X = X + U(N)*P(N,I)
      ST(I,J) = X*FAC
  400 ST(J,I) = ST(I,J)
      IF(NSF.LE.0)  GOTO 1000
      DO 550  K = 1,3
      I = K + NBF
      DO 550  L = 1,3
      FAC = QS(K,L)*AREA
      J = L + NBF
      ST(I  ,J  ) = ST(I  ,J  ) + FAC*XS(1,1)
      ST(I+3,J+3) = ST(I+3,J+3) + FAC*XS(2,2)
      ST(I  ,J+3) = ST(I  ,J+3) + FAC*XS(1,2)
  550 ST(J+3,I  ) = ST(I  ,J+3)
      DO 600  N = 1,6
      K = 15 - N
      L = K + 1
      PIVOT = ST(L,L)
      DO 600  I = 1,K
      C = ST(I,L)/PIVOT
      ST(I,L) = C
      DO 600  J = 1,K
      ST(I,J)=ST(I,J)-C*ST(L,J)
  600 ST(J,I)=ST(I,J)
      DO 700 I=1,15
      DO 700 J=1,6
  700 SCOND(I,J,NT)=ST(I,J+6)
 1000 RETURN
      END



      SUBROUTINE NLOAD ( X,Y,Z,P1,P2,P3,D1,D2,D3,PE,AREA ,
     1                   A,B,TH)
      IMPLICIT REAL*8 (A-H,O-Z)
      DIMENSION PE(3,5),Q(3,3),          TH(3),A(3),B(3)
      Q(1,1)=D1*X
      Q(1,2)=D2*X
      Q(1,3)=D3*X
      Q(2,1)=D1*Y
      Q(2,2)=D2*Y
      Q(2,3)=D3*Y
      Q(3,1)=D1*Z+P1
      Q(3,2)=D2*Z+P2
      Q(3,3)=D3*Z+P3
      C=AREA/24.
      DO 1 I=1,3
      PE(I,1)=(2.*Q(I,1)+   Q(I,2)+   Q(I,3))*D
      PE(I,2)=(   Q(I,1)+2.*Q(I,2)+   Q(I,3))*D
    1 PE(I,3)=(   Q(I,1)+   Q(I,2)+2.*Q(I,3))*D
      RETURN
      END
```

```
      SUBROUTINE TRIPLT(PR,ALP,NLVT)
      IMPLICIT REAL*8 (A-H,O-Z)
      COMMON  IQ(4),NODES,QUADT,NTRI,IX1,IBD(200,7),
     1BC(200,6),S(37,37),PT(37,5),PX3(315)
     2    ,THQ(4),ANG,TPC(5,4,5),TP1,TP2,X(4),Y(4),Z(4)
     3,011,    D12, D22, D33,EM, G1, G2,PX4(29),
     4AREA,B(3),A(3),PX5(234),P(21,15),PX6(496),IX2(50),PX8(300),IB(500)
      DIMENSION TEMP(5,4,5),TEMFAC(5),TB(3,5),C(3,9),ICURV(3,3),
     1          ILOCP(9,2),TF(9,5),ILOC1P(6,2)
      DATA ICURV/ 7,10,19, 13,16,19, 1,4,19 /
      DATA ILOCP/ 3,4,5,8,9,10,13,14,15, 3,4,5,13,14,15,18,19,20 /
      DATA ILOCIP/ 1,6,11,2,7,12, 1,11,16,2,12,17 /
      INTEGER QUADT
      NTRIF=2
      IF( NTRI .EQ. 1) NTRIF=1
      DO 100 I=1,NTRIF
      CALL TRICOR(I,TAVG,TEMP,NLVT,X,Y,THQ,TPC,B,A)
    1 AREA=A(1)*B(3) - A(3)*B(1)
      FAC=-EM*ALP*AREA/(6.*(1.-PR))
      IF( NTRI .EQ. 1) GO TO 2
      CALL SLCCT (9,0,1,1)
    2 CONTINUE
C.....FORM PLATE BENDING FORCES FOR EACH SUBTRIANGLE.
      DO 90 II=1,3
      CALL TEMCON(II,NLVT,TAVG,TEMP,1,TEMFAC,TB)
C.....FORM MATRIX CONTAINING WXX+WYY FOR SUBTRIANGLE.
      DO 9 IR=1,3
      ILOC=ICURV(IR,II)
      DO 9 J=1,9
    9 C(IR,J)=P(ILOC,J) + P(ILOC+1,J)
      DO 11 K=1,NLVT
      DO 11 IX=1,9
      TF(IX,K)=0.0
      DO 11 J=1,3
   11 TF(IX,K)=TF(IX,K) + TB(J,K)*C(J,IX)*FAC
C.....LOCATE SUBELEMENT FORCES IN FINAL FORCE VECTOR
      DO 12 K=1,9
      IFOR=ILOCP(K,I)
      DO 12 J=1,NLVT
   12 PT(IFOR,J)=PT(IFOR,J) + TF(K,J)
   90 CONTINUE
C.....FORM IN-PLANE FORCES FOR EACH TRIANGLE
      CALL TEMCON(1,NLVT,TAVG,TEMP,2,TEMFAC,TB)
      FAC1=EM*ALP/((1.-PR)*6.)
      CALL ITEMPF(FAC1,TEMFAC,TF,NLVT,A,B)
C.....LOCATE TRIANGLE IN-PLANE FORCES IN FINAL FORCE VECTOR
      DO 13 K=1,6
      IFOR=ILOCIP(K,I)
      DO 13 L=1,NLVT
   13 PT(IFOR,L)=PT(IFOR,L) + TF(K,L)
  100 CONTINUE
      RETURN
      END
```

```
      SUBROUTINE TRICOR(I,TAVG,TEMP,NLVT,X,Y,THQ,TPC,B,A)
      IMPLICIT REAL*8 (A-H,O-Z)
      DIMENSION ITRI(3,2),TEMP(5,4,5),X(4),Y(4),THQ(4),TPC(5,4,5)
     I          ,B(3),A(3)
      DATA ITRI / 1,2,3, 1,3,4 /
      ILOC=ITRI(1,I)
      JLOC=ITRI(2,I)
      KLOC=ITRI(3,I)
C.....FORM A(I) AND B(I) FOR TRAINGLE IF QUAD ELEMENT
      IF ( NTRI .EQ. 1 ) GO TO 2
      X1=X(ILOC)
      X2=X(JLOC)
      X3=X(KLOC)
      Y1=Y(ILOC)
      Y2=Y(JLOC)
      Y3=Y(KLOC)
      B(1)=Y2-Y3
      B(2)=Y3-Y1
      B(3)=Y1-Y2
      A(1)=X3-X2
      A(2)=X1-X3
      A(3)=X2-X1
    2 TAVG=(THQ(ILOC) + THQ(JLOC) + THQ(KLOC))/3.
      DO 1 J=1,NLVT
      DO 1 K=1,5
      TEMP(K,1,J)=TPC(K,ILOC,J)
      TEMP(K,2,J)=TPC(K,JLOC,J)
      TEMP(K,3,J)=TPC(K,KLOC,J)
    1 TEMP(K,4,J)=(TEMP(K,1,J)+TEMP(K,2,J)+TEMP(K,3,J))/3.
      RETURN
      END
```

```
      SUBROUTINE ITEMPF(FAC1,TEMFAC,TF,NLVT,A,B)
      IMPLICIT REAL*8 (A-H,O-Z)
      DIMENSION TEMFAC(5),TF(9,5),A(3),B(3)
      DO 1 I=1,NLVT
      TF(1,I)=B(1)
      TF(2,I)=B(2)
      TF(3,I)=B(3)
      TF(4,I)=A(1)
      TF(5,I)=A(2)
      TF(6,I)=A(3)
    1 CONTINUE
      DO 2 K=1,NLVT
      DO 2 L=1,6
    2 TF(L,K)=TF(L,K)*TEMFAC(K)*FAC1
      RETURN
      END
```

```
      SUBROUTINE TEMCON(II,NLVT,T,TEMP,ITYPE,TEMFAC,TB)
      IMPLICIT REAL*8 (A-H,O-Z)
      DIMENSION TEMP(5,4,5),ITEMP(3,3),TEMFAC(5),TB(3,5)
      DATA ITEMP / 2,3,4, 3,1,4, 1,2,4 /
      IF ( ITYPE .EQ. 2) GO TO 2
    1 IJ=ITEMP(1,II)
      IK=ITEMP(2,II)
      IL=ITEMP(3,II)
      GO TO 3
    2 IJ=1
      IK=2
      IL=3
    3 T2=T*T
      T3=T**3.
      T4=T**4.
      T5=T**5.
      DO 100 J=1,NLVT
      TT1=TEMP(1,IJ,J)
      TT2=TEMP(1,IK,J)
      TT3=TEMP(1,IL,J)
      TT41=TEMP(2,IJ,J)
      TT42=TEMP(2,IK,J)
      TT43=TEMP(2,IL,J)
      TB41=TEMP(4,IJ,J)
      TB42=TEMP(4,IK,J)
      TB43=TEMP(4,IL,J)
      TB1=TEMP(5,IJ,J)
      TB2=TEMP(5,IK,J)
      TB3=TEMP(5,IL,J)
      IF( ITYPE .EQ. 2 ) GO TO 4
      BF1=32.*(TT1-TB1-2.*(TT41-TB41))/(6.*T3)
      BF2=32.*(TT2-TB2-2.*(TT42-TB42))/(6.*T3)
      BF3=32.*(TT3-TB3-2.*(TT43-TB43))/(6.*T3)
      DF1=16.*(TT41-TB41-(TT1-TB1)/8.)/(6.*T)
      DF2=16.*(TT42-TB42-(TT2-TB2)/8.)/(6.*T)
      DF3=16.*(TT43-TB43-(TT3-TB3)/8.)/(6.*T)
      BT1=BF1*T5/80. + DF1*T3/12.
      BT2=BF2*T5/80. + DF2*T3/12.
      BT3=BF3*T5/80. + DF3*T3/12.
      TB(1,J)=BT1/6. + BT2/12. + BT3/12.
      TB(2,J)=BT1/12. + BT2/6. + BT3/12.
      TB(3,J)=BT1/12. + BT2/12. + BT3/6.
      GO TO 100
    4 TM1=TEMP(3,IJ,J)
      TM2=TEMP(3,IK,J)
      TM3=TEMP(3,IL,J)
      AF1=128.*((TT1+TB1+6.*TM1)/4.-TT41-TB41)/(3.*T4)
      AF2=128.*((TT2+TB2+6.*TM2)/4.-TT42-TB42)/(3.*T4)
      AF3=128.*((TT3+TB3+6.*TM3)/4.-TT43-TB43)/(3.*T4)
      CF1=32.*(TT41+TB41-(TT1+TB1)/16.-15.*TM1/8.)/(3.*T2)
      CF2=32.*(TT42+TB42-(TT2+TB2)/16.-15.*TM2/8.)/(3.*T2)
      CF3=32.*(TT43+TB43-(TT3+TB3)/16.-15.*TM3/8.)/(3.*T2)
      TEMFAC(J)=(AF1+AF2+AF3)*T5/80. + (CF1+CF2+CF3)*T3/12. +
     1          (TM1+TM2+TM3)*T
  100 CONTINUE
      RETURN
      END
```

```
      SUBROUTINE OVER3
      IMPLICIT REAL*8 (A-H,O-Z)
      COMMON NOEL,NOPT,NDOF( 400),PE(24),S(24,24)
      COMMON/CV/NUMEL,NUPTS,NUBPTS,IBANDP,MBAND,NBLOC,NDFRE,IFLAG,NUMAT
     1       ,ITEMP,NLVT,ISTRAN
      COMMON / ELEM / NODES,MD,IQ(36)
      COMMON / PRNT / IPO,IP1,IP2,IP3,IPA,IPN,IPB
      COMMON / SUBT / NSUB,ISUB(20),KSUB(20),NUEL,LEFT,NSTR

      REWIND 1
      REWIND 2
      REWIND 3
      REWIND 4
      REWIND 8
      NSUB=0
      IPO=0
      IP1=0
      IP2=0
      IP3=0
      IPA=0
      IPN=0
      IPB=0
      NOEL=NUMEL
      NOPT=NUPTS
      DO 100 I=1,NOPT
  100 NDOF(I)=NDFRE
          CALL PUZZLE
   60 RETURN
      END
```

```
      SUBROUTINE PUZZLE
      IMPLICIT REAL*8 (A-H,O-Z)
      COMMON NOEL,NOPT,NDOF( 400),IB( 400),IC( 400),
     .       LQ(36),LOC(36),
     .       LZ1,MD1,M1,K1,N1,NODE1,IQ1(36),MOC1(36),
     .       LZ2,MD2,M2,K2,N2,NODE2,IQ2(36),MOC2(36)
      COMMON / ELEM / NODES,MD,IQ(36)
C *** DIMENSION OF IB,IC          = NUMBER OF TOTAL NODAL POINTS
C *** DIMENSION OF IQ             = NUMBER OF ELEMENT NODAL POINTS
           CALL FRNTIQ   ( NT )
           CALL FRNTST   ( NT )
           CALL ANALYZ   ( NT )
      RETURN
      END
```

```
      SUBROUTINE FRNTIQ ( NT )
      IMPLICIT REAL*8 (A-H,O-Z)
      COMMON NOEL,NOPT,NDOF( 400),IB( 400),IC( 400),
     .       LQ(36),LOC(36),
     .       LZ1,MD1,M1,K1,N1,NODE1,IQ1(36),MOC1(36),
     .       LZ2,MD2,M2,K2,N2,NODE2,IQ2(36),MOC2(36)
      COMMON / ELEM / NODES,MD,IQ(36)
      COMMON / SUBT / NSUB,ISUB(20),KSUB(20),NUEL,LEFT,NSTR

            NUEL = NOEL
            NSTR = NOEL
            IF ( NSUB.EQ.0) GOTO 6
            NUEL = 0
      DO 1 IT = 1,NSUB
            REWIND 4
            NT = 0
            CALL LOCATE (NT,ISUB(IT),IT)
            NQ = NUM (N1,MOC1,NDOF)
            WRITE (8) N1,NQ,(MOC1(L),L=1,N1)
            NUEL    = NUEL + ISUB (IT)
            KSUB(IT)= NT
1           CONTINUE
            NSTR    = NSUB + NOEL - NUEL
            LEFT    = NOEL - NUEL
            IF (LEFT .LE. 0) GOTO 3
      DO 2 I = 1,LEFT
            READ  (1) NODES,MD,(IQ(L),L=I,NODES)
            WRITE (8) NODES,MD,(IQ(L),L=1,NODES)

2           CONTINUE

3           REWIND 1
            REWIND 8

      DO 4 I = 1,NSTR

            READ  (8) NODES,MD,(IQ(L),L=1,NODES)
            WRITE (1) NODES,MD,(IQ(L),L=1,NODES)

4           CONTINUE

            REWIND 1
            REWIND 4
            REWIND 8

      DO 5 I = 1,NOPT
5           NDOF(I) = IABS( NDOF(I) )

6           NT = 0

            CALL LOCATE (NT,NSTR,1)

            REWIND 1
            REWIND 4
            REWIND 3
      RETURN
      END
```

```
      SUBROUTINE LOCATE ( NT,NO2,IT )
      IMPLICIT REAL*8 (A-H,O-Z)
      COMMON NOEL,NOPT,NDOF( 400),IB( 400),IC( 400),
     .       LQ(36),LOC(36),
     .       LZ1,MD1,M1,K1,N1,NODE1,IQ1(36),MOC1(36),
     .       LZ2,MD2,M2,K2,N2,NODE2,IQ2(36),MOC2(36)
      COMMON / ELEM / NODES,MD,IQ(36)

      DO 1 I=1,NOPT
1           IB(I) = 0

      DO 3 LZ=1,NO2
            READ  (1) NODES,MD,(IQ(I),I=1,NODES)
            WRITE (4) NODES,MD,(IQ(I),I=1,NODES)
      DO 2 I=1,NODES
            K       = IQ(I)
2           IB(K) = IB(K) + 1
3           CONTINUE

      DO 4 I=1,NOPT
4           IC(I) = IB(I)
            REWIND 4

5     DO 8 LZ2 = 1,NO2

            READ  (4) NODES,MD,(IQ(I),I=1,NODES)
            NODE2 = NODES
            MD2   = MD

      DO 6 I = 1,NODE2
            IQ2(I) = IQ(I)
            K      = IQ2(I)
            IF ( NDOF(K).GT.0 )  IC(K) = IC(K) - 1
            IF ( NDOF(K).LT.0 )  IC(K) = IC(K) + 1
6           CONTINUE

            CALL FRONT

            IF ( LZ2.EQ.1 ) GOTO 7
            CALL EXPAND ( NT )
7           CALL UPDATE ( NT )
8           CONTINUE

            CALL FRONT
            CALL EXPAND ( NT )
            CALL UPDATE (NT)

      RETURN
      END
```

```
      SUBROUTINE FRONT
      IMPLICIT REAL*8 (A-H,O-Z)
      COMMON NOEL,NOPT,NDOF( 400),IB( 400),IC( 400),
     .       LQ(36),LOC(36),
     .       LZ1,MD1,M1,K1,N1,NODE1,IQ1(36),MOC1(36),
     .       LZ2,MD2,M2,K2,N2,NODE2,IQ2(36),MOC2(36)

           N2 = 0
      DO 1 I = 1,NOPT
           IF ( IB(I).EQ.IC(I)      ) GOTO 1
           IF ( IC(I).EQ.0          ) IB(I)=0
              N2 = N2 + 1
           LOC(N2) = I
    1      CONTINUE

C.....END OF STEP 0.

           M2 = 0
      DO 2 I = 1,N2
           MOC2(I)=0
           K = LOC(I)
           IF ( IC(K).NE.0          ) GOTO 2
           LOC(I)=0
           M2 = M2 + 1
           MOC2(M2) = K
    2      CONTINUE
           K2 = M2 + 1

C.....END OF STEP 1.

           CALL GAPS
      DO 5 I=1,N2
           K=LOC(I)
           IF ( K.EQ.0              ) GOTO 5
      DO 3 J=K2,N2
           IF ( MOC2(J).EQ.0        ) GOTO 4
    3      CONTINUE
    4      MOC2(J)=K
           LOC (I)=0
    5      CONTINUE

C.....END OF STEP 4.

      RETURN
      END
```

```
      SUBROUTINE EXPAND ( NT )
      IMPLICIT REAL*8 (A-H,O-Z)
      COMMON NOEL,NOPT,NDOF( 400),IB( 400),IC( 400),
     .       LQ(36),LOC(36),
     .       LZ1,MD1,M1,K1,N1,NODE1,IQ1(36),MOC1(36),
     .       LZ2,MD2,M2,K2,N2,NODE2,IQ2(36),MOC2(36)
      COMMON / FRNT / LZ,MD,MQ,KQ,NQ,LQT(150),LOCT(150)

      DO 1 I = 1,NODE1
      DO 1 J = 1,N1
    1      IF (  IQ1(I).EQ.MOC1(J) )  LQ(I) = J


           L = 0
      DO 2 I=1,NODE1
           LP = IQ1 ( I )
           J2 = NUM ( LQ(I),MOC1,NDOF )
           J1 = J2 - IABS(NDOF(LP)) + 1
      DO 2 J=J1,J2
           L=L+1
    2      LQT(L)=J

      IF(MQ.EQ.0) GO TO 50
      DO 60 I=1,MQ
   60 LOCT(I)=0
   50 IF(K1.GT.N1 ) GO TO 7

      DO 5 I = K1,N1
      DO 3 J = 1, N2
           IF ( MOC1(I).EQ.MOC2(J) )  GOTO 4
    3      CONTINUE
    4      LOC ( I ) = J
    5      CONTINUE


           L = MQ
      DO 6 I=K1,N1
           LP = MOC1 ( I )
           J2 = NUM ( LOC(I),MOC2,NDOF )
           J1 = J2 - IABS(NDOF(LP)) + 1
      DO 6 J=J1,J2
           L=L+1
    6      LOCT(L)=J

    7 WRITE (3) LZ,MD,MQ,KQ,NQ,LQT,LOCT

      CALL PRNT0
      CALL PRNT1

      RETURN
      END
```

```
      SUBROUTINE GAPS
      IMPLICIT REAL*8 (A-H,O-Z)
      COMMON NOEL,NOPT,NDOF( 400),IB( 400),IC( 400),
     .       LQ(36),LOC(36),
     .       LZ1,MD1,M1,K1,N1,NODE1,IQ1(36),MOC1(36),
     .       LZ2,MD2,M2,K2,N2,NODE2,IQ2(36),MOC2(36)

C.....FIX POSITIONS OF NODES COMMON TO MOC1   MOC2.

        IF ( LZ2.EQ.1                    ) GOTO 4

           I1 = MAX0 ( K1,K2 )
           I2 = MIN0 ( N1,N2 )
      DO 3 I=I1,I2
           K=MOC1(I)
           IF (    IC(K).EQ.0        )  GOTO 3
      DO 1 J=1,N2
           IF (  LOC(J).EQ.K         )  GOTO 2
    1      CONTINUE
                                        GOTO 3
    2      MOC2(I)=K
           LOC(J)=0
    3      CONTINUE

C.....END OF STEP 2.

    4 RETURN
      END
```

```
      FUNCTION NUM ( IPOS,MOC,NDOF )
      IMPLICIT REAL*8 (A-H,O-Z)
      DIMENSION MOC(1),NDOF(1)

           NUM = 0
           IF ( IPOS.EQ.0 )  GOTO 2

      DO 1 I = 1,IPOS
           K = MOC ( I )
    1      NUM = NUM + IABS ( NDOF ( K ) )

    2 RETURN
      END
```

```
      SUBROUTINE UPDATE ( NT )
      IMPLICIT REAL*8 (A-H,O-Z)
      COMMON NOEL,NOPT,NDOF( 400),IB( 400),IC( 400),
     .       LQ(36),LOC(36),
     .       LZ1,MD1,M1,K1,N1,NODE1,IQ1(36),MOC1(36),
     .       LZ2,MD2,M2,K2,N2,NODE2,IQ2(36),MOC2(36)
      COMMON / FRNT / LZ,MD,MQ,KQ,NQ,LQT(150),LOCT(150)

           IF ( LZ2.EQ.1 )  GOTO 2

      DO 1 I = 1,NT
    1      LOCT(I) = 0

    2 DO 3 I = 1,NODE2
    3      IQ1(I) = IQ2(I)

      DO 4 I = 1,N2
    4      MOC1(I) = MOC2(I)

           LZ1     = LZ2
           LZ      = LZ1
           NODE1   = NODE2
           MD1     = MD2
           MD      = MD1

           M1      = M2
           K1      = K2
           N1      = N2

           MQ = NUM ( M1,MOC1,NDOF )
           KQ = MQ+1
           NQ = NUM ( N1,MOC1,NDOF )

           NT = MAX0 ( NT,NQ )

      RETURN
      END
```

```
      SUBROUTINE FRNTST ( NT )
      IMPLICIT REAL*8 (A-H,O-Z)
      COMMON NOEL,NO(150),IX1,PE(150),S(576),B(150),A(11325)
      COMMON / ELEM / NODES,MD,IQ(36)
      COMMON / SUBT / NSUB,ISUB(20),KSUB(20),NUEL,LEFT,NSTR

           IF (NSUB.EQ.0) GOTO 7

      DO 3 IT = 1,NSUB
           READ (1) NODES,MD,(IQ(L),L=1,NODES)
           IO = KSUB (IT)
           CALL SCANIQ (IO,ISUB(IT))
           L  = ((IO+1)*IO)/2
           IF (MD.EQ.IO) GOTO 2
C.....SHRINK A FROM NT * NT SPACE TO NQ * NQ SPACE
           L  = 0
      DO 1 I  = 1,MD
           N  = NO(I) - I
      DO 1 J  = 1,MD
           L  = L + 1
    1      A(L) = A(N+J)
    2      WRITE (8) (B(J),J=1,MD),(A(J),J=1,L)

    3      CONTINUE

           IF (LEFT.LE.0) GOTO 5
      DO 4 I  = 1,LEFT
           READ (1)  NODES,MD,(IQ(L),L=1,NODES)
           L  = ((MD+1)*MD)/2
           READ (2)  (PE(I),I=1,MD),(S(I),I=1,L)
           WRITE (8) (PE(I),I=1,MD),(S(I),I=1,L)

    4      CONTINUE

    5      REWIND 1
           REWIND 2
           REWIND 8

      DO 6 I=1,NSTR
           READ  (1) NODES,MD,(IQ(L),L=1,NODES)
           L=((MD+1)*MD)/2
           READ  (8) (PE(I),I=1,MD),(S(I),I=1,L)
           WRITE (2) (PE(I),I=1,MD),(S(I),I=1,L)

    6      CONTINUE

           REWIND 2
           REWIND 8

    7      CALL SCANIQ (NT,NSTR)

      RETURN
      END
```

```
      SUBROUTINE SCANIQ ( NT,NO2 )
      IMPLICIT REAL*8 (A-H,O-Z)
      COMMON NOEL,NO(150),IX1,PE(150),S(576),B(150),A(11325)
      COMMON / FRNT / LZ,MD,MQ,KQ,NQ,LQT(150),LOCT(150)

      DO 1 I = 1,NT
    1      B(I) = 0.

           K = ((NT+1)*NT)/2
      DO 2 I = 1,K
    2      A(I) = 0.

           NO(1) = 1
           L = NT+2
      DO 3 I = 2,NT
    3      NO(I) = NO(I-1)+L - I
      CALL PRNTNO ( NT,NO )

      DO 7 LQ = 1,NO2

           READ  (3)  LZ,MD,MQ,KQ,NQ,LQT,LOCT
           L = ((MD + 1)*MD)/2
           READ  (2) (PE(I),I=1,MD),(S(I),I=1,L)

C          CALL PRNT2
C          CALL PRNTA (A,B,NO,NT,NT)
           CALL SEMBLE
C          CALL PRNTA (A,B,NO,NT,NT)

           IF ( MQ.EQ.0 )  GOTO 6
           J2 = MQ
           IF ( MQ .EQ. NQ )  J2 = NQ-1
           CALL REDUCE ( J2,NQ,NO,B,A )

C          CALL PRNTA (A,B,NO,NT,NT)

           NE = NQ ( MQ ) + NT - MQ
           WRITE (4) (B(I),I=1,MQ),(A(I),I=1,NE)


           DO 4 I = 1,MQ
    4      B(I)=0.0
           DO 5 I = 1,NE
    5      A(I)=0.0

    6      CALL SCRMBL  ( NT )

C          CALL PRNTA (A,B,NO,NT,NT)

    7      CONTINUE

      RETURN
      END
```

```
      SUBROUTINE SEMBLE
      IMPLICIT REAL*8 (A-H,O-Z)
      COMMON NOEL,NO(150),IX1,PE(150),S(576),B(150),A(11325)
      COMMON / FRNT / LZ,MD,MQ,KQ,NQ,LQT(150),LOCT(150)

           L = 0
      DO 1 M = 1,MD
           I = LQT(M)
           B(I) = B(I)+PE(M)
      DO 1 N = M,MD
           L = L + 1
           J = LQT(N)
           K = MINO ( I,J )
           K = MAXO ( I,J ) + NO(K) - K
     1     A (K) = A (K) + S(L)

      RETURN
      END
```

```
      SUBROUTINE REDUCE ( J2,NQ,NO,B,A )
      IMPLICIT REAL*8 (A-H,O-Z)
      DIMENSION NO(150),B(150),A(11325)

      DO 1 J  = 1,J2
           JO = NO(J)
           Q  = -1.0/A(JO)
           JO = JO-J
           I1 = J+1
      DO 1 I  = I1,NQ
           KO = NO(I)-I
           C  = A(I+JO)*Q
        B(I) = B(I)+B(J)*C

      DO 1 K  = 1,NQ

     1     A(K+KO) = A(K+KO) + A(K+JO)*C

      RETURN
      END
```

```
      SUBROUTINE SWITCH ( M,N,NT )
      IMPLICIT REAL*8 (A-H,O-Z)
      COMMON NOEL,NO(150),IX1,PE(150),S(576),B(150),A(11325)

C.....SWITCH LOADS.

           C    =B(M)
           B(M)=B(N)
           B(N)=C

C.....INTERCHANGE M AND N OF CONDENSED STIFFNESS MATRIX.

           MS=NO(M)-M
           NS=NO(N)-N

C.....SWITCH DIAGONAL TERMS.

           C      =A(MS+M)
           A(MS+M)=A(NS+N)
           A(NS+N)=C

C.....REGION 1.

           IF (  M.EQ.1            ) GOTO 3
           I2=M-1
      DO 2 I= 1,I2
           IS=NO(I)-I
           C      =A(IS+M)
           A(IS+M)=A(IS+N)
     2     A(IS+N)=C

C.....REGION 2.

     3     J1=M+1
           IF (  J1.EQ.N           ) GOTO 5
           J2=N-1
           DO 4 J=J1,J2
           JS=NO(J)-J
           C      =A(MS+J)
           A(MS+J)=A(JS+N)
     4     A(JS+N)=C

C.....REGION 3.

     5     IF (  N.EQ.NT           ) GOTO 7
           J1=N+1
        DO 6 J=J1,NT
           C      =A(MS+J)
           A(MS+J)=A(NS+J)
     6     A(NS+J)=C
     7  RETURN
        END
```

```
      SUBROUTINE SCRMBL  ( NT )
      IMPLICIT REAL*8 (A-H,O-Z)
      COMMON / FRNT / LZ,MD,MQ,KQ,NQ,LQT(150),LOCT(150)

            ICOUNT = 1

      DO 2 M = KQ,NQ
    1       N = LOCT(M)
            IF ( N .EQ. M .OR. N .EQ. 0) GOTO 2
            LOCT(M) = LOCT(N)
            LOCT(N) =      N
            I       = MINO(M,N)
            J       = MAXO(M,N)
            CALL SWITCH (I,J,NT)
            ICOUNT  = ICOUNT + 1
            IF (ICOUNT .GT. NT) STOP
            GOTO 1
    2 CONTINUE

      RETURN
      END
```

```
      SUBROUTINE ANALYZ  (NT)
      IMPLICIT REAL*8 (A-H,O-Z)
      COMMON NOEL,NO(150),IX1,ED(150),DUM(150),B(150),A(11325)
      COMMON / SUBT / NSUB,ISUB(20),KSUB(20),NUEL,LEFT,NSTR

            CALL SOLVE (NT,NSTR,9)
            IF (NSUB.EQ. 0) GOTO 5
            IF (LEFT.LE. 0) GOTO 2
      DO 1 I = 1,LEFT
            READ (8) MD,(ED(I),I=1,MD)
    1       CONTINUE
    2 DO 4 IT = 1,NSUB
            LT = NSUB - IT + 1
            NT = KSUB(LT)
            NO(1) = 1
            L = NT + 2
      DO 3 I = 2,NT
    3       NO(I) = NO(I-1)+L-I
            READ (8) MD,(B(I),I=1,MD)
            CALL PRNTB ( B,MD )
            CALL SOLVE (NT,ISUB(LT),0)
    4 CONTINUE

    5 RETURN
      END
```

```
      SUBROUTINE SOLVE ( NT,NO2,ISTOR )
      IMPLICIT REAL*8 (A-H,O-Z)
      COMMON NOEL,NO(150),IX1,ED(150),DUM(150),B(150),A(11325)
      COMMON / FRNT / LZ,MD,MQ,KQ,NQ,LQT(150),LOCT(150)

      DO 6 LQ = 1,NO2

            BACKSPACE 3
            READ  (3)  LZ,MD,MQ,KQ,NQ,LQT,LOCT
            BACKSPACE 3
      CALL PRNT2

            IF ( KQ.GT.NQ ) GOTO 3

      DO 1 I  = KQ,NQ
            L          = LOCT ( I )
    1       DUM ( I ) =    B ( L )

      DO 2 I  = KQ,NQ
    2       B   ( I ) =  DUM ( I )
            CALL PRNTB ( B,NQ )

    3       IF ( MQ.EQ.0 )  GOTO 4

            NE = NO ( MQ ) + NT - MQ
            BACKSPACE 4
            READ  (4)  (B(I),I=1,MQ),(A(I),I=1,NE)
            BACKSPACE 4
            CALL PRNTB ( B,NQ )
      CALL PRNTA ( A,B,NO,MQ,NT )

            CALL BPASS ( MQ,KQ,NQ,NO,B,A )

            CALL PRNTB ( B,NQ )

    4 DO 5 I  = 1,MD
            L          = LQT ( I )
    5       ED ( I ) =    B ( L )

            PRINT 110,LZ
            PRINT 130,(ED(I),I=1,MD)

            IF (ISTOR.GT.0) WRITE(8) MD,(ED(I),I=1,MD)

    6       CONTINUE

  100 FORMAT (1H1,8X,12HDISPLACEMENT,/,6X,4HNODE,8X,1HU,11X,1HV,11X,1HW)
  110 FORMAT (//,8X,7HELEMENT,I6,/)
  130 FORMAT(1P4E12.3)
      RETURN
      END
```

```
      SUBROUTINE BPASS ( MQ,KQ,NQ,NO,B,A )
      IMPLICIT REAL*8 (A-H,O-Z)
      DIMENSION NO(150),B(150),A(111325)

           IF ( MQ .EQ. NQ          ) GOTO 2

      DO 1 I = 1,MQ
           K = NO(I)-I
      DO 1 J = KQ,NQ
1          B(I) = B(I)-A(J+K)*B(J)

2          M = MQ+1
           I = NO(MQ)
           B(MQ) = B(MQ)/A(I)

           IF ( MQ.EQ.1 ) GOTO 5

      DO 4 L = 2,MQ

           I = M-L
           J1 = I+1
           K = NO(I)-I

      DO 3 J = J1,MQ
3          B(I) = B(I)-A(J+K)*B(J)

           K = NO(I)

4          B(I) = B(I)/A(K)

5     RETURN
      END
```

```
      SUBROUTINE PRNTO
      IMPLICIT REAL*8 (A-H,O-Z)
      COMMON NOEL,NOPT,NDOF( 400),IB( 400),IC( 400),
     .       LQ(36),LOC(36),
     .       LZ1,MD1,M1,K1,N1,NODE1,IQ1(36),MOC1(36),
     .       LZ2,MD2,M2,K2,N2,NODE2,IQ2(36),MOC2(36)
      COMMON / FRNT / LZ,MD,MQ,KQ,NQ,LQT(150),LOCT(150)
      COMMON / PRNT / IP0,IP1,IP2,IP3,IPA,IPN,IPB
      IF (IP0 .EQ. 0) GOTO 99
      PRINT 10,LZ1,NODE1,MD1,
     .         M1 ,K1   ,N1 ,
     .         MQ ,KQ   ,NQ
10    FORMAT (// 6X, 7HLZ1   =, I4,
     .          6X, 7HNODE1 =, I4,
     .          6X, 7HMD1   =, I4,/,
     .          6X, 7HM1    =, I4,
     .          6X, 7HK1    =, I4,
     .          6X, 7HN1    =, I4,/,
     .          6X, 7HMQ    =, I4,
     .          6X, 7HKQ    =, I4,
     .          6X, 7HNQ    =, I4 )
99    RETURN
      END
```

```
      SUBROUTINE PRNT1
      IMPLICIT REAL*8 (A-H,O-Z)
      COMMON NOEL,NOPT,NDOF( 400),IB( 400),IC( 400),
     .       LQ(36),LOC(36),
     .       LZ1,MD1,M1,K1,N1,NODE1,IQ1(36),MOC1(36),
     .       LZ2,MD2,M2,K2,N2,NODE2,IQ2(36),MOC2(36)
      COMMON / FRNT / LZ,MD,MQ,KQ,NQ,LQT(150),LOCT(150)
      COMMON / PRNT / IP0,IP1,IP2,IP3,IPA,IPN,IPB
      IF (IP1 .EQ. 0) GOTO 99
      PRINT 10,(IQ1 (I),I=1,NODE1)
      PRINT 20,(LQ  (I),I=1,NODE1)
      PRINT 30,(LQT (I),I=1,MD    )
      PRINT 40,(MOC1(I),I=1,N1    )
      PRINT 50,(MOC2(I),I=1,N2    )
      PRINT 60,(LOC (I),I=1,N1    )
      PRINT 70,(LOCT(I),I=1,NQ    )
10    FORMAT (//,6X,3HIQ ,20I4 )
20    FORMAT (   6X,3HLQ , 20I4 )
30    FORMAT (   6X,4HMLQ , 20I4 )
40    FORMAT (   6X,4HMOC1,  20I4 )
50    FORMAT (   6X,4HMOC2, 20I4 )
60    FORMAT (   6X,4HLOC , 20I4 )
70    FORMAT (   6X,4HLOCT, 20I4 )
99    RETURN
      END
```

```
      SUBROUTINE PRNT2
      IMPLICIT REAL*8 (A-H,O-Z)
      COMMON / FRNT / LZ,MD,MQ,KQ,NQ,LQT(150),LOCT(150)
      COMMON / PRNT / IP0,IP1,IP2,IP3,IPA,IPN,IPB
      IF (IP2 .EQ. 0) GOTO 99
      PRINT  1,LZ
      PRINT 10,(LQT (I),I=1,MD)
      PRINT 20,(LOCT(I),I=1,NQ)
 1    FORMAT (1H1,5X,2HLZ,I4 )
10    FORMAT (   6X,4HLQT , 20I4)
20    FORMAT (   6X,4HLOCT, 20I4)
99    RETURN
      END
```

```
      SUBROUTINE PRNTA (A,B,NO,NQ,NT)
      IMPLICIT REAL*8 (A-H,O-Z)
      DIMENSION A(1),B(1),NO(1),Q(150)
      COMMON / PRNT / IPO,IP1,IP2,IP3,IPA,IPN,IPB
      IF (IPA .EQ. 0) GOTO 99
      PRINT 20
      DO 1 I=1,NT
    1 Q(I)=0
      PRINT 10,(A(I),I=1,NT),B(1)
      IF ( NQ.EQ.1 )  GOTO 99
      DO 2 K=2,NQ
      I1=K-1
      I2=NO(K)
      I3=I2+NT-K
    2 PRINT 10,(Q(I),I=1,I1),(A(I),I=I2,I3),B(K)
   10 FORMAT ( 6X,3HA   , 20F6.0 )
   20 FORMAT (1H0)
   99 RETURN
      END
```

```
      SUBROUTINE PRNTNO ( NT,NO )
      IMPLICIT REAL*8 (A-H,O-Z)
      DIMENSION NO(1)
      COMMON / PRNT / IPO,IP1,IP2,IP3,IPA,IPN,IPB
      IF ( IPN.EQ.0 )  GOTO 99
      PRINT 100,NT,(NO(I),I=1,NT)
  100 FORMAT (6X,2HNT,14,/,6X,2HNO,20I4)
   99 RETURN
      END
```

```
      SUBROUTINE PRNT3 ( N1,LOC )
      IMPLICIT REAL*8 (A-H,O-Z)
      DIMENSION LOC(1)
      COMMON / PRNT / IPO,IP1,IP2,IP3,IPA,IPN,IPB
      IF (IP3 .EQ. 0) GOTO 99
      PRINT 10,(LOC(I),I=1,N1)
   10 FORMAT ( /,6X,3HLOC, 20I4 )
   99 RETURN
      END
```

```
      SUBROUTINE PRNTB ( B,NQ )
      IMPLICIT REAL*8 (A-H,O-Z)
      DIMENSION B(1)
      COMMON / PRNT / IPO,IP1,IP2,IP3,IPA,IPN,IPB
      IF ( IPB.EQ.0 )  GOTO 99
      PRINT 100,(B(I),I=1,NQ)
  100 FORMAT ( /,6X,2HB , 20F6.0 )
   99 RETURN
      END
```

```
      SUBROUTINE OVER4
      IMPLICIT REAL*8 (A-H,O-Z)
      COMMON/CV/NUMEL,NUPTS,NUBPTS,IBANDP,MBAND,NBLOC,NDFRE,IFLAG,LVECT,
     1 ITEMP,NLVT,ISTRAN
      COMMON/SS/IGEN,ISHEAR,JSHEAR,NREQ,IREACT,NTRUSS,ISIG,IROT
      COMMON  IQ(4), NODES, NTYPE,NQUAD, NTRI, IC(400), BX(6,400),
     1        PP(400,6), DU, AD(3,4), BD(3,4), TD(3,36), TR(3,36),
     2 TQ(3,3,4),XMQ(3,3,4),TH(5),TPC(5,4,5),TP1,TP2,PX4(12),D11,D12,
     3  D22,D33,EM,PX1(134),S(37,13),
     4        PT(13), PX2(152), DB(5), XM(3,3), XB(3,3), SM(3,3),
     5        SB(3,3), ZT(3,3,4), G1(3,3,4), ZQ(3,5), GQ(3,5),
     6        SCOND(15,6,4), PX3(9),X(4),Y(4)
      DIMENSION SIGN(5),SIG(3,5),SS(4),ST(4),TEMP(5,5),ED(6,4),
     1          DU119(119),DU437(437)
      EQUIVALENCE (DU,DU119(1)),(DU,DU437(1))
      DATA SIGN /1.,1.,0.0,-1.,-1./
      REWIND2
      REWIND3
      REWIND4
      ISTRAN=0
      DO 7 LV=1,LVECT
      REWIND9
      IF ( NTRUSS.EQ.NUMEL )  GOTO 56
```

```
C.....INITIALIZE PP,THE MATRIX STORING AVERAGED MOMENTS AND STESSES.....
      DO 1 I=1,NUPTS
      IC(I)=0
      DO 1 J=1,6
    1 PP(I,J)=0.
C.....SUM OVER NUMBER OF ELEMENTS.....
      IF ( ISIG .GT. 0 ) GO TO 800
      PRINT 90,LV
      PRINT 93
      GO TO 56
  800 PRINT 801,LV
      PRINT 802
      NEL = 0
   56 DO 50 JQ=1,NUMEL
      READ(9) IQ,NODES,NTYPE,NQUAD
      BACKSPACE8
      READ(8) MD,((ED(I,J),I=1,NDFRE),J=1,NODES)
      CALL LDISP( ED,IQ,BX,NDFRE,NODES )
      BACKSPACE8
      IF ( NODES.GT.2 )  GOTO 55
      READ(9) DU119
      IQ(3)=JQ
      IF ( LV.EQ.1 ) WRITE(2) (IQ(I),I=1,3)
      IF( LV .EQ. 1 ) WRITE(2) DU119
      GOTO 50
   55 READ(9) DU437
                THI5) = DU
      IF ( NTYPE.GT.0) READ(9) X,Y
      DO 8 I=1,NODES
      K=IQ(I)
    8 IC(K)=IC(K)+1
      IF ( ISHEAR.EQ.6) READ(9) SCOND
      IF ( NODES .EQ.4) READ(9) S
      IF ( NODES .EQ.4) READ(9) PT
C.....COMPUTE INTERIOR NODAL PT. DISPL. FOR QUAD. AND NODAL PT. DISPL. F
C.....TRI. IN ELEMENT COORDS.....
      IF (TH(5).LT..000001)  GO TO 50
      IF (XMQ(1,1,1).LT..001 .OR. XMQ(2,2,1).LT..001) GO TO 50
      CALL GDISPL
C.....COMPUTE AND TRANSFORM ELEMENT STRESSES AND MOMENTS.....
      DO 11 J=1,5
   11 DB(J)=TH(J)**3/12.
      DO 10 NTRI=1,NQUAD
      IF ( NTYPE.LE.0 )  CALL MEMBR
      IF(NTYPE .GT. 0) CALL MEMBQ(NTRI,X,Y,PT,XM,TPC,TP1,TP2)
      CALL MOMTR  ( 9,ISHEAR )
      DO 6 I=1,3
      DO 6 J=1,3
      SB(I,J)=0.
      SM(I,J)=0.
      DO 6 K=1,3
      SB(I,J)=SB(I,J)+XMQ(I,K,NTRI)*XB(K,J)
    6 SM(I,J)=SM(I,J)+XMQ(I,K,NTRI)*XM(K,J)
      K=NTRI
      KK=(NTRI-1)*9
      DO 10 J=1,3
      L=KK+(J-1)*3
      N5=1
      IF ( N5.GT.0 )  L=KK+6
      C=TR(1,L+1)
      R=TR(1,L+2)
      CS=DSQRT(C**2+R**2)
      C=C/CS
      R=R/CS
      C2=C*C
      S2=R*R
      SC=R*C
      C2MS2=C2-S2
      F=SM(1,J)
      G=SM(2,J)
      H=SM(3,J)
      IF(NTYPE.LE.0) GO TO 30
      ZT(1,J,K)=F
      ZT(2,J,K)=G
       ZT(3,J,K)=H
      GO TO 40
   30 ZT(I,J,K)=C2*F+S2*G-2.*SC*H
      ZT(2,J,K)=S2*F+C2*G+2.*SC*H
      ZT(3,J,K)=SC*(F-G)+C2MS2*H
   40 F=SB(1,J)
      G=SB(2,J)
      H=SB(3,J)
      G1(1,J,K)=C2*F+S2*G-2.*SC*H
      G1(2,J,K)=S2*F+C2*G+2.*SC*H
   10 G1(3,J,K)=SC*(F-G)+C2MS2*H
      IF(NODES.EQ.4)  GOTO 13
      DO 12 J=1,3
      DO 12 I=1,3
      GQ(I,J)=G1(1,J,1)*DB(J)
   12 ZQ(I,J)=ZT(1,J,1)*TH(J)
      GOTO  15
   13 DO 14 I=1,3
C.....COMPUTE AVERAGE MOMENTS AND STRESSES FOR QUAD.....
      GQ(I,1)=(G1(I,1,1)*G1(I,2,4))*.5*DB(1)
      GQ(I,2)=(G1(I,2,1)+G1(I,1,2))*.5*DB(2)
      GQ(I,3)=(G1(I,2,2)*G1(1,1,3))*.5*DB(3)
      GQ(I,4)=(G1(I,2,3)+G1(I,1,4))*.5*DB(4)
      GQ(I,5)=(G1(I,3,1)+G1(I,3,2)+G1(1,3,3)+G1(I,3,4))*.25*DB(5)
      ZQ(I,1)=(ZT(I,1,1)+ZT(I,2,4))*.5*TH(1)
      ZQ(I,2)=(ZT(I,2,1)+ZT(I,1,2))*.5*TH(2)
      ZQ(I,3)=(ZT(I,2,2)+ZT(I,1,3))*.5*TH(3)
      ZQ(I,4)=(ZT(I,2,3)+ZT(I,1,4))*.5*TH(4)
   14 ZQ(I,5)=(ZT(I,3,1)+ZT(I,3,2)+ZT(I,3,3)+ZT(I,3,4))*.25*TH(5)
C.....PRINT AVERAGE MOMENTS AND STRESSES FOR QUAD.....
   15 PRINT 101,JQ
      NPT=3
      IF(NODES.EQ.4)  NPT=5
              NQ = 1
          IF(NPT.EQ.5.AND.IGEN.GT.2)      NQ = 5
      DO 70 I=1,5
      DO 70 J=1,4
   70 TEMP(I,J)=TPC(I,J,LV)
      DO 71 I=1,5
      TEMP(I,5)=(TEMP(I,1)+TEMP(I,2)+TEMP(I,3)+TEMP(I,4))/4.
      IF(NPT .EQ. 3) TEMP(I,5)=(TEMP(I,1)+TEMP(I,2)+TEMP(I,3))/3.
   71 CONTINUE
      ALP=TP2
      PR=D12/D11
      IF ( ISIG .GT. 0 )  GO TO 60
          DO 3 L = NQ, NPT
```

```
      ATEMP=4.*(TEMP(1,L)+TEMP(3,L)-2.*TEMP(2,L))/(TH(L)**2)
      BTEMP=(TEMP(1,L)-TEMP(3,L))/TH(L)
      CTEMP=TEMP(2,L)
      MRES=EM*ALP*BTEMP*(TH(L)**3)/(12.*(1.-PR))
      NRES=EM*ALP*(ATEMP*(TH(L)**3/12.)+CTEMP*TH(L))/(1.-PR)
      GQ(1,L)=GQ(1,L)-MRES
      GQ(2,L)=GQ(2,L)-MRES
      ZQ(1,L)=ZQ(1,L)-NRES
      ZQ(2,L)=ZQ(2,L)-NRES
      M=0
      IF(L.LT.5) M=IQ(L)
    3 PRINT 20,((GQ(I,J),J=L,L),I=1,3),((ZQ(I,J),J=L,L),I=1,3),M
C.....ADD NODAL POINT MOMENTS AND STRESS RESULTANTS IN PP....
      DO 16 J=1,NODES
      K=IQ(J)
      DO 16 L=1,3
      M=L+3
      PP(K,L)=PP(K,L)+GQ(L,J)
   16 PP(K,M)=PP(K,M)+ZQ(L,J)
      GO TO 50
   60 CONTINUE
C.....COMPUTE STRESSES AT EACH NODE
      DO 81 LL=NQ,NPT
      IF(ISTRAN .EQ. 0) GO TO 99
C.....COMPUTE EXX AND EYY AT TOP SURFACE ONLY. ISOTROPIC MATERIAL.
      DO 86 IL=1,2
   86 SIG(IL,1)=ZQ(IL,LL)/TH(LL) + (GQ(IL,LL)*6./TH(LL)**2.)
      EXX=SIG(1,1)/EM - PR*SIG(2,1)/EM
      EYY=SIG(2,1)/EM - PR*SIG(1,1)/EM
   99 DO 80 II=1,5,2
      STTEMP=EM*ALP*TEMP(II,LL)/(1.-PR)
      DO 80 IL=1,2
      SIG(IL,II)=ZQ(IL,LL)/TH(LL)+(GQ(IL,LL)*6./TH(LL)**2)*SIGN(II)
      SIG(IL,II)=SIG(IL,II)-STTEMP
   80 SIG(3,II)=ZQ(3,LL)/TH(LL)+(GQ(3,LL)*6./TH(LL)**2)*SIGN(II)
      M = 0
      IF (LL.LT.5 )  M=IQ(LL)
      IF(ISTRAN .EQ. 0) GO TO 98
      PRINT 811,EXX,EYY,M
  811 FORMAT(5X,31HTOP SURFACE STRAINS,EXX AND EYY,2E12.4,
     1       9HFOR NODE=,I5)
   98 PRINT 810, ((SIG(IL,II),IL=1,3),II=1,5,2),M
  810 FORMAT(1X,1P9E11.3,I4)
      IF ( LL.LT.NPT)  GO TO 81
      IF ( NPT.EQ.5 )  GOTO 82
C.....AVERAGE THE STRESS RESULTANTS FOR TRI. ELEMENT
      DO 85 IL = 1,3
      GQ(IL,5) = (GQ(IL,1)+GQ(IL,2)+GQ(IL,3))/3.
   85 ZQ(IL,5) = (ZQ(IL,1)+ZQ(IL,2)+ZQ(IL,3))/3.
      TH(5)   = (TH(1)+TH(2)+TH(3))/3.
   82 CONTINUE
      WRITE(4) JQ
      NEL = NEL+1
      DO 83 II = 1,5,4
      DO 84 IL = 1,2
      SIG(IL,II)=ZQ(IL,5)/TH(5)+(GQ(IL,5)*6./TH(5)**2)*SIGN(II)
      SIG(IL,II)=SIG(IL,II)-EM*ALP*TEMP(II,5)/(1.-PR)
   84 SIG(3,II)=ZQ(3,5)/TH(5)+(GQ(3,5)*6./TH(5)**2)*SIGN(II)
      FAC1 = (SIG(1,II)+SIG(2,II))*0.5
      FAC2 = DSQRT(((SIG(1,II)-SIG(2,II))*0.5)**2+SIG(3,II)**2)
      SS(1) = FAC1+FAC2
      SS(2) = FAC1-FAC2
      SS(3) = (SS(1)-SS(2))/2.
      IF ( SS(2) .EQ. SIG(2,II) )  GOTO 87
      SS(4) = -57.272727273*DATAN(SIG(3,II)/(SIG(2,II)-SS(2)))
      GO TO 88
   87 SS(4) = 90.
   88 WRITE(4) SS
   83 CONTINUE
   81 CONTINUE
   50 CONTINUE
   20 FORMAT(1X,1P6E11.3,I4)
      IF ( NTRUSS .EQ. NUMEL )  GOTO 825
         IF (IGEN.GT.2)     GO TO 7
      IF ( ISIG .GT. 0)  GOTO 7
      PRINT 91,LV
      PRINT 92
      DO 5 I=1,NUPTS
      XP=IC(I)
      IF (XP.EQ.0.)   GO TO 5
      DO 4 J=1,6
    4 PP(I,J)=PP(I,J)/XP
      PRINT 110,I,((PP(K,L),L=1,6),K=1,1)
    5 CONTINUE
    7 CONTINUE
      IF ( ISIG.LE.0)   GOTO 824
      REWIND4
      DO 822 LV = 1,LVECT
      PRINT 820,LV
      PRINT 821
      DO 822 JJQ = 1,NEL
      READ(4) JQ
      READ(4) SS
      READ(4) ST
      PRINT 823,JQ,SS,ST
  823 FORMAT(I4,1P8E11.3)
  822 CONTINUE
  824 CONTINUE
      IF ( NTRUSS.EQ.0 )     GOTO  8000
  825 REWIND2
      REWIND3
       DO 700 LV=1,LVECT
      REWIND2
      PRINT 94,LV
      DO 600 JQ=1,NTRUSS
      CALL AXIAL ( Q,IQ,BX )
      IF ( Q.LT.0.0 )  PRINT 95,IQ(3),Q
      IF ( Q.GE.0.0 )  PRINT 96,IQ(3),Q
  600 CONTINUE
  700 CONTINUE
   90 FORMAT(1HI,2X,38HELEMENT STRESS RESULANTS FOR LOAD CASE,I4)
  101 FORMAT (12H ELEMENT NO.I4,50X,4HNODE)
   91 FORMAT (70H1AVERAGED NODAL STRESS RESULTANTS,W.R.T.,SURFACE COORDI
     1NATES,LOAD CASE,I4)
   92 FORMAT (5HONODE 2X,2HM2 9X,2HM1 9X,3HM12 8X,2HN1 9X,2HN2 9X,1HS)
C
   93 FORMAT (1H0 2X,2HM2 9X,2HM1 9X,3HM12 8X,2HN1 9X,2HN2 9X,1HS /)
   94 FORMAT (1H1,7X,43HAXIAL STRESSES FOR TRUSS ELEMENTS LOAD CASE,I4)
   95 FORMAT (7X,23HAXIAL STRESS FOR MEMBER,I5,2X,2HIS,E12.4
             ,11HCOMPRESSION )
```

```
  96 FORMAT ( 7X,23HAXIAL STRESS FOR MEMBER,I5,2X,2HIS,E12.4
     .        ,7HTENSION      )
110  FORMAT(I4,1P6E11.3)
 907 FORMAT(3014)
 801 FORMAT(1H1,2X,43HELEMENT STRESSES (TOP-BOTTOM) FOR LOAD CASE,I4)
 802 FORMAT(1H0,2X,2HN1,9X,2HN2,10X,1HS,8X,2HN1,9X,2HN2,9X,1HS,/)
 820 FORMAT(1H1,2X,45HPRINCIPAL STRESSES (TOP-BOTTOM) FOR LOAD CASE,I4)
 821 FORMAT(5HOELEM,2X,4HSMAX,7X,4HSMIN,8X,4HTMAX,5X,3HANG,8X,4HSMAX,7X
     .        ,4HSMIN,8X,4HTMAX,5X,3HANG)
8000 CONTINUE
     PRINT 330
 330 FORMAT(1H1,25HNODAL POINT DISPLACEMENTS )
     DO 331 K=1,NUPTS
 331 PRINT 332,K,(BX(J,K),J=1,NDFRE)
 332 FORMAT ( I4, 1P6E13.5 )                                    23FE77
     RETURN
     END
```

```
     SUBROUTINE GDISPL
     IMPLICIT REAL*8 (A-H,O-Z)
     COMMON IQ(4),IX1(1),NTYPE,NQUAD,IX2(401),B(6,400),PX1(2425),
    1        TD(3,36), TR(3,36), TQ(3,3,4), PX2(160), UM(5,4),
    2        VM(5,4), BP(9,4), PX3(58), S(37,13), PT(13), R2(13),
    3        P(39), D(5,5,4), PX4(512)
     DO 99 I=1,5
     DO 99 J=1,5
     DO 99 K=1,4
  99 D(I,J,K)=0.0
     IP=IQ(1)
     JP=IQ(2)
     KP=IQ(3)
     IF(NQUAD.EQ.4)  GOTO 10
     DO 15 M = 1,3
     P(M    )=TQ(M,1,1)*B(1,IP)+TQ(M,2,1)*B(2,IP)+TQ(M,3,1)*B(3,IP)
     P(M+5  )=TQ(M,1,2)*B(1,JP)+TQ(M,2,2)*B(2,JP)+TQ(M,3,2)*B(3,JP)
  15 P(M+10)=TQ(M,1,3)*B(1,KP)+TQ(M,2,3)*B(2,KP)+TQ(M,3,3)*B(3,KP)
     DO 17 M=4,5
     N = M-3
     P(M    )= TQ(N,1,1)*B(4,IP)+TQ(N,2,1)*B(5,IP)+TQ(N,3,1)*B(6,IP)
     P(M+5  )= TQ(N,1,2)*B(4,JP)+TQ(N,2,2)*B(5,JP)+TQ(N,3,2)*B(6,JP)
  17 P(M+10)= TQ(N,1,3)*B(4,KP)+TQ(N,2,3)*B(5,KP)+TQ(N,3,3)*B(6,KP)
     DO 98 M=1,5
     D(M,1,1)=P(M)
     D(M,2,1)=P(M+5)
  98 D(M,3,1)=P(M+10)
     GOTO 12
  10 LP=IQ(4)
C.....GROUP DISPL. OF CORNER NODES IN P.................................
     DO 1 M = 1,3
     P(M    )=TQ(M,1,1)*B(1,IP)+TQ(M,2,1)*B(2,IP)+TQ(M,3,1)*B(3,IP)
     P(M+5  )=TQ(M,1,2)*B(1,JP)+TQ(M,2,2)*B(2,JP)+TQ(M,3,2)*B(3,JP)
     P(M+10)=TQ(M,1,3)*B(1,KP)+TQ(M,2,3)*B(2,KP)+TQ(M,3,3)*B(3,KP)
   1 P(M+15)=TQ(M,1,4)*B(1,LP)+TQ(M,2,4)*B(2,LP)+TQ(M,3,4)*B(3,LP)
     DO 16 M=4,5
     N = M-3
     P(M    )= TQ(N,1,1)*B(4,IP)+TQ(N,2,1)*B(5,IP)+TQ(N,3,1)*B(6,IP)
     P(M+5  )= TQ(N,1,2)*B(4,JP)+TQ(N,2,2)*B(5,JP)+TQ(N,3,2)*B(6,JP)
     P(M+10)= TQ(N,1,3)*B(4,KP)+TQ(N,2,3)*B(5,KP)+TQ(N,3,3)*B(6,KP)
  16 P(M+15)= TQ(N,1,4)*B(4,LP)+TQ(N,2,4)*B(5,LP)+TQ(N,3,4)*B(6,LP)
C.....COMPUTE DISPL. AT INTERIOR NODES.................................
     DO 13 I=6,13
  13 R2(I)=0.0
     NDOFC=13
     IF ( NTYPE.GT.0 ) NDOFC=5
     DO 3 I=1,NDOFC
     L=19+I
     R2(I)=PT(I)/S(L+1,I)
     DO 2 K=1,L
   2 R2(I)=R2(I)-S(K,I)*P(K)
   3 P(I+20)=R2(I)
C.....STORE ALL THREE DISPL. COMPONENTS AT MID SIDE NODES IN P..........
     DO 5 I=1,4
     J=(I-1)*2
     K=(I-1)*3
     P(K+26)=R2(J+6)
   5 P(K+27)=R2(J+7)
     P(28)=(P( 3)+P(23))/2.
     P(31)=(P( 8)+P(23))/2.
     P(34)=(P(13)+P(23))/2.
     P(37)=(P(18)+P(23))/2.
C.....STORE DISPL. COMPONENTS FOR EACH TRI. IN D........................
     DO 6 I=1,5
     D(I,1,1)=P(I   )
     D(I,2,1)=P(I+5)
     D(I,4,1)=P(I+28)
     D(I,5,1)=P(I+25)
     D(I,3,1)=P(I+20)
     D(I,1,2)=P(I+5 )
     D(I,2,2)=P(I+10)
     D(I,4,2)=P(I+31)
     D(I,5,2)=P(I+28)
     D(I,3,2)=P(I+20)
     D(I,1,3)=P(I+10)
     D(I,2,3)=P(I+15)
     D(I,4,3)=P(I+34)
     D(I,5,3)=P(I+31)
     D(I,3,3)=P(I+20)
     D(I,1,4)=P(I+15)
     D(I,2,4)=P(I    )
     D(I,4,4)=P(I+25)
     D(I,5,4)=P(I+34)
   6 D(I,3,4)=P(I+20)
C.....TRANSFORM NODAL PT. DISPL. TO ELEMENT COORDS.....................
  12 DO 8 K=1,NQUAD
     KK=(K-1)*9
     DO 7 J=1,5
     IF(J.LT.4)  L=KK+(J-1)*3
     UM(J,K)=TD(1,L+1)*D(1,J,K)+TD(1,L+2)*D(2,J,K)+TD(1,L+3)*D(3,J,K)
     VM(J,K)=TD(2,L+1)*D(1,J,K)+TD(2,L+2)*D(2,J,K)+TD(2,L+3)*D(3,J,K)
     IF(J.GT.3)  GOTO 7
     I=(J-1)*3
     BP(I+1,K)=TD(3,L+1)*D(1,J,K)+TD(3,L+2)*D(2,J,K)+TD(3,L+3)*D(3,J,K)
```

```
      BP(I+2,K)=TR(1,L+1)*D(4,J,K)+TR(1,L+2)*D(5,J,K)
      BP(I+3,K)=TR(2,L+1)*D(4,J,K)+TR(2,L+2)*D(5,J,K)
    7 CONTINUE
    8 CONTINUE
      DO 20 I=1,4
      J=(I-1)*2
      K=(I-1)*5
      PT(J+1)=P(K+1)
   20 PT(J+2)=P(K+2)
      RETURN
      END
```

```
      SUBROUTINE MEMBR
      IMPLICIT REAL*8 (A-H,O-Z)
      COMMON  IX1(5),NTYPE,NQUAD,NTRI,IX2(400),PX1(4801),AD(3,4),
     1 BD(3,4),PX2(293),TPC(5,4,5),TP1,TP2,PX6(17),UM(5,4),VM(5,4),
     2PX3(36),U(5),          V(5), PX4(699), XM(3,3), PX5(498)
C.....GROUP MEMBRANE DISPL. IN U AND V.....
      DO 1 I=1,5
      U(I)=UM(I,NTRI)
    1 V(I)=VM(I,NTRI)
C.....MODIFY STRAIN DISPL. MATRIX IF ELEMENTT IS A CST.....
      IF(NQUAD.EQ.4)  GOTO 2
      U(4)=(U(2)+U(3))/2.
      V(4)=(V(2)+V(3))/2.
      U(5)=(U(1)+U(3))/2.
      V(5)=(V(1)+V(3))/2.
C.....COMPUTE STRAINS IN X DIR.....
    2 AREA2=-1./(AD(3,NTRI)*BD(1,NTRI))
      E=BD(1,NTRI)*AREA2
      A=AD(1,NTRI)*AREA2
      C=AD(2,NTRI)*AREA2
      D=AD(3,NTRI)*AREA2
      ITEST= NTRI+1
      IF (ITEST.GT.4)  ITEST=1
      XM(1,1)=(U(1)-U(2))*E
      XM(1,2)=(U(1)-U(2))*E
      XM(1,3)=(-U(1)+U(2)+4.*(-U(4)+U(5)))*E
C.....COMPUTE STRAINS IN Y DIR.....
      XM(2,1)=(A-2.*D)*V(1)+C*V(2)-D*V(3)+4.*D*V(5)
      XM(2,2)=A*V(1)+(C-2.*D)*V(2)-D*V(3)+4.*D*V(4)
      XM(2,3)=-A*V(1)-C*V(2)+3.*D*V(3)+4.*C*V(4) +4.*A*V(5)
C.....COMPUTE SHEAR STRAINS.....
      XM(3,1)=(V(1)-V(2))*E+(A-2.*D)*U(1)+C*U(2)-D*U(3)+4.*D*U(5)
      XM(3,2)=(V(1)-V(2))*E+A*U(1)+(C-2.*D)*U(2)-D*U(3)+4.*D*U(4)
      XM(3,3)=(-V(1)+V(2)+4.*(-V(4)+V(5)))*E
     1  -A*U(1)-C*U(2)+3.*D*U(3)+4.*C*U(4)+4.*A*U(5)
      RETURN
      END
```

```
      SUBROUTINE LDISP( ED,IQ,BX,NDFRE,NODES )
      IMPLICIT REAL*8 (A-H,O-Z)
      DIMENSION IQ(4),ED(6,4),BX(6,400)
      DO 1 K=1,NODES
      L=IQ(K)
      DO 1 I=1,NDFRE
    1 BX(I,L)=ED(I,K)
      RETURN
      END
```

```
      SUBROUTINE MOMTR ( NBF,ISHEAR )
      IMPLICIT REAL*8 (A-H,O-Z)
      COMMON  IX1(7), NTRI, IX2(400), PX1(4801), AD(3,4), BD(3,4),
     1        PX2(452), BP(9,4), PX3(10), R(12), A(3), B(3), U(3),
     2        HT(3), TX(3), TY(3), Q(3,6), PX4(660), XB(3,3),
     3        PX5(120), SCOND(15,6,4), C(6), D(3)
      DIMENSION IPERM(3),NKN(2,3)
      DATA IPERM/2,3,1/, NKN/2,5, 8,2, 5,8/
      DO 2 I=1,9
    2 R(I)=BP(I,NTRI)
      IF ( ISHEAR.NE.6)  GOTO 10
      DO 6 I=1,6
      C(I)=0.
      L= B+I
      DO 3 K=1,L
    3 C(I)=C(I)-SCOND(K,I,NTRI)*R(K)
    6 R(I+9)=C(I)
      R(2)=R(2)-C(4)
      R(5)=R(5)-C(5)
      R(8)=R(8)-C(6)
      R(3)=R(3)+C(1)
      R(6)=R(6)+C(2)
      R(9)=R(9)+C(3)
   10 DO 1 I=1,3
      D(I)=0.
      B(I)=BD(I,NTRI)
    1 A(I)=AD(I,NTRI)
      IF ( ISHEAR.NE.6)  GOTO 5
      DO 4 J=1,3
      D(1)=D(1)+B(J)*C(J)
      D(2)=D(2)+A(J)*C(J+3)
    4 D(3)=D(3)+A(J)*C(J)+B(J)*C(J+3)
    5 AREA = A(3)*B(2)-A(2)*B(3)
      DO 120  I = 1,3
      J = IPERM(I)
      X = A(I)**2+B(I)**2
      U(I) = -(A(I)*A(J)+B(I)*B(J))/X
      X = DSQRT(X)
      TX(I) =  0.5*A(I)/X
      TY(I) = -0.5*B(I)/X
      HT(I) =  4.0*AREA/X
      A1 = A(I)/AREA
```

```
      B1 = B(I)/AREA
      A2 = A(J)/AREA
      B2 = B(J)/AREA
      Q(1,I)   = B1*B1
      Q(2,I)   = A1*A1
      Q(3,I)   = 2.*A1*B1
      Q(1,I+3) = 2.*B1*B2
      Q(2,I+3) = 2.*A1*A2
  120 Q(3,I+3) = 2.*(A1*B2+A2*B1)
      M = 12 - NBF
      IF (M.LE.0)  GO TO 160
      DO 140  N = 1,M
      K = 13 - N
      L1 = NKN(1,N)
      L2 = NKN(2,N)
  140 R(K) = (R(L1)+R(L2))*TX(K-9)+(R(L1+1)+R(L2+1))*TY(K-9)
  160 DO 200  I = 1,3
      J = IPERM(I)
      K = IPERM(J)
      II = 3*I
      JJ = 3*J
      KK = 3*K
      A2 = A(J)
      A3 = A(K)
      B2 = B(J)
      B3 = B(K)
      U2 = U(J)
      U3 = U(K)
      W2 = 1.-U2
      W3 = 1.-U3
      C21 = -(2.+W2)*B2-(2.+U3)*B3
      C22 = B2*W2-B3*U3
      C31 = -(2.+W2)*A2-(2.+U3)*A3
      C32 = A2*W2-A3*U3
      C51 = 4.*B3-B2+B3*W3
      C52 = B2-B3*W3
      C61 = 4.*A3-A2+A3*W3
      C62 = A2-A3*W3
      C81 = B3-4.*B2-B2*U2
      C82 = B2*U2-B3
      C91 = A3-4.*A2-A2*U2
      C92 = A2*U2-A3
      C021 = -B2-(3.+U3)*B3
      C022 =  B3+(3.+W2)*B2
      C031 = -A2-(3.+U3)*A3
      C032 =  A3+(3.+W2)*A2
      DO 200  N = 1,3
      Q11 = Q(N,I)
      Q22 = Q(N,J)
      Q33 = Q(N,K)
      Q12 = Q(N,I+3)
      Q23 = Q(N,J+3)
      Q31 = Q(N,K+3)
      QI = Q22-Q33
      Q2 = Q22-Q23
      Q3 = Q33-Q23
      Q4 = Q23+Q1
      Q5 = Q23-Q1
      X8(N,I)  =  (-6.*Q11+3.*((U3-W2)*Q1+(U3+W2)*Q23))*R(II-2)
     1        + (6.*Q22+3.*W3*Q4)*R(JJ-2) + (6.*Q33+3.*U2*Q5)*R(KK-2)
     2        +((C21*Q1+C22*Q23+4.*(B2*Q31-B3*Q12))  *R(II-1)
     3        + (C31*Q1+C32*Q23+4.*(A2*Q31-A3*Q12))  *R(II)
     4        + (C51*Q22+C52*Q3) *R(JJ-1) + (C61*Q22+C62*Q3) *R(JJ)
     5        + (C81*Q33+C82*Q2) *R(KK-1) + (C91*Q33+C92*Q2) *R(KK)
     6        + HT(K)*Q4*R(K+9) + HT(J)*Q5*R(J+9))/2.
  200 X8(N,I)=-X8(N,I)-D(N)/AREA
      RETURN
      END



      SUBROUTINE MEMBQ(NTRI,X,Y,P,XM,TEMP,TP1,TP2)
      IMPLICIT REAL*8 (A-H,O-Z)
      DIMENSION X(4), Y(4), P(13), XM(3,3),TEMP(5,4)
      DIMENSION EPSX(4), EPSY(4), SS(4), TT(4), LOC(2,4)
      DATA LOC / 1, 2, 2, 3, 3, 4, 4, 1 /
      DATA SS /-1.,1.,1.,-1./, TT /-1.,-1.,1.,1./
      IF(NTRI.GT.1)  GO TO 300
      R12 = X(1) - X(2)
      R13 = X(1) - X(3)
      R14 = X(1) - X(4)
      R23 = X(2) - X(3)
      R24 = X(2) - X(4)
      R34 = X(3) - X(4)
      Z12 = Y(1) - Y(2)
      Z13 = Y(1) - Y(3)
      Z14 = Y(1) - Y(4)
      Z23 = Y(2) - Y(3)
      Z24 = Y(2) - Y(4)
      Z34 = Y(3) - Y(4)
      VOL=R13*Z24-R24*Z13
      CALL QM5C2 ( R13,R24,Z13,Z24,VOL,X5,X6,X7,X8,Y5,Y6,Y7,Y8 )
      EPSXY = X5*P(1)+Y5*P(2)+X6*P(3)+Y6*P(4)+X7*P(5)+Y7*P(6)+X8*P(7)+
     .        Y8*P(8)
      DO  200  I = 1, 4
      CALL QM5C1 ( SS(I),TT(I),R12,R13,R14,R23,R24,R34,Z12,Z13,Z14,Z23,
     .           Z24,Z34,VOL,X1,X2,X3,X4,XC,Y1,Y2,Y3,Y4,YC,XJAC,X(1),
     .           X(2),X(3),X(4),Y(1),Y(2),Y(3),Y(4) )
      EPSX(I) = Y1*P(1)+Y2*P(3)+Y3*P(5)+Y4*P(7)
  200 EPSY(I) = X1*P(2)+X2*P(4)+X3*P(6)+X4*P(8)
      SXAV = ( EPSX(1)+EPSX(2)+EPSX(3)+EPSX(4) ) * 0.25
      SYAV = ( EPSY(1)+EPSY(2)+EPSY(3)+EPSY(4) ) * 0.25
  300 DO 400 I=1,2
      L = LOC(I,NTRI)
      XM(1,I)=EPSX(L)
      XM(2,I)=EPSY(L)
  400 XM(3,I) = EPSXY
      XM(1,3)=SXAV
      XM(2,3)=SYAV
      XM(3,3) = EPSXY
      RETURN
      END
```

```
      SUBROUTINE QM5C1 ( S,T,R12,R13,R14,R23,R24,R34,Z12,Z13,Z14,Z23,
     .            Z24,Z34,VOL,X1,X2,X3,X4,XC,Y1,Y2,Y3,Y4,YC,XJAC,R1,R2,
     .            R3,R4,Z1,Z2,Z3,Z4 )
      IMPLICIT REAL*8 (A-H,O-Z)
C.....    THIS ROUTINE IS CALLED BY QM5 STIFFNESS AND STRESS ROUTINES
      XJ =VOL+S*(R34*Z12-R12*Z34)+T*(R23*Z14-R14*Z23)
      XJAC=XJ/8.0
      SM=1.0-S
      SP=1.0+S
      TM=1.0-T
      TP=1.0+T
      X1=(-R24+R34*S+R23*T)/XJ
      X2=( R13-R34*S-R14*T)/XJ
      X3=( R24-R12*S+R14*T)/XJ
      X4=(-R13+R12*S-R23*T)/XJ
      Y1=( Z24-Z34*S-Z23*T)/XJ
      Y2=(-Z13+Z34*S+Z14*T)/XJ
      Y3=(-Z24+Z12*S-Z14*T)/XJ
      Y4=( Z13-Z12*S+Z23*T)/XJ
      RS=0.25*(-TM*R1+TM*R2+TP*R3-TP*R4)
      ZS=0.25*(-TM*Z1+TM*Z2+TP*Z3-TP*Z4)
      RT=0.25*(-SM*R1-SP*R2+SP*R3+SM*R4)
      ZT=0.25*(-SM*Z1-SP*Z2+SP*Z3+SM*Z4)
      XC=-2.0*(T*SM*SP*RS-S*TM*TP*RT)/XJAC
      YC= 2.0*(T*SM*SP*ZS-S*TM*TP*ZT)/XJAC
      RETURN
      END
```

```
      SUBROUTINE QM5C2 ( R13,R24,Z13,Z24,VOL,X5,X6,X7,X8,Y5,Y6,Y7,Y8 )
      IMPLICIT REAL*8 (A-H,O-Z)
C.....    THIS ROUTINE IS CALLED BY QM5 STIFFNESS AND STRESS ROUTINES
      Y5 = Z24/VOL
      X6 = R13/VOL
      X7 = R24/VOL
      Y8 = Z13/VOL
      X5 =-X7
      Y6 =-Y8
      Y7 =-Y5
      X8 =-X6
      RETURN
      END
```

```
      SUBROUTINE AXIAL ( Q,IQ,BX )
      IMPLICIT REAL*8 (A-H,O-Z)
      COMMON /AX / THQ(4),ANG,TPC(5,4,5),TP1,TP2,X(4),Y(4),Z(4)
      DIMENSION IQ(4),BX(6,400)
      READ(2) (IQ(I),I=1,3)
      READ(2) THQ,ANG,TPC,TP1,TP2,X,Y,Z
      XP=X(2)-X(1)
      YP=Y(2)-Y(1)
      ZP=Z(2)-Z(1)
      Q=DSQRT ( XP*XP+YP*YP+ZP*ZP )
      X1=XP/Q
      X2=YP/Q
      X3=ZP/Q
      M=IQ(1)
      N=IQ(2)
      XR=BX(1,N)-BX(1,M)
      YR=BX(2,N)-BX(2,M)
      ZR=BX(3,N)-BX(3,M)
      Q=(X1*XR+X2*YR+X3*ZR)*THQ(2)/Q
      TEMP=0.5*(TPC(3,1,1)+TPC(3,2,1))
      QI=THQ(2)*TP2*TEMP
      Q = Q-QI
      RETURN
      END
```